| REPORT DOCUMENTATION PAGE | | | | Form Approved OMB No. 0704-0188 |
|--|-----------------------------|--|--|---|
| and maintaining the data needed, and complet | ting and rev his burden, | viewing the collection of information to Washington Headquarters Servi | n. Send comments regarding this burd ces, Directorate for information Operation | nstructions, searching existing data sources, gathering den estimate or any other aspect of this collection of ons and Reports, 1215 Jefferson Davis Highway, Suite DC 20503. |
| 1. AGENCY USE ONLY (Leave Blan | nk) | 2. REPORT DATE 1995 | 3. REPORT TYPE AND D Final | ATES COVERED |
| 4. TITLE AND SUBTITLE The Mechanism of Catalytic Halogenated Ruthenium and | • | | Molecular Oxygen and | 5. FUNDING NUMBERS |
| 6. AUTHORS Eva Rachel Birnbaum | | | | rl-sr-bl-tr-98- |
| 7. PERFORMING ORGANIZATION California Institute of Techno | |) AND ADDRESS(ES) | | 060 |
| 9. SPONSORING/MONITORING AG AFOSR/NI 110 Duncan Avenue, Room B-115 | GENCY N | IAME(S) AND ADDRESS(| ES) | AGENCY REPORT NUMBER |
| Bolling Air Force Base, DC 20332-8 11. SUPPLEMENTARY NOTES | 8080 | | | |
| 12a. DISTRIBUTION AVAILABILITY Approved for Public Release | | MENT | | 12b. DISTRIBUTION CODE |
| Approve | UTION and tox | STATEMENT A public relegan | | |
| Dies | distila | g [inlimited | | - |
| | | | | (4) |
| | | | | · |
| 14. SUBJECT TERMS | | | | 15. NUMBER OF PAGES |
| | DTIC | QUALITY INSCHO | CEU & | 16. PRICE CODE |
| 17. SECURITY CLASSIFICATION OF REPORT Unclassified | | HIS PAGE | 19. SECURITY CLASSIFICA' OF ABSTRACT Unclassified | TION 20. LIMITATION OF ABSTRACT UL |
| Onciassificu | Onciasi | SIIIEU | Oliciassilieu | OL |

6/1/

Abstract

Highly halogenated ruthenium and iron porphyrins are shown to be active catalysts for alkene oxidation with dioxygen or iodosobenzene. The synthesis and characterization of β -octachloro-tetrakis(pentafluorophenyl)porphyrinato-ruthenium(II) carbonyl [RuTFPPCl8(CO)] and β -octabromo-tetrakis(pentafluorophenyl)porphyrinato-iron(III) chloride [Fe(TFPPBr8)Cl] are reported. Crystal structures of RuTFPPCl8(CO) and the zinc and free ligand precursor complexes show extensive distortion of the halogenated porphyrin macrocycles due to steric interactions between the β -chlorine atoms and the pentafluorophenyl rings. ¹⁹F NMR is developed as a method to characterize both paramagnetic and diamagnetic fluorinated porphyrins in solution. The anodically shifted reduction potentials and red shifted absorptions in the UV-Vis spectroscopy of the halogenated porphyrins are discussed in terms of steric and electronic effects on porphyrin frontier orbitals.

Both Fe(TFPPBr₈)Cl and RuTFPPCl₈(CO) catalyze the oxidation of cyclohexene with dioxygen and without added coreductant, with 73 and 296 turnovers, respectively, in 24 hours. Although both porphyrins will catalyze reactions with iodosobenzene, showing selectivity consistent with high-valent metal-oxo formation, overall activity with dioxygen is much higher. In accord with earlier work, cyclohexene oxidation by Fe(TFPPBr₈)Cl is consistent with a mechanism involving porphyrin-mediated decomposition of alkyl peroxides, which generates free radicals in solution.

RuTFPPCl₈(CO) is shown to have a photochemical reaction mechanism involving olefin binding to the excited ruthenium porphyrin, resulting in a dramatic increase in the reaction rate upon irradiation with low energy light. This catalyst represents the first stable, effective metalloporphyrin catalyst for olefin oxidation with dioxygen and light.

THE MECHANISM OF CATALYTIC HYDROCARBON OXIDATION BY MOLECULAR OXYGEN AND HALOGENATED RUTHENIUM AND IRON PORPHYRINS

Approved firm the molecule.

Thesis by

Eva Rachel Birnbaum

In Partial Fulfillment of the Requirements for the degree of Doctor of Philosophy

California Institute of Technology

Pasadena, California

1995

(Submitted May 8th, 1995)

Mbis 30 1002

Acknowledgment



Abstract

Highly halogenated ruthenium and iron porphyrins are shown to be active catalysts for alkene oxidation with dioxygen or iodosobenzene. The synthesis and characterization of β -octachloro-tetrakis(pentafluorophenyl)porphyrinato-ruthenium(II) carbonyl [RuTFPPCl8(CO)] and β -octabromo-tetrakis(pentafluorophenyl)porphyrinato-iron(III) chloride [Fe(TFPPBr8)Cl] are reported. Crystal structures of RuTFPPCl8(CO) and the zinc and free ligand precursor complexes show extensive distortion of the halogenated porphyrin macrocycles due to steric interactions between the β -chlorine atoms and the pentafluorophenyl rings. ^{19}F NMR is developed as a method to characterize both paramagnetic and diamagnetic fluorinated porphyrins in solution. The anodically shifted reduction potentials and red shifted absorptions in the UV-Vis spectroscopy of the halogenated porphyrins are discussed in terms of steric and electronic effects on porphyrin frontier orbitals.

Both Fe(TFPPBr₈)Cl and RuTFPPCl₈(CO) catalyze the oxidation of cyclohexene with dioxygen and without added coreductant, with 73 and 296 turnovers, respectively, in 24 hours. Although both porphyrins will catalyze reactions with iodosobenzene, showing selectivity consistent with high-valent metal-oxo formation, overall activity with dioxygen is much higher. In accord with earlier work, cyclohexene oxidation by Fe(TFPPBr₈)Cl is consistent with a mechanism involving porphyrin-mediated decomposition of alkyl peroxides, which generates free radicals in solution.

RuTFPPCl₈(CO) is shown to have a photochemical reaction mechanism involving olefin binding to the excited ruthenium porphyrin, resulting in a dramatic increase in the reaction rate upon irradiation with low energy light. This catalyst represents the first stable, effective metalloporphyrin catalyst for olefin oxidation with dioxygen and light.

Table of Contents

| List of Figures | 1 |
|--|-----|
| List of Tables | vii |
| Abbreviations Used | ix |
| Introduction | 1 |
| Synthesis, Molecular Structures, and Nuclear Magnetic Resonance | |
| Spectroscopy of Halogenated Porphyrins | 18 |
| Spectroscopy and Electronic Structures of Halogenated Porphyrins | 67 |
| Oxidation of Olefins with Halogenated Iron Porphyrins | 104 |
| Mechanism of Oxidation of Hydrocarbons with Perhalogenated | |
| Ruthenium Porphyrins | 133 |
| Oxidation Chemistry in Supercritical Carbon Dioxide | 206 |
| Appendix (Chapter 2) | 247 |
| Appendix (Chapter 5) | 349 |
| | 0,, |

List of Figures

| Figure 1.1 | Catalytic Cycle of Cytochrome P-450 | 10 |
|-------------|--|----|
| Figure 1.2 | Structure of Protoporphyrin IX and Octaethylporphyrin | 1: |
| Figure 1.3 | Sterically Hindered Porphyrins | 14 |
| Figure 1.4 | Second and Third Generation Porphyrin Structures | 10 |
| Figure 2.1 | Structure and Standard Labeling of Porphyrins | 3 |
| Figure 2.2 | HPLC Trace of Separation of RuTFPPCl _x (CO) Compounds | 40 |
| Figure 2.3 | ORTEP Diagram of H ₂ TFPPCl ₈ | 42 |
| Figure 2.4 | ORTEP Diagram of ZnTFPPCl8 | 44 |
| Figure 2.5 | ORTEP Diagram of RuTFPPCl ₈ (CO) | 40 |
| Figure 2.6 | Projection of Free Ligand Series: H ₂ TPP, H ₂ TFPP, | |
| | and H ₂ TFPPCl ₈ | 48 |
| Figure 2.7 | Side-on View of RuTFPPCl ₈ (CO) | 50 |
| Figure 2.8 | ¹⁹ F NMR Spectra of a) H ₂ TFPP and b) ZnTFPP in CDCl ₃ | 52 |
| Figure 2.9 | ¹⁹ F NMR Spectrum of Fe(TFPP)Cl | 54 |
| Figure 2.10 | Curie Plot of the Temperature Dependence of Fe(TFPP)Cl | 56 |
| Figure 2.11 | ¹⁹ F NMR Spectrum of (FeTFPP) ₂ O | 58 |
| Figure 2.12 | ¹⁹ F NMR Spectrum of Fe(TFPPBr ₈)Cl | 60 |
| Figure 2.13 | ¹⁹ F NMR Spectra of Reduced Fe(TFPPBr ₈)Cl Produced by | 62 |
| | a) Bulk Electrolysis and b) Chemical Reduction | |
| Figure 3.1 | Normal Porphyrin UV-Visible Spectrum | 77 |
| Figure 3.2 | Gouterman Four Orbital Model of Porphyrin Frontier | 79 |
| | Orbitals and Modification upon Halogenation | |
| Figure 3.3 | UV-Vis Spectra of ZnTPP, ZnTFPP, ZnTFPPCl ₈ , and | |
| | ZnTFPPBr ₈ | 81 |
| Figure 3.4 | UV-Vis Spectra of Fe(TFPP)Cl and Fe(TFPPBr ₈)Cl | 83 |
| Figure 3.5 | UV-Vis Spectra of Reduced Fe(TFPPBr ₈)Cl | 85 |
| Figure 3.6 | Frontier Orbital Diagram of RuTFPPCl ₈ (CO) | 87 |
| Figure 3.7 | UV-Vis Spectra of RuTPP(CO) and RuTFPPCl8(CO) | 89 |
| Figure 3.8 | UV-Vis Spectra of RuTPP(py)2 and RuTFPPCl8(py)2 | 91 |
| Figure 3.9 | UV-Vis Spectra of RuTFPPX _n (CO) Series | 93 |
| Figure 3.10 | Charge Transfer Bands in Halogenated Ruthenium | |
| | Porphyrins | 95 |
| Figure 3.11 | Spectroelectrochemical Reduction of RuTFPPCl ₈ (py) ₂ | 97 |

| Figure 3.12 | Spectroelectrochemical Reduction of RuTFPPCl ₈ (CO) | 9 |
|-------------|---|-----|
| Figure 4.1 | Proposed Intermediates in Epoxidation by a High-Valent | |
| | Metal-Oxo | 11: |
| Figure 4.2 | Competing Mechanisms for Epoxidation by a High-Valent | |
| | Metal-Oxo | 11′ |
| Figure 4.3 | Mechanism of Cyclohexene Epoxidation and | |
| | Hydroxylation | 119 |
| Figure 4.4 | Turnovers of Cyclohexene Oxidation by Iron Porphyrins | |
| | with Iodosobenzene or Dioxygen | 12: |
| Figure 4.5 | Cyclohexene Oxidation by Fe(TFPPBrg)Cl with Dioxygen | |
| | versus Time | 123 |
| Figure 4.6 | Activity of Iron Porphyrins versus Iron Reduction Potential | 125 |
| Figure 4.7 | Dioxygenase Activity by Halogenated Iron Porphyrins | 127 |
| Figure 4.8 | Alkyl Peroxide Decomposition by Fe(TFPPBr ₈)Cl | 129 |
| Figure 4.9 | Diagram of Reaction Vessel Used for Oxidation Reactions | 131 |
| Figure 5.1 | Groves Mechanism for Aerobic Olefin Epoxidation with | |
| | Ruthenium Porphyrins | 161 |
| Figure 5.2 | Cyclohexene Oxidation by RuTFPPCl ₈ (CO) with PhIO | 163 |
| Figure 5.3 | Cyclohexene Oxidation by RuTFPPCl ₈ (CO) with Oxygen | 165 |
| Figure 5.4 | Hydrogen Peroxide Decomposition by RuTFPPC18(CO) | |
| | and Fe(TFPPBr ₈)Cl | 167 |
| Figure 5.5 | Titration of RuTFPPCl ₈ (CO) with mCPBA | 169 |
| Figure 5.6 | Oxidation of Cyclohexene by RuVITFPPCl ₈ (O) ₂ | 171 |
| Figure 5.7 | Oxidation of Triphenylphosphine by RuVITFPPCl ₈ (O) ₂ | 173 |
| Figure 5.8 | Mechanism for Dioxygen Activation via Loss of CO | 175 |
| Figure 5.9 | Effect of CO Removal from RuTFPPCl ₈ (CO) | 177 |
| Figure 5.10 | Effect of t-Butyl Hydroperoxide Addition | 179 |
| Figure 5.11 | Effect of Stir Rate | 181 |
| Figure 5.12 | Mixed Atmosphere Reaction | 183 |
| Figure 5.13 | UV-Vis of RuTFPPCl ₈ (CO) after Exposure to 1100 psi CO | 185 |
| Figure 5.14 | Isotope Effect | 187 |
| Figure 5.15 | Cyclohexene Oxidation by RuTFPPCl ₈ (CO) with | |
| | Dioxygen in the Absence of Light | 189 |
| Figure 5.16 | Effect of Photolysis on an Oxidation Reaction | 191 |
| Figure 5.17 | Transient Absorption Spectrum of RuTFPPCl ₈ (CO) | 193 |
| Figure 5.18 | 5 μs Transient Spectrum of RuTFPPCl ₈ (CO) at 415 nm | 195 |

| Figure 5.19 | 50 μs Transient Spectrum of RuTFPPCl ₈ (CO) at 415 nm | 197 |
|-------------|---|-----|
| Figure 5.20 | 50 μs Transient Absorption Spectrum of RuTFPPCl ₈ (CO) | |
| | under CO, Ar, Ethylene, and Dioxygen Atmospheres | 199 |
| Figure 5.21 | UV-Vis Spectra of RuTFPPCl ₈ (CO) after Photolysis | 201 |
| Figure 5.22 | Proposed Photochemical Mechanism for Olefin Oxidation | |
| | by RuTFPPCl8(CO) with Dioxygen | 203 |
| Figure 6.1 | Phase Diagram of Carbon Dioxide | 220 |
| Figure 6.2 | Apparatus for UV-Vis Spectroscopy in Supercritical | |
| | Carbon Dioxide | 222 |
| Figure 6.3 | UV-Vis Spectrum of Fe(TFPP)Cl in Supercritical Carbon | |
| | Dioxide | 224 |
| Figure 6.4 | UV-Vis Spectrum of Fe(TFPPBr ₈)Cl in Supercritical | |
| | Carbon Dioxide | 226 |
| Figure 6.5 | UV-Vis Spectrum of RuTFPPCl ₈ (CO) in Supercritical | |
| | Carbon Dioxide | 228 |
| Figure 6.6 | Solubility of Halogenated Porphyrins versus Pressure CO ₂ | 230 |
| Figure 6.7 | Corrected UV-Vis Spectrum of RuTFPPCl ₈ (CO) | 232 |
| Figure 6.8 | UV-Vis Spectrum of RuTFPPCl ₈ (CO) in the Presence of | |
| | Cyclohexene | 234 |
| Figure 6.9 | Apparatus for Oxidation Reactions in Supercritical Carbon | |
| | Dioxide | 236 |
| Figure 6.10 | Cyclohexene Oxidation by Fe(TFPP)Cl in SC CO ₂ | 238 |
| Figure 6.11 | Cyclohexene Oxidation by Fe(TFPPBr ₈)Cl in SC CO ₂ | 240 |
| Figure 6.12 | Cyclohexene Oxidation by RuTFPPCl ₈ (CO) in SC CO ₂ | 242 |
| Figure 6.13 | Partitioning to Multiple Oxidation Products | 242 |

viii

List of Tables

| Table 2.1 | X-ray Experimental Parameters | 64 |
|-----------|---|-----|
| Table 2.2 | Average Bond Lengths in Halogenated Porphyrins | 65 |
| Table 2.3 | Average Angles in Halogenated Porphyrins | 65 |
| Table 2.4 | Atom Displacements from the Mean Porphyrin Plane | 65 |
| Table 2.5 | ¹⁹ F and ¹ H NMR Chemical Shifts of Halogenated | |
| | Porphyrins | 66 |
| Table 3.1 | Electronic Absorptions of Halogenated Zinc, Free Base, | |
| | and Ruthenium Porphyrins | 101 |
| Table 3.2 | Reduction Potentials of Halogenated Porphyrins | 102 |
| Table 3.3 | Electronic Absorptions of Iron Porphyrins | 103 |
| Table 5.1 | Oxidation of Olefins by RuTFPPCl ₈ (CO) | 205 |

Abbreviations Used

mCPBA
OEP
SCF
SC CO₂
TBHP
TDBPP
TDCPP
TDFPP
TFPP
TFPPBr₈
TFPPCl₈
TMP
TPP

m-chloroperoxybenzoic acid octaethylporphyrin supercritical fluid supercritical carbon dioxide tert-butyl hydroperoxide tetrakis-(2,6-dibromophenyl)porphyrin tetrakis-(2,6-dichlorophenyl)porphyrin tetrakis-(2,6-difluorophenyl)porphyrin tetrakis(pentafluorophenyl)porphyrin β-octabromo-tetrakis(pentafluorophenyl)porphyrin tetramesitylporphyrin tetramesitylporphyrin tetramesitylporphyrin tetraphenylporphyrin

Chapter 1

Introduction to Catalysis with Metalloporphyrins

Science has "explained" nothing; the more we know the more fantastic the world becomes and the profounder the surrounding darkness.

-- Aldous Huxley, *Along the Road*, pt. 2 (1925).¹

The whole of science is nothing more than a refinement of everyday thinking.

-- Albert Einstein, Out of My Later Years, ch. 12 (1950).²

Oxidation chemistry is one of many arenas in which chemists are attempting to devise catalysts that achieve the remarkable efficiency, selectivity, and specificity of enzymes. Cytochrome P-450, a heme-based enzyme involved in respiration, has long been a target for the generation of a biomimetic catalyst.^{3,4} Found in a wide variety of tissues, this membrane-bound enzyme catalyzes the oxidation of a wide variety of organic substrates with reductively activated dioxygen.⁴ In particular, the ability of P-450 to selectively activate the more inert C-H bonds is quite desirable for industrial applications. Although many catalysts have been investigated, this selectivity has yet to be duplicated by a synthetic system.

The catalytic cycle of cytochrome P-450 is shown in Figure 1.1. From the resting state as the ferric porphyrin, two reducing equivalents from NADH are required to fully activate the enzyme. The first reduces the porphyrin to the ferrous state, enabling it to bind dioxygen. A second electron reduces the bound oxygen complex, and subsequent addition of two protons induces heterolytic cleavage of the dioxygen bond and release of a water molecule to form a high-valent metal-oxo iron porphyrin. The iron oxo

intermediate, which has never been isolated from P-450 due to its high reactivity, is generally believed to be an iron(IV)oxo porphyrin radical cation. Although early steps in the cycle are well documented, assignment of the active species is largely by analogy to Compound I of the enzyme horseradish peroxidase (HRP), which has been definitively characterized as an iron(IV)oxo porphyrin π radical cation.^{4,5} The active intermediate can also be directly generated with an O-atom donor such as iodosobenzene or peroxide; this "peroxide shunt" pathway is a convenient test for P-450 monooxygenase-like activity in model complexes.

A general technique in catalyst design is to model the active site of an enzyme, in the hope that one small section of the protein will exhibit the same activity as the whole. The porphyrin core of P-450 lends itself to this type of study for several reasons: reliable syntheses for porphyrins have been developed, the periphery of the porphyrin ligand is easily modified to alter the properties of the porphyrin, and the ligand has distinctive spectroscopy which facilitates investigation. Indeed, the past two decades have produced a plethora of work on metalloporphyrin derivatives.^{4,6,7}

Initial investigations on a derivative of the naturally occurring protoporphyrin IX (Figure 1.2) demonstrated that a species spectroscopically similar to compound I could be generated with an O-atom donor. ⁸ However, rather than oxidizing substrate, this intermediate hydroxylated its own β -side chain. A synthetic analog, octaethylporphyrin, was even less stable outside of the protective protein environment. Although a high-valent iron-oxo was believed to be generated in the presence of iodosobenzene, the planar porphyrin degraded by hydroxylation at the meso position, followed by complete destruction of the porphyrin chromophore. Oxidation of a second porphyrin molecule was clearly more favorable than oxidizing substrate. ⁸ The protein fold, which protects the porphyrin against autooxidation, prohibits unproductive μ -oxo dimer formation, and enhances substrate-porphyrin interactions, is clearly vital for these simple planar hemes to act as catalysts. A more stable porphyrin molecule would be necessary to mimic

monooxygenase behavior in solution. And so the quest to design a better porphyrin ligand began.

A simple iron tetraphenylporphyrin, Fe(TPP)Cl, was found to oxidize hydrocarbons in the presence of PhIO. Substitution at the meso position with a bulky phenyl moiety was found to reduce aggregation in solution and protect the reactive meso position from reactions leading to porphyrin degradation. Oxidation of tetramesitylporphyrinato-iron(III) chloride (Fe(TMP)Cl) with *m*-chloroperoxybenzoic acid at low temperatures produced a species that both shares spectral features with Compound I and is capable of epoxidizing alkenes. Although more promising than OEP, these ligands still showed substantial degradation in solution.

The second generation of metalloporphyrin catalysts were designed to increase the lifetime of porphyrins in solution by reducing their susceptibility to oxidative degradation. Halogenation of the meso phenyl rings would raise the reduction potential as well as increase steric bulk along the porphyrin periphery, decreasing the likelihood of dimerization or hydrogen abstraction by other porphyrin molecules. Tetrakis-(pentafluorophenyl)porphyrin (TFPP) was indeed found to be more stable than TPP, and iron complexes were found to show high selectivity for epoxidation of olefins. ¹¹
Similarly, tetrakis(2,6-dichlorophenyl)porphyrinato-iron(III) chloride [Fe(TDCPP)CI] was found to show high activity with pentafluoroiodosobenzene. ¹² Iron(III), manganese(III) and chromium(III) complexes of TDCPP all exhibited higher activity for cyclohexene oxidation with iodosobenzene than their TPP analogs, as well as higher selectivity for epoxide formation. Furthermore, the 2,6-dichlorophenylporphyrin complexes remained intact after an oxidation reaction, while the tetraphenylporphyrin complexes were completely degraded. ¹³

In addition to halogenation, other elegant methods have been developed for generating steric barriers against the close approach of two porphyrin molecules. Tailed porphyrins (Figure 1.3) have an imidazole or other nitrogen containing function linked to

the porphyrin ring by a flexible hydrocarbon chain, allowing it to swing around and axially bind to the metal center in simulation of histidine coordination. ¹⁴ Picket fence, ¹⁵ strapped, ¹⁶ basket handle, ¹⁷ and capped ¹⁸ porphyrins have large organic groups that project perpendicular to the plane of the porphyrin as pickets, or, in the latter cases, actually bridge across from one side of the porphyrin ring to the other. All of the above methods provide some steric protection as well as a pocket in which the substrate may bind. Although these types of porphyrins have led to some extremely interesting work in the area of enantioselective and regioselective oxidation chemistry, ¹⁹ they have not been further pursued as general oxidation catalysts. The hydrocarbon side chains that drive the selectivity found with these metalloporphyrins, while stable enough under mild conditions, are susceptible to degradation in a highly oxidizing environment.

Instead of building a pocket around the porphyrin, the third generation catalysts have completely protected the porphyrin periphery by full substitution at both the meso and beta positions (Figure 1.4). Steric bulk from mesityl, 20,21 pentafluorophenyl, $^{21-28}$ or 2,6-dihalophenyl $^{22,29-32}$ groups at the meso carbons is paired with electron-withdrawing substituents at the β -carbons. The electronic and steric crowding created by the full periphery imparts unusual structural and spectroscopic features to the porphyrin ligand, while the steric bulk of these complexes causes severe distortion of the porphyrin macrocycle, preventing dimerization (Chapter 2 and 3). The electronic demands of the substituents have been shown to decrease oxidative degradation of the porphyrin, thereby increasing net activity. 22,28,29,33,34

Indeed, these highly halogenated porphyrins are found to be active catalysts. Iron and manganese complexes of β -octachloro, β -octabromo, $^{20,22,26,28-30,34-40}$ and β -octanitro 32 tetraphenylporphyrin derivatives are reported to catalyze the oxidation of both alkanes and alkenes with a variety of O-atom donors, with tremendous increases in both activity and catalyst lifetime over the second generation porphyrins. For example, β -octabromo-tetramesitylporphyrinato-manganese(III) chloride catalyzes the epoxidation

of cyclooctene with hydrogen peroxide in 96% yield,³⁴ and the hydroxylation of adamantane with KHSO₅ in 62% yield.²⁰ Iron(III) chloride complexes of β-octachlorotetrakis(2,6-dichlorophenyl)porphyrin catalyze the hydroxylation of heptane with iodosobenzene in 80% yield.²² These reactions show increases in rate, total activity, selectivity, and porphyrin lifetime relative to the unhalogenated derivatives.

An even more unique finding is the activity of the third generation porphyrins with dioxygen. At 80 °C and 75 atm O₂, β-octabromo-tetrakis(pentafluorophenyl)-porphyrinato-iron(III) chloride (Fe(TFPPBr₈)Cl) catalyzes 17,150 turnovers of isobutane to *tert*-butyl alcohol in three hours. At slightly lower temperatures, the selectivity of the reaction for the desired alcohol can be increased to 92%.²⁶

The unprecedented activity of a metalloporphyrin with dioxygen and without a coreductant gave rise to new ideas for mechanisms for O₂ activation. Most recent porphyrin literature examines catalysis with O-atom donors that attempt to directly mimic enzymatic P-450 reactions. The reports of Fe(TFPPBr₈)Cl activity imply that alternate mechanisms may exist in addition to traditional high-valent metal-oxo chemistry, and prompted a more thorough investigation of this and similar third generation compounds in our lab.

This brief review of recent metalloporphyrin catalysis literature is not meant to be comprehensive, but rather to explain some of the history behind the development of the unusual perhalogenated porphyrin ligand. The more contemporary metalloporphyrin catalysts are now only distant cousins to the natural hemes they were initially designed to model. The following chapters are a more thorough investigation of the spectroscopy and catalytic properties of several fluorinated metalloporphyrins.

Chapter 2 describes the synthesis of halogenated iron and ruthenium porphyrins and their precursors. Molecular structures of β-octachloro-tetrakis(pentafluorophenyl)-porphyrinato-ruthenium(II) carbonyl, [RuTFPPCl₈(CO)] and the zinc and free ligand precursor complexes, are shown to be extremely distorted, in line with other halogenated

porphyrin structures. ¹⁹F NMR is developed as a method for characterizing the solution structure of both paramagnetic and diamagnetic fluorinated porphyrin structures.

The unusual spectroscopy and electrochemistry of halogenated porphyrins is discussed in Chapter 3. The changes in the frontier orbital energies upon phenyl and pyrrole halogenation are described. A full molecular orbital diagram is shown for RuTFPPCl₈(CO) and discussed in terms of the distortion and electron-withdrawing effects of halogenation.

Enhanced catalytic activity is observed with the highly halogenated complexes. Alkene oxidation by halogenated iron porphyrins is described in Chapter 4. Fe(TFPPBr₈)Cl is an active catalyst with both iodosobenzene and dioxygen, and shows a significant increase in activity and catalyst lifetime relative to Fe(TFPP)Cl. Observations support a mechanism involving porphyrin-mediated decomposition of alkyl peroxide, as proposed earlier in our group. ^{37,41}

Chapter 5 is a discussion of catalysis with RuTFPPCl₈(CO). Similar to the iron complex, this porphyrin is an extremely active catalyst for the oxidation of olefins under very mild conditions: 1 atm dioxygen, room temperature, and without addition of coreductant. Alkene oxidation is also observed with iodosobenzene. Observations of oxidation reactions catalyzed by RuTFPPCl₈(CO) with dioxygen are not consistent with mechanisms proposed for the activity of either the iron analog, Fe(TFPPBr₈)Cl, or other ruthenium porphyrins. Instead, olefin oxidation is dependent on light, possibly initiated by an interaction of the alkene with a RuTFPPCl₈(CO) excited state. As oxidation mechanisms in metalloporphyrins involving electronic excited states are rare, a photochemical reaction mechanism would be an interesting result, suggesting intermediates and ideas completely distinct from traditional high-valent metal-oxo chemistry.

The final chapter investigates the use of halogenated porphyrin catalysts in supercritical carbon dioxide. An apparatus was set up to measure the solubility of three

halogenated porphyrins in supercritical carbon dioxide by optical spectroscopy. Each porphyrin was tested with both iodosobenzene and dioxygen as a catalyst for the oxidation of cyclohexene in a supercritical medium. Although the results are extremely preliminary, they suggest that selectivity was more affected than net activity by the change in solvent. More multiple oxidations of the same substrate molecule were observed relative to reactions run in methylene chloride. Supercritical carbon dioxide was shown for the first time to be a good medium for oxidation catalysis.

References

- (1) Huxley, A. In Along the Road; George Doran: New York, 1925; pp 266.
- (2) Einstein, A. Out of my Later Years; Greenwood Press: Westport, CT, 1950, pp 282.
- (3) McMurray, T. J.; Groves, J. T. In *Cytochrome P-450*; P. K. Ortiz de Montellano, Ed.; Plenum Press: New York, 1986; pp 1-28.
- (4) Gunter, M. J.; Turner, P. Coord. Chem. Rev. 1991, 108, 115-161.
- (5) Cytochrome P-450; Ortiz de Montellano, P. K., Ed.; Plenum Press: New York, 1986.
- (6) Meunier, B. Chem. Rev. 1992, 92, 1411-1456.
- (7) Mansuy, D. Coord. Chem. Rev. 1993, 125, 129-142.
- (8) Chang, C. K.; Kuo, M.-S. J. Am. Chem. Soc. 1979, 101, 3413-3415.
- (9) Groves, J. T.; Nemo, T. E.; Myers, R. S. J. Am. Chem. Soc. 1979, 101, 1032-1033.
- (10) Groves, J. T.; Haushalter, R. C.; Nakamura, M.; Nemo, T. E.; Evans, B. J. J. Am. Chem. Soc. 1981, 103, 2884-2886.
- (11) Chang, C. K.; Ebina, F. J. Chem. Soc., Chem. Commun. 1981, 778-779.
- (12) Traylor, P. S.; Dolphin, D.; Traylor, T. G. J. Chem. Soc., Chem. Commun. 1984, 279-280.
- (13) Traylor, T. G.; Miksztal, A. R. J. Am. Chem. Soc. 1989, 111, 7443-7448.
- (14) Collman, J. P.; Groh, S. E. J. Am. Chem. Soc. 1982, 104, 1391-1403.
- Gunter, M. J.; McLaughin, G. M.; Berry, K. J.; Murray, K. S.; Irving, M.; Clark,P. E. *Inorg. Chem.* 1984, 23, 283-300.
- (16) Battersby, A. R.; Howson, W.; Hamilton, A. D. J. Chem. Soc., Chem. Commun. 1982, 1266-1268.
- (17) Lexa, D.; Mamenteau, M.; Saveant, J. M.; Xu, F. *Inorg. Chem.* **1986**, 25, 4857-4865.
- (18) Kim, K.; Ibers, J. A. J. Am. Chem. Soc. 1991, 113, 6077-6081.
- (19) Collman, J. P.; Zhang, X.; Lee, V. J.; Uffelman, E. S.; Brauman, J. I. *Science* **1993**, *261*, 1404-1411.
- (20) Hoffmann, P.; Robert, A.; Meunier, B. Bull. Chem. Soc. Fr. 1992, 129, 85-97.
- (21) Mandon, D.; Ochsenbein, P.; Fischer, J.; Weiss, R.; Jayaraj, K.; Austin, R. N.; Gold, A.; White, P. S.; Brigaud, O.; Battioni, P.; Mansuy, D. *Inorg. Chem.* 1992, 31, 2044-2049.

- (22) Bartoli, J. F.; Brigaud, O.; Battioni, P.; Mansuy, D. J. Chem. Soc., Chem. Commun. 1991, 440-442.
- (23) Marsh, R. E.; Schaefer, W. P.; Hodge, J. A.; Hughes, M. E.; Gray, H. B.; Lyons, J. E.; Ellis, P. E., Jr. Acta Crystallogr. 1993, C49, 1339-1342.
- (24) Schaefer, W. P.; Hodge, J. A.; Hughes, M. E.; Gray, H. B.; Lyons, J. E.; Ellis, P. E., Jr.; Wagner, R. W. Acta Crystallogr. 1993, C49, 1342-1345.
- (25) Henling, L. M.; Schaefer, W. P.; Hodge, J. A.; Hughes, M. E.; Gray, H. B.; Lyons, J. E.; Ellis, P. E., Jr. Acta Crystallogr. 1993, C49, 1745-1747.
- (26) Lyons, J. E.; Ellis, P. E., Jr.; Durante, V. A. In Structure-Activity and Selectivity Relationships in Heterogeneous Catalysis; R. K. Grasselli and A. W. Sleight, Eds.; Elsevier Science Publishers B.V.: Amsterdam, 1991; pp 99-116.
- (27) D'Souza, F.; Villard, A.; Caemelbecke, E. V.; Franzen, M.; Boschi, T.; Tagliatesta, P.; Kadish, K. M. *Inorg. Chem.* 1993, 32, 4042-4048.
- (28) d'A. Rocha Gonsalves, A. M.; Johnstone, R. A. W.; Pereira, M. M.; Shaw, J.; Sobral, D. N.; Abilio, J. F. *Tetrahedron Lett.* 1991, 32, 1355-1358.
- (29) Traylor, T. G.; Tsuchiya, S. Inorg. Chem. 1987, 26, 1338-1339.
- (30) Hoffmann, P.; Meunier, B. New J. Chem. 1992, 16, 559-561.
- (31) Lu, W. Y.; Bartoli, J. F.; Battioni, P.; Mansuy, D. New J. Chem. 1992, 16, 621-628.
- (32) Bartoli, J. F.; Battioni, P.; Foor, W. R. D.; Mansuy, D. J. Chem. Soc., Chem. Commun. 1994, 23-24.
- (33) Ellis, P. E., Jr.; Lyons, J. E. Catal. Lett. 1989, 3, 389-398.
- (34) Banfi, S.; Mandelli, R.; Montanari, F.; Quici, S. Gazz. Chim. Ital. 1993, 123, 409-415.
- (35) d'A. Rocha Gonsalves, A. M.; Pereira, M. M.; Serra, A. C.; Johnstone, R. A. W.; Nunes, M. L. P. G. J. Chem. Soc., Perkin Trans. 1 1994, 2053-2057.
- (36) Ellis, P. E., Jr.; Lyons, J. E. Coord. Chem. Rev. 1990, 105, 181-193.
- (37) Grinstaff, M. W.; Hill, M. G.; Labinger, J. A.; Gray, H. B. Science 1994, 264, 1311-1313.
- (38) Lyons, J. E.; Ellis, P. E., Jr. Catal. Lett. 1991, 8, 45-52.
- (39) Traylor, T. G.; Hill, K. W.; Fann, W.; Tsuchiya, S.; Dunlap, B. E. J. Am. Chem. Soc. 1992, 114, 1308-1312.
- (40) Wijesekera, T.; Matsumoto, A.; Dolphin, D.; Lexa, D. Angew. Chem., Int. Ed. Eng. 1990, 29, 1028-1030.
- (41) Labinger, J. A. Catal. Lett. 1994, 26, 95-99.

Figure 1.1 -- The proposed catalytic cycle for oxidation reactions by cytochrome P-450.

All steps before the generation of the high-valent metal-oxo are well documented, but the actual active intermediate has not been isolated.

Addition of an O-atom donor such as iodosobenzene to the ferric porphyrin (peroxide shunt) will directly form the oxidizing species, generally believed to be Fe^{IV}(P)(O)*+ (diagram modified from reference 1).

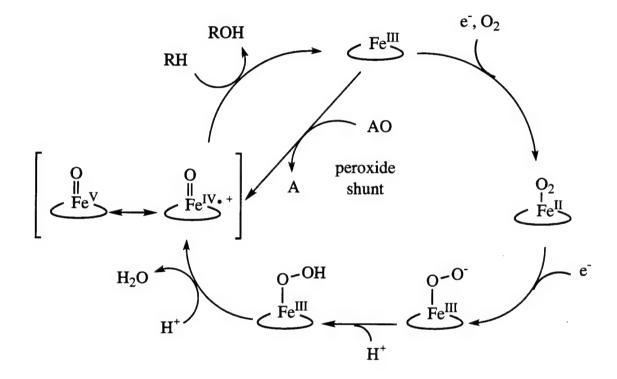


Figure 1.2 -- Diagram of the heme center from cytochrome P-450, protoporphyrin IX, and a synthetic equivalent, octaethylporphyrin (OEP). Naturally occurring hemes commonly bear alkyl or vinyl substituents at the pyrrole carbons.

Protoporphyrin IX (above) and Octaethylporphyrin (OEP)

Figure 1.3 -- Representations of tailed, picket fence, basket handle, and capped porphyrins. The bulky ligands create a steric barrier in the plane perpendicular to the porphyrin to prevent μ -oxo dimerization.

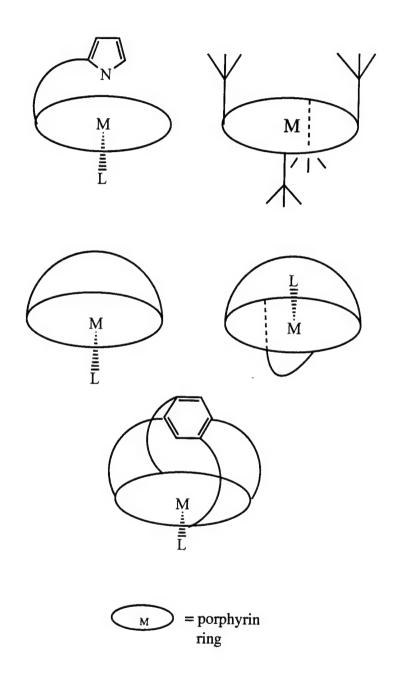


Figure 1.4 -- Drawings of three iron complexes of second generation porphyrins showing the groups commonly substituted at the meso positions: mesityl, 2,6-dichlorophenyl, and pentafluorophenyl groups. Halogenation of the pyrrole carbons would form third generation catalysts.

Chapter 2

Synthesis, Molecular Structures, and Nuclear Magnetic Resonance Spectroscopy of Halogenated Porphyrins

Introduction

Biomimetic metalloporphyrin oxidation catalysts are often based on a tetraphenylporphyrin template because these complexes are not as susceptible to aggregation and are protected from degradation to oxophlorins (oxo substitution at the meso position) by meso-phenyl substitution. Mesityl (TMP) or 2,6-dichlorophenyl (TDCPP) groups at the meso positions are more successful than unsubstituted phenyl rings, since the additional steric bulk of a substituted phenyl moiety decreases the tendency to form μ -oxo dimers in solution. The next generation of metalloporphyrins further enhanced the tetraphenylporphyrin ligands with electron-withdrawing substituents at the beta positions, removing reactive C-H bonds from the porphyrin periphery and increasing the steric bulk of the molecules. Many β -substituted TDCPP and TMP metalloporphyrins have been synthesized and investigated as oxidation catalysts (see Chapter 4). In addition to these ligands, another option is to begin with a tetrakis(pentafluorophenyl)porphyrin (TFPP) template, and then halogenate the β -positions to give a perhalogenated macrocycle. These "Teflon" porphyrins are designed to be extremely resistant to normal porphyrin decomposition in oxidizing environments.

Although extremely efficient porphyrin condensation reactions have been developed, lallowing porphyrins to be made in high yield from the appropriate benzaldehyde and pyrrole, this methodology has not been reported to be successful for β-halo derivatives. Recent advances have developed a the synthesis for the required

3,4-halogenated pyrroles, 2,3 but these compounds readily polymerize and are difficult to purify. Instead, halogenation of the β -positions is accomplished on an intact porphyrin macrocycle. $^{4-14}$ The fluorinated porphyrin, 5,10,15,20-tetrakis(pentafluorophenyl)-porphyrinato-zinc(II) (ZnTFPP), is commercially available or can be synthesized from pyrrole and pentafluorobenzaldehyde. The zinc, rather than the unmetallated porphyrin, is used because the metallated porphyrins are found to better withstand the halogenation reactions. 14

Synthesis

Halogenation to form β -octachloro- or β -octabromo-tetrakis(pentafluorophenyl)-porphyrinato-zinc(II) (ZnTFPPCl8 and ZnTFPPBr8; Figure 1.1) was initially accomplished with direct addition of $Cl_{2(g)}$ or $Br_{2(l)}$. However, a less hazardous synthesis with N-halo-succinamide was developed and found to proceed in good yield. Addition of excess N-halosuccinamide to a refluxing solution of ZnTFPP in methanol gave the desired product in 1-3 hours. Synthesis of the octabromo porphyrin was easier to drive to completion than that of the octachloro. The relative size of chlorine (atomic radii = 0.99) versus bromine $(1.14 \ \text{Å})^{15}$ would have predicted a more difficult synthesis for ZnTFPPBr8 based on the greater steric demands of eight bromines on the porphyrin periphery . However, the relative ease of synthesis of the two ligands suggests that the electronic effect, which leads to a decrease in reactivity for further substitution on the ligand, (electronegativity = $3.617 \ Cl$, $3.365 \ Br$) is more significant. If the trend follows to fluorine, the lack of success in our lab and the population of the porphyrin is not surprising.

Although ZnTFPPBr8 was readily purified by column chromatography, the large amount of partially halogenated porphyrins in the ZnTFPPCl8 reaction mixture necessitated high performance liquid chromatography (HPLC). Once the β -octahalo porphyrins were isolated, they were demetallated with HCl_(g) and purified from the zinc salts by alumina

chromatography. The yields for H₂TFPPCl₈ and H₂TFPPBr₈ were 40 and 82%, respectively, based on ZnTFPP.

Iron was inserted into the porphyrins by the standard methods: iron(II) acetate in refluxing glacial acetic acid or iron(II) chloride in DMF.^{17,18} With the TFPPBr₈ ligand, the metal is oxidized to iron(III) during the aqueous workup, and the porphyrin isolated as the chloride salt, Fe(TFPPBr₈)Cl. The iron porphyrins were found to demetallate during standard column chromatography, and could only be purified by washing or recrystallization. Therefore, high quality free ligand was a prerequisite for generation of pure iron porphyrin.

Addition of pyridine to a solution of Fe(TFPPBr₈)Cl reduced the metal and formed the bis-pyridine adduct. Both Fe^{III}(TFPPBr₈)Cl¹⁹ and Fe^{II}(TFPPBr₈)py2²⁰ have been crystallographically characterized. The absorption spectrum of [Fe(TFPPCl₈)] in the presence of pyridine indicates formation of Fe(TFPPCl₈)py₂, but this species was not isolated. Attempts to synthesize [Fe(TFPPCl₈)] were made using air-free, high vacuum techniques, in hopes of isolating a clean, oxygen-free sample for the anticipated investigation of O_2 activation. In retrospect, the removal of oxygen is believed to have complicated its synthesis. Allowing oxygen into the synthesis of Fe(TFPPBr₈)Cl did not lead to oxygen coordination, but clean oxidation of the Fe^{II} porphyrins to Fe^{III}(TFPPBr₈)Cl. In the absence of oxygen, the β -octachloro porphyrin appeared to form an iron(II) complex, based on the red shifted Soret band (see Chapter 3), but with mixed axial ligands. Due to the difficulty in isolating any pure Fe(TFPPCl₈) species, further work concentrated on the β -octabromo species.

Insertion of Ru from Ru₃(CO)₁₂ into H₂TFPPX₈ in perfluorobenzene yields a bright red (X = Cl) or green (X = Br) RuTFPPX₈(CO) compound.²¹ In perprotiobenzene, the extended time at reflux necessary to insert the ruthenium atom results in partial porphyrin dehalogenation and decomposition. In these reactions, ruthenium also inserts into the partially chlorinated derivatives H₂TFPPCl₇ and H₂TFPPCl₆ to form

RuTFPPCl₇(CO) and RuTFPPCl₆(CO), which can be isolated by sequential column chromatography and HPLC (Figure 2.2).

A single band attributable to CO stretching (1990, Cl₈; 1973 cm⁻¹, Br₈) is observed in the IR spectrum of RuTFPPX₈(CO), confirming a single carbonyl ligand.²² Identification of the other axial ligand is problematic; this ligand is labile in Ru(CO) porphyrins due to the strong trans effect of the CO.²³ Photolysis of RuTFPPCl₈(CO) in pyridine results in the formation of RuTFPPCl₈(py)₂. After photolysis, a single symmetrically coordinated species is observed by ¹⁹F NMR spectroscopy, indicating that the multiple signals in the spectrum of the carbonyl complex are due to variations in trans ligation and not dehalogenation of the porphyrin ring (*vide infra*).

Ruthenium insertion from $Ru_3(CO)_{12}$ was found to proceed in very low yield: approximately 10-20 % for TFPPCl₈, and less than 5 % for TFPPBr₈. Attempts to modify the reaction were unsuccessful. Solvent choice is limited, since any proton bearing solvent will exchange protons with the β -halogens of the porphyrin. Other ruthenium starting materials were tried, including $Ru(DMSO)_4Cl_2$, $[Ru(DMSO)_6]Cl_2$, $RuCl_3$, and $[Ru_5Cl_{12}]^{2-}$ (generated in situ). None showed significant reactivity with the TFPPCl₈ ligand.

Surprisingly, attempts to insert ruthenium into TFPP were also unsuccessful. Similar reaction conditions as above showed no reaction with H₂TFPP before substantial decomposition of the ligand occurred. No reports of RuTFPP have been found in the literature, although many metallated derivatives of TFPP have been synthesized.

Molecular Structures

ORTEP diagrams for H₂TFPPCl₈, ZnTFPPCl₈,¹⁰ and RuTFPPCl₈(CO)H₂O²⁴ complexes are shown in Figure 2.3 - 2.5, with the atom numbering shown. Complete crystallographic reports are included in Appendix 2.

H₂TFPPCl₈ crystallized from an acetone/water solution in space group P $\bar{1}$, with two porphyrins in the unit cell. The two parallel porphyrin molecules are 4.74 Å apart, with the porphyrin centers slightly offset (center to center distance 6.1 Å). The zinc derivative, ZnTFPPCl₈, crystallized from a saturated o-dichlorobenzene solution with a solvent molecule in a parallel plane both above and below the porphyrin molecule. The solvent molecules are located 3.4 Å from the mean plane of the porphyrin (defined as the average plane of the four nitrogen atoms), a distance suggestive of a π -stacking interaction between the π systems of the porphyrin and the o-dichlorobenzene molecules. Aromatic solvent molecules were found to stack in a similar fashion in the crystal structure of tetraphenylporphyrinato-zinc(II) bis-toluene, ZnTPP(C₆H₅CH₃)₂, where two toluene molecules occupy these positions.²⁵ The π donor ability of the aromatic solvent may help stabilize the zinc ion in the electron deficient macrocycle. Similarly, H₂TFPPBr₈ was found to crystallize with an o-dichlorobenzene molecule stacked above each porphyrin molecule.¹⁰

Recrystallization of RuTFPPCl₈(CO) in air from ethyl acetate and hexane gave RuTFPPCl₈(CO)H₂O (Figure 2.5). An ethyl acetate molecule is hydrogen bonded to the water ligand (O ··· O 2.668 Å), and the stability provided by this hydrogen bond network may explain why no crystals were obtained with other solvents. Trans coordination of CO and H₂O to Ru is unusual, but is precedented in RuOEP(CO)H₂O and the non-porphyrin compound *trans*-RuCl₂(PEt₃)₂(CO)H₂O.^{26,27}

Chlorination of the β -pyrrole carbons induces severe tetrahedral distortions (Figures 2.6 and 2.7) reducing the molecular symmetry of the porphyrin from D_{4h} to D_2 . The pairs of β -halogen atoms are located alternately above and below the average plane determined by the four central nitrogen atoms, and the phenyl rings are rotated slightly towards the mean porphyrin plane to minimize steric contact between the halogen atoms at the pyrrole positions and the ortho carbons of the pentafluorophenyl rings. The distortion of the macrocycle is quantified as the distances of the *meso* and β -carbons from the mean

plane of the porphyrin (Table 2.2). A view of the free ligand porphyrins H₂TFPP, H₂TFPPCl₈, and H₂TFPPBr₈ (Figure 2.6), generated from crystal structure coordinates, shows the increasing distortion along the series.

The three β -octachloro porphyrins described above exhibit severe distortions common to perhalogenated and other highly substituted porphyrins: 7,10,13,20,28-32 'ruffling' or twist (distortion manifested at the *meso*- carbons) and 'saddling' (distortion manifested at the β -carbons). As expected, saddling increases with halogenation (Figure 2.6), as manifested by increasing average C_{β} displacements from the plane from 0.051 to 0.62 to 0.90 Å in the free ligand series. The free ligand, H₂TFPPCl₈, is the least distorted of the structurally characterized chlorinated porphyrins [ZnTFPPCl₈, H₂TFPPCl₈, RuTFPPCl₈(CO)H₂O, CuTFPPCl₈²⁹], as reflected by the smaller perpendicular displacements of atoms from the mean porphyrin plane and a lack of the twisting or ruffling observed in the metallated derivatives. The saddle distortion in the free ligand (average C_{β} displacement = 0.62 Å) is smaller than in the metallated derivatives ZnTFPPCl₈ (0.75), and CuTFPPCl₈ (0.70), ²⁹ but greater than in the octahedrally coordinated RuTFPPCl₈(CO)H₂O (0.48 Å). ²⁴

Though saddled, the unmetallated $H_2TFPPCl_8$ has essentially no twist distortion (average C_m displacement = 0.023 Å). When the metal atom sits inside the core, a large twist distortion is observed: ZnTFPPCl₈ (0.13), RuTFPPCl₈(CO)H₂O (0.20),²⁴ and CuTFPPBr₈ (0.16 Å).²⁸ Extended to the porphyrin periphery, this results in one halogen atom of each pyrrole being significantly farther out of the mean plane than the other. In ZnTFPPCl₈ the displacements differ by 0.31 Å,¹⁰ and in RuTFPPCl₈(CO)H₂O by 0.43 Å.²⁴ The twist distortion is apparent in the side-on view of RuTFPPCl₈(CO)H₂O (Figure 2.7).

A final measure of distortion is one based on the phenyl dihedral angles; to minimize steric contact with the β-substituents, the phenyl rings rotate towards the mean porphyrin plane (Figure 2.6). The dihedral angles decrease with halogenation from 79° in

H₂TFPP to 73° in H₂TFPPCl₈ to 54° in H₂TFPPBr₈. Metallation also affects the dihedral angle. In the TFPPCl₈ complexes, octahedral RuTFPPCl₈(CO) has a much larger dihedral angle (81°) than the free ligand (73°) or the zinc complex (59°) (Table 2.3).

Remarkably, bond lengths (Table 2.4) in the porphyrin skeleton are essentially preserved throughout the series of metalloderivatives of TPP, ^{25,34,35} TFPP, and TFPPX₈ (X=Cl, Br). ^{10,36} Bond lengths and angles in the porphyrin skeleton are very similar for all three TFPPCl₈ species, indicating that metallation does not greatly affect porphyrin bond lengths.

The Ru-C bond is slightly longer in RuTFPPCl₈(CO)H₂O (Table 2.2) than in RuOEP(CO)H₂O (1.785)²⁶ or RuTPP(CO)EtOH (1.77 Å),³⁷ consistent with the relatively high value of v_{CO}.²² The Ru-C-O bond is nearly linear in the three porphyrins, at 178.9, 178.5, and 175.8°, respectively. The Ru-O bond length (2.172 Å) is shorter for the perhalogenated porphyrin than for RuOEP(CO)H₂O (2.253 Å), and closer to the distance found for *trans*-RuCl₂(PEt₃)₂(CO)H₂O (2.189 Å).^{26,27} Interestingly, although the Ru-N bond lengths in RuTFPPCl₈(CO)H₂O and RuTPP(CO)EtOH are the same (~2.05 Å), the TPP derivative is planar, whereas the metal in the halogenated derivative is 0.11 Å out of the mean plane towards the carbonyl ligand. The distorted structure decreases the core size, and may explain why ruthenium insertion is so difficult for TFPPCl₈ and has almost no yield for TFPPBr₈.

NMR Spectra

Fluorine-19 NMR has been extremely helpful in ascertaining both the identity and purity of halogenated compounds. The 100% natural abundance of spin 1/2 19 F and its high gyromagnetic ratio allow 19 F NMR spectra to be obtained readily. As observed in 1 H NMR of tetraphenylporphyrins, the corresponding fluorine atoms from all four phenyl rings appear equivalent in 19 F NMR. The four phenyl rings on the porphyrin are related in the high degree of symmetry of the approximate D_{4h} or D_{2d} point groups of these

compounds. The chemical shifts of the fluorine atoms on the meso-phenyl rings are extremely sensitive to the metal center, its axial ligands, and the pyrrole carbon substituents, however, such that each porphyrin has a unique spectrum. Correlations in ¹⁹F shifts and splitting patterns may be related to various TFPP structures.

The 19 F NMR for the unmetallated and zinc TFPP and TFPPCl₈ complexes (Figure 2.8; Table 2.5) display one set of signals each for the ortho, meta, and para fluorines. The para signal, identified by its intensity of $^{1/2}$ relative to the ortho and meta signals, is most sensitive to metallation, and shifts 1.7 ppm upfield from 19 FPPCl₈ to 19 FPPCl₈. The signal appears as a triplet due to coupling to the meta-Fs (3 J_{F-F} = -21 Hz). The ortho signal, farthest downfield, is split into a doublet of doublets, and the meta is a triplet of doublets. The additional splitting is attributed to coupling of fluorines positioned para to one another, as only the para signal does not show any additional structure, with 5 J_{F-F} = 6.7 Hz. Computer simulation of the observed spectrum with only these parameters was not satisfactory. Additional coupling between meta fluorines of 4 J \approx -2 Hz was needed to increase linewidth and generate the proper intensities in the model spectrum. The signs of the coupling constants are consistent with literature values, as are the magnitudes of the various Js (ortho > para > meta).

Substitution with a paramagnetic or an axially unsymmetric metal center results in significantly different NMR spectra. As with proton NMR, fluorine resonances of the paramagnetic species exhibit a large isotropic shift from those of the diamagnetic derivatives. High spin five-coordinate Fe^{III}TFPP(Cl) (Figure 2.9) or Fe^{III}TFPP(OH) samples, identified by their characteristic UV-Vis and EPR spectra, ⁴⁰ show *five* separate ¹⁹F NMR signals that fall over a much larger window than those of the diamagnetic porphyrins. The ortho and ortho' (and meta and meta') fluorines, no longer related by an S₄ axis, now have chemical shifts separated by several ppm, and previously observed fine structure is lost due to paramagnetic line broadening. The resonances do not coalesce at temperatures up to 298 K, indicating that rotation of the phenyl rings is slow on the NMR

time scale at room temperature. A Curie plot (Figure 2.10) shows a linear relationship between the isotropic shift and inverse temperature. The isotropic shift is the sum of a contact shift (dependent on 1/T) and a dipolar shift (dependent on 1/T²)⁴¹; the linear dependence on 1/T suggests that the dipolar contribution is small. However, the lines do not intersect the origin, which may indicate some dipolar contribution is present.⁴²

The axial ligand is known to affect the 1H NMR shifts of paramagnetic Fe^{III} porphyrins. In general terms, the porphyrin and the axial ligand compete for bonding interactions with the metal, and the strength of these interactions affects the ring current and π electron density on the protons and therefore their chemical shift. 43 A substantial downfield shift of all five resonances (Table 5) is observed upon substitution of an ^{-}OH for a Cl- ligand on FeTFPP, consistent with axial ligand effects observed with p-CH₃-TPPMnX complexes. Increased π bonding between the metal and the stronger field axial ligand reduces π electron density in the porphyrin, resulting in smaller contact shifts in the ^{1}H NMR spectrum. 44 Although the direction of the shift is similar in the fluorine spectrum, the different magnitudes for the contact shift at the ortho and para positions relative to the meta are not observed. Therefore, contact shift alone is not sufficient to explain the ^{19}F NMR spectrum. This is consistent with theory that expects a large temperature independent paramagnetic contribution to fluorine chemical shifts (relative to proton). Further study involving additional compounds would be needed to fully explore this effect.

The five-coordinate (FeTFPP)₂O dimer also shows 5 peaks in its NMR spectrum (Figure 2.11); however, the signals show significantly less broadening and appear in a much narrower window than the other Fe^{III} porphyrins. Strong antiferromagnetic coupling between the two metal centers⁴⁰ reduces the paramagnetic shift in the ¹⁹F NMR of the μ -oxo dimer. Similarly, the resonance for the β -hydrogens in the ¹H NMR spectrum is shifted less in the dimer relative to the monomeric iron(III) complexes. The pyrrole protons of (FeTFPP)₂O and (FeTPP)₂O⁴² show similar isotropic shifts of 5.1 and 5.02 ppm,

respectively, from the diamagnetic Zn complexes, whereas the pyrrole protons are shifted over 70 ppm downfield in the spectrum of Fe(TFPP)Cl.

The distinctive patterns observed in ¹⁹F NMR play important roles in the structural assignment of other perhalogenated compounds. The ¹⁹F NMR spectrum of Fe^{III}TFPPBr₈(Cl) (Figure 2.12) shows a broadened five-signal pattern similar to that of Fe^{III}TFPP(Cl). The ortho fluorine resonances exhibit a smaller paramagnetic shift in the perhalogenated compound, consistent with the mixed spin character of the Fe^{III}TFPPBrg(Cl) ground state.²⁰ The addition of pyridine to Fe^{III}TFPPBrg(Cl) results in reduction of the iron and formation of the symmetric bis-pyridine compound, Fe^{II}TFPPBr₈(py)₂. The assignment of this compound was confirmed as low-spin iron(II) due to the sharp signals and splitting pattern consistent with an axially symmetric. diamagnetic species. Most unusual is the NMR of [Fe^{II}TFPPBrg(Cl)], produced by electrochemical reduction of Fe^{III}TFPPBr₈(Cl) (Figure 2.13a). The relatively sharp signals support the reduction of the metal center, but the splitting of the ortho and meta signals suggests an axially unsymmetric porphyrin; the Fe(II) porphyrin appears to retain an association with the chloride ligand even in the reduced state. 19 Chemical reduction in methanol with ascorbic acid, however, gives a very different spectrum. Only three resonances appear instead of five, indicating a symmetric porphyrin, most likely the bismethanol derivative [Fe^{II}TFPPBr₈(OMe)₂].

NMR also revealed interesting properties of RuTFPPCl₈(CO)H₂O.²⁴ Although an X-ray structure for this compound was obtained, ¹⁹F NMR on crystalline material fails to yield a simple spectrum. Instead, several 5-signal patterns are observed, suggesting that the strong trans effect of the carbonyl ligand results in lability of the sixth ligand. The unsymmetric trans coordination around the Ru again leads to dual ortho and meta signals (as in FeTFPP(Cl)), but with the diamagnetic metal center, the fine structure is retained. Upon photolysis in pyridine, a single species, RuTFPPCl₈(py)₂, is obtained. The simple pattern now seen in the ¹⁹F NMR shows that previous overlapping signals were due to

multiple species with varying ligands trans to the CO rather than to partial decomposition or dehalogenation of the porphyrin macrocycle.

Conclusions

A series of tetrakis(pentafluorophenyl)- and β -octahalo-tetrakis(pentafluorophenyl)porphyrins have been synthesized. TFPP derivatives have been studied to provide a
comparison for understanding the spectroscopy and catalytic properties of the
perhalogenated iron and ruthenium complexes (Chapters 3 - 6).

Crystal structures of unmetallated, zinc, and ruthenium octachlorotetrakis(pentafluorophenyl) porphyrins are consistent with other structures that demonstrate that halogenation of the β-pyrrole carbons causes a severe saddling of the porphyrin macrocycle. The free base porphyrin, however, does not show the twisting distortion seen in the metallated octahalo derivatives, suggesting that the metal plays a significant role in determining the type and degree of distortion.

The distortions and metal effects observed in the structures of the halogenated metalloporphyrins are analogous to those reported for the octamethyl and octaethyl derivatives of TPP; 2,3,7,8,12,13,17,18- β -octaalkyl-5,10,15,20-tetraphenylporphyrin (TPPX₈, X = methyl, and ethyl).^{32,45} ZnTPPMe₈ and ZnTPPEt₈ are essentially the steric analogs of ZnTFPPCl₈ and ZnTFPPBr₈, respectively. The implication is that the observed distortion is a result of the steric interactions involving the β -halo substituents, and is not electronic in origin.

Fluorine-19 NMR has been shown to be a useful tool for characterization of perhalogenated porphyrin compounds. The identification of various FeTFPPX species will allow another mechanism to study catalysis reactions, for example, by monitoring deactivation of the catalyst via formation of a μ -oxo dimer. Trends in linewidths, shift dispersions, and multiplicities all provide information on the oxidation state and coordination sphere of the metal center. As a supplement to crystallographic data, NMR

allows a more direct examination of the behavior of these highly halogenated porphyrins in solution.

Experimental

Materials Omnisolv grade methanol, acetone, dichloromethane, benzene, pyridine, dimethylformamide, and hexane were purchased from EM Science. N-chloro- and N-bromosuccinimide, glacial acetic acid, iron(II) chloride, triruthenium dodecacarbonyl, and tetraphenylporphyrinato ruthenium(II) carbonyl were purchased from Aldrich and used as received. ZnTFPP and H₂TFPP were purchased from Porphyrin Products and used as received. UV-Vis (CH₂Cl₂): ZnTFPP λ_{max} nm (ε 10⁵ M⁻¹ cm⁻¹); 414 (5.0), 544 (0.24); H₂TFPP λ_{max} nm 412, 506, 584. Fe^{III}TFPPCl was purchased from Aldrich and purified by chromotography on alumina before use. UV-Vis (acetone): λ_{max} nm (ε 10⁵ M⁻¹ cm⁻¹) 350 (0.7), 410 (1.0), 50 (0.11), 629 (0.06). RuTPP(py)₂ was prepared by a literature method.⁴⁶

Methods UV-Vis spectra were recorded on a Hewlett Packard HP8452 diode array interfaced to an IBM or a Cary-14 spectrophotometer with an Olis 3820 conversion system. Infrared spectra were recorded as solutions in carbon tetrachloride or benzene on a Perkin-Elmer Model 1600 FT-IR spectrophotometer. Separation of the ruthenium porphyrins was accomplished with a Beckman Model 126 dual pump and 166 single channel detector on a Vydac C-18 reverse phase column. A 1000 W tungsten lamp was used for photolysis experiments. ¹H and ¹⁹F NMR spectra were recorded on a Brüker AM-500 (tuned down to 470.56 MHz for fluorine detection) instrument in CDCl₃ or deuterated acetone and referenced internally to C₆H₅F at -113.6 ppm (vs. CFCl₃ at 0 ppm). Porphyrin purification was accomplished with alumina (Fluka or Baker 40 μ alumina) or silica (Analtech 150 Å pore, 75-100 particle size silica) column chromatography. Further purification of the zinc and ruthenium perhalogenated porphyrins was accomplished with a Beckman Model HPLC system (126 dual pump and 166 single channel detector) on a

Vydac C-18 reverse phase column with isocratic acetone:water elution. Mass spectroscopy was performed at Caltech with a cesium ion fast atom bombardment spectrometer. Elemental analysis on the perhalogenated compounds was obtained, and varied greatly by compound. Results were not satisfactory, even on crystalline samples that were pure by other criteria.

Fe^{III}TFPP(OH) and (Fe^{III}TFPP)₂O: Fe^{III}TFPP(OH) and (Fe^{III}TFPP)₂O were synthesized from the chloride by published methods:⁴⁰ Fe^{III}TFPP(Cl) was dissolved in benzene, and a small amount of NaOH solution was added. After stirring for several hours, the water was removed using a separatory funnel, and the benzene solution was chromatographed on neutral alumina with a benzene/acetone solution. The μ-oxo elutes first, and the hydroxide elutes with a higher percent acetone. Fe^{III}TFPPP(OH): UV-Vis (acetone): λ_{max} 406, 563 nm. (Fe^{III}TFPP)₂O: UV-Vis; CH₂Cl₂; λ_{max} 398, 415(shoulder), 560 nm.

H2TFPPCl8: Chlorination of ZnTFPP was accomplished by a modification of earlier methods. ^{8,47,48} Approximately 500 mg ZnTFPP was dissolved in 50 mL dry methanol with forty equivalents of N-chlorosuccinimide, and the mixture refluxed for an hour. When chlorination of the pyrrole positions was complete, as determined by the red shift of the Soret band in the UV-Vis and thin layer chromatography on silica plates (1:1 hexane: dichloromethane) the solution was allowed to cool. The product was precipitated with water, filtered, and washed with cold hexane to remove decomposed porphyrin by-products. Further purification by HPLC was necessary to separate partially chlorinated species. Yield ZnTFPPCl₈ 60 to 80%. UV-Vis (CH₂Cl₂): λ_{max} nm (ε 10⁵ M⁻¹ cm⁻¹); 364, 440 (1.6), 572 (0.13). Mass spectrum m/z = 1314 (calc. 1313). The chlorinated zinc porphyrin was demetallated as previously by Lyons, et al.:⁴⁷ ZnTFPPCl₈ was redissolved in approximately 50 mL chloroform, and HCl gas was passed through a gas dispersion tube into the solution for 1-2 minutes. The volume of the reaction mixture was reduced, and the solution was chromatographed on alumina, eluting with 95% chloroform - 5%

methanol. The product, $H_2TFPPCl_8$, was collected and rotary evaporated to dryness, with a yield of approximately 95%. UV-Vis (CH₂Cl₂): λ_{max} nm (ϵ 10⁵ M⁻¹ cm⁻¹); 436 (16), 536 (1.3), 622 (0.46).

H₂TFPPBr₈: The bromo analog was similarly synthesized via bromination of ZnTFPP with N-bromosuccinimide. ZnTFPPBr₈: UV-Vis (CH₂Cl₂): λ_{max} nm (ε 10⁵ M⁻¹ cm⁻¹); 460 (1.9), 594 (0.17). The free ligand was obtained by demetallation with HCl gas, and the product chromatographed on alumina. UV-Vis (CH₂Cl₂): λ_{max} 454, 552, 636 nm.

FeTFPPBr₈(Cl) and [FeTFPPCl₈]: Iron was inserted into H₂TFPPX₈ with freshly prepared iron(II) acetate in glacial acetic acid, ¹⁷ or with Fe^{II}Cl₂ in DMF. ¹⁸ Insertion was evident by the red color of the solution. The iron porphyrin was precipitated with brine, dried, and washed with hexane to remove impurities. UV-Vis (CH₂Cl₂) Br₈: λ_{max} nm(ϵ 10⁵ M⁻¹ cm⁻¹) 402 (8.1), 442 (8.5), 560 (1.4). With H₂TFPPCl₈, reactions were conducted on a high vacuum line and precipitated with deoxygenated water. UV-Vis (CH₂Cl₂): λ_{max} 404, 582 nm. Addition of pyridine to a solution of FeTFPPX₈(Cl) led to formation of Fe^{II}TFPPX₈(py)₂. UV-Vis (CH₂Cl₂) Br₈: λ_{max} 450, 556, 588 nm; Cl: λ_{max} 438, 542, 574 nm.

RuTFPPCl₈(CO): The preparation of RuTFPPCl₈(CO) was based on the methods of Tsutsui⁴⁹ and Chow.⁵⁰ 300 mg H₂TFPPCl₈¹⁰ reacts with 300 mg Ru₃(CO)₁₂ (48 h, refluxing benzene) to form RuTFPPCl₈(CO). RuTFPPCl₇(CO) and RuTFPPCl₆(CO) also were isolated from the reaction mixture. RuTFPPCl_n(CO) (n = 6,7,8) complexes were separated from unreacted free ligand by column chromatography on silica gel eluting with hexane and increasing percentages of methylene chloride. The partially chlorinated isomers were purified by HPLC, and the identity of each fraction was confirmed by mass spectroscopy. The parent peak in each mass spectrum appears at the mass for RuTFPPCl_n (n = 6,7,8), with a smaller peak appearing at the mass for the monocarbonyl complex. Parent peaks appeared at m/z = 1351.2 (RuTFPPCl₉), 1315.8

(RuTFPPCl₇), and 1280.1 (RuTFPPCl₆). UV-Vis (CH₂Cl₂): λ_{max} nm (ϵ 10⁵ M⁻¹ cm⁻¹) 416 (1.7), 542 (0.14). RuTFPPBr₈(CO) (mass spectrum; m/z =1703) was synthesized from Ru₃(CO)₁₂ and H₂TFPPBr₈ (50 h refluxing benzene). UV-Vis (CH₂Cl₂): λ_{max} 424, 560 nm.

RuTFPPCl₈(py)₂: Photolysis of the carbonyl was accomplished by modification of Chow's methods.⁵⁰ Pyridine solutions of RuTFPPCl_n(CO) exposed to a 1000W mercury lamp for several hours lose a carbonyl ligand to form RuTFPPCl_n(py)₂. Loss of the carbonyl was confirmed by the disappearance of the CO stretch (IR, CCl₄ solution) and by ¹⁹F-NMR spectroscopy (CDCl₃ solution): d (RuTFPPCl₈(py)₂) = -138.7 (2F, q, ortho); -152.3 (1F, t, para); -163.2 ppm (2F, m, meta). UV-Vis (CH₂Cl₂): λ_{max} 415, 510, 536 nm. ¹⁹F-NMR: -138.7 (2F, q, ortho), -152.3 (1F, t, para), -163.2 ppm (2F, m, meta).

Crystal Structure Analysis: Since the halogenated porphyrin crystals lost solvent easily, a single crystal was removed directly from the crystallization solution and mounted in a capillary with silicon grease. Data were collected on an Enraf-Nonius CAD-4 diffractometer using Mo Ka radiation. Atomic scattering factors and values for f' were taken from Cromer and Waber⁵¹ and Cromer,⁵² and CRYM,⁵³ MULTAN,⁵⁴ and ORTEP⁵⁵ computer programs were used for calculations. The weights were taken as $1/\sigma^2(F_0^2)$; variances ($\sigma^2(F_0^2)$) were derived from counting statistics plus an additional term, $(0.014I)^2$; variances of the merged data were obtained by propagation of error plus another additional term, $(0.014\bar{I})^2$.

Purple crystals of ZnTFPPCl₈ were grown from a saturated solution of odichlorobenzene at 0 °C. Crystals of this compound lost solvent quickly, so one was covered with epoxy glue before being cooled to -44 °C on the diffractometer. The zinc crystal was found to be tetragonal, belonging to space group P \(\frac{1}{4}\)21c. The structure was solved by location of the zinc atom from a Patterson map. Structure factors and Fourier calculations showed Cl1 and Cl2, and subsequent structure factor Fourier calculations gave the rest of the porphyrin. Solvent molecules were found in difference Fourier maps

calculated in their planes. The solvent molecules occupy two separate regions in the cell, each region holding one dichlorobenzene molecule. The molecules are disordered in these regions, and were initially modeled with idealized C₆H₄Cl₂ groups. Eventually, some of the chlorine atoms of the solvent were refined, as well as the population parameters for alternate orientations, but the carbon atoms were always positioned based on Fourier maps. For one region (C31-36 and C41-46) anisotropic displacement parameters were assigned by hand based on the maps and the refined parameters of the Cl atoms of the solvent; the other carbon atoms of the solvent were left isotropic. The disordered solvent regions are the cause, in all probability, of the somewhat larger than usual values for R and goodness of fit.

Brown crystals of H_2 TFPPCl₈ were grown by slow evaporation from an acetone/water solution. The crystals were found to be triclinic, belonging to space group $P\bar{1}$. Porphyrin molecules were located from a Patterson map, and the two inner hydrogen atoms were located in a difference map as disordered among the four nitrogen atoms. Their positional parameters were refined, with B values fixed at 1.2 times the isotropic equivalent U_{ij} value of the bonded nitrogen atoms and the population factors assigned at one-half.

Deep red crystals of RuTFPPCl₈(CO)(H₂O) were grown by slow evaporation from an ethyl acetate/hexane solution. Ruthenium atom coordinates were obtained from a Patterson map, and the remaining atoms located with structure factor-Fourier calculations. Hydrogen atoms on the solvent molecules were positioned by calculation in idealized locations with staggered geometry and a C-H bond length of 0.95 Å. Of the solvent molecules, only one ethyl acetate site is fully populated (C71,C72, O2, O3, C73, and C74). The second (C81, C82, O4, O5, C83, and C84) is half-populated, near a center of symmetry. The region occupied by hexane is not easily interpreted. There are five peaks in a difference map in an area of broadly diffuse electron density. These five were co-planar within 0.15 Å, so we fitted idealized hexane molecules to the difference density in this plane. Our model has three orientations of the hexane; there may be twice that many. We

kept the positional and thermal parameters of these idealized molecules fixed but refined their population parameters independently. The sum of the three was 0.84; we believe this represents some loss of hexane from the crystal during data collection. We kept the populations fixed in the final refinement. The final difference map has peaks of 0.88, 0.82 and 0.79 Å-3 and valleys of -1.24 and -0.84 Å-3 in this region.

Appendix 2 contains unit cell diagrams, final heavy atom parameters, anisotropic displacement parameters, complete distances and angles, and structure factors for $H_2TFPPCl_8$, $ZnTFPPCl_8$, and $RuTFPPCl_8$ (CO) H_2O , H atom parameters for $H_2TFPPCl_8$, and intermolecular distances less than 3.5 Å for $ZnTFPPCl_8$ and $RuTFPPCl_8$ (CO) H_2O .

References and Notes

- (1) Lindsey, J. S.; Wagner, R. W. J. Org. Chem. 1989, 54, 828-836.
- (2) Bray, B. L.; Mathies, P. H.; Naef, R.; Solas, D. R.; Tidwell, T. T.; Artis, D. R.; Muchowski, J. M. J. Org. Chem. 1990, 55, 6317-6328.
- (3) Qui, Z.-M.; Burton, D. J. Tetrahedron Lett. 1994, 35, 4319-4322.
- (4) Traylor, T. G.; Tsuchiya, S. Inorg. Chem. 1987, 26, 1338-1339.
- (5) Wijesekera, T.; Matsumoto, A.; Dolphin, D.; Lexa, D. Angew. Chem., Int. Ed. Eng. 1990, 29, 1028-1030.
- (6) Bartoli, J. F.; Brigaud, O.; Battioni, P.; Mansuy, D. J. Chem. Soc., Chem. Commun. 1991, 440-442.
- (7) Mandon, D.; Ochsenbein, P.; Fischer, J.; Weiss, R.; Jayaraj, K.; Austin, R. N.; Gold, A.; White, P. S.; Brigaud, O.; Battioni, P.; Mansuy, D. Inorg. Chem. 1992, 31, 2044-2049.
- (8) Hoffmann, P.; Robert, A.; Meunier, B. Bull. Chem. Soc. Fr. 1992, 129, 85-97.
- (9) D'Souza, F.; Villard, A.; Caemelbecke, E. V.; Franzen, M.; Boschi, T.; Tagliatesta, P.; Kadish, K. M. *Inorg. Chem.* 1993, 32, 4042-4048.
- (10) Birnbaum, E. R.; Hodge, J. A.; Grinstaff, M. G.; Schaefer, W. P.; Marsh, R. E.; Henling, L. M.; Labinger, J. A.; Bercaw, J. E.; Gray, H. B. *Inorg. Chem.* in press.
- (11) d'A. Rocha Gonsalves, A. M.; Johnstone, R. A. W.; Pereira, M. M.; Shaw, J.; Sobral, D. N.; Abilio, J. F. *Tetrahedron Lett.* 1991, 32, 1355-1358.
- (12) Banfi, S.; Mandelli, R.; Montanari, F.; Quici, S. Gazz. Chim. Ital. 1993, 123, 409-415.
- (13) Ochsenbein, P.; Ayougou, K.; Mondon, D.; Fischer, J.; Weiss, R.; Austin, R. N.; Jayaraj, K.; Gold, A.; Terner, J.; Fajer, J. Angew. Chem., Int. Ed. Eng. 1994, 33, 348-350.
- (14) Bartoli, J. F.; Battioni, P.; Foor, W. R. D.; Mansuy, D. J. Chem. Soc., Chem. Commun. 1994, 23-24.
- (15) Tables of Interatomic Distances and Configurations in Molecules and Ions; Sutton,
 L. E., Ed.; The Chemical Society: London, 1965; Vol. Special Publication 18.
- (16) Allred, A. L. J. Inorg. Nucl. Chem. 1961, 17, 215-221.
- (17) Warburg, O.; Negelein, E. Z. Biochem 1932, 14-32.
- (18) Adler, A. D.; Longo, F. R.; Kampas, F.; Kim, J. J. Inorg. Nucl. Chem. 1970, 32, 2443-2445.

- (19) Grinstaff, M. W.; Hill, M. G.; Labinger, J. A.; Gray, H. B. Science 1994, 264, 1311-1313.
- (20) Grinstaff, M. W.; Hill, M. G.; Birnbaum, E. R.; Schaefer, W. P.; Labinger, J. A.; Gray, H. B. *Inorg. Chem.* in press.
- (21) The axial ligand trans to the carbonyl ligand in ruthenium porphyrins is usually assumed to be solvent, and is not specifically mentioned. Unless otherwise indicated, the oxidation state of ruthenium is 2+.
- (22) For reference, the CO stretch in the IR spectrum of RuTPP(CO) is at 1945 cm⁻¹: Chow, B. C.; Cohen, I. A. *Bioinorg. Chem.* 1971, 1, 57. Since the probable trans ligands (water, ethanol, acetone) are all O-atom donors, we would not expect any splitting of v_{CO}.
- (23) Buchler, J. W.; Kokisch, W.; Smith, P. D. Struct. Bonding 1978, 34, 79-134.
- (24) Birnbaum, E. R.; Schaefer, W. P.; Labinger, J. A.; Bercaw, J. E.; Gray, H. B. *Inorg. Chem.* 1995, 34, 1751-1755.
- (25) Scheidt, W. R.; Kastner, M. E.; Hatano, K. Inorg. Chem. 1978, 17, 706-710.
- (26) Kadish, K. M.; Hu, Y.; Mu, X. H. J. Heterocycl. Chem. 1991, 28, 1821-1824.
- (27) Sun, Y.; Taylor, N. J.; Carty, A. J. Inorg. Chem. 1993, 32, 4457-4459.
- (28) Henling, L. M.; Schaefer, W. P.; Hodge, J. A.; Hughes, M. E.; Gray, H. B.; Lyons, J. E.; Ellis, P. E., Jr. Acta Crystallogr. 1993, C49, 1745-1747.
- (29) Schaefer, W. P.; Hodge, J. A.; Hughes, M. E.; Gray, H. B.; Lyons, J. E.; Ellis, P. E., Jr.; Wagner, R. W. Acta Crystallogr. 1993, C49, 1342-1345.
- (30) Marsh, R. E.; Schaefer, W. P.; Hodge, J. A.; Hughes, M. E.; Gray, H. B.; Lyons, J. E.; Ellis, P. E., Jr. Acta Crystallogr. 1993, C49, 1339-1342.
- (31) Bhyrappa, P.; Krishnan, V. Inorg. Chem. 1991, 30, 239-245.
- (32) Barkigia, K. M.; Berber, M. D.; Fajer, J.; Medforth, C. J.; Renner, M. W.; Smith, K. M. J. Am. Chem. Soc. 1990, 112, 8851-8857.
- (33) Scheidt, W. R.; Lee, Y. J. In *Metal Complexes with Tetrapyrrole Ligands I*; J. W. Buchler, Ed.; Springer-Verlag: New York, 1987; Vol. 64; pp 2-70.
- (34) Hoard, J. L. Ann. N.Y. Acad. Sci. 1973, 206, 18-31.
- (35) Fleischer, E. B.; Miller, C. K.; Webb, L. E. J. Am. Chem. Soc. 1964, 86, 2342-2347.
- (36) Hodge, J. A. Thesis, California Institute of Technology, 1995.
- (37) Bonnet, J. J.; Eaton, S. S.; Eaton, G. R.; Holm, R. H.; Ibers, J. A. J. Am. Chem. Soc. 1973, 95, 2141-2149.
- (38) Harris, R. K. Nuclear Magnetic Resonance Spectroscopy; Pitman Publishing, Inc.: Marshfield, MA, 1983.

- (39) Bovey, F. A.; Jelinski, L. *Nuclear Magnetic Resonance Spectroscopy*; 2nd ed.; Academic Press, Inc. San Diego, CA, 1988, pp 437-488.
- (40) Jayaraj, K.; Gold, A.; Toney, G. E.; Helms, J. H.; Hatfield, W. E. *Inorg. Chem.* 1986, 25, 3516-3518.
- (41) La Mar, G. N.; Eaton, G. R.; Holm, R. H.; Walker, F. A. J. Am. Chem. Soc. 1971, 95, 63-75.
- (42) La Mar, G. N.; Walker, F. A. J. Am. Chem. Soc. 1973, 95, 1782-1790.
- (43) Caughey, W. S.; Johson, L. F. J. Chem. Soc., Chem. Commun. 1969, 1362-1363.
- (44) La Mar, G. N.; Walker, F. A. J. Am. Chem. Soc. 1975, 97, 5013-5106.
- (45) Sparks, L. D.; Medforth, C. J.; Park, M.-S.; Chamberlain, J. R.; Ondrias, M. R.; Senge, M. O.; Smith, K. M.; Shelnutt, J. A. J. Am. Chem. Soc. 1993, 115, 581-592.
- (46) Brown, G. M.; Hopf, F. R.; Ferguson, J. A.; Meyer, T. J.; Whitten, D. G. J. Am. Chem. Soc. 1973, 95, 5939-5942.
- (47) Lyons, J. E.; Ellis, P. E., Jr.; Myers, H. K., Jr.; Wagner, R. W. J. Catal. 1993, 141, 311-315.
- (48) Ellis, P. E., Jr.; Lyons, J. E. Coord. Chem. Rev. 1990, 105, 181-193.
- (49) Tsutsui, M.; Ostfeld, D.; Hoffman, L. M. J. Am. Chem. Soc. 1971, 93, 1820-1823.
- (50) Chow, B. C.; Cohen, I. A. Bioinorg. Chem. 1971, 1, 57-63.
- (51) Cromer, D. T.; Waber, J. T. *International Tables For X-ray Crystallography*; Kynoch Press: Birmingham, 1974; Vol. IV, pp 99-101.
- (52) Cromer, D. T. *International Tables For X-ray Crystallography*; Kluwer Academic Publishers: Dordrecht, 1974; Vol. IV, pp 149-151.
- (53) Duchamp, D. J. In Am. Crystallogr. Assoc. Meet., Paper B14: Bozeman, Montana, 1964; pp 29-30.
- (54) Debaerdemaeker, T.; Germain, G.; Main, P.; Refaat, L. S.; Tate, C.; Woolfson, M. M. MULTAN 88. Computer Programs for the Automatic Solution of Crystal Structures from X-ray Diffraction Data, University of York, England and Louvain, Belgium, 1988.
- (55) Johnson, C. K. *ORTEPII*, Report ORNL-3794: Oak Ridge National Laboratory, Oak Ridge, Tennessee, 1976.

Figure 2.1 -- The general structure of third generation pentafluorophenyl metalloporphyrins discussed in this chapter. The α , β , and meso carbons are marked.

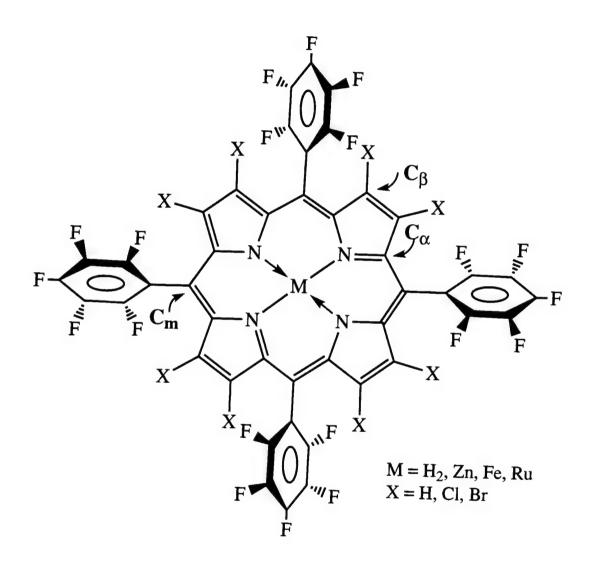


Figure 2.2 -- HPLC trace showing separation of partially halogenated ruthenium porphyrins on a reverse phase C_{18} column with isocratic elution of 88% ethanol in water. Excess free ligand comes off the column earliest, followed by ruthenium porphyrins bearing increasing numbers of β -chlorines. Zinc porphyrin is likely produced from metallation of the free ligand in the stainless steel HPLC tubing.

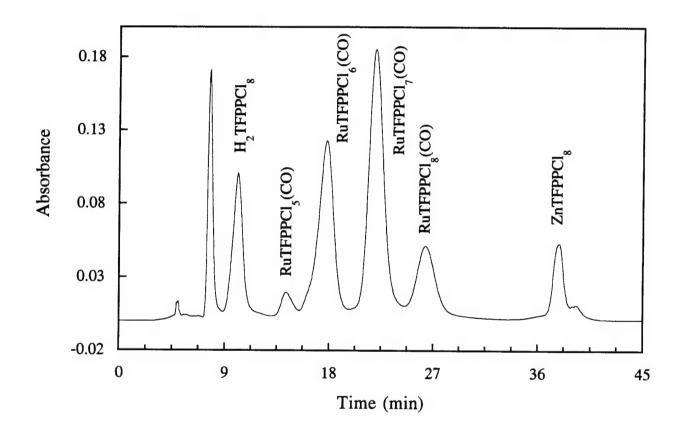


Figure 2.3 -- ORTEP diagram of H₂TFPPCl₈ with 50% probability ellipsoids of the molecule showing the numbering used. Only two hydrogen atom sites are shown.

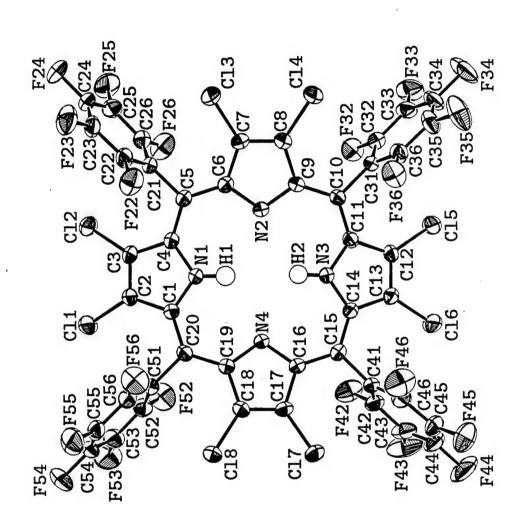


Figure 2.4 -- ORTEP diagram of ZnTFPPCl₈ with 50% probability ellipsoids of the molecule showing the numbering system used.

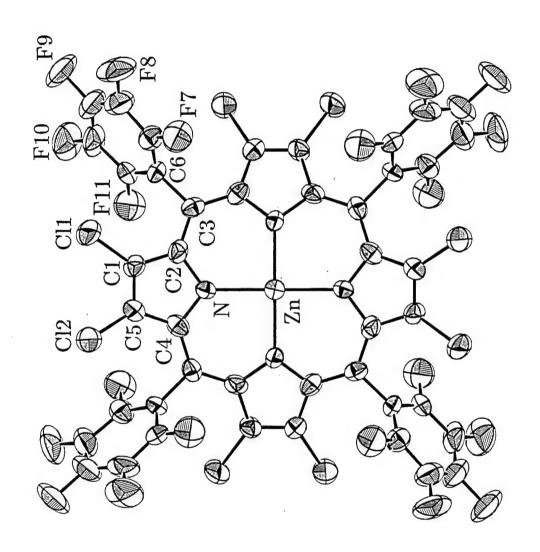


Figure 2.5 -- ORTEP diagram of RuTFPPCl₈(CO)H₂O with 50% probability ellipsoids showing the numbering system used. Atoms C21, C31, C41, and C51 (not numbered) are bonded to C3, C8, C13, and C18, respectively; carbon atoms in the pentafluorophenyl groups have the same numbers as the attached fluorine atoms.

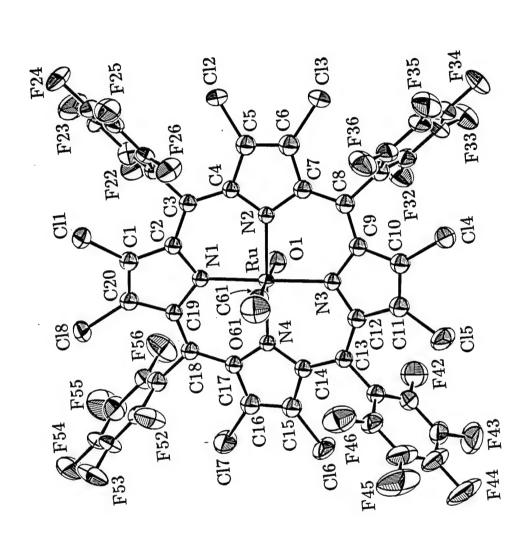


Figure 2.6 -- Molecular representations of the series H_2TFPP , $H_2TFPPCl_8$, and $H_2TFPPBr_8$ using the actual crystal structure coordinates. From the planar H_2TFPP , the saddle distortion clearly increases upon further halogenation.

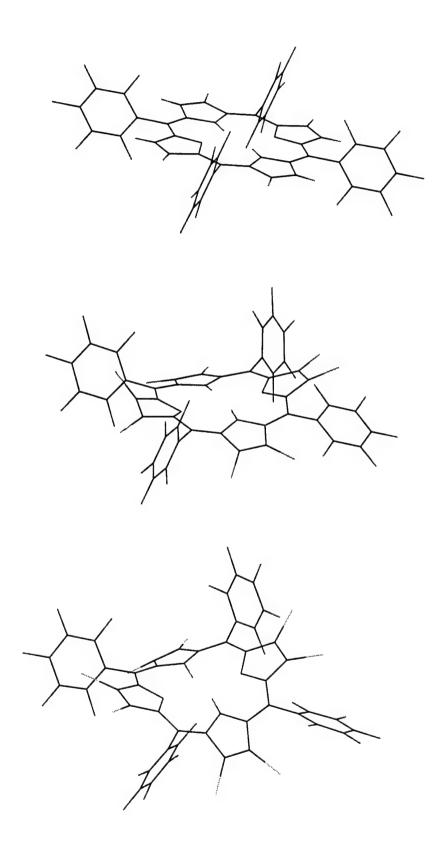


Figure 2.7 -- Edge-on view of a Chem 3D drawing of RuTFPPCl₈(CO)H₂O using crystal structure coordinates. The ruffle in the porphyrin macrocycle is apparent in the different displacements of the chlorine atoms (striped) from the mean porphyrin plane.

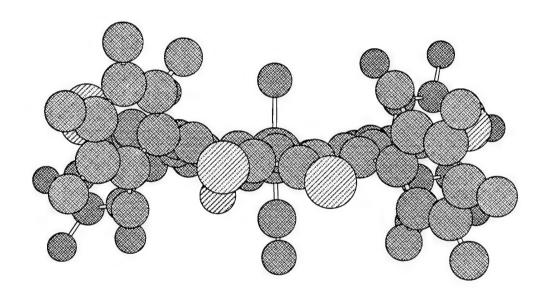


Figure 2.8 -- ¹⁹F-NMR spectra of a) H₂TFPPCl₈ and b) ZnTFPPCl₈ in CDCl₃. The signals are assigned ortho, para, meta, from left to right. The signals for the free ligand have been enlarged to show the fine structure observed in the spectra of free ligand, zinc, and other diamagnetic metal porphyrins.

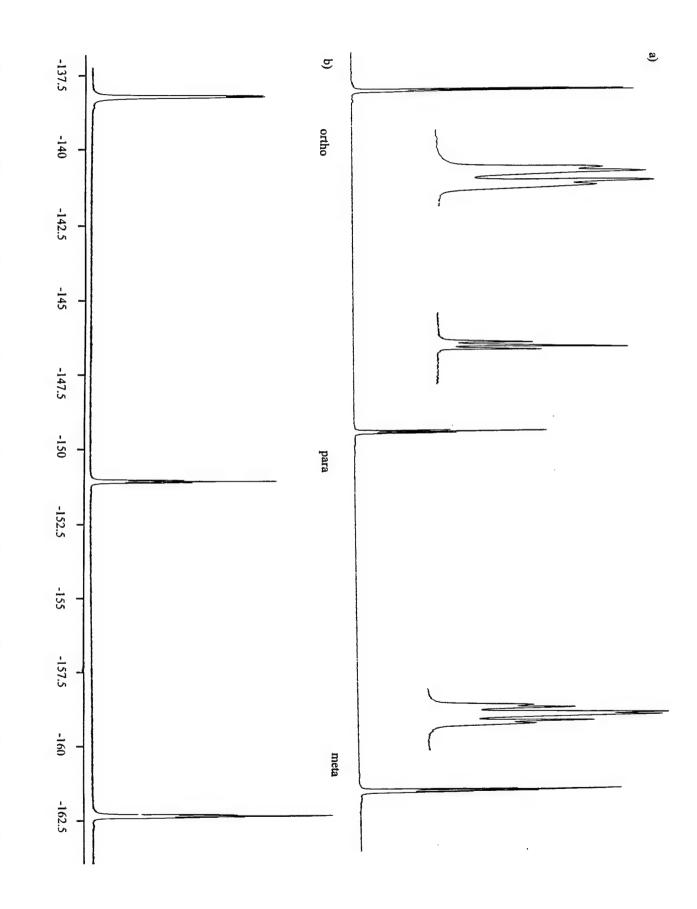


Figure 2.9 -- ¹⁹F-NMR spectrum of Fe^{III}TFPP(Cl). The ortho resonances are shifted over 20 ppm downfield from those of H₂TFPP.

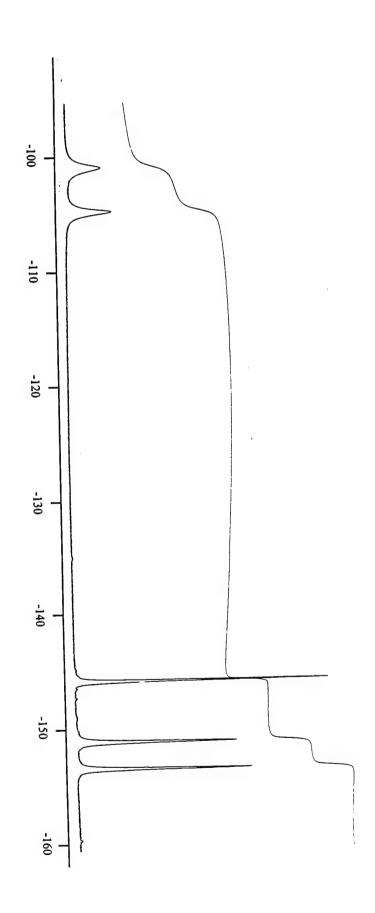


Figure 2.10 -- Curie plot showing the temperature dependence of the chemical shift of $Fe^{III}TFPP(Cl)$ resonances. The isotropic shift is calculated relative to the diamagnetic $Zn^{II}TFPP$ complex.

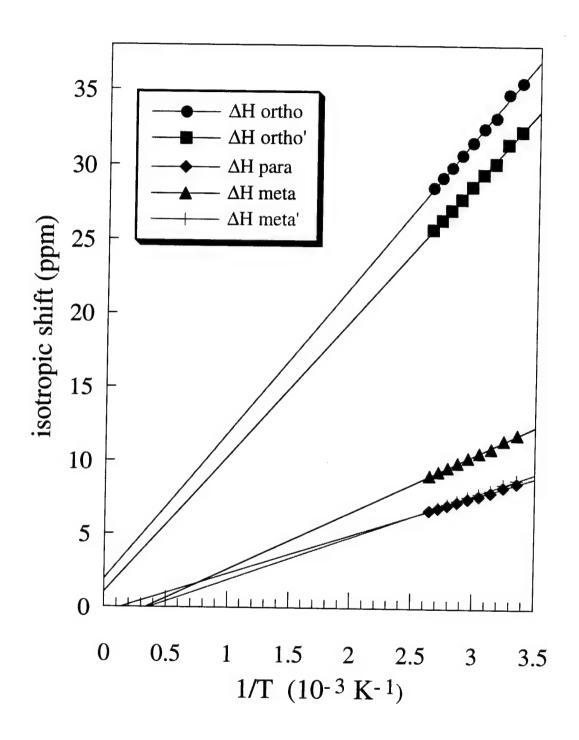


Figure 2.11 -- 19 F-NMR spectrum of (Fe^{III}TFPP)₂O in acetone- d_6 . The window is much smaller than that of the paramagnetic FeTFPP(Cl) monomer due to antiferromagnetic coupling between the two iron atoms.

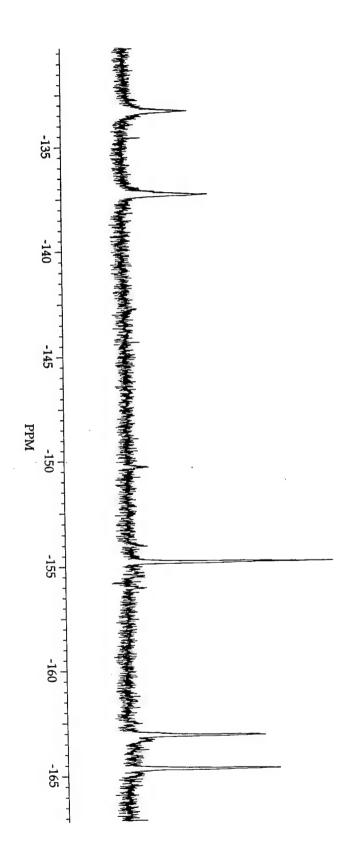


Figure 2.12 -- 19 F-NMR spectrum of Fe^{III}TFPPBr₈Cl in acetone- d_6 . The paramagnetic shift is less than in the partially halogenated FeTFPP(Cl).

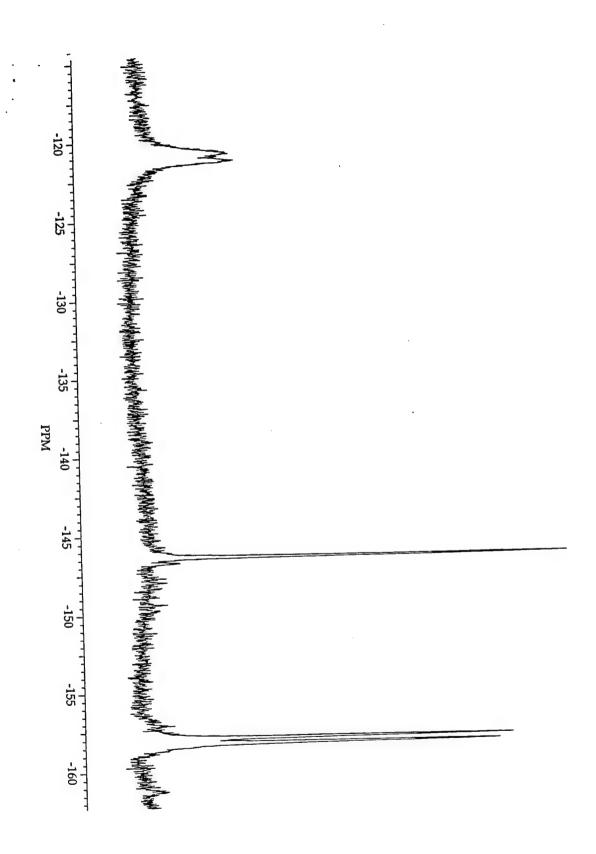


Figure 2.13 -- ¹⁹F-NMR spectra of electrochemically (bottom) and chemically (top) generated [Fe^{II}TFPPBr₈]. The five line pattern in the electrochemically generated spectrum indicates an axially unsymmetric species, [Fe^{II}(TFPPBr₈)Cl]⁻, while the lack of splitting in the ortho and meta resonances in the top spectrum is suggestive of a symmetric coordination sphere, i.e. Fe^{II}(TFPPBr₈)(OMe)₂. The five spikes in the bottom spectrum are instrument noise.

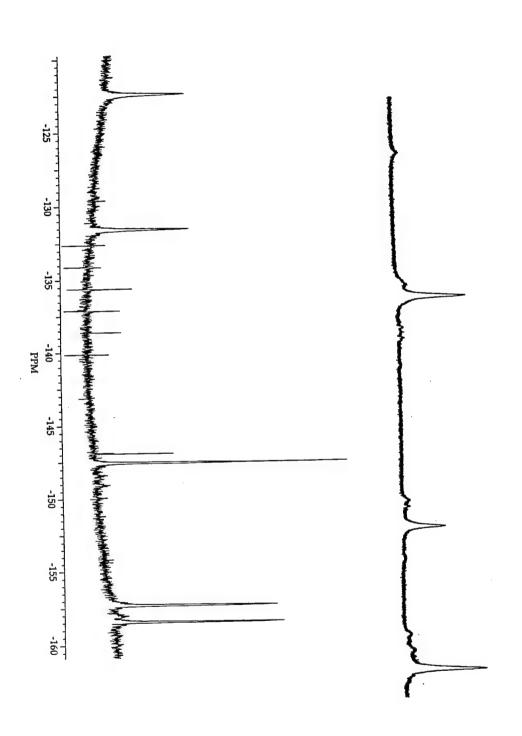


Table 2.1. X-ray Experimental Parameters.

| | H ₂ TFPPCl ₈ | ZnTFPPCl ₈ | RuTFPPCl ₈ (CO)H ₂ O | |
|-------------------------------------|---|---|---|--|
| formula | C ₄₄ H ₂ Cl ₈ F ₂₀ N ₄ | C ₄₄ Cl ₈ F ₂₀ N ₄ Zn | C ₅₇ H ₂₈ Cl ₈ F ₂₀ N ₄ O ₅ | |
| | | \cdot 6(C ₆ H ₄ Cl ₂) | Ru | |
| molecular weight | 1250.12 | 2139.48 | 1613.53 | |
| color | brown | dull red | dark red | |
| shape | plate | thick needles | rectangular tablet | |
| crystal system | triclinic | tetragonal | monoclinic | |
| space group | ΡĪ | P 421c | P2 ₁ /c | |
| a, A | 11.066(1) | 19.502(20) | 14.364(3) | |
| b, Å | 14.641(3) | | 16.012(4) | |
| c, À | 14.678(2) | 10.916(8) | 26.679(8) | |
| a, ° | 88.97(1) | | | |
| β, ° | 76.05(1) | | 90.29(2) | |
| γ, ° | 71.29(1) | | | |
| V, Å ³ | 2181.4(6) | 4152(6) | 6136(3) | |
| Z | 2 | 2 | 4 | |
| D _x , g cm ⁻³ | 1.90 | 1.71 | 1.75 | |
| radiation | | ΜοΚα | | |
| μ, cm ⁻¹ | 6.4 10.41 | | 7.11 | |
| temperature, K | 293 | 229 | 295 | |
| crystal size, mm | 0.11 X 0.35 X | 0.19 X 0.19 X | 0.16 x 0.29 x 0.44 | |
| | 0.42 | 0.59 | | |
| diffractometer | Enraf-Nonius Cad-4 | | | |
| collection method | omega scans | | | |
| h _{min/max} | ± 12 | 0/23 | -15/+15 | |
| k _{min/max} | ± 16 | 0/23 | -17/+17 | |
| l _{min/max} | ± 16 | ± 13 | 0/28 | |
| reflections measured | 12455 | 8027 | 16,813 | |
| indep. reflections | 6054 | 2050 | 8006 | |
| reflections used | 6054 | 2050 | 8005 | |
| R _{int} (F) | 0.019 | 0.033 | 0.043 | |
| R(F) | 0.042 | 0.0949 | | |
| $R_{W}(F^{2})$ | 0.0061 | 0.0286 0.028 | | |
| $(\Delta/\sigma)_{max}$ | 0.01 | 0.07 0.00 (for porphyrin | | |
| goodness of fit | 2.05 | 3.29 | 2.14 | |

Table 2.2. Selected Average Bond Lengths (Å).

| Bond | H ₂ TFPPCl ₈ | ZnTFPPCl ₈ | RuTFPPCl ₈ (CO)H ₂ O |
|---------------------------------|------------------------------------|-----------------------|--|
| N-C _α | 1.372 | 1.380 | 1.378 |
| C _α - C _β | 1.448 | 1.427 | 1.448 |
| C_{β} - C_{β} | 1.347 | 1.337 | 1.339 |
| C_{α} - C_{m} | 1.402 | 1.403 | 1.399 |
| N - M (or H) | 0.94 | 2.032 | 2.059 |
| N - Ct | 2.075 | 2.029 | not determined |
| Ru - C | | | 1.828 |
| Ru - O | _ | | 2.172 |

Table 2.3. Selected Average Angles (°).

| Angle | H ₂ TFPPCl ₈ | ZnTFPPCl ₈ | RuTFPPCl ₈ (CO)H ₂ O |
|---|------------------------------------|-----------------------|--|
| N - M - N | _ | 90.2 | 175.5 |
| C_{α} - N - C_{α} | 109.5 | 106.9 | 177.6 |
| $N - C_{\alpha} - C_{m}$ | 125.4 | 124.2 | 125.1 |
| $N - C_{\alpha} - C_{\beta}$ | 107.2 | 107.4 | 107.8 |
| $C_{\alpha} - C_{\beta} - C_{\beta}$ | 107.9 | 108.8 | 108.0 |
| C_{α} - C_{m} - C_{α} | 125.8 | 126.5 | 126.0 |
| $C_m - C_{\alpha} - C_{\beta}$ | 127.2 | 128.4 | 127.0 |
| Dihedral (C ₆ F ₅ groups) | 72.6 | 59.1 | 80.7 |
| C - Ru - O | _ | | 177.6 |

Table 2.4. Average Deviations of Atoms from the Least-Squares Plane (Å).

| Atom | H ₂ TFPPCl ₈ | ZnTFPPCl ₈ | RuTFPPCl ₈ (CO)H ₂ O |
|-------------------|------------------------------------|-----------------------|--|
| N | 0.088 | 0.10 | 0.06 |
| C _m | 0.023 | 0.13 | 0.20 |
| C_{β} | 0.625 | 0.79, 0.68 | 0.48 |
| Cl _{odd} | 1.06 | 1.17 | 1.11 |
| Cleven | 1.06 | 1.48 | 0.68 |
| M | | 0.0 | 0.11 (towards CO) |

Table 2.5: NMR Shifts for Halogenated Porphyrins.

| | NMR values in acetone- d_6 ^a | | | | |
|---|---|------------|----------------|-------------------|------|
| Compound | ¹⁹ F | | | ¹ H | β-Η |
| | ortho | para | meta | N-H | • |
| | | | | | 9.17 |
| ZnTFPP | -138.5 (d) | -154.8 (t) | -163.7 (m) | _ | 9.40 |
| H ₂ TFPP | -136.9 (d) | -151.7 (t) | -161.8 (m) | -2.91 | 83 |
| FeTFPP(Cl) | -105.8, -107.7 | -150.2 | -153.9, -156.0 | | 83 |
| FeTFPP(OH) | -108.0, -114.5 | -152.0 | -156.6, -158.0 | _ | 14.3 |
| (FeTFPP) ₂ O | -133.3, -137.1 | -154.8 | -163.1, -164.7 | | |
| 1 | | | | | |
| ZnTFPPCl ₈ | -138.9 (d) | -151.5 (t) | -163.4 (m) | | |
| H ₂ TFPPCl ₈ | -140.0 (d) | -149.8 (t) | -162.4 (m) | -1.0 ^b | |
| RuTFPPCl ₈ (CO) ^c | -138.8, -139.3 | -151.3 (t) | -163.2, -163.6 | | |
| RuTFPPCl ₈ (py) ₂ | -136.9 (d) | -149.7 (t) | -161.1 (m) | _ | |
| | | | | | |
| ZnTFPPBr ₈ | -138.4 (d) | -151.7 (t) | -163.4 (m) | | |
| H ₂ TFPPBr ₈ | -139.7 (d) | -150.1 (t) | -162.7 (m) | -0.5b | _ |
| FeTFPPBr ₈ (Cl) | -121.4, -122.3 | -146.5 | -158.1, -158.5 | _ | |
| [FeTFPPBr ₈ (Cl)]-d | -124, -133 | -148 | -158, -160 | _ | _ |
| [FeTFPPBr ₈]e | -136 | -152 | -163 | | _ |
| FeTFPPBr ₈ (py) ₂ f | -138.6 | -152.0 | -163.1 | | |

- a. ¹⁹F-NMR values are versus CFCl₃ at 0 ppm. ¹H-NMR values are versus TMS at 0 ppm. Fine structure given as follows: (d) doublet of doublets, (t) triplet, (m) multiplet.
- b. Very broad; the inner nitrogen protons are much more distinct in chlorocarbon solvents such as CDCl₃.
- c. Major set of resonances, each with fine structure as observed in diamagnetic species; other resonances are also observed, as discussed in text.
- d. Produced by bulk electrolysis.
- e. Produced by reduction with ascorbic acid in methanol. Presumably the bis-methanol complex (see text).
- f. Values in CDCl₃.

Spectroscopy and Electronic Structures of Halogenated Porphyrins

Introduction

Metalloporphyrins have distinctive UV-visible spectroscopy due to the aromatic porphyrin chromophore. Two strong $\pi \to \pi^*$ absorptions in the near UV (log $\varepsilon \approx 5$ M⁻¹ cm⁻¹) and visible regions (log $\varepsilon \approx 4$ M⁻¹ cm⁻¹) dominate the spectrum. The higher energy transition is known as the Soret (or B) band, and the less intense, lower energy transition as the Q band. Other higher energy bands of moderate intensity often appear, designated N, L, and M with increasing energy. A typical porphyrin spectrum is pictured in Figure 3.1, with the various transitions labeled with standard porphyrin nomenclature.

A satisfactory theoretical basis for these bands was developed by extension of work on polyarenes, 2,3 which developed a new method for calculating frontier molecular orbital energies for extended π systems. LCAO calculations were based on a postulate assuming free electron movement along the perimeter of the π system. Essentially, this allowed the porphyrin macrocycle to be treated as an 18-electron polyarene; after several iterations, the now-standard Gouterman four orbital model for porphyrin spectroscopy evolved from these calculations. The frontier orbital picture is as follows (Figure 3.2); in D_{4h} symmetry, the two lowest occupied molecular orbitals consist of a nearly degenerate a_{1u} and a_{2u} pair, and the highest unoccupied molecular orbitals are a degenerate e_g set, both of π symmetry. Generally, the a_{1u} orbital is found at slightly lower energy than the a_{2u} , resulting in the two observed electronic transitions. Strong configurational interactions between the lowest energy states give rise to the different intensities in the Soret and Q bands.

Although $\pi \to \pi^*$ in origin, the two intense transitions observed in porphyrin spectra are remarkably sensitive to the metal coordination sphere and oxidation state. In

combination with NMR data, UV-visible spectroscopy is a valuable tool for porphyrin characterization, and in some situations, is the sole method of characterization for some intermediates in metalloporphyrin oxidation reactions.

The substituents on the porphyrin periphery are found to effect the relative energies of the porphyrin frontier molecular orbitals. Substitution at the β -positions of the porphyrin ring with electron withdrawing groups such as halogens or cyano groups has been found to substantially red-shift the Soret band. A combination of theoretical and experimental work has separated the effects of halogenation into electronic and steric 14-17 factors. Electrochemical data and semi-empirical calculations have both suggested that electron withdrawing substituents on the porphyrin periphery stabilize both the HOMO and the LUMO. This effect is offset by the distortion of the porphyrin macrocycle, which results in a large destabilization of the HOMO, and a smaller destabilization of the LUMO (Figure 3.2). The different magnitude of these shifts results in a red shifted electronic transition. A.15,18,19 Characterization of non-planar β -alkyl porphyrins supports this separation of electronic and steric effects. Similar to β -haloporphyrins, these complexes have red-shifted Soret bands from the distortion-induced destabilization of frontier orbitals; however, the reduction potentials for these compounds are substantially more negative than in halogenated derivatives.

Results and Discussion

The electronic spectroscopy of the perhalogenated porphyrins described in Chapter 2 is consistent with this electronic model. The UV-Vis spectra for the zinc(II) tetraphenylporphyrin series are in Figure 3.3. Fluorination of the phenyl moiety has little effect on the Soret or Q band positions, consistent with the planar structures for both these compounds. ^{20,21} In fact, rather than the red shift observed with pyrrole halogenation, a slight blue shift in the Soret band is observed for both the zinc and free base porphyrins. The direction of the change may be explained by the effect of meso substitution on the

relative energy of the porphyrin HOMOs. The a_{2u} orbital, which has greater electron density at meso position,⁵ is stabilized by the pentafluorophenyl groups such that it falls at lower energy than the a_{1u} orbital.²² The a_{1u} orbital, with no density at the meso position, remains relatively unchanged in energy, resulting in a larger HOMO-LUMO gap for the TFPP compounds. Electrochemical experiments also show that the HOMO shifts more than the LUMO, as ZnTFPP is 0.57 V more difficult to oxidize, but only 0.38 V harder to reduce than ZnTPP.

The effect of pyrrole substitution is more substantial. Chlorination induces a 1405 cm^{-1} red shift in the Soret energy of ZnTFPPCl₈ relative to ZnTFPP; as expected, the larger bromine atom induces a greater shift (2405 cm^{-1}) in ZnTFPPBr₈. The magnitude of the shift is consistent with other halogenated porphyrins, i.e., H₂TMP exhibits a 2210 cm^{-1} red shift upon bromination.²³ The decrease in Soret intensity is offset by increasing strength of the Q bands (Table 3.1), consistent with a decrease in the configurational interaction upon β -halogenation.¹⁸ However, the oscillator strength throughout the zinc porphyrin series remains fairly constant: 2.58, 3.40, 2.5, and $2.8 \text{ M}^{-1} \text{ cm}^{-2}$ (from ZnTPP to ZnTFPPBr₈).²⁴

The anodic shift in the reduction potentials of ZnTFPPX $_8^{25}$ and H_2 TFPPX $_8$ relative to the TFPP complexes (Table 3.2) also indicate that electron-withdrawing groups at the β positions stabilize both the highest occupied and lowest unoccupied molecular orbitals of tetraphenylporphyrins. Furthermore, the reduction potentials reflect the contraction of the HOMO-LUMO gap observed in the spectroscopy. Relative to H_2 TFPP, H_2 TFPPCl $_8$ is 0.46 V easier to reduce, but only 0.13 V harder to oxidize.

Addition of a redox active metal does not alter the observed trends. The Soret transition red shifts 1808 cm⁻¹ from Fe^{III}(TFPP)Cl to Fe^{III}(TFPPBr₈)Cl (Figure 3.4), and the Soret bands of the bis-pyridine derivatives, Fe^{II}(TFPPBr₈)py₂ and Fe^{II}(TFPPCl₈)py₂, are also found at lower energy than those of Fe^{II}(TFPP)py₂ (Table 3.3). Although Fe^{III}(TFPPBr₈)Cl may appear to have a split Soret at 404 and 440 nm, the higher energy

absorbance may be a chloride to iron charge transfer, as is the 351 nm band in the spectrum of Fe^{III}(TFPP)Cl. As the LMCT falls at closer energy to the Soret, it steals intensity from it, resulting in the unusually large extinction coefficient for this absorption. The reduction potential of the metal (Fe^{III}/II) follows the same trend as the ligand upon halogenation, increasing from -0.29, to -0.08, to 0.31 V vs. AgCl/Ag along the series Fe(TPP)Cl, Fe(TFPP)Cl, and Fe(TFPPBr₈)Cl.²⁶

Electrochemical reduction of Fe(TFPPBr₈)Cl is found to red shift the Soret from 440 nm to 478 nm, similar to the 25 nm shift observed in the reduction of Fe(TPP)Cl. Chemical reduction with ascorbic acid in methanol results in a similar but less shifted spectrum (Figure 3.5). NMR (Chapter 2) of both species suggests that the first is a five-coordinate anion, [Fe^{II}(TFPPBr₈)Cl]⁻, and the second a low spin six-coordinate species, likely Fe^{II}(TFPPBr₈)(OMe)₂. The spectrum obtained during the attempted synthesis of Fe(TFPPCl₈) was also at very low energy, 440 nm, suggesting that an Fe^{II} species was transiently formed. Addition of pyridine resulted in an optical spectrum very similar to that of Fe(TFPPBr₈)py₂, but no single species was isolated.

Following the same trends, the RuTFPPX8(CO) complexes are harder to oxidize and easier to reduce than RuTPP(CO). Notably, the RuTFPPX8(CO)+/0 potentials are within 0.07 V of those of the unmetallated H_2 TFPPX8 molecules, indicating that the first electron is removed from a ligand-based orbital. Oxidation of RuTFPPCl8(py)2 occurs 0.63 V lower than RuTFPPCl8(CO), suggesting that the HOMO is a $d\pi$ level in the pyridine derivative. The magnitude of this shift is similar to the 0.64 V shift between the metal-centered oxidation of RuTPP(py)2²⁸ and the ligand-centered oxidation of RuTPP(CO). 29

This sterically induced contraction of the HOMO-LUMO gap is surprisingly small for RuTFPPCl₈(CO) (0.11 V relative to RuTPP(CO))²⁷ as extracted from the values of the +/0 and 0/- potentials). Enhanced backbonding from Ru^{II} to TFPPCl₈ is the likely explanation of this finding, as discussed below.

The electronic properties of perhalogenated Ru^{II} porphyrins can be interpreted in terms of a Gouterman four-orbital model^{4,9} modified by the inclusion of the Ru d π orbitals (Figure 3.6).³⁰ Increased backbonding in the TFPPX8 complexes promotes mixing of $\pi \to e\pi^*$ and $Ru^{II} \to e\pi^*$ excited states, with the result that the Soret (mainly $\pi \to e\pi^*$) transition falls at higher energies than would be predicted by a simple one-electron (HOMO-LUMO) model.^{1,31,32} The Soret band of RuTFPPCl8(CO) (418 nm) is substantially blue-shifted from that of H_2 TFPPCl8 (440 nm). A blue shift upon metalation with a 2nd or 3rd row metal is often observed; i.e., the Soret band of PdTFPPCl8 is 705 cm⁻¹ shifted from the free ligand. The magnitude of the shift in RuTFPPCl8(CO), ~ 1300 cm⁻¹, is surprisingly high, indicating that the electronic coupling of Ru^{II} to the porphyrin is unusually strong. The offsetting effect of extensive backbonding in the distorted porphyrins is the reason that the Soret bands for both RuTFPPCl8(CO) and RuTFPPCl8(py)₂ (414 nm) are only slightly red-shifted from those of RuTPP(CO) (412 nm) and RuTPP(py)₂ (413 nm) (Figure 3.7 and 3.8).

IR data also indicate that halogenated porphyrins are π acceptors. The peak attributable to the CO stretch appears at much higher energy in the halogenated porphyrins relative to the 1945 cm⁻¹ band observed for RuTPP(CO).³³ The transition energy decreases according to RuTFPPCl₈(CO) (1990) > RuTFPPCl₇(CO) (1987) > RuTFPPCl₆(CO) (1984) > RuTFPPBr₈(CO) (1973 cm⁻¹), further reflecting the increased competition between the porphyrin and the carbonyl ligand for π electron density upon halogenation.

The distortion-induced contraction of the HOMO-LUMO gap^{9,10,12,14,17,18} is evidenced by a decrease of the Soret transition energy according to RuTFPPCl₆(CO) (410) > RuTFPPCl₇(CO) (413.5) > RuTFPPCl₈(CO) (418 nm) (Figure 3.9). The Soret band of RuTFPPBr₈(CO) is further red-shifted to 424 nm; as predicted,⁹ the larger halogen atoms generate a greater distortion of the porphyrin, thereby producing a smaller HOMO-LUMO

gap. Porphyrin saddling also is responsible for the red shifts of the Q(0,1) bands of RuTFPPX8 complexes from those of the corresponding TPP derivatives (Figure 3.7 and 3.8).

Relatively weak bands at 670 ($\varepsilon \approx 800$) and 792 nm ($\varepsilon \approx 300 \text{ M}^{-1}\text{cm}^{-1}$) are observed in the spectrum of RuTFPPCl₈(py)₂ (Figure 3.10). Low-lying Ru^{II} \rightarrow e π^* (TFPPCl₈) transitions are expected, since the electrochemical data show that both Ru^{II} oxidation and TFPPCl₈ reduction are accessible. Extensive backbonding to e π^* (TFPPCl₈) orbitals would stabilize d_{xz} , d_{yz} relative to d_{xy} (Figure 3.6); it is likely, then, that a d_{xy} electron is involved in both electrochemical and the 792-nm spectroscopic oxidation of Ru^{II} to Ru^{III}. No bands above 650 nm were observed in the spectrum of RuTFPPCl₈(CO), consistent with the absence of any Ru^{II} oxidations in the electrochemical experiments. The d π orbitals for RuTFPPCl₈(CO) are anticipated to fall at a similar energy as the porphyrin b_2 π orbital. Any charge transfer band in this region would be obscured by the intense porphyrin $\pi \to \pi^*$ transition. However, a b_2 d $\pi \to e\pi^*$ transition may be contributing to the slight tailing on the low energy side of the Soret band of RuTFPPCl₈(CO).

Spectroelectrochemistry was performed to confirm the assignment of the LUMO as metal or ligand based in the ruthenium porphyrins. Reduction of RuOEP(CO)³⁴ and RuTPP(CO)³⁵ has demonstrated distinct differences in the UV-Vis depending on the site of reduction. Formation of a radical porphyrin anion is accompanied by a broadening of the Soret, with a concomitant decrease in intensity. The Q bands disappear, and a new band around 600 - 700 nm grows into the spectrum. RuOEP(CO)(THF)³⁴ and RuTPP(CO)³⁵ in THF both show these type of spectral features upon reduction. Reduction of RuTFPPCl₈(py)₂ (Figure 3.11) is accompanied by a decrease in the Soret intensity, with a red shift to 420 nm, as well as a decrease in the Q band intensity. A new band appears at 580 nm, consistent with formation of a porphyrin based radical anion.

Spectroelectrochemistry in a different solvent has been shown to have completely different

characteristics, indicating that the axial ligand can alter the site of reduction. Upon reduction in benzonitrile, the Soret band of RuOEP(CO) is still sharp, and shows a slight red shift. No new features are observed in the lower wavelength regions.³⁴ Reduction of RuTFPPCl₈(CO) is shown in Figure 3.12. The Soret band decreases in intensity, and shows a similar red shift as in RuTFPPCl₈(py)₂, but the broadening generally associated with radical anion formation is not observed. In addition, there is no major change in the Q-band region. Isosbestic points at 270, 376, 420, and 440 nm indicate that clean reduction is occurring, but the decrease in Soret intensity suggests that this reduction may have both metal and ligand character.

Conclusion

The distortion of the porphyrin macrocycle, as observed in the crystal structures of the halogenated free ligand, zinc, and ruthenium porphyrins (Chapter 2), gives rise to the expected red shifted optical spectra and anodically shifted electrochemistry common to porphyrins substituted with electron withdrawing ligands. Only the RuTFPPX8 complexes show Soret transitions at higher energy, which has been demonstrated to stem from strong coupling between the ruthenium and porphyrin orbitals. Attempts to photolyze the carbonyl ligand further support strong interactions between these orbitals; despite a relatively high VCO (indicating a correspondingly weak Ru-C bond), it is difficult to remove the carbonyl ligand with light energy. Rather than leading to dissociation, the excited state appears to decay by non-radiative pathways. No emission is observed for either the RuTFPPCl8(CO) or Ru(TFPPCl8)py2 complexes.

The highly positive reduction potentials of the perhalogenated ruthenium and iron complexes indicate that these compounds will be quite stable in a highly oxidizing environment. Further experiments will test to see if they display the high activity as oxidation catalysts for which they were designed.

Methods

Infrared spectra were recorded as solutions in carbon tetrachloride or benzene on a Perkin-Elmer Model 1600 FT-IR spectrophotometer. Electronic absorption spectra were recorded on an Olis-modified Cary-14 spectrophotometer. Electrochemistry was performed under Ar in three compartment cell consisting of a highly polished glassy carbon working electrode, a Ag/AgCl reference electrode in 1M KCl, and a platinum auxiliary electrode. The working electrode and reference electrode are connected by a modified Luggin capillary. Spectroelectrochemical experiments were performed in an optically transparent platinum working electrode. Spectral changes were monitored with a Hewlett Packard 8452A diode array spectrophotometer. A 1000 W tungsten lamp was used for photolysis experiments.

Materials

Porphyrins were obtained as described in Chapter 2. Solvents were Omnisolv grade from EM Science, and used as received.

References and Notes

- (1) Gouterman, M. In *The Porphyrins*; D. Dolphin, Ed.; Academic Press, Inc.: New York, NY, 1978; Vol. III; pp 1-156.
- (2) Platt, J. R. J. Chem. Phys. 1949, 17, 484.
- (3) Simpson, W. T. J. Chem. Phys. 1949, 17, 1218.
- (4) Gouterman, M. J. Mol. Spectrosc. 1961, 6, 138-163.
- (5) Gouterman, M. J. Chem. Phys. 1959, 30, 1139-1161.
- (6) Callot, H. J. Bull. Chem. Soc. Fr. 1974, 7, 1492-1496.
- (7) Callot, H. J.; Giraudeau, A.; Gross, M. J. Chem. Soc., Perkin Trans. 2 1975, 1321-1324.
- (8) Wijesekera, T.; Matsumoto, A.; Dolphin, D.; Lexa, D. Angew. Chem., Int. Ed. Eng. 1990, 29, 1028-1030.
- (9) Takeuchi, T.; Gray, H. B.; Goddard, W. A., III J. Am. Chem. Soc. 1994, 116, 9730-9732.
- (10) Barkigia, K. M.; Chantranupong, L.; Smith, K. M.; Fajer, J. J. Am. Chem. Soc. 1988, 110, 7566-7567.
- (11) Binstead, R. A.; Crossley, M. J.; Hush, N. S. Inorg. Chem. 1991, 30, 1259-1264.
- (12) Giraudeau, A.; Callot, J. H.; Gross, M. Inorg. Chem. 1979, 18, 201-206.
- (13) Hodge, J. A.; Hill, M. G.; Gray, H. B. Inorg. Chem. 1995, 34, 802-812.
- (14) Ochsenbein, P.; Ayougou, K.; Mondon, D.; Fischer, J.; Weiss, R.; Austin, R. N.; Jayaraj, K.; Gold, A.; Terner, J.; Fajer, J. Angew. Chem., Int. Ed. Eng. 1994, 33, 348-350.
- (15) Barkigia, K. M.; Berber, M. D.; Fajer, J.; Medforth, C. J.; Renner, M. W.; Smith, K. M. J. Am. Chem. Soc. 1990, 112, 8851-8857.
- (16) Mandon, D.; Ochsenbein, P.; Fischer, J.; Weiss, R.; Jayaraj, K.; Austin, R. N.; Gold, A.; White, P. S.; Brigaud, O.; Battioni, P.; Mansuy, D. *Inorg. Chem.* 1992, 31, 2044-2049.
- (17) Senge, M. O.; Medforth, C. J.; Sparks, L. D.; Shelnutt, J. A.; Smith, K. M. Inorg. Chem. 1993, 32, 1716-1723.
- (18) Bhyrappa, P.; Krishnan, V. Inorg. Chem. 1991, 30, 239-245.
- (19) D'Souza, F.; Villard, A.; Caemelbecke, E. V.; Franzen, M.; Boschi, T.; Tagliatesta, P.; Kadish, K. M. *Inorg. Chem.* 1993, 32, 4042-4048.
- (20) Scheidt, W. R.; Kastner, M. E.; Hatano, K. Inorg. Chem. 1978, 17, 706-710.

- (21) Birnbaum, E. R.; Hodge, J. A.; Grinstaff, M. G.; Schaefer, W. P.; Marsh, R. E.; Henling, L. M.; Labinger, J. A.; Bercaw, J. E.; Gray, H. B. *Inorg. Chem.* in press.
- (22) Gross, Z.; Barzilay, C. Angew. Chem., Int. Ed. Eng. 1992, 1615-1617.
- (23) Hoffmann, P.; Robert, A.; Meunier, B. Bull. Chem. Soc. Fr. 1992, 129, 85-97.
- (24) Oscillator strength is calculated as 4.6 x 10^{-9} ε $v_{1/2}$.
- (25) The ZnTFPPX₈ compounds also show anoidcally shifted electrochemistry, but are complicated by two-electron waves. See reference 13.
- (26) Grinstaff, M. W.; Hill, M. G.; Birnbaum, E. R.; Schaefer, W. P.; Labinger, J. A.; Gray, H. B. *Inorg. Chem.* in press.
- (27) The potentials of RuTPP(CO) are 0.87 (+/0) and -1.59 (0/-) V vs. SCE (CH₂Cl₂, 0.1M TBAP): Mu, X. H.; Kadish, K. M. Langmuir **1990**, 6, 51-56.
- (28) Brown, G. M.; Hopf, F. R.; Ferguson, J. A.; Meyer, T. J.; Whitten, D. G. J. Am. Chem. Soc. 1973, 95, 5939-5942.
- (29) Kadish, K. M.; Chang, D. Inorg. Chem. 1982, 21, 3614-3619.
- (30) Since pyridine is a much weaker π acceptor than CO, we would expect Ru^{II} to backbond more strongly to TFPPCl₈ in the bis(pyridine) than in the carbonyl derivative. For discussions of M^{II} (M = Fe, Ru, Os) backbonding to CO and py in porphyrin complexes, see: Gentemann, S.; Albaneze, J.; Garcia-Ferrer, R.; Knapp, S.; Potenza, J. A.; Schugar, H. J.; Holten, D. J. Am. Chem. Soc. 1994, 116, 281-289; Kim, D.; Su, Y. O.; Spiro, T. G. Inorg. Chem. 1986, 25, 3993-3997; Schick, G. A.; Bocian, D. F. J. Am. Chem. Soc. 1984, 106, 1682-1694.
- (31) Buchler, J. W.; Kokisch, W.; Smith, P. D. Struct. Bonding 1978, 34, 79-134.
- (32) Antipas, A.; Buchler, J. W.; Gouterman, M.; Smith, P. D. J. Am. Chem. Soc. 1978, 100, 3015-3024.
- (33) Chow, B. C.; Cohen, I. A. Bioinorg. Chem. 1971, 1, 57-63.
- (34) Kadish, K. M.; Tagliatesta, P.; Hu, Y.; Deng, Y. J.; Mu, X. H.; Bao, L. Y. *Inorg. Chem.* **1991**, *30*, 3737-3743.
- (35) Mu, X. H.; Kadish, K. M. Langmuir 1990, 6, 51-56.
- (36) Hill, M. G.; Mann, K. R. Inorg. Chem. 1991, 30, 1429-1431.

Figure 3.1 -- An absorption spectrum of ZnTPP, a normal porphyrin. The Soret (or B) absorption usually lies around 410 nm, and the Q bands are at lower energy. The shoulder on the Soret has been assigned as a $\pi \to \pi^*$ transition (N band).

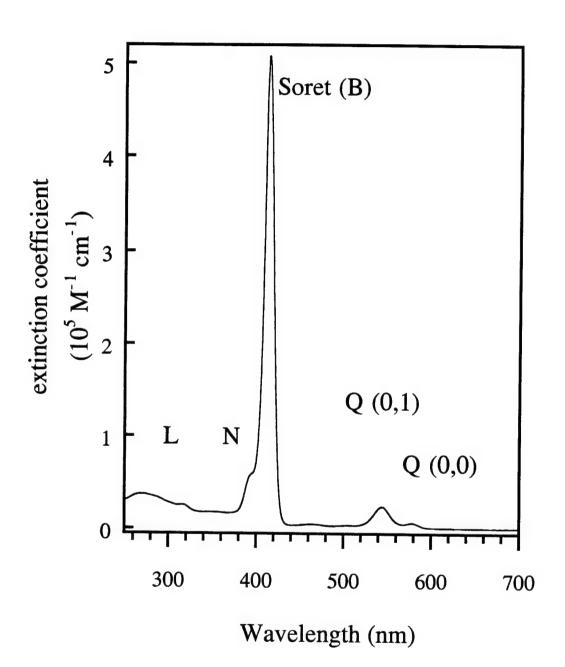
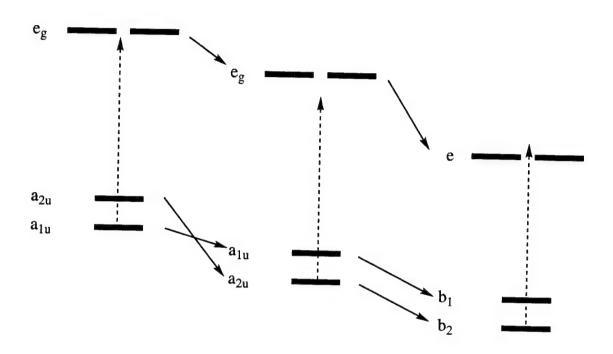


Figure 3.2 -- The Gouterman four orbital model for normal porphyrins is shown on the left (with D_{4h} symmetry labels). Upon fluorination of the phenyl rings, both the HOMO and the LUMO are stabilized, and the relative energy of the a_{1u} and a_{2u} HOMOs are reversed. Halogenation of the pyrrole carbons results in a further stabilization of all of the orbitals (pictured on the right). The distortion of the molecule drops the symmetry to approximately D_{2d} . The Soret transition is marked on each molecular orbital diagram with an arrow of equal length, showing the increase in the HOMO-LUMO gap in TFPP and the decrease in TFPPCl₈.

Gouterman Four Orbital Model



Normal orbital ordering

Addition of pentafluorophenyl groups to meso carbons

Addition of halogens to pyrrole carbons

TPP

TFPP

TFPPCl₈

Figure 3.3 -- The UV-Vis spectra of the ZnTPP series of porphyrins in methylene chloride. As shown in the molecular orbital diagrams in Figure 3.2, the energy of the Soret transition decreases as ZnTFPP > ZnTPP > ZnTFPPCl₈ > ZnTFPPBr₈.

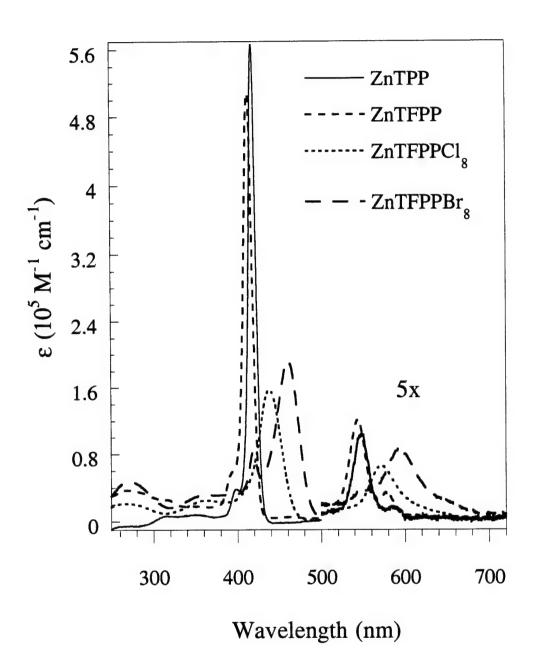


Figure 3.4 -- The UV-Vis spectra of Fe(TFPP)Cl and Fe(TFPPBr₈)Cl in methylene chloride. The LMCT of Fe(TFPPBr₈)Cl mixes with the Soret band, increasing the extinction coefficient of this transition relative to the 350 nm band in Fe(TFPP)Cl.

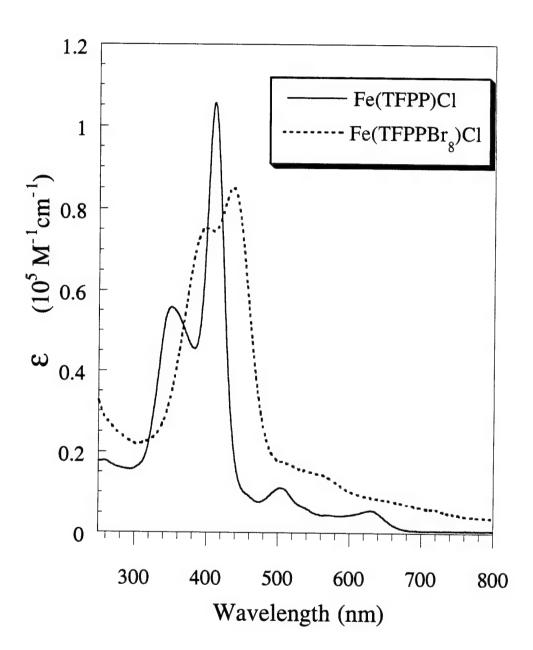


Figure 3.5 -- The UV-Vis spectra of [Fe^{II}(TFPPBr₈)Cl]⁻ and [Fe^{II}(TFPPBr₈)(OCH₃)₂] produced by bulk electrolysis or chemical reduction in methylene chloride.

The red shifted Soret band and the single Q band are consistent with formation of an iron(II) porphyrin. The axial ligands for the two complexes are determined from a combination of electrochemical data and ¹⁹F NMR.

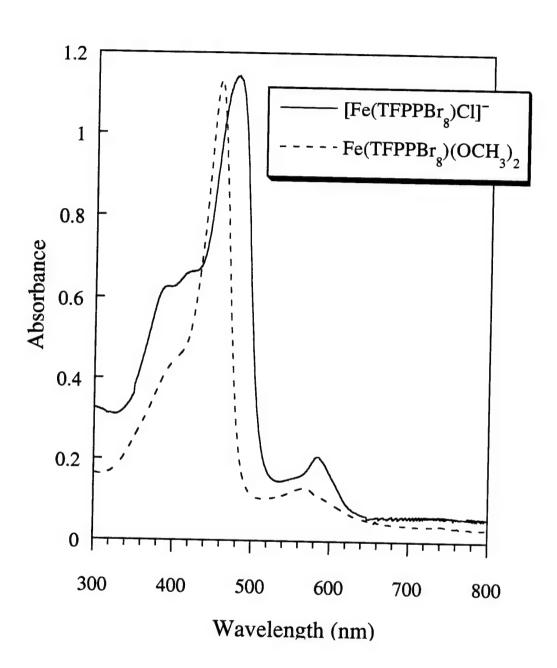
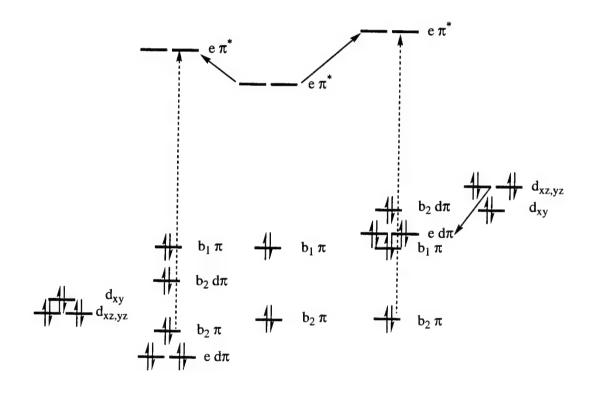


Figure 3.6 -- The Gouterman four orbital model for RuTFPPX₈ complexes. The porphyrin TFPPX₈ orbitals are allowed to interact with the $d\pi$ orbitals of carbonyl or bis-pyridine ruthenium fragments (D_{2d} symmetry). Extensive π -backbonding to the carbonyl ligand strongly stabilizes the d_{xz} , d_{yz} orbitals, resulting in a ligand based HOMO for RuTFPPX₈(CO). Weaker interactions in the bis-pyridine complex leaves the $d\pi$ orbitals at higher energies, consistent with a Ru-based HOMO and low energy charge transfer transitions in RuTFPPX₈(py)₂. The Soret transition is shown with an arrow for both complexes.

"Ru(CO)" RuTFPPX $_8$ (CO) H $_2$ TFPPX $_8$ RuTFPPX $_8$ (py) $_2$ "Ru(py) $_2$ "



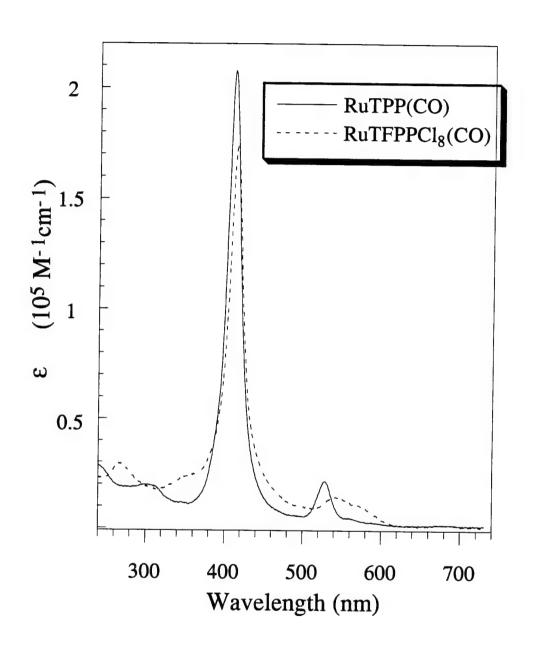


Figure 3.7 -- The UV-Vis spectra of RuTPP(CO) and RuTFPPCl $_8$ (CO) in methylene chloride. Although the Soret energy is similar for the two complexes, the Q(1,0) transition is red shifted for the perhalogenated complex.

Figure 3.8 -- The UV-Vis spectra of RuTPP(py)₂ and RuTFPPCl₈(py)₂ in methylene chloride.

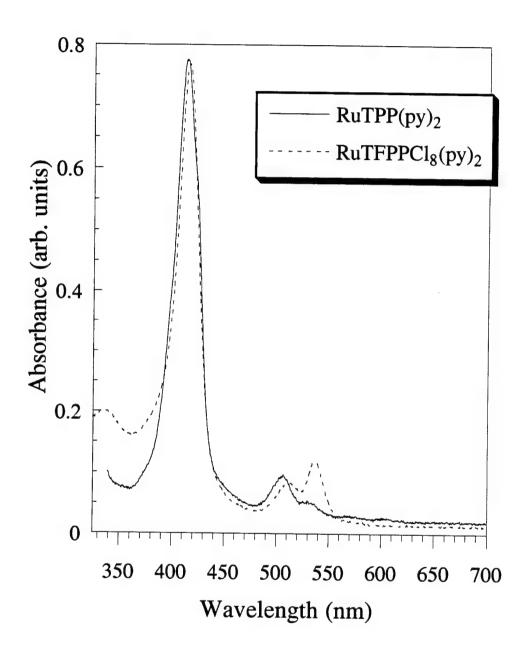


Figure 3.9 -- The UV-Vis spectra of the RuTFPPX_n(CO) complexes in methylene chloride. The Soret energy decreases with halogenation: RuTFPPCl₆(CO) $> \text{RuTFPPCl}_7(\text{CO}) > \text{RuTFPPCl}_8(\text{CO}) > \text{RuTFPPBr}_8(\text{CO}), \text{ with the larger bromine atoms inducing a larger red shift than chlorine. The Q bands (not shown) show a similar change in energy.}$

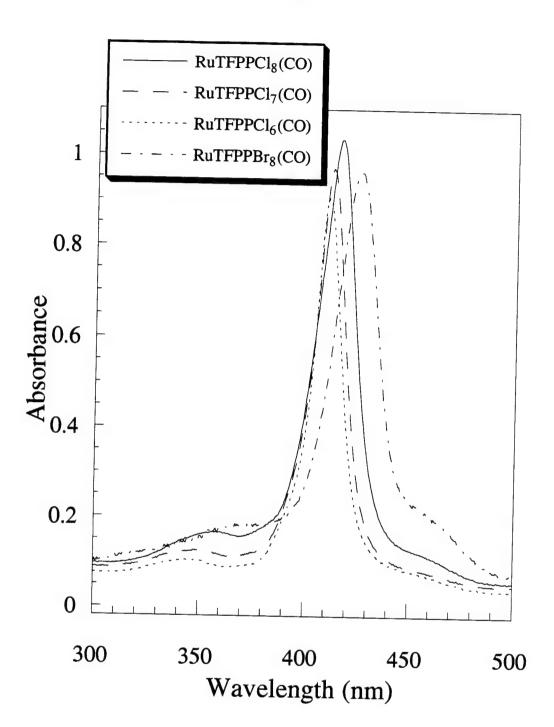


Figure 3.10 -- The low energy visible spectrum of RuTFPPCl₈(CO) and RuTFPPCl₈(py)₂. The two absorptions at 670 and 792 nm in the bispyridine spectrum are assigned to Ru^{II} \rightarrow e π^* (TFPPCl₈) transitions. MLCT transitions in the carbonyl complex are anticipated to lie at higher energy and are obscured by porphyrin $\pi \rightarrow e\pi^*$ transitions.

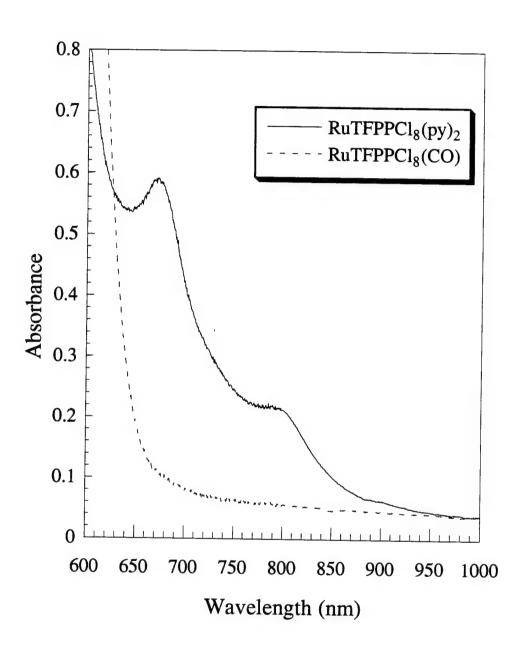


Figure 3.11 -- Spectroelectrochemical reduction of RuTFPPCl $_8(py)_2$ in methylene chloride. The reduced species shows clear porphyrin radical character.

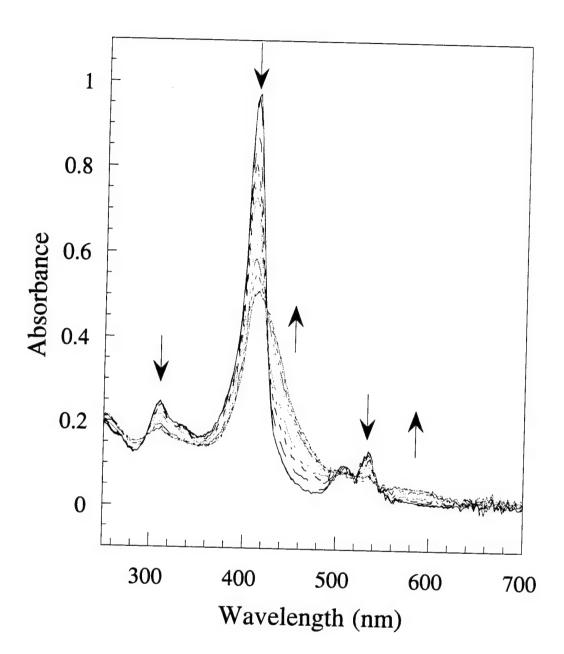
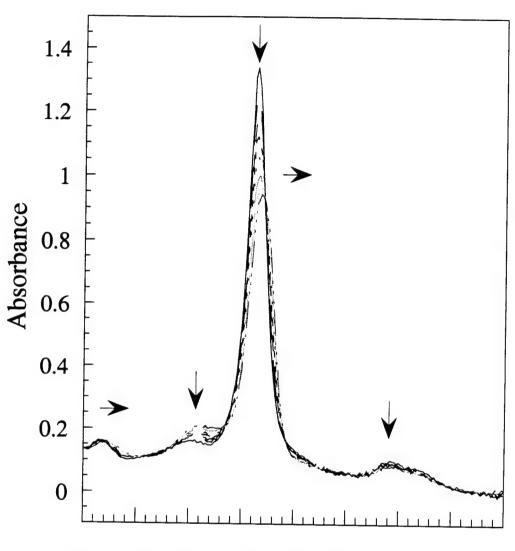


Figure 3.12 -- Spectroelectrochemical reduction of RuTFPPCl₈(CO) in methylene chloride. While the reduced species shows a decrease in the Soret intensity, consistent with formation of a porphyrin radical anion, no change in the Q band region is observed.



250 300 350 400 450 500 550 600 650 Wavelength (nm)

Table 3.1. Electronic Absorptions of Halogenated Porphyrins.

| Porphyrin | L, M bands | Soret, nm | Q bands, nm | | | |
|---|-----------------------------------|---|--|--------|------------------|---------|
| • | $(\epsilon, 10^3 \text{M}^{-1})$ | $(\epsilon, 10^5 \mathrm{M}^{-1} \mathrm{cm}^{-1})$ | $(\varepsilon, 10^4 \mathrm{M}^{-1} \mathrm{cm}^{-1})$ | | | |
| | cm ⁻¹) | | | | | |
| ZnTPP | 315 (1.0) | 418 (5.6) | 548 | 0 | | |
| | 350 (1.5) | | (2.1) | | | |
| ZnTFPP | 318 (4) | 413.5 (5.0) | 544 | | | |
| | | | (2.4) | | | |
| ZnTFPPCl ₈ | 360 (3.0) | 439 (1.6) | 572 | | į | |
| | | (4.6) | (1.3) | ļ | | |
| ZnTFPPBr ₈ | 364 (3.3) | 460 (1.9) | 594 | | | |
| | | | (1.7) | | | |
| H ₂ TPP ^a | | 419 (4.7) | 514 | 549 | 591 | 647 |
| 112111 | | 125 () | (1.9) | (0.77) | (0.54) | (0.34) |
| H ₂ TFPP ^a | | 412 (2.4) | 506 | 584 | 659 | |
| 2 | | ` / | (1.9) | (0.58) | (0.36) | |
| H ₂ TFPPCl ₈ | | 438 (1.6) | 538 | 626 | | |
| | | | (1.3) | (0.46) | | |
| H ₂ TFPPBr ₈ | | 454 | 532 | 636 | | |
| | | | | | - | |
| RuTPP(CO) | 300 (20) | 412 (2.0) | 528 | | | |
| | 355 (35) | 416 (1.5) | (2.1) | 500 | | |
| RuTFPPCl ₈ (CO) | 355 (25) | 416 (1.7) | 548 | 580 | | |
| D-TEDDCI-(CO) | 345 | 413 | (1.4) | (1.0) | | |
| RuTFPPCI ₇ (CO) | 343 | 411 | 539 | 572 | | |
| RuTFPPCl ₆ (CO) | | | | 312 | | |
| RuTFPPBr ₈ (CO) | 370 | 426 | 595 | | | |
| | | | | | | |
| RuTPP(py) ₂ | | 413 | 507 | 534 | | |
| RuTFPPCl ₈ (py) ₂ | 355 | 414 (1.6) | 512 | 536 | 670 ^b | 790⁵ |
| 101111 C18(PJ)2 | 333 | (1.0) | (2.0) | (2.5) | (0.08) | (0.03) |
| RuTFPPCl ₇ (py) ₂ | | 414 | 510 | 536 | 672 ⁶ | 790⁵ |
| RuTFPPCl ₆ (py) ₂ | | 412 | 508 | 534 | 674 ^b | 790⁵ |
| RuTFPPBr ₈ (py) ₂ | | 424 | 518 | 572 | | |

<sup>a. Extinction coefficients in benzene, from Longo, F. R.; Finarelli, M. G.; Kim, J. B. J. Hetero. Chem., 1969, 6, 927-931.
b. Assigned as MCLT absorptions.</sup>

Table 3.2. Reduction Potentials of Halogenated Porphyrins.

| Porphyrin ^a | E°'+/0 | $E^{"}_{M(III)/M(II)}$ | E'' _{0/-} | |
|---|-------------------|------------------------|--------------------|--|
| ZnTPPb | 0.80 | | -1.33 | |
| ZnTFPP ^b | 1.37 | | -0.95 | |
| ZnTFPPCl8b | 1.60 ^c | | -0.76 | |
| ZnTFPPBr ₈ b | 1.55° | | -0.75 | |
| H ₂ TPP ^d | 1.08 | | -1.21 | |
| H ₂ TFPP | 1.53 | | -0.78 | |
| H ₂ TFPPCl ₈ | 1.66e | | -0.78 | |
| H ₂ TFPPBr ₈ | 1.56e | _ | -0.31 | |
| RuTPP(CO)f | 0.86 | | -1.46 | |
| RuTFPPCl ₆ (CO) | 1.64 | _ | -0.76 | |
| RuTFPPC17(CO) | 1.69 | | -0.69 | |
| RuTFPPCl ₈ (CO) | 1.71 | _ | -0.64 | |
| RuTFPPBr ₈ (CO) | 1.63 | _ | -0.84 | |
| RuTPP(py)2 ^d | | 0.21 | | |
| RuTFPPC16(py)2 | | 0.89 | -1.12 | |
| RuTFPPCl ₇ (py) ₂ | | 1.04 | -0.98 | |
| RuTFPPCl ₈ (py) ₂ | | 1.08 | -0.94 | |
| Fe(TPP)Clg | 1.14 | -0.29 | 1.07 | |
| Fe(TFPP)Cl | 1.65 | -0.29 -0.08 | -1.07 | |
| Fe(TFPPBr ₈)Cl | 1.03 | | -1.10 | |
| 10(1111 b18)C1 | | 0.31 | -0.63 | |

a. Potentials in CH₂Cl₂ solution at room temperature (V vs. AgCl/Ag, 0.1M TBAPF₆).

b. The zinc potentials are from reference 13.

c. E°'2+/0.

d. V. vs SCE in 0.05M THAP. From reference 12.

e. Ena

f. V. vs. SCE in 0.1 M TBAP in CH₃CN. From reference 29.

g. From reference 26.

Table 3.3. Electronic Absorptions of Halogenated Iron Porphyrins.

| Porphyrin | L, M bands | Soret, nm (ε,10 ⁵ M ⁻¹ cm ⁻¹) | Q bands, nm (E, 10 ⁴ M ⁻¹ cm ⁻¹) | | | |
|---|---------------|--|---|----------------|------------------------------|--|
| Fe ^{III} (TPP)Cl ^a | | 419 (1.7) | 510 (1.2) | 573 (0.037) | 656, 692 (0.028, 0.32) | |
| Fe ^{II} (TPP)Cl ² | | 444 (1.7) | 530 (0.32) | 571 (0.75) | 612 (0.65) | |
| Fe ^{III} (TFPP)Cl | | 411 (1.0) | 351 (0.70) | 504 (1.1) | 621 (0.56) | |
| "Fe ^{II} (TFPPCl ₈)" ^b | 398 | 440 | 566 | | | |
| Fe ^{III} (TFPPBr ₈)Cl | 404 (0.81) | 440 (0.85) | 560 (2.0) | | | |
| [Fe ^{II} (TFPPBr ₈)Cl]- | 388, 420 | 478 | 585 | | | |
| Fe ^{II} (TFPPBr ₈)(OMe) ₂ | | 454 | 568 | | | |
| Fe(TPP)py ₂ | | | | | | |
| Fe(TFPP)py ₂ | | 418 | 525 | 552 | | |
| Fe(TFPPCl ₈)py ₂ | | 438 | 542 | 574 | | |
| Fe(TFPPBr ₈)py ₂ | | 452 | 556 | 588 | | |
| (FeTFPP) ₂ O ^c | | 398 (0.62) | 577 (0.7) | 590 (sh) | | |
| Fe(TFPP)OH ^c | | 406 (7.6) | 563 (1.2) | | | |

a. Spectra taken in PhCN; from reference 8.

b. Appears to be iron (II) based on the red color. See text.

c. Extinction coefficients from reference 40, Chapter 2.

Chapter 4

Mechanism of Catalytic Alkene Oxidation with Molecular Oxygen or Iodosobenzene and Halogenated Iron Porphyrins

Introduction

Since the discovery that tetraphenylporphyrinato-iron(III) chloride [Fe(TPP)Cl] catalyzes olefin epoxidation with iodosobenzene, a variety of porphyrins have been tested for the ability to mediate hydrocarbon oxidation reactions utilizing assorted oxygen sources. These studies have generally striven to generate high-valent metal-oxo intermediates to mimic the putative active species in cytochrome P-450. Most experiments take advantage of the peroxide shunt pathway to directly form the desired metal-oxo species, while reactions with dioxygen are usually carried out in the presence of a reductant to follow the complete P-450 oxygen activation mechanism.

The reaction of iodosobenzene (PhIO) with metalloporphyrins has been well documented. $^{1,3-8}$ The iodosobenzene polymer oxidizes $M^{III}(P)X$ complexes to $M^{V}(P)(O)$ species as shown in Eq. 1, where P = porphyrin, X = halide, ^{-}OH , etc., R = phenyl, and R' is the continuing iodosobenzene polymer. 9 Some evidence also exists for the transient

formation of a μ -oxo dimer intermediate, (P)M^{IV} - O - M^{IV}(P)*+, formed from a reaction of M^V(P)(O) with another porphyrin molecule. ^{10,11}

Whether the last oxidizing equivalent is more appropriately characterized as a MV or as a M^{IV}(P^{+*}) depends on the metal and porphyrin involved. Spectroscopic evidence indicates that most iron porphyrins are oxidized to form porphyrin radical cations, ¹²⁻¹⁴ as does the heme center in the enzyme horseradish peroxidase (HRP) The high-valent metal-oxo of HRP (compound I) is well characterized as Fe^{IV}(P^{+*})(O) and is often used as a standard for comparisons with model complexes. ¹⁵ Oxidation of Fe^{III}(TMP)Cl with

m-chloroperbenzoic acid (mCPBA) at -77 °C is reported to give UV-Vis and ¹H NMR spectra consistent with formation of an iron(IV) porphyrin π-radical cation. ¹⁴ EXAFS and Mössbauer spectra are similar to those of HRP compound I, further supporting this assignment. ¹⁶ With other metals, such as chromium, the last electron is removed from a metal based orbital. ¹⁷ For Cr^{III}TPPCl, UV-Vis and IR spectroscopy, in combination with magnetic susceptibility measurements, indicate formation of Cr^VTPP(O) upon oxidation with mCPBA or PhIO. ¹⁸

Once the high-valent metal-oxo is generated, there are a number of mechanisms for interaction with an olefin. Possible intermediates include a metallaoxetane (I), a π -radical cation (II), a carbocation (III), a carbon radical (IV), or a process of concerted oxene insertion (V) (Figure 4.1). ¹⁹ The metallocyclo intermediate has been excluded, especially for sterically encumbered porphyrins, since modeling demonstrates that the reaction coordination sphere is not large enough to accommodate formation of the four-membered ring. ^{20,21} Although many elegant experiments have been conducted to further probe the transition state, there is no consensus indicating a general metalloporphyrin oxidation mechanism. The academically unsatisfying conclusion seems to be that the mechanism is dependent on the metal ion and the electron density of the porphyrin and alkene substrate. ¹⁹

Nevertheless, a few general concepts concerning the mechanism have been proposed (Figure 4.2). $^{17,21-23}$ The first step has been proposed to be association of the metal-oxo and the olefin, in some cases called a charge transfer (CT) complex. With $Cr^{V}(TDBPP)(O)$ (TDBPP = tetrakis-(2,6-dibromophenyl)porphyrin), the formation of this complex is rate limiting, 17 and other evidence suggests this is also true for the iron derivative. The reaction of Fe(TMP)Cl with mCPBA and cyclooctene at -43 °C resulted in an observable intermediate prior to epoxide formation, again suggested to be an olefin π -complex. 13 The charge transfer complex may then react through various pathways, including concerted oxene transfer (V), electrophillic addition (III), or electron

transfer (IV). 19-21 The relative rates for each pathway are determined in each case by the electron density on the olefin and the electrochemical potential of the metal center.

Unfortunately, the actual oxo transfer step is after the rate limiting formation of the CT complex, precluding its direct observation.

For the specific case of cyclohexene oxidation, different pathways are implicated for hydroxylation and epoxidation (Figure 4.3). Oxidation of deuterated cyclohexene with Fe(TPP)Cl and Cr(TPP)Cl has shown that allylic oxidation occurs via allylic hydrogen atom abstraction followed by geminate radical recombination. ²⁴ Further experiments with partially halogenated porphyrins supported this mechanism for hydroxylation²⁵ and suggested that formation of cyclohexene epoxide occurs by direct electron transfer to form a carbocation intermediate (Figure 4.3). Competition between direct hydrogen abstraction and electron transfer depends on the electron density at the metal, allowing for different selectivity as observed with different metals. ²⁵ The higher selectivity for epoxidation observed with electron-withdrawing iron porphyrins suggests that the higher reduction potential favors the electron transfer mechanism. ²⁵ Correlations of epoxidation rates with the reduction potential or the Hammett parameter of the olefin have also been argued to support an electron transfer mechanism for Fe(TDCPP)Cl. ²⁶

The perhalogenated porphyrin, 2,3,7,8,12,13,17,18-octabromo-5,10,15,20-tetrakis(pentafluorophenyl)porphyrinato-iron(III) chloride, [Fe(TFPPBr₈)Cl], is an active catalyst for the selective oxidation of light alkanes at elevated temperatures (80 °C) and under high dioxygen pressure (80 atm).^{27,28} Recently, we reported that at room temperature and one atmosphere of molecular oxygen, Fe(TFPPBr₈)Cl will oxidize 3-methylpentane to 3-methylpentan-3-ol.²⁹ We have now found that this metalloporphyrin is also an efficient catalyst for the oxidation of cyclohexene with either dioxygen or single O-atom donors such as iodosobenzene.

Results

In the presence of Fe(TFPPBr8)Cl, cyclohexene oxidation to a mixture of cyclohexene oxide, 2-cyclohexen-1-ol, and 2-cyclohexen-1-one, was observed (Figures 4.4 and 4.5). The product distribution and activity varied greatly with the oxidant. With PhIO, the majority of product (77%) consisted of the epoxide. With dioxygen, mainly allylic oxidation products were generated (49 and 44% of alcohol and ketone, respectively). Reactions with styrene exhibited similar differences in product distribution with oxidant. With PhIO, the majority of the product (67%) was styrene oxide, while with dioxygen, only the cleavage product, benzaldehyde (> 95%), was observed.

Catalytic activity also varied with oxidant. Iodosobenzene reactions deactivated in 1 to 5 hours, accompanied by a shift in the Soret band from 442 to 418 nm. However, 18 ± 4 turnovers (TO) were completed during this time period, and the product distribution (Figure 4.4) was consistent between runs. Although the initial activity with PhIO was greater, overall activity was higher with dioxygen, suggesting an induction period for the latter reaction. Furthermore, in reactions with dioxygen, the perhalogenated porphyrin showed much higher activity at 24 hours (73 TO) as compared to the related porphyrins tetrakis(pentafluorophenyl)porphyrinato-iron(III) chloride (Fe(TFPP)Cl) (31 TO) and tetraphenylporphyrinato-iron(III) chloride (Fe(TPP)Cl) (< 1 TO) (Figure 4.6).

The variations in selectivity with Fe(TFPPBr₈)Cl can be explained by invoking different mechanisms for the two oxidants. Iodosobenzene is believed to react with metalloporphyrins to generate a high-valent metal-oxo intermediate, as described above. ³⁰ Indeed, the large percentage of epoxide formed with PhIO and Fe(TFPPBr₈)Cl is consistent with a ferryl as the oxidizing species. The increase in activity from Fe(TFPPBr₈)Cl relative to Fe(TFPP)Cl, however, is not as great as one might predict: the positive E* Fe^{3+/2+} (0.31 V vs. AgCl/Ag)²⁹ of the perhalogenated porphyrin would make an "FeV=O" of this porphyrin high in energy and difficulty to attain.²³ In line with

this prediction, reductive generation of a ferryl (O₂, Zn, H⁺) has been shown to be inefficient for highly halogenated porphyrins.^{31,32} The lower potentials of Fe(TFPP)Cl (-0.08 V)²⁹ and Fe(TPP)Cl (-0.29 V vs. SCE)³³ suggest that a ferryl complex can be generated more readily in these complexes. However, once formed, the ferryl can attack the C-H bonds on other porphyrins, leading to catalyst decomposition and lower net activity with these two complexes.

With dioxygen, the formation of a metal-oxo is not observed. Previously in the literature, ³⁴ the active species was proposed to be (P)Fe^{IV}=O, formed by reaction of dioxygen with (P)Fe^{II} to form a μ-peroxy bridged dimer (Figure 4.7). Homolytic cleavage of the dimer to (P)Fe^{IV}=O would result in dioxygenase-type oxygen activation. ^{27,34,35} With electron-withdrawing porphyrins, it was proposed that an iron(IV)-oxo would have as much oxidizing power as a typical iron(V)-oxo porphyrin. Although the positive reduction potential of Fe(TFPPBr₈)Cl is consistent with this mechanism, the increased stability of the ferrous state causes both the iron(II) and iron(III) oxidation states to be stable to oxygen. A solution of electrochemically generated [Fe^{II}(TFPPBr₈)Cl]- only shows minimal oxidation after several weeks under an O₂ atmosphere, ³⁶ indicating that this pathway is not operative. ²⁹ Attempts to generate an iron(IV)-oxo directly, by addition of iodosobenzene to electrochemically produced [Fe^{II}(TFPPBr₈)Cl]- in methylene chloride, resulted only in immediate conversion to Fe^{III}(TFPPBr₈)Cl.

The possibility of reductive ferryl generation with Fe(TFPPBr₈)Cl is eliminated for several reasons. First, the lack of an added co-reductant allows no mechanism for the reduction of the ferric porphyrin to the ferrous state. Furthermore, [Fe^{II}(TFPPBr₈)Cl]⁻ is stable to dioxygen, meaning that the oxygen binding step from the P-450 cycle does not occur. As mentioned above, reductive ferryl generation has been shown to be inefficient for halogenated iron porphyrins, ^{31,32} suggesting that a high-valent metal-oxo is not

implicated in reactions of Fe(TFPPBr₈)Cl with dioxygen. A mechanism less common to metalloporphyrins must be investigated.

Indeed, the reaction has been shown to involve formation and porphyrin-catalyzed decomposition of alkyl peroxides (Figure 4.8). 29,37 Free radicals present in solution react with oxygen to form alkyl peroxides. The alkyl peroxides, unlike dioxygen, react more readily with highly electron-deficient porphyrins such as Fe(TFPPBr₈)Cl (*vide infra*). The radicals generated by the Fe(TFPPBr₈)Cl-catalyzed peroxide decomposition react with additional molecules of substrate to form the observed products, propagating a radical chain reaction. A plot of moles product produced versus time (Figure 4.5) indicates that the reaction is autocatalytic. Competitive experiments with cyclohexene and cyclohexene- d_{10} show an isotope effect of 8.2, consistent with a mechanism involving hydrogen abstraction in the rate-determining step. Addition of a radical trap, BHT, completely inhibits the reaction. The radical chain mechanism is also consistent with the high percentage of allylic oxidation products observed in the reaction of cyclohexene with dioxygen.

Moreover, this mechanism explains the greater reactivity observed with dioxygen and Fe(TFPPBr8)Cl compared to tetraphenylporphyrinato-iron(III) chloride or tetrakis(pentafluorophenyl)porphyrinato-iron(III) chloride. The electron-withdrawing TFPPBr8 ligand stabilizes the ferrous state, thereby enhancing the rate of alkyl peroxide oxidation. In contrast, the lower reduction potentials of Fe(TFPP)Cl and Fe(TPP)Cl make these species poor oxidants, greatly slowing the ferric \rightarrow ferrous step in the catalytic cycle. Furthermore, as with ferryl complexes, any radicals generated in the presence of Fe(TFPP)Cl or Fe(TPP)Cl may decompose the porphyrin by attacking C-H bonds. Halogenation of the β positions of the porphyrin is also believed to prevent formation of a μ -oxo dimer, which is a mode of deactivation for both Fe(TPP)Cl and Fe(TFPP)Cl in reactions with dioxygen. Thus the perhalogenated porphyrin has a faster rate of catalysis but a lower rate of catalyst degradation in solution

In order to further explore the possibility of an active iron(IV) or iron(V) oxo species, the synthesis of Fe^{III}(TFPPBr₈)OH was attempted. Either chemical oxidants or bulk electrolysis could be used to generate a high-valent metal-oxo from an iron(III) hydroxide porphyrin. The pentafluorophenyl derivative, Fe(TFPP)OH, has been produced by washing Fe(TFPP)Cl with NaOH in benzene. 39 Instead, we attempted to isolate the hydroxide salt directly from the iron insertion reaction. As described in Chapter 2, Fe^{II}(OAc)₂ in glacial acetic acid inserts into H₂TFPPBr₈. The red color and red shifted Soret band of this species (in situ, λ_{max} = 448 and 578 nm) are consistent with formation of Fe^{II}(TFPPBr₈)(OAc)₂. Instead of brine, a weak sodium hydroxide solution was used to quench the metal insertion reaction, which would provide a hydroxide ligand for the iron ion. The porphyrin that precipitated from the reaction was filtered and washed with water; the absorption spectrum of resulting solid has a maximum at 434 and a Q band at 584 nm. The blue shift from Fe(TFPPBr₈)Cl, as well as the shape of the spectrum, is analogous to the change from Fe(TFPP)Cl to Fe(TFPP)OH, suggesting formation of Fe(TFPPBr₈)OH. Purification by column chromatography resulted in a new species, with a Soret at 418, a strong shoulder at 486, and a Q band at 600 nm. This species had the same spectrum as Fe(TFPPBr₈)Cl after 48 hours in a methylene chloride/PhIO solution, and may be the μ -oxo dimer. The blue shift of the Soret band and red shift in the Q bands is again the same as observed in the TFPP complexes. Although modeling has suggested that formation of [Fe(TFPPBr8)]₂O is unfavorable due to poor steric interactions, a weak complex may form. Rather than becoming a permanently unreactive species, however, this dimer may be able to break apart and undergo further reactions, as has been suggested for (FeTFPP)₂O. ⁴⁰ An alternative explanation of catalysis with a μ -oxo dimer is that dimerization protects one side of the porphyrin ligand, allowing oxidation to occur on the opposite side.⁴¹ Attempts to obtain a ¹⁹F NMR of this material were unsuccessful, and due to the small amounts of compound obtained, this chemistry was not further pursued.

Conclusion

Fe(TFPPBr₈)Cl is a remarkably active catalyst for the oxidation of cyclohexene with dioxygen, without added coreductant or light. The mechanism does not involve traditional high-valent metal-oxo intermediates, but interacts through the lower oxidation states of the porphyrin. Catalytic oxidation and reduction of alkyl peroxides by Fe(TFPPBr₈)Cl generates radicals that continue free-radical chemistry in solution.

Other than halogenated porphyrins, only the highly activated porphyrin RuTMP(O)₂ [dioxo(tetramesitylporphyrinato)-ruthenium(VI)] is known to catalyze the aerobic epoxidation of alkenes at ambient temperatures and pressures. Although able to catalyze 26 turnovers of cyclooctene in 24 hours (versus 73 TO of cyclohexene by Fe(TFPPBr₈)Cl), the Ru catalyst decomposes within this time period.⁴² Another electron-deficient porphyrin, β-hexanitro-tetrakis(2,6-dichlorophenyl)porphyrinato iron (III) chloride, has been shown to activate alkanes at higher temperatures and high pressures of O₂.⁴³ Considering the similarity of the two porphyrins, it is likely that they operate by the same peroxide decomposition mechanism. Unfortunately, the exceptional reactivity of Fe(TFPPBr₈)Cl with dioxygen appears to come at the expense of the selectivity found with high-valent metal-oxo species.

Methods

Oxidation reactions were run as follows. 3-4 mg of porphyrin (approximately 2-3 µmol) were added to a clean, oven-dried reaction vessel with a stir bar. For iodosobenzene experiments, 20-30 mg of PhIO were also weighed out into the flask (~ 50 eq PhIO/Fe). The reaction vessel was then fully assembled (Figure 4.9) and flushed from the top with Ar (for PhIO reactions) or O₂, allowing gas to escape through the open stopcock. 15 mL freshly distilled methylene chloride (under Ar or saturated with dioxygen) was added by syringe into the reaction vessel, followed by 1 mL of freshly

distilled substrate. From the solubility of oxygen in methylene chloride and the volume of the flask, the dioxygen reactions were calculated to have approximately 1240 μ mol of O₂, or ~ 450 equivalents based on iron. The Kontes valve and stopcock were then closed, isolating the flask from the external atmosphere. The reactions were stirred for the next 24 - 48 hours, and aliquots taken by syringe every few hours for analysis of oxidation products.

The reactions were carried out in special flasks designed to minimize evaporation from the vessel during a reaction. A stopcock was attached to the side of a 25 mL Kjeldahl flask as shown in Figure 4.9. A hose could be attached to one of the two tubes on the stopcock, such that sample aliquots were not exposed to oxygen, and additional air did not leak into the flasks when an aliquot was removed. Unfortunately, this method prohibited clean kinetic measurements, since the concentration of oxygen in the flask at any given time was unknown. However, the rather excessive caution in sealing the flask was found to be necessary, since experiments run in round bottom flasks sealed only with a rubber septum had evidence of significant evaporation and/or leakage. Even with these precautions, the reaction volume decreased due to evaporation of the volatile solvent, and measurement reliability decreased significantly after 24 hours.

Gas chromatography was performed on a Hewlett Packard with a SD 1 column. Samples were identified by retention times relative to authentic samples. An internal standard (toluene) was added to each aliquot before injection in the GC and used to determine the concentration of each product.

Materials

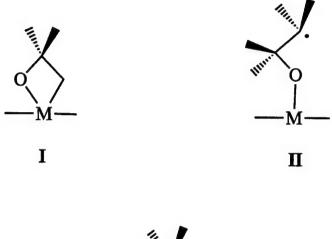
Porphyrins were obtained as described in Chapter 2. Iodosobenzene was purchased from TCI. Some batches were rather yellow in color, and were washed with benzene to remove impurities, with only some success. Methylene chloride, styrene, cyclohexene, *tert*-butyl hydroperoxide, and GC standards were purchased from Aldrich.

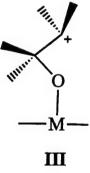
- (23) Traylor, T. G.; Nakano, T.; Dunlap, B. E.; Traylor, P. S.; Dolphin, D. J. Am. Chem. Soc. 1986, 108, 2782-2784.
- (24) Groves, J. T.; Subramanian, D. V. J. Am. Chem. Soc. 1984, 106, 2177-2181.
- (25) Traylor, T. G.; Miksztal, A. R. J. Am. Chem. Soc. 1989, 111, 7443-7448.
- (26) Traylor, T. G.; Xu, F. J. Am. Chem. Soc. 1988, 110, 1953-1958.
- (27) Ellis, P. E., Jr.; Lyons, J. E. Coord. Chem. Rev. 1990, 105, 181-193.
- (28) Lyons, J. E.; Ellis, P. E., Jr. Catal. Lett. 1991, 8, 45-52.
- (29) Grinstaff, M. W.; Hill, M. G.; Labinger, J. A.; Gray, H. B. Science 1994, 264, 1311-1313.
- (30) Smegal, J. A.; Schardt, B. C.; Hill, C. L. J. Am. Chem. Soc. 1983, 105, 3510-3515.
- (31) Ji, L.-N.; Liu, M.; Hsieh, A.-K.; Hor, T. S. A. J. Mol. Catal. 1991, 70, 247-257.
- (32) Lu, W. Y.; Bartoli, J. F.; Battioni, P.; Mansuy, D. New J. Chem. 1992, 16, 621-628.
- (33) Bottomley, L. A.; Kadish, K. M. Inorg. Chem. 1981, 20, 1348-1357.
- (34) Lyons, J. E.; Ellis, P. E., Jr.; Durante, V. A. In Structure-Activity and Selectivity Relationships in Heterogeneous Catalysis; R. K. Grasselli and A. W. Sleight, Eds.; Elsevier Science Publishers B.V.: Amsterdam, 1991; pp 99-116.
- (35) Ellis, P. E., Jr.; Lyons, J. E. J. Chem. Soc., Chem. Commun. 1989, 1315-1316.
- (36) Grinstaff, M. W.; Hill, M. G.; Birnbaum, E. R.; Schaefer, W. P.; Labinger, J. A.; Gray, H. B. submitted to *Inorg. Chem*.
- (37) Labinger, J. A. Catal. Lett. 1994, 26, 95-99.
- (38) Gunter, M. J.; Turner, P. Coord. Chem. Rev. 1991, 108, 115-161.
- (39) Jayaraj, K.; Gold, A.; Toney, G. E.; Helms, J. H.; Hatfield, W. E. *Inorg. Chem.* 1986, 25, 3516-3518.
- (40) Ellis, P. E., Jr.; Lyons, J. E. Catal. Lett. 1989, 3, 389-398.
- (41) Chang, C. K.; Kuo, M.-S. J. Am. Chem. Soc. 1979, 101, 3413-3415.
- (42) Groves, J. T.; Quinn, R. J. Am. Chem. Soc. 1985, 107, 5790-5792.
- (43) Bartoli, J. F.; Battioni, P.; Foor, W. R. D.; Mansuy, D. J. Chem. Soc., Chem. Commun. 1994, 23-24.

References

- (1) Groves, J. T.; Nemo, T. E.; Myers, R. S. J. Am. Chem. Soc. 1979, 101, 1032-1033.
- (2) Meunier, B. Chem. Rev. 1992, 92, 1411-1456.
- (3) Smith, J. L.; Sleath, P. J. Chem. Soc., Perkin Trans. 2 1982, 1009-1014.
- (4) Traylor, T. G.; Tsuchiya, S. Inorg. Chem. 1987, 26, 1338-1339.
- (5) Traylor, P. S.; Dolphin, D.; Traylor, T. G. J. Chem. Soc., Chem. Commun. 1984, 279-280.
- (6) Groves, J. T.; Quinn, R. Inorg. Chem. 1984, 23, 3844-3846.
- (7) Chang, C. K.; Ebina, F. J. Chem. Soc., Chem. Commun. 1981, 778-779.
- (8) Bartoli, J. F.; Brigaud, O.; Battioni, P.; Mansuy, D. J. Chem. Soc., Chem. Commun. 1991, 440-442.
- (9) Traylor, T. G.; Hill, K. W.; Fann, W.; Tsuchiya, S.; Dunlap, B. E. J. Am. Chem. Soc. 1992, 114, 1308-1312.
- (10) Assis, M. d. D.; Serra, O. A.; Iamamoto, Y.; Nascimento, O. R. Inorg. Chim. Acta 1987, 187, 107-114.
- (11) Iamamoto, Y.; Assis, M. d. D.; Baffa, O.; Nakagaki, S.; Nascimento, O. R. J. Inorg. Biochem. 1993, 52, 191-200.
- (12) Fujii, H. J. Am. Chem. Soc. 1993, 115, 4641-4648.
- (13) Groves, J. T.; Watanabe, Y. J. Am. Chem. Soc. 1986, 108, 507-508.
- (14) Groves, J. T.; Haushalter, R. C.; Nakamura, M.; Nemo, T. E.; Evans, B. J. J. Am. Chem. Soc. 1981, 103, 2884-2886.
- (15) Hewson, W. D.; Hager, L. P. Porphyrins 1979, 7, 295-315.
- (16) Penner-Hahn, J. E.; Eble, K. S.; McMurry, T. J.; Renner, M.; Balch, A. L.; Groves, J. T.; Dawson, J. H.; Hodgson, K. O. J. Am. Chem. Soc. 1986, 108, 7819-7825.
- (17) He, G.-X.; Arasasingham, R. D.; Zhang, G.-H.; Bruice, T. C. J. Am. Chem. Soc. 1991, 113, 9828-9833.
- (18) Groves, J. T.; W. J. Kruper, J. J. Am. Chem. Soc. 1979, 101, 7613-7615.
- (19) Ostovic, D.; Bruice, T. C. Acc. Chem. Res. 1992, 25, 314-320.
- (20) Ostovic, D.; Bruice, T. C. J. Am. Chem. Soc. 1988, 110, 6906-6908.
- (21) Ostovic, D.; Bruice, T. C. J. Am. Chem. Soc. 1989, 111, 6511-6517.
- (22) Naruta, Y.; Tani, F.; Ishihara, B.; Maruyama, K. J. Am. Chem. Soc. 1991, 113, 6865-6872.

Figure 4.1 -- Intermediates that have been proposed in the literature for epoxidation by a high-valent metal-oxo. The metallaoxetane (I) and carbon radical (II) have been ruled out by recent experiments (see text), although this is not universally accepted. The carbocation (III) and carbocation radical (IV) are still considered viable intermediates, as is concerted oxygen insertion (V).





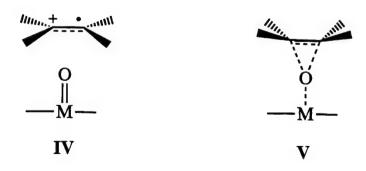


Figure 4.2 -- A proposed mechanism for epoxidation where the rate limiting step involves association of the olefin with the metal-oxo to form a charge transfer complex (CT). The CT can form an epoxide by concerted oxygen insertion, electrophillic addition, or electron transfer (shown from left to right). The carbocation radical (IV) can either recombine and form an epoxide, or continue on a radical pathway leading to hydroxylation or other rearrangement products. Mechanism modified from reference 19.

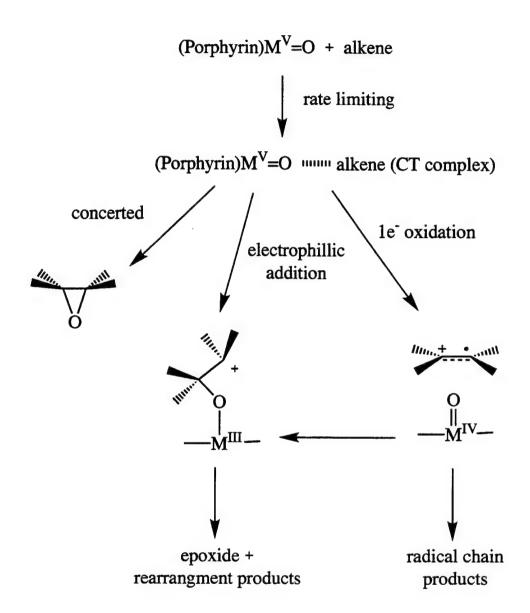


Figure 4.3 -- Multiple pathways are believed to be responsible for epoxidation and hydroxylation of cyclohexene. Hydroxylation is generally believed to occur via hydrogen abstraction. In addition to the electron-transfer epoxidation mechanism shown, direct oxygen insertion may also occur. The branching ratio is dependent on the nature of the olefin, the porphyrin, and the solvent.

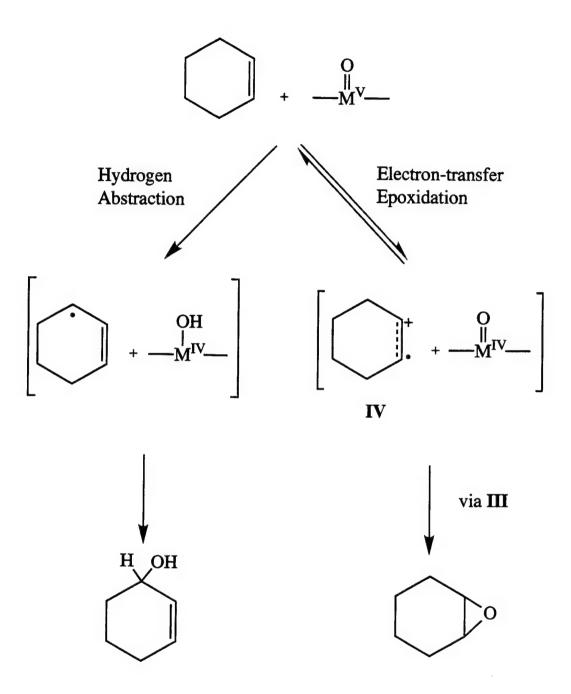


Figure 4.4 -- Turnovers and product distributions with cyclohexene and iron(III) porphyrins with dioxygen (at 3 hours) and PhIO (at 4 hours).

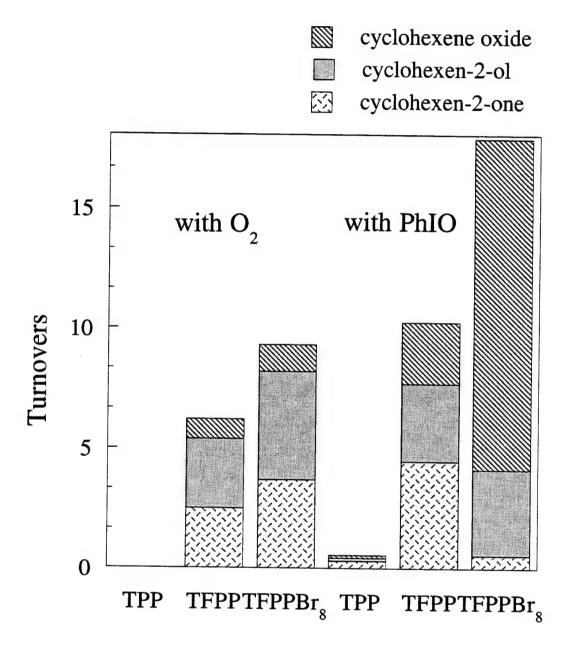


Figure 4.5 — Product formation during cyclohexene oxidation with Fe(TFPPBr₈)Cl and dioxygen. The curvature of the plot indicates the autocatalytic nature of the reaction.

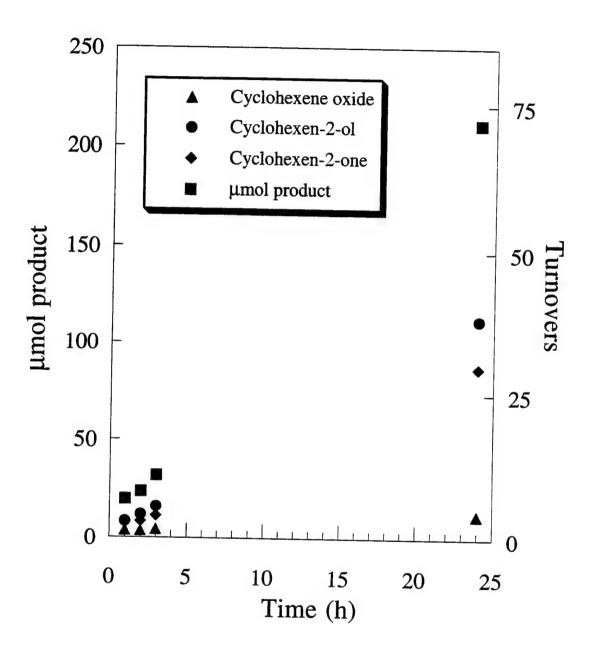


Figure 4.6 -- A plot of the catalytic activity (turnovers at 24 hours) observed for cyclohexene oxidation with dioxygen versus the reduction potential of the iron(III)-porphyrin catalyst (E* values: Fe(TPP)Cl < Fe(TFPP)Cl < Fe(TFPPBr₈)Cl).

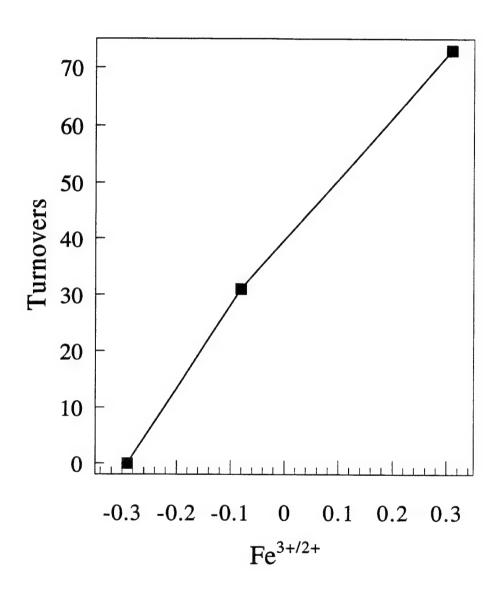
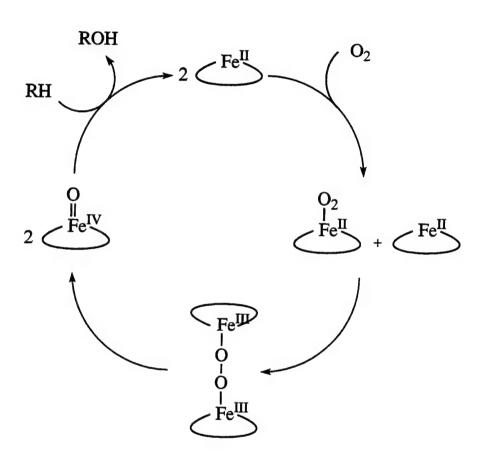


Figure 4.7 -- A proposed mechanism for direct activation of dioxygen initiated by oxygen binding to a ferrous porphyrin (modified from reference 34). The positive electrochemical potential (Fe^{2+/3+}) of the halogenated iron porphyrins were proposed to generate an iron(IV) oxo of comparable activity to that of a biological iron(V) oxo.



$$egreentering Fe^{II} = Fe^{II}(TFPPBr_8)$$

Figure 4.8 -- The alkyl peroxide decomposition mechanism for dioxygen reactions with Fe(TFPPBr₈)Cl. Initiated by radicals in solution, the peroxides thereby generated are catalytically decomposed by the iron porphyrin. These radicals can further propagate the reaction.

Initiation by radicals present in solution.

$$R \cdot + O_2 \longrightarrow ROO \cdot$$
 $ROO \cdot + RH \longrightarrow ROOH + R \cdot$

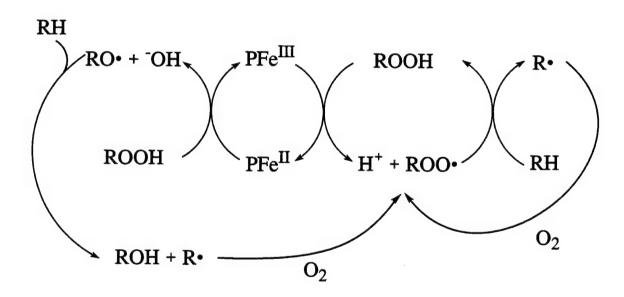
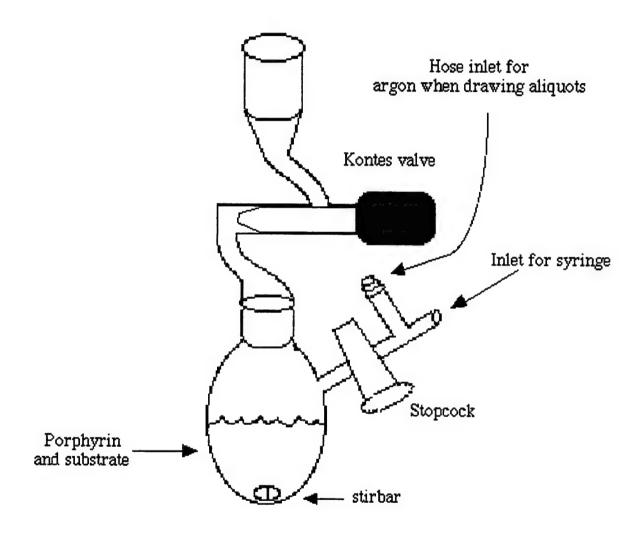


Figure 4.9 -- The modified Kjeldahl flask used for oxidation reactions. The porphyrin and iodosobenzene are added dry, then solvent and substrate are added.

Aliquots can be removed without exposing the sample to air.

\$24/40 Joint, Could evacuate on a vacuum line or flush with argon or dioxygen.



Chapter 5

On the Mechanism of Alkene Oxidation by Ruthenium Porphyrins and Molecular Oxygen

Introduction

As described in the preceding chapter, iron tetraphenylporphyrin derivatives are catalysts for the oxidation of alkenes and alkanes with oxygen donors. A smaller number of ruthenium porphyrins have also been synthesized to further explore biomimetic metalloporphyrin oxidation chemistry. Although a few have been investigated as oxidation catalysts, a greater portion of work has focused on using ruthenium porphyrins as model complexes for iron porphyrins or as systems for dihydrogen or dinitrogen activation. For example, cofacial ruthenium porphyrin dimers have been shown to bind dihydrogen in the core between the two porphyrin molecules. ¹

Ruthenium porphyrins are commonly isolated as six-coordinate $Ru^{II}(porphyrin)L_2$ species with $2e^-$ donor ligands such as pyridine or CO as compared to five-coordinate $Fe^{III}(porphyrin)X$ complexes. Greater ligand field stabilization energy for the second row metal and π bonding from π acid ligands give ruthenium(II) porphyrins greater stability relative to iron hemes.² This increase in stability is exploited for mechanistic investigations, as intermediates in ruthenium oxidation reactions, such as $(P)Ru^{IV}=O$, can be isolated and better characterized than the corresponding iron porphyrin species. Furthermore, comparisons of iron, ruthenium, and osmium porphyrin spectroscopy have been useful in determining orbital energies in iron porphyrin compounds.³⁻⁹

Ruthenium tetramesitylporphyrins have been investigated as catalysts for the oxidation of hydrocarbons. Groves 10 found that RuTMP(CO) is oxidized to RuVITMP(O)₂ with two equivalents of m-chloroperoxybenzoic acid (mCPBA). This species is moderately stable, and has been characterized by NMR, elemental analysis, and

UV-Vis spectroscopy. The ruthenium dioxo porphyrin complex is a competent stoichiometric oxidant of norbornene, resulting in 1.6 equivalents (eq) norbornene oxide per mole of porphyrin and a solvated Ru^{II}TMP complex. ¹¹ Transfer of the first oxygen occurs more readily than the second, indicating that the monooxo complex is not as effective an oxo transfer agent as the dioxo complex. ¹² However, various N-oxides have been used as O-atom donors with Ru^{VI}TMP(O)₂ to catalytically oxidize alkenes ^{13,14} and alkanes ¹⁵ in good yields (30-90% based on N-oxide).

The carbonyl complexes RuTMP(CO), RuTPP(CO), RuOEP(CO) and RuTDFPP(CO) (TDFPP = 2,6-difluororphenylporphyrin) are also observed to catalyze hydrocarbon oxidation. ^{15,16} With *tert*-butyl hydroperoxide (TBHP) or sodium hypochlorite as the oxidant, over 100 turnovers of styrene in 24 hours are reported for RuTDFPP(CO), and even higher activity was reported with RuOEP(CO). ¹⁶ RuTMP(CO) and RuTPP(CO) do not show activity until addition of strong acid to the solution; once activated, both porphyrins catalyze the oxidation of adamantane with 2,6-dichloropyridine N-oxide. Activity is higher when the dioxo complex is used. ¹⁵ No mechanism was proposed to explain either the high activity with planar, unhalogenated OEP, or the "activation" of the carbonyl porphyrins by acid.

In addition to catalysis observed with N-oxides and peroxides, the dioxo ruthenium porphyrins are a unique example of porphyrin catalysis with dioxygen but without addition of a coreductant. RuVITMP(O)₂ catalyzes the aerobic oxidation of olefins under mild conditions. ¹¹ The proposed mechanism (Figure 5.1) suggests that RuIVTMP(O), formed upon a single oxidation of substrate, disproportionates to reform the active RuVI species and a solvated ruthenium(II) porphyrin, RuIITMP(S)₂. ¹² The weakly coordinated ruthenium(II) reacts with O₂ to complete the cycle. While other porphyrins such as RuVIOEP(O)₂ and RuVITPP(O)₂ share the ability to stoichiometrically oxidize alkenes, the less sterically bulky compounds dimerize to (RuIVP(OH))₂O rather than reform RuVIP(O)₂ in the presence of dioxygen. ^{17,18}

RuTMP(O)₂ has been utilized as a catalyst for the aerobic oxidation of thioethers, steroids, and esters. ¹⁹⁻²² Although these papers describe catalysis by RuTMP(O)₂ in good yield, few experiments have been conducted to probe the validity of the initially proposed Groves mechanism (Figure 5.1). Furthermore, there has been little comment on the unusual ability to activate dioxygen in combination with the inability of this species to oxidize alkanes. The mechanism of RuP(CO) activation by strong acid, or the possibility of a different mechanism with N-oxides (versus dioxygen) have also not been adequately addressed. In summary, although some of the extremely interesting and unique chemistry displayed by ruthenium porphyrins has been noted, little of it is well understood.

Our investigations into oxidation catalysis with perhalogenated iron porphyrins (Chapter 4) led to the synthesis and characterization of a perhalogenated ruthenium porphyrin complex, β-octachloro-tetrakis(pentafluorophenyl)porphyrinato-ruthenium(II) carbonyl (RuTFPPCl₈(CO)) (Chapters 2 and 3). Initially, the ruthenium porphyrin was to be used to generate stable ruthenium analogs to iron peroxy intermediates proposed in the decomposition of alkyl peroxides by Fe(TFPPBr₈)Cl, allowing a better understanding of the iron oxidation mechanism. Alternatively, the halogenated porphyrin could share the unusual reactivity of Ru^{II}TMP with dioxygen. Catalytic activity in iron porphyrins has been shown to increase with the anodic shift in the iron reduction potential, suggesting that a halogenated ruthenium porphyrin may show higher activity than RuTMP. Indeed, RuTFPPCl₈(CO) is an extremely active catalyst for olefin oxidation with dioxygen. The mechanism does not appear to be related to either the other halogenated metalloporphyrins or the unhalogenated ruthenium porphyrins, but is unique to RuTFPPCl₈(CO).

Results

RuTFPPCl₈(CO) is an efficient catalyst for the oxidation of alkenes with PhIO or molecular oxygen. The oxidation reactions were run under comparable conditions to those with Fe(TFPPBr₈)Cl described in Chapter 4. Each reaction was initiated by addition of 1 mL substrate to 15 mL of a 0.1 mM solution of RuTFPPCl₈(CO) in methylene chloride. The reaction vessel (Figure 4.9) also contained 40 equivalents iodosobenzene under argon, or if O₂ was the oxygen source, the solution and head space in the reaction vessel were saturated with dioxygen. Aliquots were taken every 2 hours and products detected by GC.

Iodosobenzene is not a very efficient oxygen source for cyclohexene oxidation with RuTFPPCl₈(CO) (Figure 5.2, Table 5.1). Only 10 turnovers are observed in 24 hours, with formation of 42% epoxide. The selectivity for epoxide is less than with Fe(TFPPBr₈)Cl, but a notable lack of ketone is produced (< 2%). The reaction rate is highest initially, tapering off after the first 6 hours. The UV-Vis spectrum remains unchanged at the end of 24 hours, indicating that the decrease in rate is not due to porphyrin decomposition. Styrene is better oxidized by iodosobenzene and RuTFPPCl₈(CO), with 26 turnovers in only 3 hours, 81% of which are styrene oxide.

The high selectivity for epoxidation observed with PhIO and RuTFPPCl₈(CO) is consistent with formation of Ru^{IV}TFPPCl₈(O). As described in Chapter 4, iodosobenzene reacts with metalloporphyrins to form a metal-oxo intermediate. In the presence of olefin, the oxo species forms a charge transfer complex that may lead to epoxidation via concerted oxene transfer or electrophillic addition to the carbon-carbon double bond (Figure 4.3). The decreased activity for cyclohexene oxidation by Ru^{IV}TFPPCl₈(O) relative to "Fe^V(TFPPBr₈)Cl(O)" is not surprising, since the ruthenium porphyrin is one oxidation state lower than the iron analog.

Activity with dioxygen is quite substantial (Table 5.1). In 24 hours, 42 equivalents of cyclooctene are epoxidized to cyclooctene oxide. Benzaldehyde is the

sole product of styrene oxidation, producing only 2.5 turnovers in 3 hours. The greatest activity is seen in the oxidation of cyclohexene; 296 turnovers consisting of cyclohexene oxide (15%), 2-cyclohexen-1-ol (58%) and 2-cyclohexen-1-one (27%) are observed in 24 hours (Figure 5.3).

The mechanism with dioxygen is not as obvious. The different product selectivity observed in oxidation of both styrene and cyclohexene with dioxygen versus iodosobenzene suggests there is a different mechanism for the two O-atom sources. The increased amount of allylic and carbon-carbon bond cleavage oxidation products suggests that the mechanism with O₂ has a substantial radical contribution. Since reactions with PhIO are believed to go through a Ru^{IV} oxo intermediate, a different oxidizing species must be generated upon reaction with O₂. Unfortunately, the difficulty in obtaining large quantities of porphyrin has precluded the direct observation of intermediates in the dioxygen reactions. Instead, indirect methods have been used to probe the reaction mechanism. As many modes of interaction between oxygen and the porphyrin are possible, we have tried to test the viability of the most likely candidates.

A simple, direct method of dioxygen activation mimics dioxygenase rather than monooxygenase activity (Figure 4.7). Such a mechanism, initially proposed to explain oxidations with highly halogenated iron porphyrins,²³ is even more attractive for the ruthenium analogs, since no addition of coreductant would be required to initiate the cycle. Oxygen binds to RuTFPPClg(CO), which reacts with another porphyrin molecule to form a μ-peroxo dimer, (TFPPClg)Ru^{III}-O-O-Ru^{III}(TFPPClg). Homolytic O-O bond cleavage forms the active oxidant, Ru^{IV} monooxo, which returns to the catalyst resting state after oxidizing substrate. This mechanism is unlikely for two reasons. First, cleavage of the μ-peroxo bond to form (P)Ru^{IV}=O would produce the same oxidizing species as PhIO, and would therefore be expected to yield the same product distribution. This mechanism does not allow for the different selectivity observed with different oxidants. Furthermore, Ru^{II}TFPPClg(CO) is air stable and shows no reaction with

dioxygen, even upon recrystallization from an air saturated solution. Thus the first step in the cycle does not occur.

A second possibility is that RuTFPPCl₈(CO) and Fe(TFPPBr₈)Cl operate by the same mechanism with oxygen (Figure 4.8). A plot of moles of cyclohexene product versus time for catalysis by RuTFPPCl₈(CO) (Figure 5.3) shows a slight curvature, suggesting some initiation for this catalyst, although not as significant as observed for the iron analog. More importantly, no metal couple is accessible in the ruthenium porphyrin electrochemistry (Chapter 3), so no orbital of reasonable energy is available to transfer electrons to or from an alkyl peroxide.

The best evidence that RuTFPPClg(CO) does not operate by an alkyl peroxide decomposition mechanism, however, is that it does not decompose peroxides at an appreciable rate. Fe(TFPPBrg)Cl has been shown to rapidly decompose *tert*-butyl hydroperoxide^{24,25}; when TBHP is added to a solution of Fe(TFPPBrg)Cl, oxygen is vigorously evolved. A similar concentration of RuTFPPClg(CO) does not exhibit a visible reaction. A more sensitive analysis of hydrogen peroxide decomposition shows that the ruthenium porphyrin only decomposes 4.5 equivalents of peroxide in four hours, as measured by oxygen evolution. The iron porphyrin is much more efficient, with 68 turnovers in the same time period (Figure 5.4). The opposite relative activity is observed for cyclohexene oxidation with dioxygen, where RuTFPPClg(CO) catalyzes 296 turnovers compared to only 73 by Fe(TFPPBrg)Cl in 24 hours. A purely radical peroxide decomposition mechanism is not consistent with these observations.

A third possibility is that this catalyst mimics the behavior of RuTMP(CO) with oxygen. A RuVI dioxo complex would be expected to exhibit different reactivity than a monooxo, thus resolving the problem of dissimilarity with the iodosobenzene results. Therefore an attempt was made to reproduce the Groves cycle with RuTFPPCl₈(CO). As in the conversion of RuTMP(CO) to RuVITMP(O)₂, ¹⁰ careful titration of a solution of RuTFPPCl₈(CO) with mCPBA resulted in complete formation of a new species

 $(\lambda_{max} = 420, 514, 552 \text{ nm})$ after addition of two equivalents peroxide (Figure 5.5). Isosbestic points at 390, 417, 525, and 585 nm indicate that only a single species is formed. The slight red shift in the Soret band and the blue shift in the Q bands are consistent with spectral changes observed in the oxidation of RuOEP(CO) to RuOEP(O)₂, ¹⁸ suggesting that Ru^{VI}TFPPCl₈(O)₂ is formed. The disappearance of the carbonyl stretch in the IR indicates removal of the CO ligand, but no strong stretch is observable in the 700 to 900 cm⁻¹ region, as would be expected for a ruthenium oxo. ^{12,18} However, this region contains strong solvent stretches, making detection of $v_{Ru=O}$ difficult by solution infrared spectroscopy.

The anodically shifted reduction potentials of RuTFPPCl₈(CO) would destabilize the higher oxidation states relative to those of RuTPP complexes, making RuVITFPPCl8(O)2 extremely reactive. In line with this expectation, any attempt to concentrate or isolate this species led to decomposition to a variety of porphyrin products. However, at low concentrations, such as in a range where UV-Visible spectroscopy of the porphyrin ligand is feasible $(1 - 10 \mu M)$, the steps of the catalytic cycle can be observed (Figure 5.6). Addition of mCPBA to form RuVITFPPCl₈(O)₂, followed by addition of a small amount of cyclohexene, results in a large decrease in the intensity of both the Soret and Q band absorptions. The bleach is not due to porphyrin decomposition, because addition of carbon monoxide gas regenerates the original spectrum with over 85% of the original intensity. The new spectrum is similar to that of Ru^{IV}OEP(O)²⁶ or Ru^{IV}TPP(O), ¹⁷ with a slight blue shift in the Soret band and broad absorptions in the Q band region relative to the dioxo complex, suggesting formation of Ru^{IV}TFPPCl₈(O). Increased recovery of the Soret band after 24 hours in the presence of substrate could indicate transfer of the second oxo ligand from Ru^{IV}TFPPCl₈(O) to form another molecule of oxidized substrate and Ru^{II}TFPPCl₈(S)₂. Unfortunately, the amount of product generated was too small to be detected by the GC method used for the general catalysis experiments, and oxo-transfer to the olefin could not be confirmed.²⁷

Oxidation of triphenylphosphine to triphenylphosphine oxide can be confirmed by ³¹P NMR. Addition of two equivalents PPh₃ to a solution of Ru^{VI}TFPPCl₈(O)₂ led to a decrease in the 514 nm band and the 600 nm tailing associated with dioxo formation, and new Q bands at 542 and 553 nm (Figure 5.7a). Continued addition of PPh₃ resulted in a blue shift of the Q bands to 517 and 540 nm, which may correspond to the coordination of triphenylphosphine to Ru^{II}TFPPCl₈ (Figure 5.7b). These two steps are believed to correspond to oxidation of 2 eq PPh₃ by the dioxo porphyrin followed by coordination of PPh₃ to the solvated ruthenium(II) porphyrin.

The ³¹P NMR of this sample after the reaction is complete does show a resonance for Ph₃PO at 29.9 ppm. A second signal, consistent with PPh₃ coordination to Ru^{II}, appears at 40 ppm in the ³¹P NMR (no signal is observed at -6 ppm for free triphenyl-phosphine). For example, Ru(COOMe)₂(CO)₂PPh₃ has a chemical shift of 30.5 ppm.²⁸ Although the UV-Vis showed isosbestic conversion to "RuTFPPCl₈(PPh₃)₂", the ¹⁹F NMR was not clean, indicating that coordination of triphenylphosphine is not quantitative. Additional peaks in the ¹⁹F NMR may be due to partial degradation of the porphyrin ligand after treatment with a harsh oxidant such as mCPBA.

Addition of styrene to a solution of RuVITFPPCl₈(O)₂ led to similar spectroscopic changes, indicating that the decrease in Soret intensity ("oxo transfer") is not dependent on the substrate. In the absence of a potential ligand, the Soret bleach was even more pronounced. Addition of a small amount of pyridine to this solution led to the formation of RuTFPPCl₈(py)₂ (confirmed by UV-Vis). The ease of formation of the bis-pyridine adduct is consistent with oxidation of substrate by RuVITFPPCl₈(O)₂ to form RuIITFPPCl₈(S)₂ that is able to coordinate an available ligand.

These experiments suggest that RuTFPPCl₈(CO) can undergo Groves type chemistry. The catalytic oxidation reactions with O₂, however, were conducted without any additional oxidant, allowing no mechanism for the initial formation of RuVITFPPCl₈(O)₂ from the carbonyl species. In addition, oxo transfer is generally

accepted to be more selective than the catalysis observed in the dioxygen reactions.

Although Groves chemistry is possible, it does not seem probable for the main mechanism for catalysis by RuTFPPCl₈(CO) with dioxygen.

Therefore a modified mechanism is proposed, which reacts through the lower oxidation states, involving both a monooxo and a peroxo intermediate. As mentioned above, RuIVTMP(O) is a weak oxo transfer agent; the more electron-withdrawing TFPPClg ligand would be expected to result in a much more reactive monooxo complex. The reaction is initiated by a slow loss of CO (Figure 5.8). The solvated ruthenium(II) porphyrin, without the strong π acid effect of the carbonyl, would have a much lower Ru^{III/II} couple, increasing the possibility of a reaction with dioxygen. Instead of forming Ru^{IV}TFPPCl₈(O), as in the direct oxygen activation mechanism (Figure 4.7), the ruthenium(II) dioxygen complex could rearrange to a ruthenium peroxo species that can react with substrate. The peroxide intermediate can either abstract a hydrogen atom from substrate to form Ru^{III}TFPPCl₈(OOH) or attack olefin to epoxidize one substrate molecule and form Ru^{IV}TFPPCl₈(O). The branching at this point in the mechanism would accommodate the observation of allylic oxidation products from escape of R. which could initiate a free radical reaction. Decomposition of the alkyl peroxide radical to product and RuTFPPClg(O) would result in a larger amount of epoxide formation relative to the purely radical alkyl peroxide mechanism of Fe(TFPPBrg)Cl. This mechanism is similar to one proposed for stoichiometric oxidation by vanadium(V) peroxo complexes where a mixture of epoxidation and hydroxylation was observed.²⁹

The modified peroxo intermediate mechanism does implicate an initiation period for the catalyst, as loss of the carbonyl ligand is required before interaction with dioxygen can occur. Chemical removal of the carbonyl ligand should abolish the initiation period and increase the amount of active catalyst, resulting in higher overall product formation. However, addition of a small amount of triethylamine-N-oxide (10 eq) or mCPBA (5-10 eq) to remove the carbonyl ligand did not increase the rate of reaction. The oxidation

reactions were initiated by addition of oxygen and cyclohexene to a solution of RuTFPPCl₈(CO) and (Et)₃NO or mCPBA. No change in the rate of catalysis was observed with triethylamine-N-oxide (Figure 5.9), though the product distribution was much more similar to that of Fe(TFPPBr₈)Cl with dioxygen, with only 6% epoxide and 59% 2-cyclohexen-1-ol. The porphyrin spectrum was also affected by addition of (Et)₃NO. The Q band absorptions grew in intensity and moved to 510 and 535 nm, similar to the spectrum of RuTFPPCl₈(py)₂, suggesting that triethylamine may bind to ruthenium.

Reactions with mCPBA were substantially different; only 20 turnovers were observed, all within the first 2 hours. More epoxide was produced: 35% versus 15% with dioxygen alone. The lack of products suggests that the catalyst deactivated, although the spectrum was unchanged. It is possible that RuIITFPPCl8(L)2 remaining after the reaction with mCPBA dimerizes or forms another porphyrin product with a Soret at similar energy to RuTFPPC18(CO). Although titrations with mCPBA suggest relatively stable formation of RuVITFPPCl8(O)2, the catalysis experiments are run at significantly higher concentration of porphyrin (> 25 X). The lack of activity suggests that the carbonyl free porphyrin is not stable at higher concentrations, and perhaps dimerizes to a catalytically inactive species. In a normal cyclohexene oxidation reaction, only a small amount of ruthenium porphyrin is an active catalyst (has lost CO) at any given time. Therefore the concentration of Ru^{IV}TFPPCl₈(O) is quite low, and reacts with substrate before deactivation (via dimerization) can occur. Alternatively, the mechanism proposed in Figure 5.9 may be incorrect; the carbonyl ligand may remain on the ruthenium for the duration of the reaction, and activation of the catalyst occurs by some other means.

Addition of TBHP could also serve to initiate the reaction. Unlike mCPBA,
TBHP is not a strong enough oxidant to remove the carbonyl ligand. However, it is
capable of generating free radicals, and could initiate a radical based reaction in solution.

Addition of 10 equivalents TBHP to a solution of RuTFPPCl₈(CO) in the presence of cyclohexene and O₂ results in no increase in the number of moles of products produced (Figure 5.10a). The product distribution in these reactions is the same as with dioxygen alone.

If a larger amount of TBHP is added, the reaction is much faster, with 200 turnovers in the first hour. The product distribution is also significantly different, with 10% epoxide and 50% 2-cyclohexen-1-ol throughout the run. It is not clear if the porphyrin is involved in this chemistry, or if the TBHP has simply initiated a free radical reaction. If the data is replotted in terms of turnovers, then a significant increase in rate is observed with either 10 or 300 equivalents of TBHP (Figure 5.10b). Interpretation of this result is complicated by the fact that only 50% as much porphyrin catalyst was used in the peroxide experiment.

Phase transfer of dioxygen into the solution is not rate limiting. Although solubility of dioxygen in methylene chloride is only 10 mM, this does not limit the reaction rate. A decrease in the stir rate (Figure 5.11) or even a complete lack of stirring does not curtail the rate of product formation. In fact, as seen in Figure 5.11, the slower stirred reaction showed more turnovers in an equal time period. A completely unstirred reaction also showed slightly higher activity, suggesting that a lower concentration of oxygen in solution may enhance reactivity.

A further test of the peroxo mechanism used the presence of additional carbon monoxide to inhibit the reaction. If catalyst activation involves spontaneous loss of CO, exposure to a carbon monoxide atmosphere should shut down catalysis by pushing the equilibrium towards the inactive CO bound form. As mentioned above, both UV-Vis and IR spectroscopy indicate that the carbonyl ligand remains bound both during and after a catalytic run. However, the presence of a small amount of ruthenium porphyrin without CO would be difficult to detect by these methods. To further explore the role of the carbonyl ligand, oxidation of cyclohexene by RuTFPPCl₈(CO) was conducted under a

mixture of oxygen and carbon monoxide. Rather than preventing oxidation, identical rates of product formation were observed under a $50/50 \, \text{O}_2/\text{CO}$ atmosphere. The mixed atmosphere reaction only produced less product at the 24 hour time point, since only half as much total oxygen was in the reaction vessel (Figure 5.12).

The lack of inhibition by CO, while not encouraging, does not completely rule out the loss of CO as the first step in the reaction mechanism. As described above, if the carbonyl ligand is never lost, the subsequent reaction with dioxygen would never occur. However, if the reaction with dioxygen is much faster than recombination with carbon monoxide, some ruthenium porphyrin would remain active, allowing oxidation chemistry to take place in the presence of CO. However, it is surprising that absolutely no decrease in rate is observed.

A more interesting result from the mixed atmosphere experiments is the decrease in epoxide formation. At 24 hours, epoxide comprises only 7% of the total products, compared to 15% in a pure dioxygen environment. The decrease in epoxidation is offset by an increase in the amount of 2-cyclohexen-1-one to 36%. A possible explanation for the change in product distribution is that multiple oxidation pathways with dioxygen are available, and one that favors epoxidation is inhibited by carbon monoxide, while the other is not.

To insure that a small amount of uncarbonylated porphyrin is not present, a sample was exposed to a high pressure of CO. A small amount of RuTFPPCl₈(CO) in CCl₄ or CH₂Cl₂ was placed into a Parr reactor and sealed under 1100 psi of carbon monoxide for 2 or 4 days. The pressure was released from the Parr bomb, and a measured amount of the porphyrin solution (containing ~ 2 µmol porphyrin) was injected directly into a solution of methylene chloride and cyclohexene to initiate a dioxygen catalysis reaction. Some carbon monoxide remained in the porphyrin solution, but as the mixed atmosphere experiments demonstrated, the presence of a small amount of CO does not inhibit the oxidation reaction.

Catalysis with the CO treated RuTFPPCl₈(CO), however, had an extremely long initiation period. In 24 hours, only ten turnovers are observed, composed entirely of allylic oxidation products. By 48 hours, the reaction has fully initiated, with 238 turnovers comprised of 7% epoxide, 53% 2-cyclohexen-1-ol, and 40% 2-cyclohexen-one, similar to the product distribution observed in the mixed atmosphere reactions.

Spectroscopy of the CO treated porphyrin showed that the porphyrin had been modified during the long exposure to CO. The infrared spectrum of the porphyrin shows a new peak at 2112 cm⁻¹ in addition to the peak assigned to the CO stretch of monocarbonyl complex at 1981 cm⁻¹. The shift of V_{CO} to higher energy is consistent with formation of RuTFPPCl₈(CO)₂; calculations indicate that a single CO stretch is expected for the bis-carbonyl porphyrin (approximating the porphyrin as D_{2d} symmetry). An intense peak also appeared in the IR spectrum at 1730 cm⁻¹, as discussed below.

The UV-Vis spectrum in either methylene chloride or carbon tetrachloride showed a slight red shift of the Soret to 420 nm and a slight blue shift and broadening of the Q bands (Figure 5.13). A strong absorption was also observed at 280 nm, but is not believed to be related to the porphyrin, since it appeared at different intensity relative to the porphyrin bands in the two runs. The high energy electronic transition and the 1730 cm⁻¹ IR band are consistent with signals from a ketone. It is possible that some reaction between the reactive halogenated solvent and carbon monoxide could have occurred, resulting in formation of an acyl chloride or halogenated ketone. Low molecular weight acyl chlorides have a strong absorption around 1800 cm⁻¹, while halogenated ketones are at slightly lower energy. ¹H NMR of the carbon tetrachloride solution after removal from the Parr reactor showed a weak resonance at 4.3 ppm; chloroacetyl chloride has a chemical shift of 4.6 ppm. Unfortunately, it is impossible to do more than speculate on the source of these organic-type absorptions. However, repurification of the porphyrin by column chromotography does remove the 280 nm band from the UV-Vis and the 2112 cm⁻¹ band from the IR. The purified porphyrin regains

catalytic activity, suggesting that chromotography removes the second CO from the ruthenium. In the absence of another axial ligand to displace the second carbonyl, such as water or acetone available in the usual post-synthesis workup, the second carbonyl ligand remains bound. The bis-carbonyl complex has no coordination sites available for chemistry, and no catalysis is observed. The pressure experiments suggest some interesting activation of CO under high pressures, but do not elucidate the role of the carbonyl ligand in catalysis.

Oxidation reactions with cyclohexene- d_{10} show a large isotope effect in reactions with dioxygen (Figure 5.14). In competitive experiments with equal amounts of deuterated and non-deuterated cyclohexene, the ratio of products at 24 hours gives an isotope effect of 7.0. The product distribution indicates a significant difference between epoxidation and allylic oxidation. Epoxide formation has no isotope effect (ratio = 1.0), 2-cyclohexen-1-ol has an isotope effect of 14.1, and the isotope effect for 2-cyclohexen-1-one formation is twice that number (29.5), suggesting that different processes are responsible for epoxidation and hydroxylation. Both the total isotope effect (8.2) and the individual isotope effects (1.15 for epoxidation, 9.2 and 19.3 for allylic oxidation) are of similar magnitude to those of Fe(TFPPBr₈)Cl, suggesting that hydrogen abstraction is involved in the rate determining step.

Non-competitive experiments reveal that the two cases are not the same. With Fe(TFPPBrg)Cl, no reaction was seen with cyclohexene- d_{10} alone. Presumably, spontaneous radical formation from deuterated cyclohexene is slow due to the stronger C-D bond, and the reaction is never initiated. With RuTFPPClg(CO), however, some reaction with cyclohexene- d_{10} was observed, indicating that the ruthenium porphyrin does not initiate solely by the same mechanism as the iron porphyrin. The non-competitive isotope effect is extremely large, (mol cyclohexene products)/(mol cyclohexene- d_{10} products) = 85. A large non-competitive isotope effect (50) has been reported for the oxidation of alcohols by $[(bpy)_2(py)Ru^{IV}(O)]^{2+}$. The mechanism

involves hydride transfer followed by rapid proton equilibration from the aqueous medium, which is not applicable to the organic solvent reaction of RuTFPPCl₈(CO).

Further experiments probed the possibility of a photochemical reaction. Since the reaction vessel is made of glass, ambient light enters the reaction, allowing the possibility of a light activated mechanism. Porphyrins are known to sensitize singlet oxygen .31 and the actual oxygen transfer step could be completely unrelated to the ruthenium center. To test the possibility of singlet oxygen production, ZnTFPPCl₈ was used in place of RuTFPPClg(CO). Visible light has enough energy to cause a $\pi \to \pi^*$ transition in either the zinc or ruthenium porphyrin to form a triplet excited state. The triplet can act as a sensitizer to generate singlet oxygen, which could then react with cyclohexene. Under similar conditions to catalysis with RuTFPPClg(CO), ZnTFPPClg produced only 3 turnovers of cyclohexene in 24 hours, all of which were allylic oxidation products. This is within the range of products observed without any catalyst (between zero and 20 µmol product, approximately equal to up to 10 turnovers), suggesting that ZnTFPPC18 does not catalyze the oxidation of cyclohexene by any mechanism. The lack of activity from the porphyrin suggests that the TFPPCl₈ ligand is not an efficient oxygen sensitizer. Furthermore, the products are not consistent with an organic singlet oxygen reaction. 102 generates ketones and carbon - carbon bond cleavage products rather than epoxides and alcohols. 32

A second control was performed by excluding light from a catalysis reaction of RuTFPPCl₈(CO) with dioxygen and cyclohexene. The initiation period increased dramatically, with almost no reaction in the first 10 hours. The initiation period for one reaction was longer than the second trial, resulting in very different turnover numbers at 24 hours (Figure 5.15). Once started, however, the reaction rate does increase; at 24 hours, Run 1 has 75% of the products of an average reaction in ambient light. The second reaction, which was slower to initiate, has only 16% as much activity in 24 hours. Product distributions are similar to a reaction in the light, suggesting that the same

mechanism is operating in both cases. Although singlet oxygen is not implicated, ambient light does play a role in initiating the reaction with RuTFPPCl8(CO) and O_2 . The catalyst appears to be both thermally and photochemically activated.

Photolysis with visible light dramatically increases the rate of reaction (Figure 5.16). Two identical reactions were set up, one in the presence of normal room light (one light bulb from a hood lamp), and one continuously irradiated with a tungsten lamp (150W). The visible photolysis reaction shows 3.5 times as many turnovers in 8 hours (270 vs. 77), a tremendous enhancement by relatively low energy light. No porphyrin decomposition was observed. Product distributions are similar in the two reactions, indicating that a similar reaction is occurring in both cases.

To further explore the effect of light, the photophysics of RuTFPPCl₈(CO) were investigated. Samples of RuTFPPCl₈(CO) in methylene chloride were irradiated with pulses from a Nd-YAG or dye laser. Laser photolysis is known to photodissociate carbonyl ligands, ⁸ allowing an investigation of the reactivity of the bare ruthenium porphyrin. Excitation with 355 or 480 nm light produced a transient difference spectrum consistent with promotion of an electron into the π^* e_g orbital. A positive absorbance at 620 nm (Figure 5.17) and a negative change in optical density (Δ OD) in the Soret region indicate formation of a porphyrin triplet.

The kinetics describing decay of the excited state were dependent on the atmosphere over the solution. Both the 5 μ s and 50 μ s transient absorption spectra from 390 to 440 nm were obtained under carbon monoxide, ethylene, oxygen, and argon atmospheres; the transient spectra at 415 nm are shown in Figures 5.18 and 5.19 (additional traces are in Appendix 5). Under CO, biexponential decay of the excited state is observed. The faster rate, 33 k₁ = 3.9 x 106 s⁻¹, most likely corresponds to the decay of the porphyrin triplet excited state. The lifetime, 286 ns, is much shorter than the 36 μ s porphyrin-based triplet excited state of RuTPP(CO), 34 but longer than the 15 ns charge transfer excited state of RuTPP(py)₂. Generally, ruthenium porphyrin complexes have

 $^3(\pi - \pi^*)$ lifetimes of tens of microseconds, while $(d - \pi^*)$ lifetimes are only a few nanoseconds. Although the transient spectrum (at t = 0; Figure 5.17) shows porphyrin triplet characteristics, the short lifetime suggests that substantial mixing of the triplet and charge transfer states is occurring. The molecular orbital diagram of RuTFPPCl8(CO) (Figure 3.6) indicates that these two transitions are expected to be very close in energy. No emission was detected either at room temperature or from 2-methyl-tetrahydrofuran glass (77 K) at any wavelength out to 1100 nm.

The second kinetic term, $k_2 = 1.3 \times 10^5 \, s^{-1}$, is believed to be due to recombination of CO. The concentration of CO in chloroform is 8.5 mM; assuming pseudo first order kinetics (and a similar concentration in CH₂Cl₂), the CO recombination rate is calculated as $1.5 \times 10^7 \, M^{-1} \, s^{-1}$.

As observed in the laser traces at 415 nm on a 50 μ s time base (Figure 5.19), the signal does not completely return to zero. The transient at 50 μ s is after the excited state has decayed, and should correspond to the spectrum of the photoproduct from loss of the carbonyl ligand. The magnitude of the Δ OD indicates that the quantum yield for loss of CO is quite small, consistent with quantum yields observed for other ruthenium porphyrins. ⁸ Comparisons of the transient spectra under different atmospheres at 50 μ s may give some indication of the reactivity of the carbonyl free ruthenium.

Oxygen efficiently quenches the triplet at a rate of 1.25 x 10⁷ s⁻¹. However, comparison of the transient absorption spectra at 50 µs under CO and O₂ does not suggest that oxygen binds to ruthenium (Figure 5.20). In fact, none of the spectra from the four samples have a distinct photoproduct at 50 µs, not supporting a mechanism involving oxygen binding to RuTFPPCl₈ after loss of CO. Furthermore, a spectrum taken of each sample after laser photolysis (Figure 5.21) indicates that significant amounts of porphyrin decomposition occur under an oxygen atmosphere.

An ethylene atmosphere results in decay rates of $k_1 = 8.9 \times 10^6 \text{ s}^{-1}$ and $k_2 = 4.2 \times 10^5 \text{ s}^{-1}$, indicating substantial quenching of the porphyrin excited state. Since ethylene is

unable to quench an excited state by energy transfer, it must be interacting more directly with the porphyrin to protect it from decomposition. The 50 μs transient under ethylene shows the greatest bleach in the Soret region, suggesting some interaction between ruthenium and olefin on this time scale. The ethylene sample shows no decomposition after photolysis, and even shows a slight increase in the Soret intensity. One explanation for these results is that ethylene binds to the excited state of RuTFPPCl₈(CO) (k₁), and also to the photodissociated ruthenium porphyrin (k₂). Approximating the concentration of ethylene in solution as 5 mM gives an ethylene recombination rate with the photodissociated RuTFPPCl₈ of 8.4 x 10⁷ M⁻¹ s⁻¹. However, olefin complexation after loss of CO is not likely to be relevant to the catalytic mechanism since the quantum yield is very small. Photolysis of CO is only observed with high energy light (355 nm), and the oxidation reactions are only irradiated with visible wavelengths.

Under an atmosphere of argon, the excited state again shows biexponential decay kinetics with $k_1 = 7.1 \times 10^6 \, \text{s}^{-1}$ and $k_2 = 7.6 \times 10^5 \, \text{s}^{-1}$. These results are not consistent with the description of the ethylene and dioxygen chemistry above. It is difficult to find an explanation for the increase in the decay rates under an inert atmosphere. One possibility is that the in the absence of another ligand, the excited state interacts with methylene chloride, which is not a completely inert solvent. However, the decay rate would still be expected to be slower than rates under a CO atmosphere. A second possibility is that with the high energy light needed to observe the Soret band transients, multiple reactions may occur, complicating the kinetics.

Despite these problems, it is clear that excitation under ethylene results in a different product than photolysis under an inert atmosphere. Furthermore, although oxygen quenches the triplet excited state, there is no evidence for the substantial red shift normally observed upon binding of dioxygen.⁴ These experiments suggest another possible mechanism that would initiate not with oxygen binding but with olefin binding. RuTFPPCl₈(CO) is not able to catalyze the hydroxylation of alkanes with dioxygen,

suggesting that the electron richness of the carbon - carbon double bond is somehow important. Toluene, which has weak methyl C-H bonds, is not oxidized, either alone or in the presence of olefin to initiate reaction. Cumene or 3-methyl pentane, which is oxidized in low yield by Fe(TFPPBr₈)Cl, is also inactive with the ruthenium porphyrin and dioxygen.

Some evidence for olefin binding does exist. The carbonyl stretch in the solution IR of RuTFPPCl₈(CO) in CCl₄ shifts 2.2 cm⁻¹ upon addition of a small amount of cyclohexene. The shift to higher energy is consistent with weak competition by the π * orbitals of the olefin for backbonding density from the ruthenium ion.

¹H NMR of RuTFPPCl₈(CO) in acetone- d_6 after 24 hours under an ethylene atmosphere showed a weak resonance at -3.6 ppm. RuTMP(C₂H₄) has a singlet at -3.27 ppm, assigned to a π complex of ethylene, ³⁶ suggesting a similar assignment for RuTFPPCl₈(C₂H₄). The carbonyl ligand may remain bound to trans to the olefin, but it is not clear from the NMR data. As the signal is present under an atmosphere of ethylene gas, exchange of the bound ethylene must be slow on the NMR time scale. The ¹⁹F NMR of this sample still showed several different porphyrin species, indicating that only a small fraction of the porphyrin has ethylene bound.

UV-Vis data indicates that olefin binding, if occurring, is not highly favored. A solution of RuTFPPCl₈(CO) with cyclohexene showed no change after 24 hours, suggesting that any olefin complex is of low enough concentration to be swamped by the signal of the carbonyl porphyrin. Alternatively, a weak interaction with olefin might cause only small changes in the UV-Vis spectrum.

If olefin binding is not favored for the ground state, the transient spectroscopy suggests that olefin binding may be more favorable in the excited state. A mechanism for catalytic olefin oxidation via the excited state is shown in Figure 5.22. The mixing of the $3(\pi - \pi^*)$ and $(d - \pi^*)$ orbitals indicate that visible excitation of RuTFPPCl₈(CO) might populate the MLCT state which results in an oxidized metal center in the excited state.

Olefin binding to the strongly oxidizing Ru^{III} would then be more likely to occur (Figure 5.22). Once a π olefin complex is formed, it may rearrange to form a ruthenium(IV) alkyl radical complex, which would readily combine with dioxygen. The bound alkyl peroxide radical could abstract a hydrogen atom from another substrate molecule, forming a peroxide complex. From this point, several different pathways could occur. The peroxide could homolytically cleave, either thermally or photochemically, initiating a free radical reaction (not shown). Alternatively, the peroxide could decompose via an intermolecular epoxidation reaction, leaving Ru^{III}TFPPCl₈(OH) (after the formal π radical anion recombines with the ruthenium), which may recombine with another radical, R*, to form ROH and return the porphyrin to the resting state of the catalytic cycle.

This mechanism has several advantages over the mechanism involving loss of CO. First, spontaneous loss of the π acid carbonyl ligand is not likely for such an electron deficient porphyrin. Second, a partial carbon monoxide mechanism would not inhibit a photochemical reaction. Third, the dramatic increase in reactivity with light is explained by a greater amount of olefin complexation, which decomposes to lead directly to product or free radicals. The branching for a radical mechanism explains the large amount of allylic radical products observed. In addition, the large non-competitive isotope effect suggests that branching for the intermolecular mechanism is favored over C-D bond cleavage by a substantial amount, as is the high percentage of epoxidation formed with cyclohexene- d_{10} .

The peroxide experiments are also consistent with this mechanism. Addition of mCPBA removes the carbonyl ligand, which leads to a less oxidizing MLCT state with less or no affinity for olefin interaction. Addition of small amounts of TBHP may enhance the branching to the radical pathway by providing radicals to propagate radical reactions.

Conclusion

Traditional scientific method has always been at the very best, 20-20 hindsight. It's good for seeing where you've been. It's good for testing the truth of what you think you know, but it can't tell you where you ought to go.

-- Robert M. Pirsig, Zen and the Art of Motorcycle Maintenance, (1974).³⁷

RuTFPPCl₈(CO) has unprecedented ability for a carbonyl porphyrin to catalyze the oxidation of olefins with dioxygen. The mechanism does not appear to be radical decomposition of alkyl peroxides, as observed with Fe(TFPPBr₈)Cl, or the Groves dioxo ruthenium(VI) chemistry observed with RuTMP. Instead, a novel mechanism is proposed that involves an interaction of olefin with a mixed $3(\pi - \pi^*) - (d - \pi^*)$ excited state. The electron-withdrawing porphyrin ligand creates a highly oxidizing excited state ruthenium center, which can be stabilized by an interaction with a π donor ligand. Photochemically driven oxidation chemistry with such low energy, low intensity light is quite amazing.

The involvement of light in the mechanism is indisputable. The dramatic enhancement of catalysis by even low-energy irradiation clearly favors a photochemical reaction mechanism. This is unprecedented for this class of porphyrin catalysts.

RuTFPPCl₈(CO) is unique in being the first stable, effective photocatalyst for olefin oxidation with dioxygen. Moreover, the catalyst would be extremely interesting for potential commercial applications since it fulfills the desired requirements of intense, low-energy light absorption.

Once olefin binding has occurred, the following steps in the reaction mechanism are not as clear. Although a logical mechanism can be proposed, further work would be necessary to completely understand the decomposition of the bound olefin/oxygen complex to form product. The potential also exists to tune the mechanism to favor one

branches of the proposed mechanism over another to increase the selectivity for epoxidation over hydroxylation. For example, selective photolysis at 420 nm (into the Soret band) could decrease undesired radical side reactions (such as decomposition of the bound alkylperoxide). Other conditions, such as solvent, temperature, and oxygen concentration have obvious potential to change the reaction selectivity. Since phase transfer is not rate limiting, perhaps a lower concentration of oxygen would increase the activity by decreasing unfavorable quenching of the excited state by oxygen (as suggested by the higher activity in the unstirred reactions).

A continuation of this project would include a more thorough investigation of the proposed photochemical activation of olefin. The photophysics of RuTFPPCl₈(CO) could be better understood, especially the fast excited state decay under an argon atmosphere. Furthermore, if ethylene is quenching the $^{3}(\pi - \pi^{*})$ excited state, varying the concentration of olefin would allow the quenching rate to be determined by Stern-Volmer kinetics. The possibility of a reaction with solvent could also be eliminated by repeating the reaction in a more inert solvent.

Experimental

Materials -- Ruthenium porphyrins were obtained as described in Chapter 2. Iodosobenzene and cyclohexene- d_{10} was purchased from TCI. Cyclohexene, cyclooctene (Aldrich), and methylene chloride (EM Science) were distilled under argon before use. Cyclohexene oxide, 2-cyclohexen-1-ol, 2-cyclohexen-1-one, m-chloroperoxybenzoic acid (mCPBA), tert-butyl hydroperoxide (TBHP), triethylamine-N-oxide, pyridine, and styrene were purchased from Aldrich. Hydrogen peroxide and acetone were purchased from EM Science. Carbon monoxide, ethylene, and dioxygen lecture bottles were purchased from Matheson.

Methods -- General oxidation reactions were conducted as described in Chapter 4. UV-Vis, NMR, and IR spectra were obtained as described in Chapters 2 and 3.

Reaction with peroxide -- Reactivity with TBHP was only determined in a qualitative fashion. Approximately 0.2 mL TBHP was added to a mM solution of either RuTFPPCl8(CO) or Fe(TFPPBr8)Cl in methylene chloride and allowed to stir for several hours. During this time, the solution was monitored visually for the evolution of gas that would indicate peroxide decomposition. A similar reaction with hydrogen peroxide was also monitored. In this case, 10 mg of porphyrin in 10 mL acetone was degassed on a high vacuum line. Five mL of 0.6 % hydrogen peroxide in acetone (degassed) was added, and the solution allowed to stir at room temperature. Every hour, the pressure of evolved gas was measured with a Toeppler pump and the number of moles calculated. An IR of the gas indicated that it was not carbon dioxide or carbon monoxide (from the carbonyl ligand of the ruthenium porphyrin), and was assumed to be dioxygen from the recombination of radicals produced from peroxide decomposition by the porphyrin.

Titration with mCPBA -- A solution of RuTFPPClg(CO) in methylene chloride, such that the absorbance at either the Soret or Q band was close to 1, was prepared and

the exact concentration determined by either serial dilution or from the extinction coefficient. A solution of mCPBA (mM) was prepared by serial dilution. The porphyrin solution (2.5 mL) was titrated with 10 to 20 μ L aliquots of mCPBA, and monitored by UV-Vis. The changes in the spectrum were complete after addition of less than 100 μ L mCPBA solution, such that the porphyrin concentration remained relatively constant.

Titration with triphenylphosphine -- Aliquots from a mM solution of PPh₃ were added to the porphyrin solution immediately after addition of mCPBA, and monitored by UV-Vis. The solution was concentrated and spiked with CDCl₃ for NMR analysis.

Initiation with mCPBA or (Et)₃NO -- Five to ten equivalents of oxidant (approximately 1-3 mg) were added with the porphyrin to the reaction flask. Under argon, 15 mL of methylene chloride were added, and the solution allowed to stir for two minutes. The reaction vessel was flushed with dioxygen as 1 mL of cyclohexene was added to start the oxidation reaction. Product formation was measured as before.

Mixed atmosphere reactions — RuTFPPCl₈(CO), solvent, and cyclohexene were mixed together in the reaction flask under argon. A mixture of carbon monoxide and oxygen was used to flush the argon from the flask and start the oxidation reaction.

Pressurized carbon monoxide reaction -- A mM solution of RuTFPPCl₈(CO) in either methylene chloride or carbon tetrachloride was placed in a glass lined Parr reactor. The reactor was connected to a carbon monoxide tank, and flushed twice before full pressurization to 1100 psi of CO. The reaction was not stirred, but allowed to rest under CO pressure for 2 or 4 days (in CCl₄ or CH₂Cl₂, respectively). The pressure was let down, the Parr reactor opened and the porphyrin solution transferred to a Teflon capped vial. One mL of solution was used to run an oxidation reaction by injecting it into the reaction just before addition of dioxygen and substrate. The concentration of RuTFPPCl₈(CO) in the reaction was calculated from the absorbance of the porphyrin solution.

Initiate with TBHP -- Attempts to initiate cyclohexene oxidation reactions with peroxide were accomplished by addition of TBHP to the reaction before addition of substrate. A small amount of a dilute TBHP solution was added to a solution of RuTFPPClg(CO) in methylene chloride. Three separate reactions were run, adding 10, 225, or 380 equivalents of TBHP, respectively.

Stir rate -- The stir rate was lowered to half of normal for these reactions. One reaction was also run without any stirring.

Isotope effect -- The isotope effect was calculated from both competitive and non-competitive experiments. Competitive experiments were run with 15 mL of methylene chloride, 2 mg RuTFPPCl8(CO), and 1 mL each of cyclohexene and cyclohexene- d_{10} . The deuterated oxidation products ran slightly slower on the GC, allowing individual determination of deuterated and non-deuterated turnover numbers. Non-competitive experiments were run with 1 mL of cyclohexene- d_{10} , and compared to reactions run with perprotio cyclohexene. The isotope effect was calculated as a ratio of turnover numbers at 24 hours, since actual rates of product formation were not determined from these experiments.

Singlet oxygen generation -- A cyclohexene oxidation reaction was run as described above, with 3 µmol ZnTFPPCl₈ in place of RuTFPPCl₈(CO).

Light experiments -- A cyclohexene oxidation reaction was run as described above, except the entire reaction flask was wrapped in foil to prevent incidental light from affecting the reaction. The light catalyzed reaction was accomplished by photolysis of an oxidation reaction with a normal 150 watt light bulb. The light was turned on before addition of substrate, and kept on for the duration of the experiment. The reaction was placed in a water bath to maintain ambient temperature.

Laser experiments -- Solutions of RuTFPPCl₈(CO) in methylene chloride were degassed by three cycles of the freeze/pump/thaw method on a high vacuum line in a quartz laser cuvette. The cuvettes were then backfilled with the desired gas (argon,

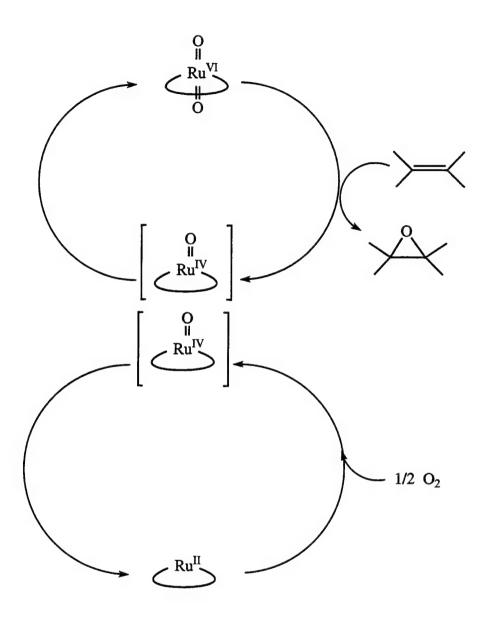
carbon monoxide, oxygen, or ethylene) to 1 atm pressure. The excitation source for the time resolved absorption experiments was the third harmonic of a Quanta-Ray Nd-YAG laser with a 20 nm pulse width; a PTi arc lamp supplied the white probe light source, and a DH 10 SA Inc. monochrometer was placed before the R955 Hamamatsu PMT detector. The analog signal was analyzed by a RTD 710A digitizer, and worked up on a 386 PC. The arc lamp power was 68 W, and in the case of weak signals the arc lamp was pulsed at 6 Hz. The signal was amplified with a fast amplifier designed at Brookhaven National Laboratories. Further data manipulation was accomplished on either a 486 PC or a Macintosh IISi with computer programs written at Caltech.

References and Notes

- (1) Collman, J. P.; Hutchison, J. E.; Ennics, M. S.; Lopez, M. A.; Guilard, R. J. Am. Chem. Soc. 1992, 114, 8074-8080.
- (2) Chow, B. C.; Cohen, I. A. Bioinorg. Chem. 1971, 1, 57-63.
- (3) Antipas, A.; Buchler, J. W.; Gouterman, M.; Smith, P. D. J. Am. Chem. Soc. 1978, 100, 3015-3024.
- (4) Barringer, L. F.; Rillema, D. P.; Ham, J. H. J. Inorg. Biochem. 1984, 21, 195-207.
- (5) Brown, G. M.; Hopf, F. R.; Ferguson, J. A.; Meyer, T. J.; Whitten, D. G. J. Am. Chem. Soc. 1973, 95, 5939-5942.
- (6) Brown, G. M.; Hopf, F. R.; Meyer, T. J.; Whitten, D. G. J. Am. Chem. Soc. 1975, 97, 5385-5390.
- (7) Eaton, G. R.; Eaton, S. S. J. Am. Chem. Soc. 1975, 97, 235-236.
- (8) Hopf, F. R.; O'Brien, T. P.; Scheidt, W. R.; Whitten, D. G. J. Am. Chem. Soc. 1975, 97, 277-281.
- (9) Tsutsui, M.; Ostfeld, D.; Hoffman, L. M. J. Am. Chem. Soc. 1971, 93, 1820-1823.
- (10) Groves, J. T.; Quinn, R. Inorg. Chem. 1984, 23, 3844-3846.
- (11) Groves, J. T.; Quinn, R. J. Am. Chem. Soc. 1985, 107, 5790-5792.
- (12) Groves, J. T.; Ahn, K.-H. *Inorg. Chem.* 1987, 26, 3831-3833.
- (13) Ohtake, H.; Higuchi, T.; Hirobe, M. Tetrahedron Lett. 1992, 33, 2521-2524.
- (14) Higuchi, T.; Ohtake, H.; Hirobe, M. Tetrahedron Lett. 1991, 32, 7435-7438.
- (15) Ohtake, H.; Higuchi, T.; Hirobe, M. J. Am. Chem. Soc. 1992, 114, 10660-10662.
- (16) Takagi, S.; Miyamoto, T. K.; Hamaguchi, M.; Sasaki, Y.; Matsurmura, T. *Inorg. Chim. Acta* 1990, 173, 215-221.
- (17) Ho, C.; Leung, W.-H.; Chi-Ming-Che J. Chem. Soc., Dalton Trans. 1991, 2933-2939.
- (18) Leung, W.-H.; Chi-Ming-Che J. Am. Chem. Soc. 1989, 111, 8812-8818.
- (19) Rajapakse, N.; James, B. R.; Dolphin, D. Catal. Lett. 1989, 2, 219-226.
- (20) Tavares, M.; Ramasseul, R.; Marchon, J.-C.; Maumy, M. Catal. Lett. 1991, 8, 245-252.
- (21) Tavares, M.; Ramasseul, R.; Marchon, J.-C.; Bachet, B.; Brassy, C.; Marnon, J.-P. J. Chem. Soc., Perkin Trans. 2 1992, 1321-1329.
- (22) Tavares, M.; Ramasseul, R.; Marchon, J.-C. Catal. Lett. 1990, 4, 163-168.
- (23) Ellis, P. E., Jr.; Lyons, J. E. Coord. Chem. Rev. 1990, 105, 181-193.

- (24) Lyons, J. E.; Ellis, P. E., Jr.; Myers, H. K., Jr.; Wagner, R. W. J. Catal. 1993, 141, 311-315.
- (25) Grinstaff, M. W.; Hill, M. G.; Birnbaum, E. R.; Schaefer, W. P.; Labinger, J. A.; Gray, H. B. submitted to *Inorg. Chem.*
- (26) Sugimoto, H.; Higashi, T.; Mori, M.; Nagano, M.; Yoshida, Z.-I.; Ogoshi, H. Bull. Chem. Soc. Jpn. 1982, 55, 822-828.
- (27) Attempts to repeat this experiment on a larger scale were not successful. Oxidation of RuTFPPCl₈(CO) was not clean, and although product formation was observed, it was impossible to differentiate between oxo transfer from the dioxo ruthenium porphyrin and direct reaction with excess mCPBA.
- (28) Evans, E. W.; Howlader, M. B. H.; Atlay, M. T. Inorg. Chim. Acta 1995, 230, 193-197.
- (29) Mimoun, H.; Saussine, L.; Daire, E.; Postel, M.; Fischer, J.; Weiss, R. J. Am. Chem. Soc. 1983, 105, 3101-3110.
- (30) Roecker, L.; Meyer, T. J. J. Am. Chem. Soc. 1987, 109, 746-754.
- (31) Kalyanasundaram, K. Photochemistry of Polypyridine and Porphyrin Complexes; Academic Press, Inc.: San Diego, 1992.
- (32) March, J. Advanced Organic Chemistry; 4th ed.; John Wiley & Sons: New York, 1992, pp 708.
- (33) The faster rates are taken from the 5 μs transient spectra, and the slower rates from the 50 μs data. The two sets of rates do not show good agreement, suggesting that additional processes are contributing to the kinetics.
- (34) Rillema, D. P.; Nagle, J. K.; Barringer, L. F., Jr.; Meyer, T. J. J. Am. Chem. Soc. 1981, 103, 57-82.
- (35) Levine, L. M. A.; Holten, D. J. Phys. Chem. 1988, 92, 714.
- (36) Rajapakse, N.; James, B. R.; Dolphin, D. Can. J. Chem. 1990, 68, 2274-2277.
- (37) Pirsig, R. Zen and the Art of Motorcycle Maintanence; Morrow: New York, 1974, pp 412.
- (38) McCleskey, T. M. Thesis, California Institute of Technology, 1994.

Figure 5.1 -- The Groves mechanism for catalytic oxidation of olefins with dioxygen by RuVITMP(O)₂. The ruthenium(IV) monooxo porphyrin disproportionates to reform the active ruthenium(VI) catalyst (see reference 11).



Ru^{II} = Ruthenium tetramesitylporphyrin

Figure 5.2 - Turnovers of cyclohexene by RuTFPPCl₈(CO) with iodosobenzene in 24 hours, showing the observed product distribution. Only 25% of the available oxidant is used.

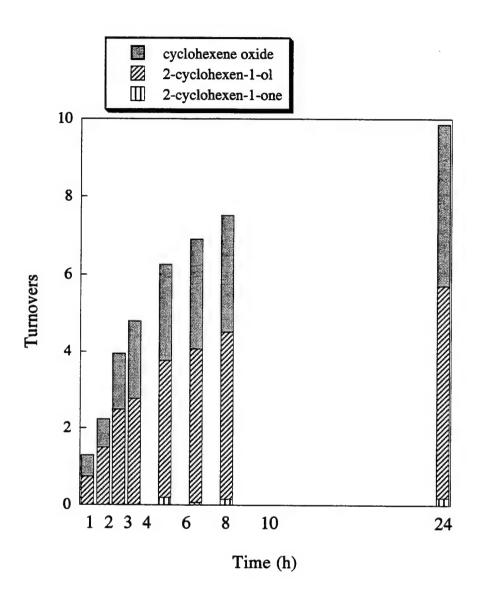


Figure 5.3 -- Turnovers of cyclohexene by RuTFPPCl₈(CO) with dioxygen in 24 hours, showing the observed product distribution. More allylic oxidation products are observed than with PhIO as the oxidant.

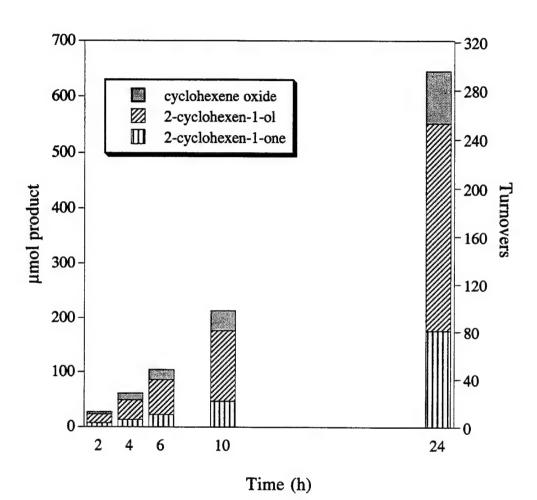


Figure 5.4 — Hydrogen peroxide decomposition by RuTFPPCl₈(CO) and Fe(TFPPBr₈)Cl in acetone, as determined by oxygen evolution. The iron porphyrin decomposes 68 turnovers in 4 hours, while the ruthenium porphyrin shows much less activity in the same time period (4.5 TO).

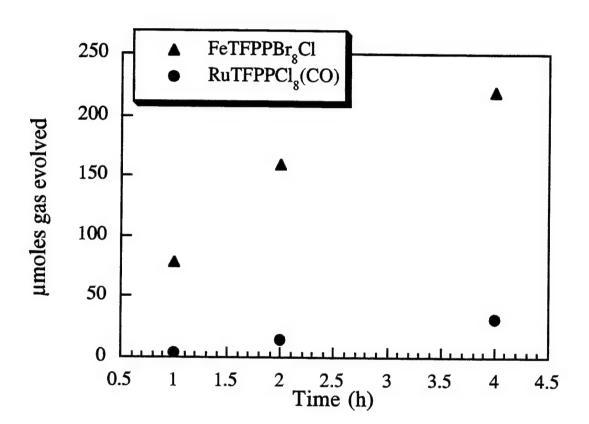


Figure 5.5 -- UV-Vis spectrum of RuTFPPCl₈(CO) upon titration with 2 equivalents of mCPBA to form RuVITFPPCl₈(O)₂. The red shift of the Soret band to 420 nm is consistent with dioxo formation.

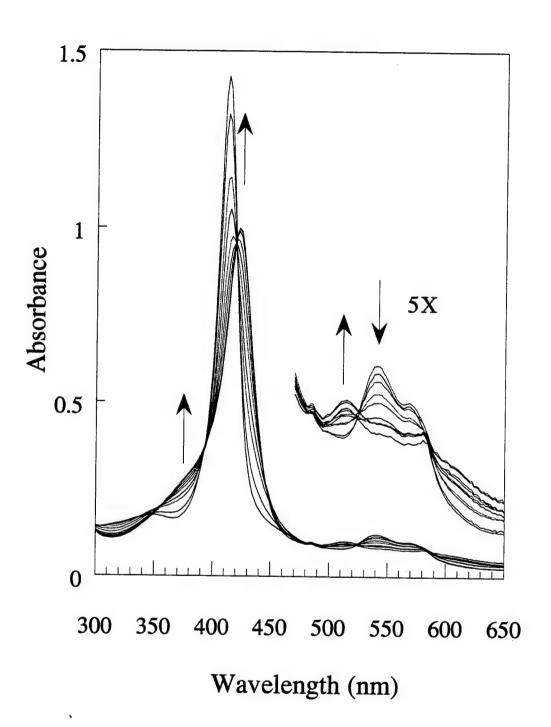


Figure 5.6 -- Addition of cyclohexene to RuVITFPPCl₈(O)₂. The initial decrease in Soret intensity corresponds to a single oxidation of substrate and formation of RuIVTFPPCl₈(O). Eventually, the second oxo also transfers, and addition of carbon monoxide gas regenerates the original spectrum of RuIITFPPCl₈(CO) with 85% of the original intensity.

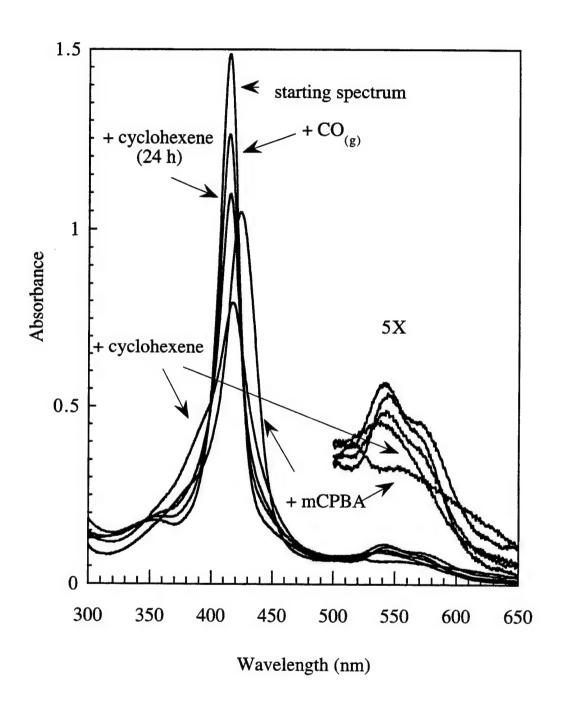


Figure 5.7 — Addition of triphenylphosphine to RuVITFPPCl₈(O)₂. The first 2 eq (a) are believed to correspond to transfer of both oxo ligands. Further addition of PPh₃ (2 eq, spectrum b) results in new spectral features consistent with coordination of triphenylphosphine to the ruthenium porphyrin.

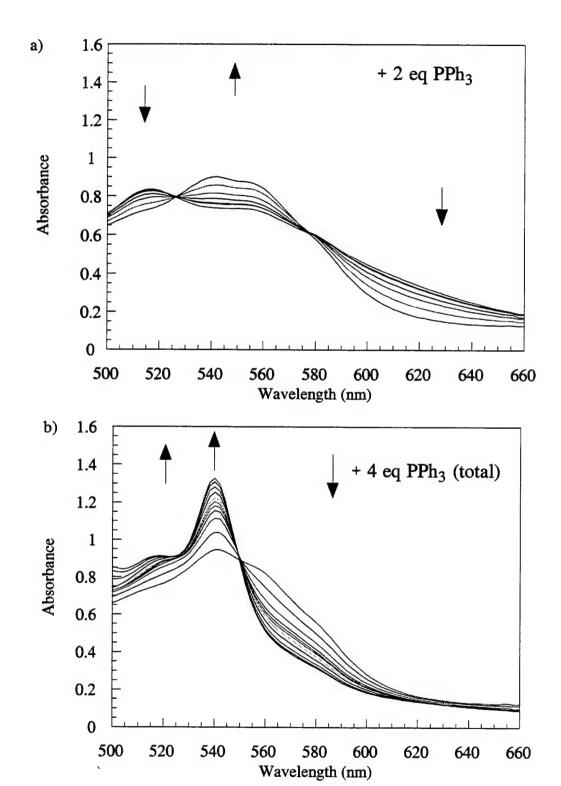


Figure 5.8 — A potential mechanism for oxidation of olefins by Ru^{II}TFPPCl₈(CO).

Initial loss of CO allows oxygen to bind to the electron poor metal center, initiating the chemistry.

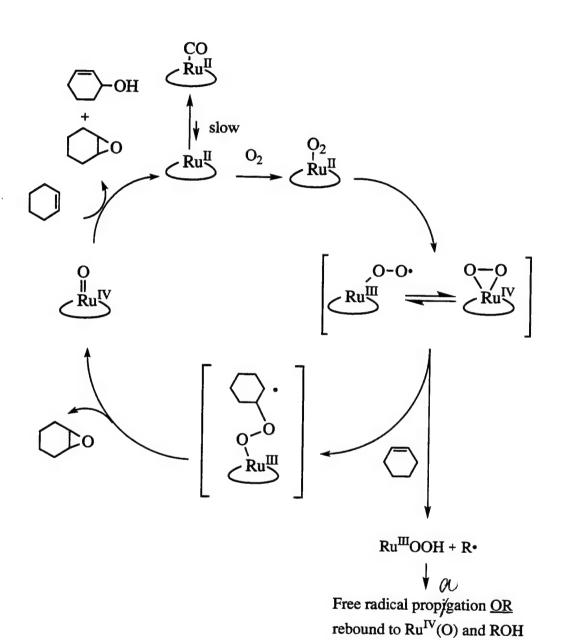


Figure 5.9 -- Relative rates of reaction for RuTFPPCl₈(CO) with dioxygen (a "normal" reaction) or in the presence of small amounts of (Et)₃NO or mCPBA before addition of substrate.

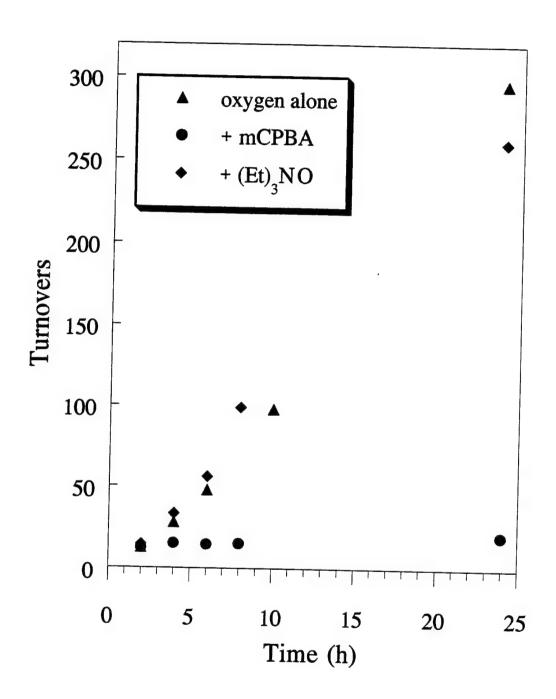


Figure 5.10 -- The relative rates of cyclhexene oxidation after the addition of 10 or 300 equivalents of TBHP. Although a small addition of peroxide only induces a minor enhancement of the chemistry, the large addition appears to initiate a free radical reaction that may not be related to the ruthenium catalyst.

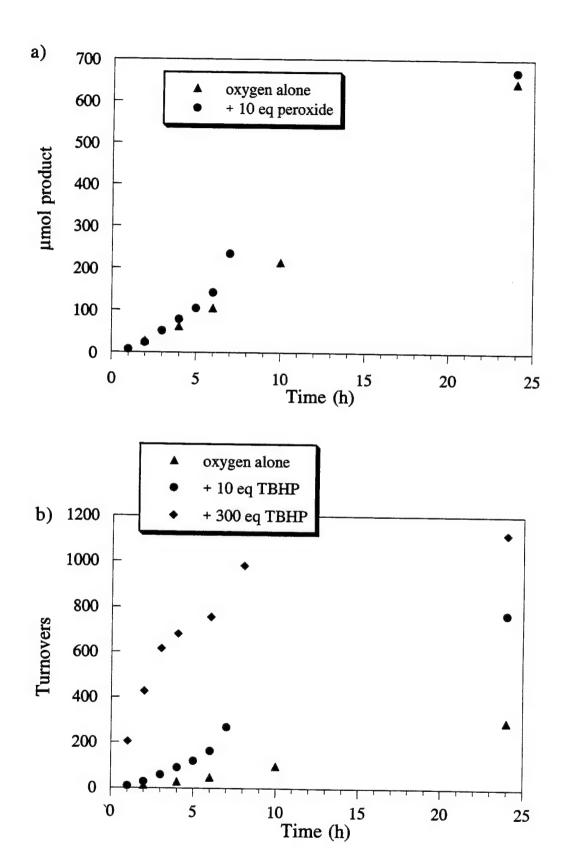


Figure 5.11 -- Relative turnovers in experiments stirred at two different rates indicate that phase transfer was not rate limiting. Experiments that were stirred more slowly showed slightly more activity than average.

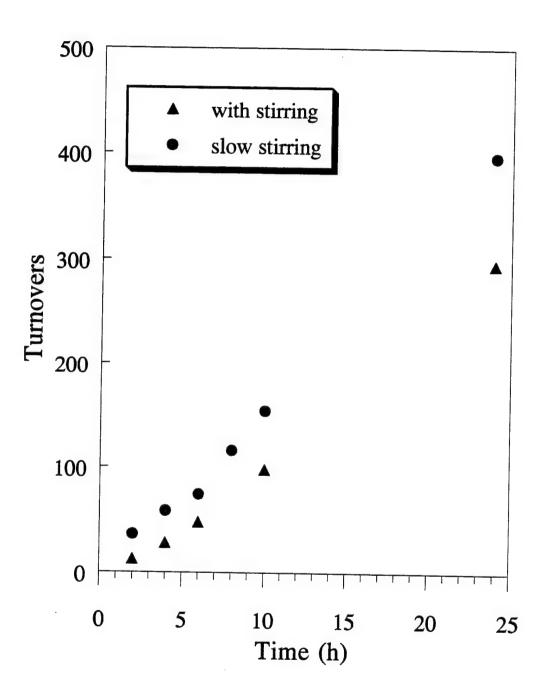


Figure 5.12 -- Relative rates of cyclohexene oxidation under dioxygen or under a mixture of oxygen and carbon monoxide, indicating that CO does not inhibit catalysis by Ru^{II}TFPPCl₈(CO).

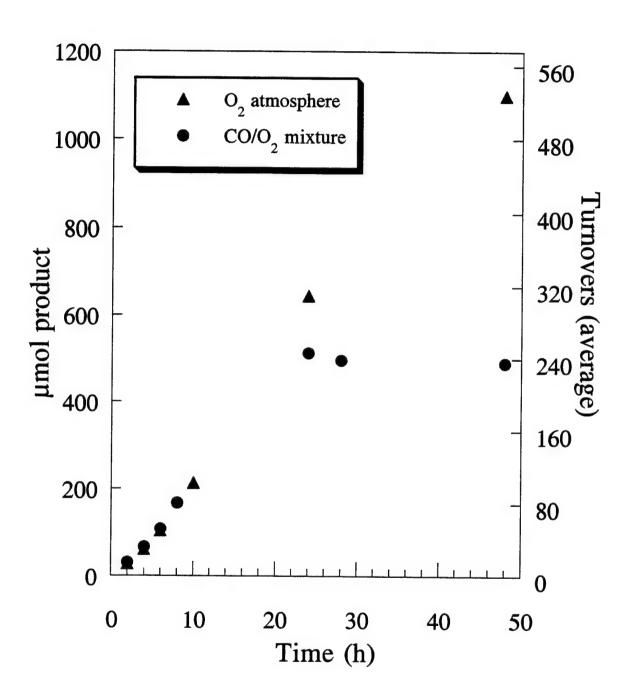


Figure 5.13 -- UV-Vis spectrum of Ru^{II}TFPPCl₈(CO) in carbon tetrachloride after two days in a Parr reactor under 1100 psi of carbon monoxide. The Soret band is slightly red shifted and the Q bands are slightly blue shifted from the spectrum before the Parr reactor. The absorption at 280 nm is believed to be from an organic product (see text).

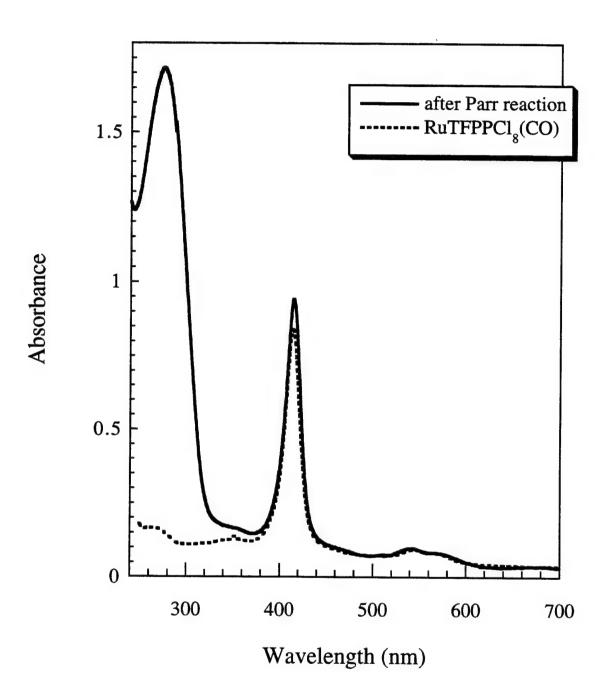


Figure 5.14 -- Relative rates of cyclohexene and cyclohexene- d_{10} oxidation by $Ru^{II}TFPPCl_8(CO)$ with dioxygen.

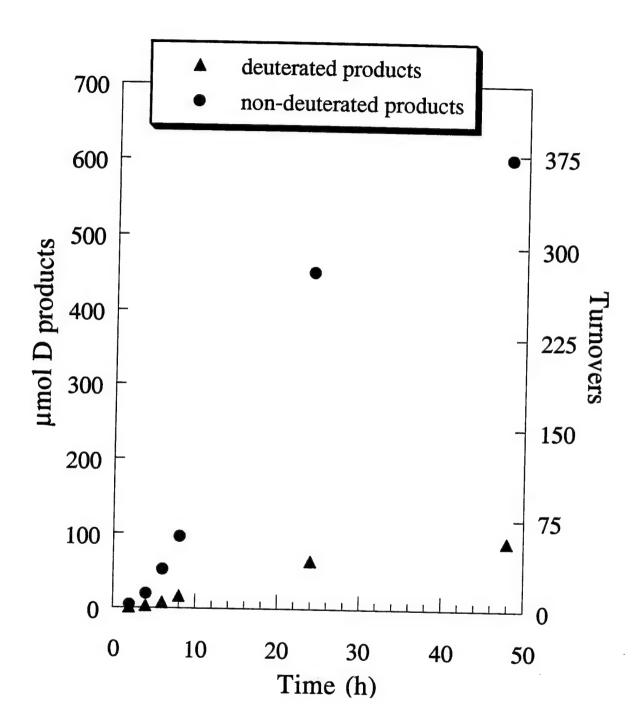


Figure 5.15 -- Cyclohexene oxidation experiments carried out in the dark showed great variability in the initiation period. Eventually both reactions showed significant reactivity.

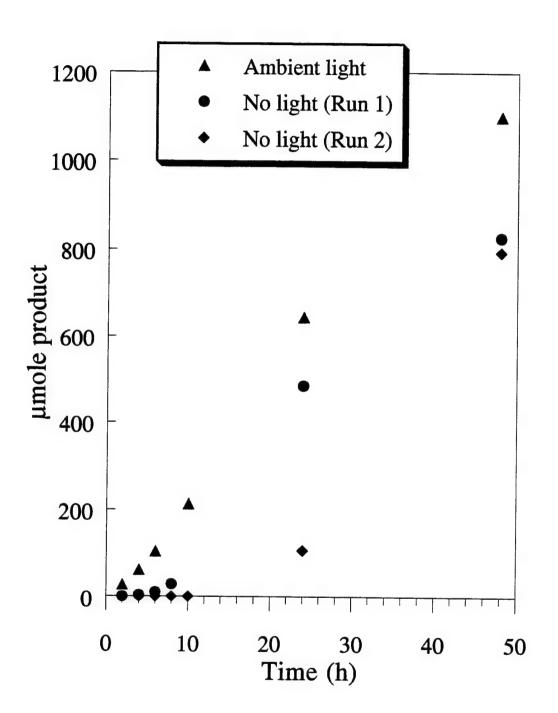


Figure 5.16 -- Photolysis of a cyclohexene oxidation reaction by Ru^{II}TFPPCl₈(CO) with dioxygen with a tungsten lamp dramatically increased the reaction rate.

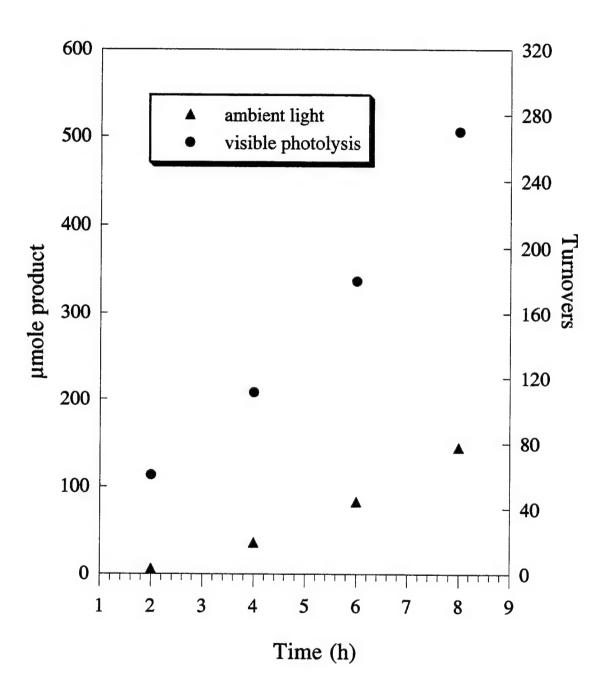


Figure 5.17 -- Transient absorption spectrum in the Q band region immediately following irradiation at 480 nm. The appearance of a low energy band is consistent with formation of a porphyrin triplet excited state.

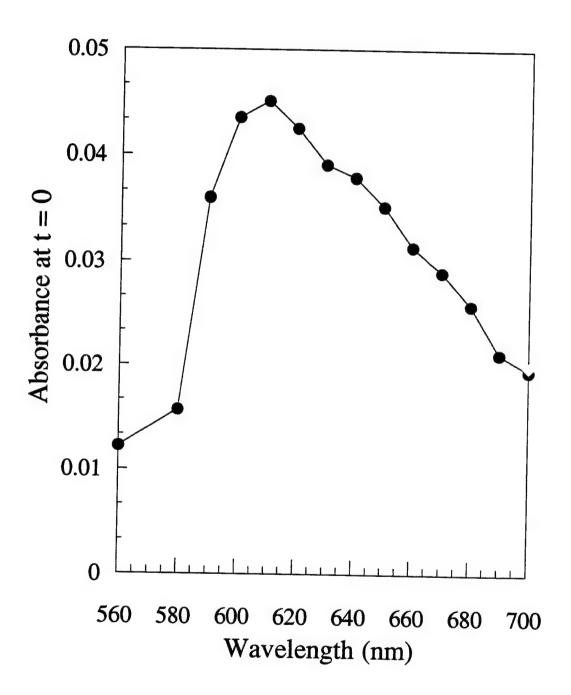


Figure 5.18 -- A 5 μs transient spectrum at 415 nm for excitation of Ru^{II}TFPPCl₈(CO) with 355 nm light. The sample is in methylene chloride and under an atmosphere of CO. Other transient spectra are in appendix 5.

DATA FILE: RUCO.006

1995-2-23 9:27:49

INPUT V RANGE: 0.320V

INPUT OFFSET: 0 %

TIME RANGE: 5.0 µs INPUT V RAY EXPERIMENT: TRANSIENT ABSORBTION FAST (200 MHz) QUASI-DIFFERENTIAL AMP

MODE: SINGLE-ENDED

PMT VOLTIGE: 702 V

SHOTS PRE CYCLE: 10 CYCLES: 5 PMT VOLTIGE: EXCITATION WAVELENGTH: 355 nm OBSERVATION WAVELENGTH: 415 nm

SAMPLE: RuCl8(CO) SOLVENT: CH2Cl2 TEMPERATURE: rt COMMENT: under CO

COMMENT:

---> FIXED PARAMETER; ! ---> FIXED SIGN

$$y(t) = C0 + C1*e^{-k1*t} + C2*e^{-k2*t}$$

C0 = -1.941E-2 C1 = -1.023E-1 C2 = -4.168E-2 $!k1 = 3.951E6 \text{ s}^{-1}$ $!k2 = 8.530E5 \text{ s}^{-1}$

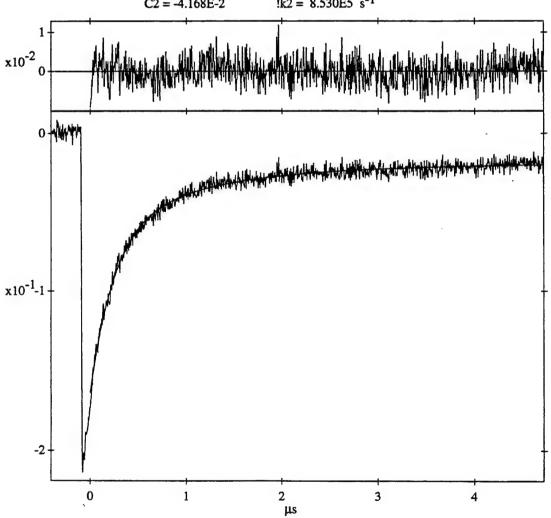


Figure 5.19 - A 50 μs transient spectrum at 415 nm for excitation of Ru^{II}TFPPCl₈(CO) with 355 nm light. The sample is in methylene chloride and under an atmosphere of CO. Other transient spectra are in appendix 5.

DATA FILE: RUCO.002

INPUT V RANGE: 0.320V

1995-2-23 8:56:56

INPUT OFFSET: 0 %

TIME RANGE: 50 µs INPUT V RAI EXPERIMENT: TRANSIENT ABSORBTION

FAST (200 MHz) QUASI-DIFFERENTIAL AMP

MODE: SINGLE-ENDED

PMT VOLTIGE: 700 V

SHOTS PRE CYCLE: 10 CYCLES: 5 PMT VOLTIGE: EXCITATION WAVELENGTH: 355 nm OBSERVATION WAVELENGTH: 415 nm

SAMPLE: RuCl8(CO) SOLVENT: CH2Cl2 TEMPERATURE: rt COMMENT: under CO

COMMENT:

---> FIXED PARAMETER; ! ---> FIXED SIGN

$$y(t) = C0 + C1*e^{-k1*t} + C2*e^{-k2*t}$$

C0 = -7.483E-3

C1 = -7.385E-2

 $!k1 = 2.196E6 \text{ s}^{-1}$ $!k2 = 1.318E5 \text{ s}^{-1}$

C2 = -2.381E-2

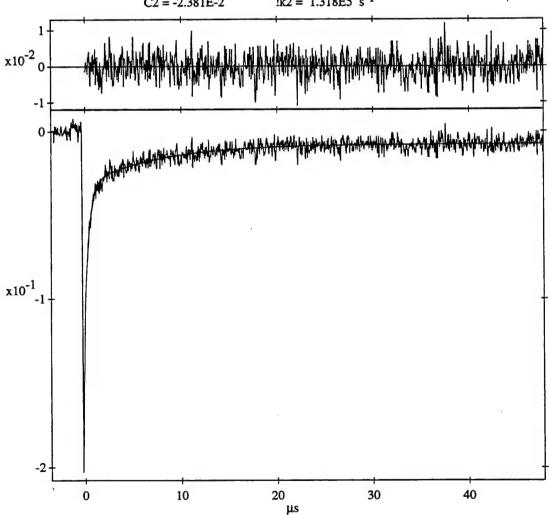


Figure 5.20 -- The 50 µs transient absorption spectrum after excitation with 355 nm light of equally concentrated solutions of RuTFPPCl₈(CO) in methylene chloride under different atmospheres. The spectra are very similar; only the ethylene spectrum has a larger decrease in Soret intensity relative to the other samples.

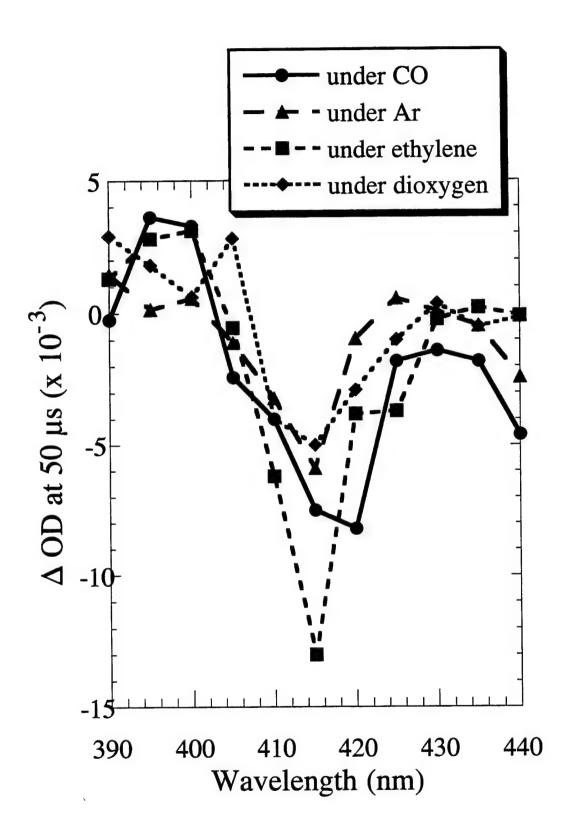


Figure 5.21 -- UV-Vis spectra of the samples shown in Figure 5.20 after the completion of the laser photolysis experiments. The samples under argon and dioxygen show significant broadening and a decrease in the Soret intensity, but CO or ethylene atmospheres protected the porphyrin from decomposition.

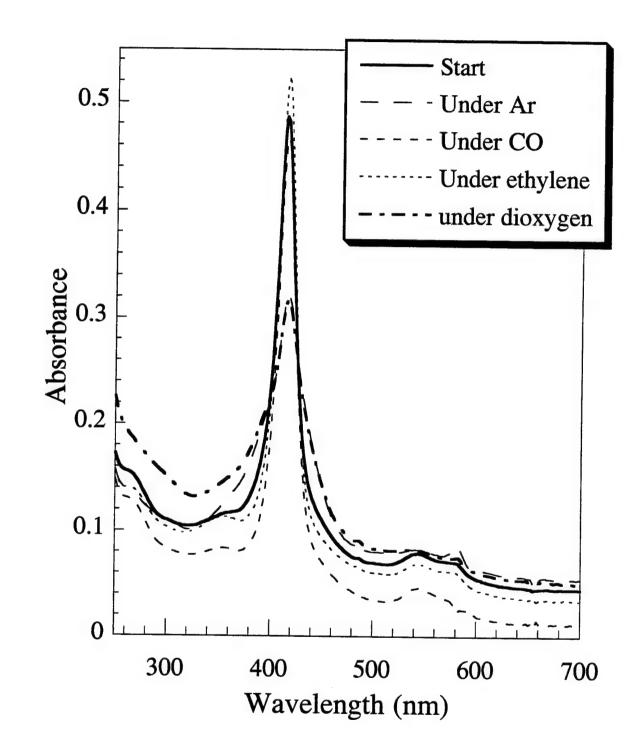


Figure 5.22 -- A mechanism for catalytic olefin oxidation by RuTFPPCl₈(CO) with dioxygen involving an excited state of the porphyrin. Olefin binding is enhanced in the excited state due to the photochemical oxidation of the metal. The excited state could also be quenched by oxygen, forming singlet oxygen that could also lead to product formation.

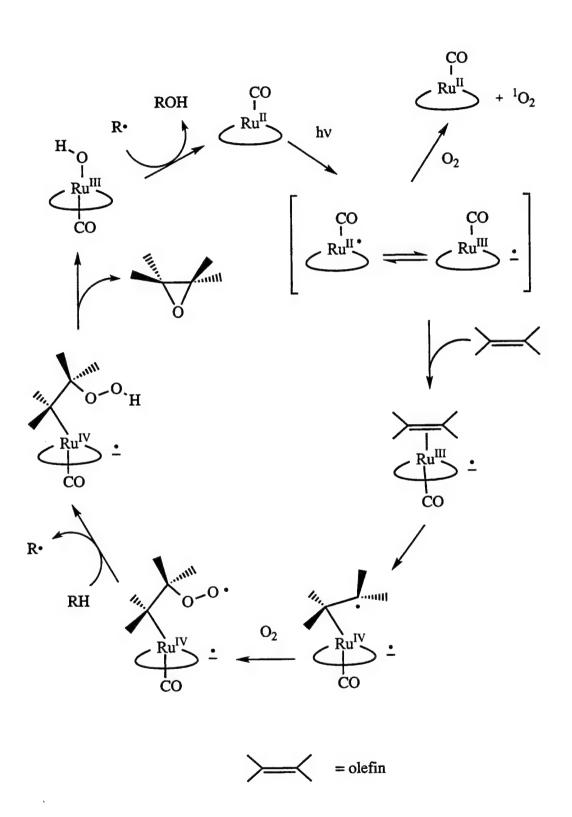


Table 5.1. Oxidation Chemistry with RuTFPPCl₈(CO).

| Reaction Conditions ^a | % 0 | % ОН | % | Turnovers |
|--|-----|------|----|---------------|
| PhIO | 42 | 56 | 2 | 9.9 |
| O_2 | 15 | 58 | 27 | 296 |
| O ₂ + 10 eq (Et) ₃ NO | 7 | 59 | 35 | 260 |
| O ₂ + 5 eq mCPBA | 35 | 52 | 13 | 20 |
| O ₂ + 10 eq TBHP | 14 | 54 | 32 | 770 |
| O ₂ + 300 eq TBHP | 7 | 65 | 28 | 1119 |
| slow str rate | 14 | 61 | 25 | 258 |
| CO/O ₂ | 7 | 57 | 36 | 258 |
| No light | 16 | 59 | 25 | 200 (average) |
| Visible Photolysis | 15 | 61 | 24 | 531 |

a. Reactions run in 15 mL of methylene chloride with approximately 1.5 - $2.0~\mu mol$ of RuTFPPClg(CO) and 1 mL of cyclohexene. All reactions were run under 1 atm of dioxygen, except the PhIO reaction, which was under an argon atmosphere. See text and experimental section for more details.

Chapter 6

Solubility and Reactivity of Iron and Ruthenium Halogenated Porphyrins in Supercritical Carbon Dioxide

Introduction

The investigation of biomimetic metalloporphyrin catalysis has two general long range goals: first, to better understand oxidation chemistry *in vivo*, and second, the more economic objective of applying this knowledge to the design of efficient oxidation catalysts for industrial applications. The latter aim of efficiency is not specific to oxygenation, but also drives research in other areas of catalysis. Increasing pressure from the government to reduce waste as well as burgeoning costs of waste disposal have necessitated fundamental changes in catalysis methodology. Consideration of the catalyst efficiency and longevity are no longer sufficient; solvent disposal, waste stream reduction, and chemical toxicity are of increasing importance.

Supercritical carbon dioxide (SC CO₂) has recently received great attention as an environmentally friendly solvent. Non-toxic, inexpensive, and nonflammable, it is currently used for commercial extraction of hops and decaffination of coffee. SC CO₂ is being further explored as a medium for uses ranging from the extraction of lanthanides from nuclear reprocessing waste² to dry-cleaning. The primary applications and research related to SC CO₂ have focused on separation technology. The use of supercritical carbon dioxide as a solvent for chemical reactions has not been widely explored, an area where the unique attributes of supercritical fluids (SCFs) could possibly affect the desired enhancements in catalysis.

In general, SCFs have properties that range between those of gases and liquids.

Gases are miscible in SCFs, eliminating phase transfer problems during hydrogenation or oxygenation catalysis in homogeneous solution. The density of a SCF is extremely

dependent on the pressure and temperature, and can vary between being "gas-like" or "liquid-like". The polarity of SC CO₂ is similar to that of halogenated hydrocarbons, indicating that it may be an excellent replacement for hazardous solvents such as carbon tetrachloride or methylene chloride.⁴

Carbon dioxide has an unusually low critical point. A phase diagram (Figure 6.1) shows the critical point at 72.8 atm and 31 °C, which is far lower than that of water (218 atm and 374 °C).⁵ These conditions are easily achievable in the laboratory, albeit with care and respect, and are also feasible for industrial applications.

Supercritical carbon dioxide has recently begun to be explored as a medium for catalysis. DiSimmone conducted the free radical polymerization of methyl methacrylate in SC CO₂. High yields of quality poly(methyl methacrylate) were obtained from a single phase reaction, avoiding the aqueous and organic dispersing media used in classical polymerization techniques.⁶ Noyori et. al. have achieved formation of dimethylformamide from hydrogen gas, dimethylamine, and supercritical carbon dioxide with a ruthenium phosphine catalyst. The CO₂ serves as both solvent and reactant, driving the reaction at a rate an order of magnitude above that in an organic solvent.⁷ Similarly, the miscibility of H₂ in SC CO₂ leads to very high initial rates of reaction for the formation of formic acid, catalyzed by Ru(PMe₃)₄(H)₂.⁸ Asymmetric hydrogenation reactions with ruthenium and rhodium catalysts have demonstrated that enantioselectivity can be increased by moving from a conventional solvent to supercritical CO₂.³ The above examples demonstrate several methods in which SCFs have improved catalytic processes.

Despite these recent successes, only one oxidative system has been investigated in SC CO₂. The uncatalyzed free radical oxidation of cyclohexane with dioxygen in SC CO₂ has been reported. The conversion of cyclohexane and the ratio of cyclohexanol and cyclohexanone produced are controlled by the pressure and temperature near the critical region. No other oxidations in supercritical carbon dioxide have been reported. Catalytic olefin oxidation by halogenated metalloporphyrins seems an ideal system for analysis in

SC CO₂. Since dioxygen is the only additive in these reactions (no coreductant is needed), the miscibility of O₂ with SC CO₂ has potential to increase reactivity in the SCF. Furthermore, the different solvation properties of SC CO₂ could lead to different selectivity in the oxidation reactions.

Before investigating reactivity, we determined the solubility of three halogenated porphyrins in SC CO₂. Although the dielectric constant of supercritical carbon dioxide increases with pressure, it remains quite low (only 1.8 at 2000 psi), making SC CO₂ a rather poor solvent.⁴ However, since chlorinated solvents able to dissolve halogenated porphyrins (i.e., CCl₄) also have low dielectric constants, the porphyrins were anticipated to be soluble in the supercritical medium. Fe(TFPP)Cl, Fe(TFPPBr₈)Cl and RuTFPPCl₈(CO) were investigated, since their chemistry in methylene chloride had been previously studied in our laboratory.

Results

Solubility Studies

An apparatus allowing UV-Vis spectroscopy under high pressures is pictured in Figure 6.2. A tank of liquid carbon dioxide was connected to allow flow directly into the cell or into an ISCO syringe pump, which is capable of condensing CO₂ up to 5000 psi. The cell was secured with a stand on top of a stirplate in between the lamp and detector. Rubber heating tape was wrapped around the cell to maintain the temperature at 40°C during the UV-Vis experiments (Figure 6.2).

After the cell was aligned in the spectrophotometer setup, a solution of porphyrin in methylene chloride was injected into the cell through the thermocouple inlet. The thermocouple was then reattached, and the cell evacuated to remove the organic solvent. CO₂ was added, and the absorbance calculated from light intensity measurements taken at 500 psi intervals (Figure 6.3-6.6). A spectrum of each compound in methylene chloride is also displayed in each figure for comparison. The concentration of porphyrin in solution is

calculated assuming the extinction coefficients are similar in methylene chloride and in SC CO₂. Although porphyrin spectra are known to be sensitive to solvent, generally the position of the band shifts more than the extinction coefficient.

In general, solubility was found to increase with pressure. Although the spectra are quite noisy, due to refraction from mixing lines in the large cell, the main features of the porphyrin are still observable. Fe(TFPP)Cl (Figure 6.3) is the least sensitive to pressure, but has the highest solubility, with the concentration only changing from 0.27 to $0.30 \,\mu\text{M}$ from 2000 to 5000 psi CO₂. The Q band region is most distinct in these spectra, with a shoulder at 500 and a stronger band at 610 nm corresponding to the solution spectrum bands at 504 and 620 nm.

The resolution of the Soret band of Fe(TFPPBr₈)Cl is lost in SC CO₂ (Figure 6.4). However, there is a definite increase in absorbance from 1400 to 3500 psi, and the solubility increases from 0.07 to 0.20 μ M. Further increases in pressure do not cause much change in absorbance.

Unlike the iron porphyrins, the Soret band of RuTFPPCl8(CO) is quite distinct in SC CO₂. The Q band region in this spectrum, however, has a substantial amount of instrument noise (Figure 6.5). The solubility increased from almost nothing in liquid carbon dioxide (800 psi) to $0.16~\mu M$ (5000 psi). The changes of solubility with pressure for all three porphyrins are plotted in Figure 6.6. Although none of the porphyrins were soluble in liquid CO₂ (data not shown), all of them were soluble once the critical point was achieved (> 1200 psi). Surprisingly, little change in the concentration was observed at higher pressures.

Solubility Studies Discussion

The solubility of halogenated porphyrins in supercritical carbon dioxide was significantly less than in halogenated solvents. Although solubility increased with pressure as the dielectric constant increased (became more like that of a halogenated solvent), the

maximum solubility achieved was quite low (< 1 μ M). Presumably SC CO₂ never became polar enough to dissolve large amounts of porphyrin.

The observed pressure broadening of electronic absorption bands is not unexpected. The $d\sigma^* \to p\sigma$ transitions in single crystals of Pt₂Cl have been shown to red shift and broaden with pressure. 11 However, the rather dramatic change in the shape of the spectrum from room temperature and one atmosphere pressure relative to SC pressure and temperature for both of the iron porphyrins is rather puzzling. The loss of resolution in the Soret bands of Fe(TFPP)Cl and Fe(TFPPBr₈)Cl could be ascribed to pressure broadening. Other aspects of the spectra are not as readily explained. A single intense O band has appeared in the spectrum of Fe(TFPPBr₈)Cl; although absorption maxima often shift with solvent, the appearance of a new absorptions suggests that the porphyrin has been chemically altered. A blue shift in the Soret band and an increase in intensity of a band around 600 nm may be attributed to dimerization at high pressures. Relative to the 410, 510, and 620 nm bands in Fe(TFPP)Cl, (FeTFPP)2O has absorption bands at 398 and 600 nm; these values match well with the observed SC CO₂ spectrum ($\lambda_{max} = 390$, 610 nm). Similarly, a μ-oxo dimer of Fe(TFPPBrg)Cl would be expected to have a blue shifted Soret band and a more intense Q band relative to the monomer. The SC CO2 spectrum of Fe(TFPPBr₈)Cl has maximum absorbance at 420 and 600 nm, relative to a 442 nm Soret band and weak Q bands in the solution spectrum. Although formation of a µ-oxo dimer should not have been possible in these experiments, since no oxygen was present in the cell, other dimerization modes are possible and could also account for the observed spectral changes. Contaminants from the carbon dioxide are also possible; although high purity carbon dioxide should be fairly free of impurities, no scrubbers were used. Dimerization is further suggested by the lack of pressure shifting with RuTFPPClg(CO); the ruthenium porphyrins are not as susceptible to dimerization as the iron analogs. Higher resolution spectra would have to be obtained to fully address this question.

A second complication was introduced by the use of methylene chloride. Methylene chloride was found to extract plasticizers from the O-rings used to make the seal between the sapphire windows and the cell. When the pressure was decreased, the plasticizers formed a film on the interior of the cell, possibly causing interference patterns and reducing the quality of the spectra. Furthermore, the plasticizers seem to reduce the solubility of RuTFPPCl₈(CO). Addition of RuTFPPCl₈(CO) as a solid to the cell resulted in much high solubility (Figure 6.7). By 3000 psi, the Soret band had already reached the maximum absorbance able to be measured by the instrument (~ 0.4).

Addition of cyclohexene resulted in a higher quality spectrum for RuTFPPClg(CO) (Figure 6.8). No solubility is observed in liquid carbon dioxide, but the transition limit of the spectrophotometer is reached by 2000 psi, indicating that cyclohexene is an excellent co-solvent for RuTFPPClg(CO). Cyclohexene also reduces the noise level in the ruthenium porphyrin spectrum; this effect is not understood. The structure in the Q band region changes in the presence of olefin, with a slight red shift and different intensity for the Q(1,0) and the Q(0,0) bands relative to the methylene chloride spectrum, indicating that cyclohexene may coordinate at high pressure, since no distinct Q bands were observed with SC CO₂ alone.

Despite the complications and noise levels of the spectra, lower limits for the solubility of the three halogenated porphyrins were determined. The minimal solubility of these complexes is not expected to limit the reactivity of the catalysts in supercritical carbon dioxide since the co-solvent properties of the substrate, cyclohexene, will increase the net solubility of Fe(TFPP)Cl, Fe(TFPPBr₈)Cl, and RuTFPPCl₈(CO) in the oxidation reaction mixture.

The ability to perform UV-visible spectroscopy at high pressures is a valuable tool for studying reaction intermediates in SCF reactions. This will help determine if reaction pathways change at higher pressures. Further work to enable transient IR and emission spectroscopy in SCF systems is currently in progress at LANL.

Oxidation of Cyclohexene

We investigated the ability of Fe(TFPP)Cl, Fe(TFPPBr₈)Cl, and RuTFPPCl₈(CO) to oxidize cyclohexene in supercritical carbon dioxide. The oxidation reaction had been studied in methylene chloride (Chapter 4 and 5), providing a comparison for data in a SCF. For oxidations with dioxygen, it was thought that the miscibility of O₂ would increase the reaction rate relative to the solution chemistry.

In order to help separate solvent and pressure effects, oxygenation reactions with iodosobenzene as an oxygen source were also investigated. This chemistry should be relatively unaffected by pressure, and should help isolate the different solvation properties at high pressure.

The oxidation reactions were conducted in a small autoclave reactor (Figure 6.9). Constructed in a similar fashion to the UV-Vis apparatus, this system had an additional inlet for pressurized air. The porphyrin, cyclohexene, and iodosobenzene (if used) were added to the reactor, which was then sealed and connected to the carbon dioxide inlet. As with the UV-Vis cell, the system temperature was maintained at 40 °C and the reaction stirred to maintain equilibrium. All reactions were run at 5000 psi of CO₂ to maximize solubility of the porphyrin. At the end of the batch reaction, the pressure was let down through a metering valve, and volatile organics were collected in cold acetone. The cell was washed with additional acetone, and products were detected by GC/MS.

Two reactions were run in the UV-Vis cell in order to determine the effect of light on the ruthenium porphyrin oxidation reaction. Since irradiation with visible light dramatically enhances catalysis by RuTFPPCl₈(CO) with dioxygen in methylene chloride, we wanted to determine if light would also enhance cyclohexene oxidation in SC CO₂.

The results of the oxidation reactions are shown in Figures 6.10 - 6.12. With iodosobenzene, the overall activity was similar to the methylene chloride reactions for Fe(TFPP)Cl and Fe(TFPPBr₈)Cl. RuTFPPCl₈(CO) activity was considerably higher in

SC CO₂, with 21 turnovers compared to only 5 in methylene chloride (4 hour points). The product distributions for these reactions showed more variation. Notably, Fe(TFPP)Cl produced only cyclohexene oxide. For the perhalogenated iron and ruthenium complexes, higher oxidation products were observed. While reactions in methylene chloride have only been found to produce 2-cyclohexen-1-ol and 2-cyclohexen-1-one, the SC CO₂ reactions showed large peaks in the GC at later retention times. The first was identified by comparison to a library mass spectrum as 7-oxa-bicyclo[4.1.0]heptan-2-one (Figure 6.13). The second was assumed to be 4-hydroxy-2-cyclohexen-1-one due to a similar relationship in the retention times of cyclohexene oxide and 2-cyclohexen-1-ol, and since it is the logical partitioning product from the oxidation of 2-cyclohexen-1-one. Both Fe(TFPPBr₈)Cl and RuTFPPCl₈(CO) reactions with PhIO showed less 2-cyclohexen-1-ol than in methylene chloride, and more 2-cyclohexen-1-one, as well as 7-oxa-bicyclo[4.1.0]heptan-2-one and 4-hydroxy-2-cyclohexen-1-ol. None of the reactions used more than 30% of the available oxidant in 4 hours. A batch reaction of Fe(TFPPBr₈)Cl run for 12 hours showed no more epoxide formation, but more allylic oxidation products were observed.

With air, the catalyst activities were similar in the two solvents. It is difficult to make a direct comparison, because the batch reactions in SC CO₂ were run for different times than the methylene chloride experiments. Nevertheless, it is clear that all catalysts are quite active in the supercritical solvent. Fe(TFPP)Cl (at 4 hours), Fe(TFPPBr₈)Cl, and RuTFPPCl₈(CO) (at 12 hours) showed 11, 59, and 51 turnovers, respectively. If the higher oxidation products are considered as more than one turnover, the numbers for the latter reactions increase to 127 and 90 turnovers. As with iodosobenzene, substantial amounts of multiple oxidation products were observed in all reactions, with a decrease in the amount of 2-cyclohexen-1-ol produced. Surprisingly, a greater percentage of epoxide was also produced.

Both Fe(TFPPBr₈)Cl and RuTFPPCl₈(CO) had substantial initiation periods in SC CO₂. Batch reactions run for only 4 hours showed no trace of products. After 12

hours, however, significant activity was observed, as described above. Only Fe(TFPP)Cl showed activity with air in the 4 hour time period. Attempts to shorten the initiation period for RuTFPPCl₈(CO) by the addition of light were not successful. Two experiments with RuTFPPCl₈(CO) were conducted in the larger UV-Vis cell. Upon addition of CO₂, the solution turned a bright red, indicating that cyclohexene serves as an excellent co-solvent for the catalyst. A flashlight was used to irradiate the reaction through the cell window for the duration of the batch reaction. However, after only a few hours, the pressure dropped and the solution bleached. A reaction in the UV-Vis cell was attempted twice. The first reaction, with one atmosphere of air, bleached after 20 hours. The second, with 5 atm air, bleached within 6 hours. After bleaching was observed, the cell was let down as previously described. No product formation was detected in either light reaction.

Discussion Oxidation Experiments

The iodosobenzene reactions in supercritical carbon dioxide all showed an increase in the percent epoxide formed relative to reaction in CH₂Cl₂. As discussed in Chapter 4, epoxidation with a high-valent metal-oxo is believed to occur by a different mechanism than hydroxylation. The different solvation properties of SC CO₂ may increase the probability for electron transfer (leading to epoxidation) over hydrogen abstraction (leading to hydroxylation). The success of free radical polymerization reactions conducted in SC CO₂ suggests that radicals are quite stable in a supercritical medium. However, the solvent may change the stability of the caged radical species such that electron transfer becomes more favorable. SC CO₂ may provide a new medium for probing the oxo-transfer step in olefin oxidation reactions.

In addition to the increase in epoxide formation, there is also an increase in multiple oxidations of the same substrate molecule, both with PhIO and dioxygen. The supercritical fluid did not greatly increase the observed turnover numbers, suggesting that phase transfer is not the limiting step in the dioxygen reactions for any of the porphyrins. However, the

different solvent properties of SC CO₂ may be changing the selectivity; perhaps the catalysts are more soluble in the oxidized cyclohexene derivatives than in cyclohexene itself. Therefore, the catalyst could re-oxidize a single substrate multiple times before encountering other substrate molecules.

For RuTFPPCl₈(CO), fewer turnovers are observed in the dark cell, consistent with the photochemical reaction mechanism described in Chapter 5. However, the UV-Vis suggests a greater interaction between the porphyrin and substrate in SC CO₂, indicating that olefin binding may occur in the ground state in this medium, whereas it only is effective in the excited state in a methylene chloride solution. Alternatively, a different reaction mechanism may take precedence in this solvent. Unfortunately, attempts to photolyze the reaction were complicated by the cell design. The Buna-N O-rings used to seal the sapphire windows, while having excellent resistance to supercritical carbon dioxide, are reported to have unsatisfactory resistance to alkanes, ¹² suggesting that the "bleach" observed upon photolysis was not due to porphyrin decomposition but a leaking cell.

Conclusion

The preliminary results described above demonstrate that supercritical carbon dioxide is an adequate solvent replacement for methylene chloride for porphyrin-catalyzed oxidation of cyclohexene. Large rate enhancement was not observed, but changes in the reaction selectivity did occur. Most notable was the 100% selectivity observed for epoxidation of cyclohexene with Fe(TFPP)Cl and PhIO, and increased epoxidation selectivity for both RuTFPPCl₈(CO) and Fe(TFPPBr₈)Cl in reactions with either PhIO or O₂. For allylic oxidation products, multiple oxidations of the same substrate molecule was observed, suggesting that destruction of organics in a supercritical medium may be favorable under different conditions. A repeat of the oxidation experiments at different temperatures and pressures would reveal if the selectivity could be tuned to favor one

pathway more completely. Further experiments would be needed to determine the source of these effects.

Methods

RuTFPPCl8(CO) and Fe(TFPPBr8)Cl were synthesized as in Chapter 2.

Fe(TFPP)Cl was used as received (Aldrich). Cyclohexene was from Aldrich, and distilled under argon before use. Acetone and methylene chloride were used as received from EM Science. Iodosobenzene was from TCI and used as received. Air and carbon dioxide were from Albuquerque Welding. Oxidation products were determined by injection onto an Hewlett Packard GC/MS with an auto injector and a JW Scientific DB-5 30m column. Sample identification was determined by injection of an authentic sample for cyclohexene oxide, 2-cyclohexen-1-ol, and 2-cyclohexen-1-one (Aldrich). The identity of one higher boiling peak was determined by the library on the GC MS.

Standard NPT, Swagelock, and HiP pressure rated valves and connections were used to build the high pressure systems. Stainless steel tubing (1/16" - 1/4") was used for longer connections. An ISCO brand syringe pump was used to pressurize the carbon dioxide. All systems were barricaded behind Lexan shielding, and tubing and valves were secured to the work tables to minimize damage in case of a pressure failure. All systems were equipped with relief valves or rupture discs, so the system would blow at the designed weak point in case of over-pressurization.

UV-Vis spectra were measured on a Hewlett Packard 8452 spectrophotometer. The lamp and detector were removed from the instrument cavity and placed on a laser table to allow room for the large cell. Additional focusing mirrors were placed after the lamp and before the detector to increase light intensity. Intensity data was collected in ASCII format, and loaded onto a Macintosh computer, where absorbance readings were calculated ($A = log (I_0/I)$). I_0 readings were taken at each pressure since the absorbance of CO_2 was found to change considerably around the supercritical transition. This is due to the variable

density of SC CO₂; the change in the index of refraction between the cell windows and solvent decreased at higher pressures. The stirplate was turned off when spectra were taken, in order to minimize refraction by mixing lines in solution. The large cell volume (≈ 75 mL) made it difficult to maintain a constant temperature in the cell, causing visible sheer lines due to the temperature gradient in solution. Averaging intensity data helped decrease the noise in the spectra.

The cell used for UV-Vis experiments was constructed of 316 stainless steel, with a 13.2 cm path length and 1 inch aperture on each side. The seal between the 1 cm thick sapphire windows and the metal cell was made by a Buna-N rubber O-ring, which was replaced after each use. The cell had three inlets for a thermocouple, an inlet valve, and a t-joint which contained a relief valve, an analog pressure gauge, and an outlet line. The outlet could be directed to a vacuum pump or vented to a hood.

For each sample, the cell was first mounted on the stand and aligned for maximum lamp intensity. A solution of porphyrin in methylene chloride was added through the thermocouple inlet, and then the thermocouple was fastened down. By this method, a known amount of porphyrin could be added, such that the possible absorbance in a 13.2 cm path length cell would not be above 1. The cell was evacuated, removing the solvent, and then carbon dioxide was added. The cell was sealed off at each pressure, and allowed to equilibrate to 40 ± 0.5 °C for each intensity reading. Alternatively, excess solid porphyrin was added to the cell before the windows were sealed down (the large nuts for the windows had to be tightened down on a vise).

Oxidation reactions were conducted in a cell designed by Dave Morgenstern and Sam Borkowsky at Los Alamos National Laboratory. This cell was a single 2.5" cylinder of 316 stainless steel, with a 5/8" hole bored into the center. The only openings were for a rupture disc (rated to 10000 psi), an analog pressure gauge, a thermocouple, and the main reactor valve. The total cell volume was \approx 12 mL. The inlet lines allowed the sequential addition of compressed air and carbon dioxide to the cell. Air was always added first, so

that the CO₂ would flush any oxygen from the lines before the system was brought up to pressure. Although air or pure oxygen gas could be used with this reactor, air was used for safety reasons.

Solid porphyrin, cyclohexene, and iodosobenzene (if used) were added to the reactor, the valve was sealed on the vise, and the reactor was then attached to the inlet and letdown tubing. Air was added first, up to the pressure of the tank (110 psig) and then CO₂ up to 5000 psi. As with the UV-Vis experiments, the cell rested on a stirplate and the cell temperature was maintained at 40 °C with heating tape. As soon as the pressure reached 5000 psi, the main reactor valve was closed, and the system allowed to stir for the desired reaction time.

Oxidation reactions were let down by a HiP metering valve through 1/16" tubing, and the end of the tubing was crimped with a hammer to reduce the flow rate. The pressure was let down slowly over a period of 1-2 hours into a vial containing approximately 20 mL of cold acetone to catch volatile organics. The vial rested in a cold block of steel to maintain its temperature and reduce loss of organics. The reaction vessel was then opened and rinsed with acetone to remove residual cyclohexene and products. The rinse was collected, and the volume measured. An aliquot was taken, diluted with a known amount of toluene in acetone to standardize the GC/MS analysis, and injected onto the GC. Although there is undoubtedly some loss to evaporation, it is believed that most of the organic products are collected by this method. No mass balance calculation was attempted.

References and Notes

- (1) Kaupp, G. Angew. Chem., Int. Ed. Eng. 1994, 33, 1452-1455.
- (2) Laintz, K. E.; Tachikawa, E. Anal. Chem. 1994, 66, 2190-2193.
- (3) Personal communication from William Tumas, Los Alamos National Laboratory, January 1995.
- (4) Wenclawiak, B. In Analysis with Supercritical Fluids: Extraction and Chromatography; B. Wenclawiak, Ed.; Springer-Verlag: Berlin, 1992.
- (5) Dickerson, R. E.; Gray, H. B.; Darensbourg, M. Y.; Darensbourg, D. J. Chemical Principles; 4th ed.; The Benjamin/Cummings Publishing Co., Inc.: Menlo Park, CA, 1984.
- (6) DeSimone, J. M.; Maury, E. E.; Meneceloglu, Y. Z.; McClain, J. B.; Romack, T. J.; Combes, J. R. Science 1994, 265, 356-359.
- (7) Jessop, P. G.; Hsiao, Y.; Ikariya, T.; Noyori, R. J. Am. Chem. Soc. 1994, 116, 8851-8852.
- (8) Jessop, P. G.; Ikariya, T.; Noyori, R. Nature 1994, 368, 231-233.
- (9) A substantial amount of oxidation chemistry has been investigated in supercritical water. Complete oxidation of organics has been observed under these harsh conditions. For example, see Webley, P. A.; Tester, J. W. Energy Fuels. 1991, 30, 411.
- (10) Srinivas, P.; Mukhopadhyay, M. Ind. Eng. Chem. Res. 1994, 33, 3118-3124.
- (11) Stroud, M. A.; Drickamer, H. G.; Zietlow, M. H.; Gray, H. B.; Swanson, B. I. J. Am. Chem. Soc. 1989, 111, 66-72.
- (12) Seymour, R. S. Engineering Polymer Source Book; McGraw-Hill: New York, 1990, pp 102.

Figure 6.1 -- Phase diagram of carbon dioxide (modified from reference 5). The critical point of CO₂ is at relatively low temperature and pressure, facilitating its use as a supercritical solvent.

Phase Diagram of Carbon Dioxide

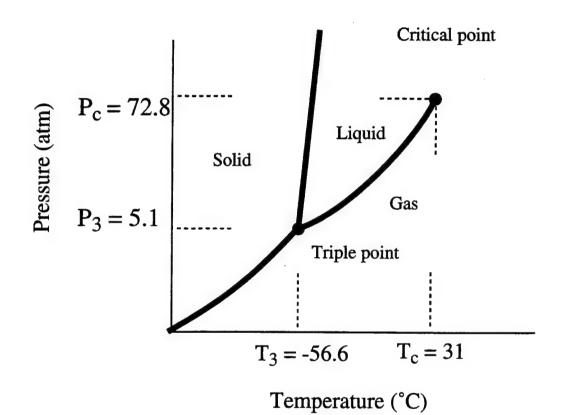
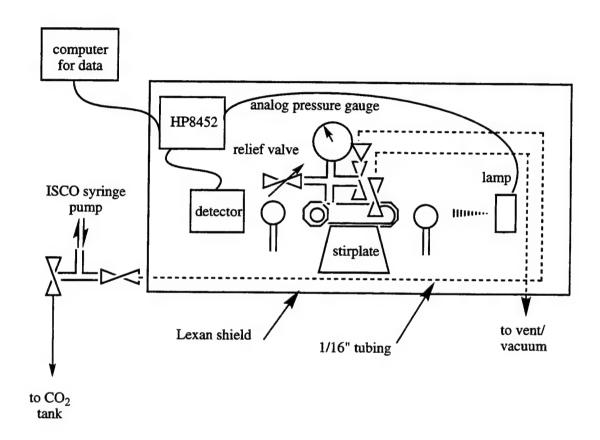


Figure 6.2 - Apparatus used for UV-Visible spectroscopy in supercritical carbon dioxide.

UV Vis in Supercritical CO₂



Cell characteristics: 6 inches long, 13.2 cm path length

1 inch diameter aperture with sapphire windows

75 mL cell volume, including dead space

316 stainless steel rated to 5000 psi

Figure 6.3 -- Spectra of Fe(TFPP)Cl in methylene chloride and carbon dioxide. The spectrum in SC CO₂ is smoothed to remove noise from refracted light. The solubility did not change much with pressure, increasing only from 0.27 to 0.30 μ M from 2000 to 5000 psi of CO₂.

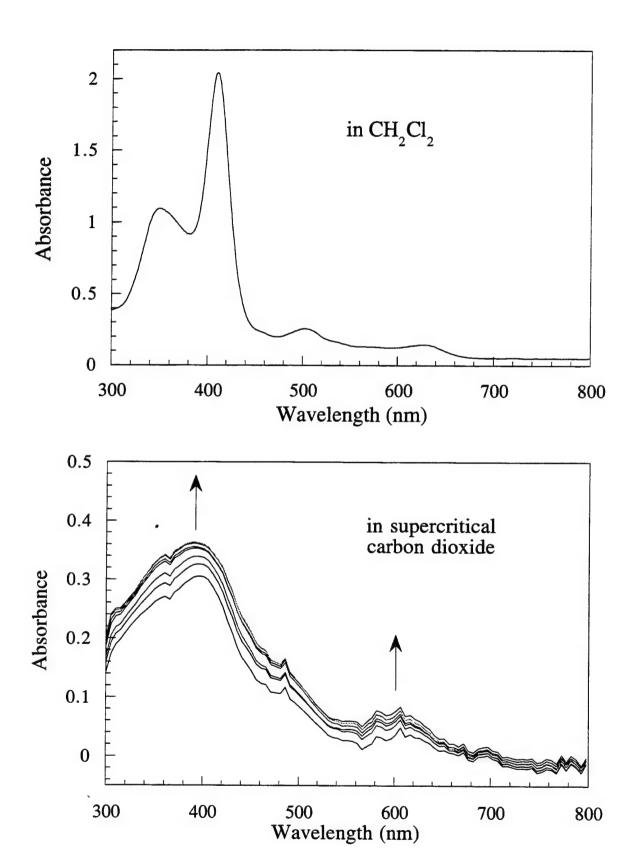
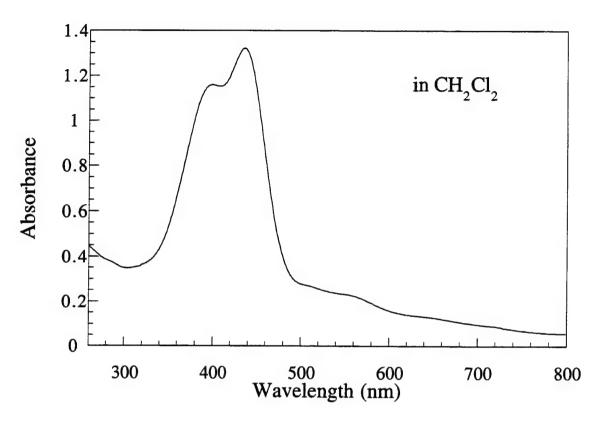


Figure 6.4 -- Spectra of Fe(TFPPBr₈)Cl in methylene chloride and carbon dioxide. The spectrum in SC CO₂ is smoothed to removed noise from refracted light. The solubility increased from 0.07 to 0.20 μM from 2000 to 3500 psi of CO₂, remaining fairly constant after this pressure.



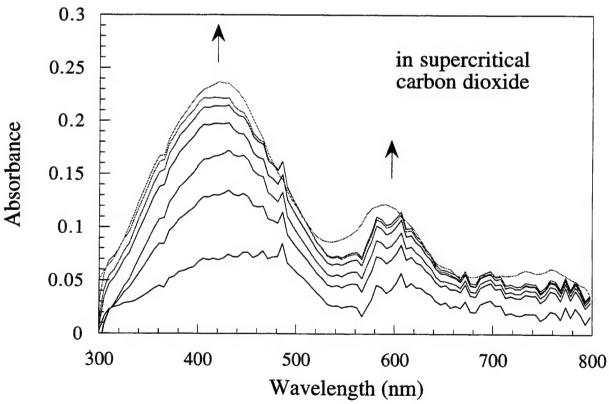
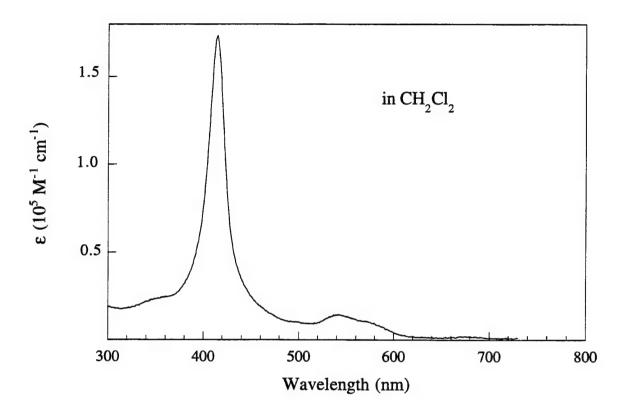


Figure 6.5 – Spectra of RuTFPPCl₈(CO)in methylene chloride and carbon dioxide. The porphyrin is almost insoluble in liquid CO₂, but solubility increased to 0.16 μM at 5000 psi of CO₂. The spectra in the two different solvents match best for RuTFPPCl₈(CO), suggesting no unusual interactions in the supercritical solvent.



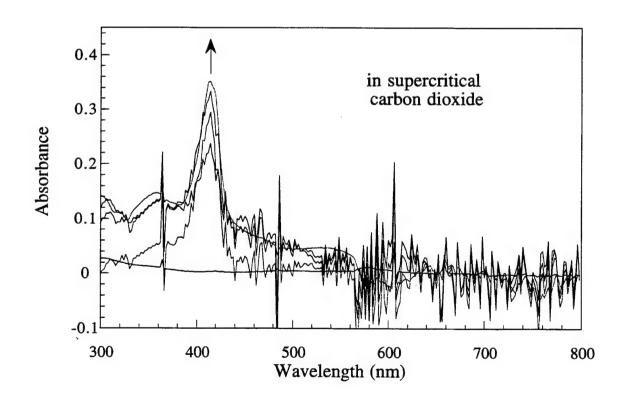


Figure 6.6 -- A plot of solubility versus pressure for the halogenated porphyrins.

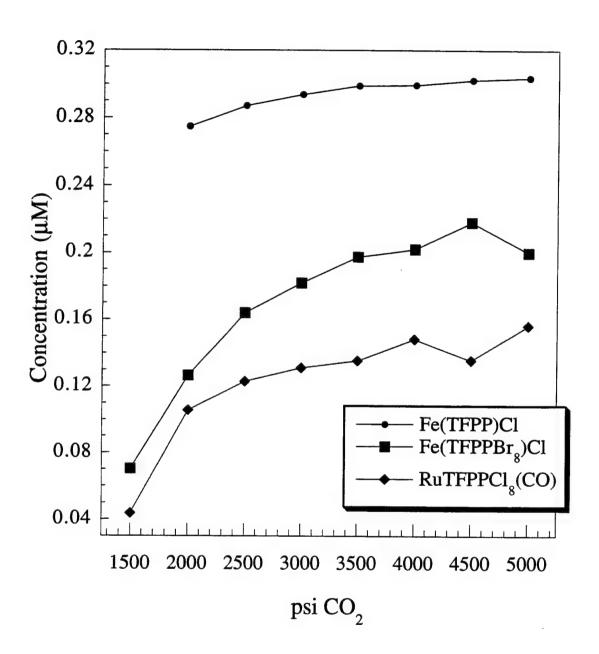


Figure 6.7 -- Spectrum of RuTFPPCl₈(CO) in carbon dioxide. This differs from the spectrum in Figure 6.3 in that the porphyrin was added as a solid, and not as a methylene chloride solution. The solubility is much higher in this case, reaching the maximum transmission of the instrument by 3000 psi, suggesting that a deleterious interaction occurs when the porphyrin is added as a CH₂Cl₂ solution (data at 2000, 3000, and 4000 psi).

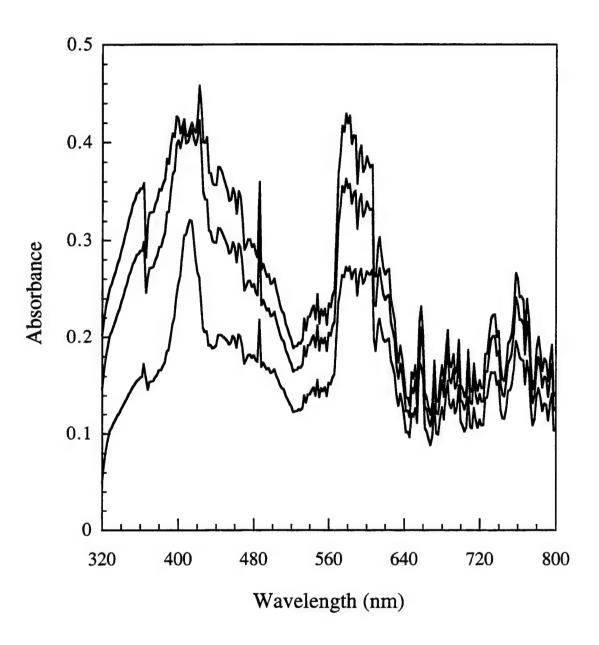


Figure 6.8 -- Spectrum of RuTFPPCl₈(CO) with cyclohexene in carbon dioxide. The Q band structure is significantly different than without cyclohexene, suggesting a possible interaction or binding of alkene in the supercritical solvent (data at 800, 1200, 2000, 3000, 4000, and 5000 psi).

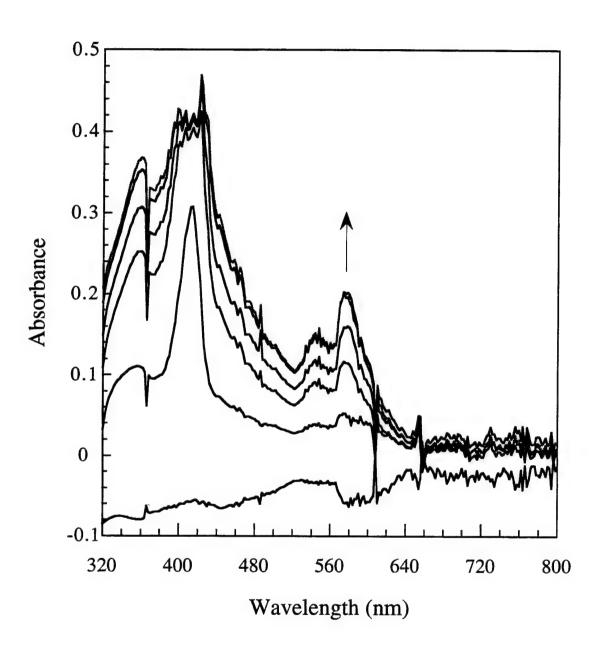


Figure 6.9 -- Cell used for oxidation reactions with iodosobenzene or air by halogenated porphyrins in supercritical carbon dioxide.

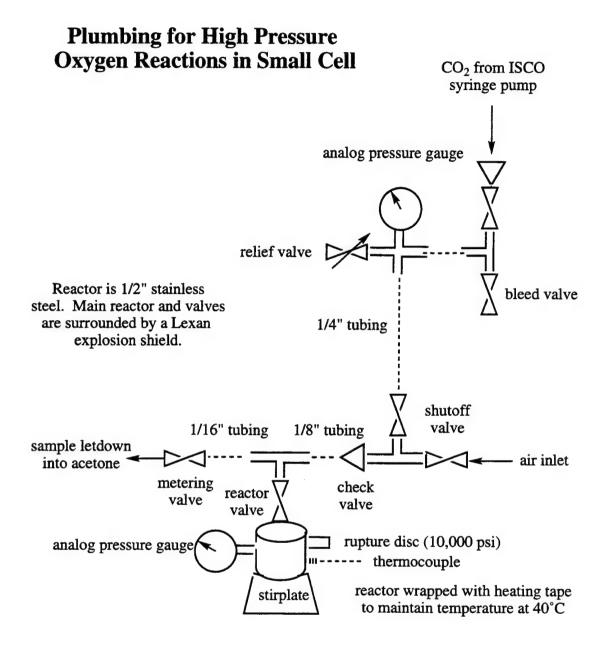


Figure 6.10 -- Turnovers of cyclohexene observed in oxidation reactions with Fe(TFPP)Cl and either iodosobenzene (left) or dioxygen (right). PhIO data is after 4 hours, and the dioxygen results are at 24 hours (CH₂Cl₂) or 12 hours (SC CO₂) in the different solvents. 100% selectivity for epoxide formation is observed with PhIO in SC CO₂.

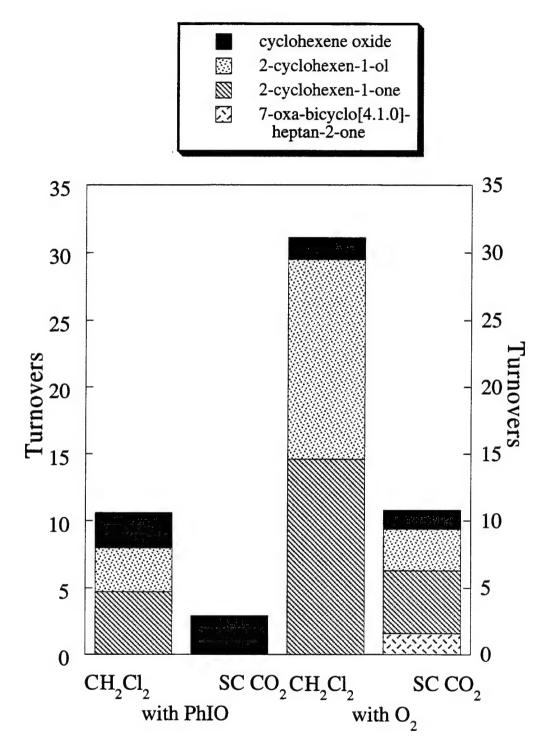


Figure 6.11 — Turnovers of cyclohexene observed in oxidation reactions with Fe(TFPPBr₈)Cl and either iodosobenzene (left) or dioxygen (right). PhIO data is after 4 hours, and the dioxygen results are at 24 hours (CH₂Cl₂) or 12 hours (SC CO₂) in the different solvents. Higher selectivity for epoxide formation is observed with dioxygen in SC CO₂ relative to CH₂Cl₂. Significant amounts of higher oxidation products are also observed.

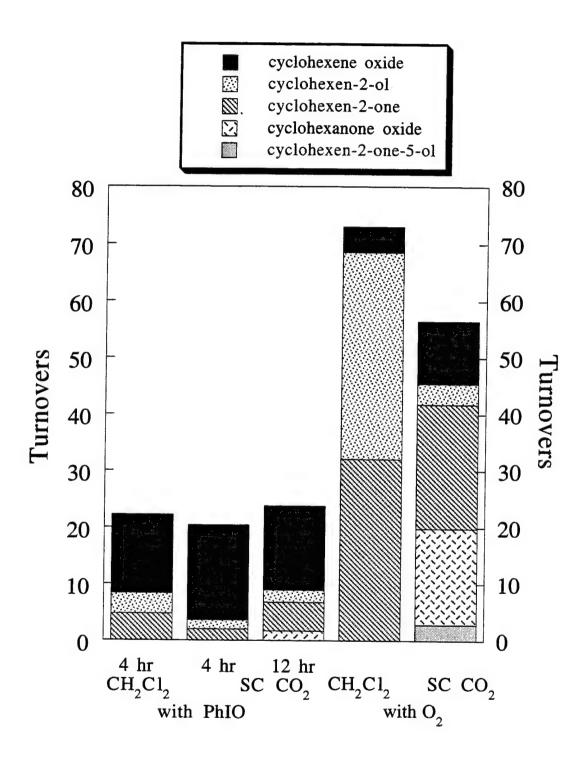
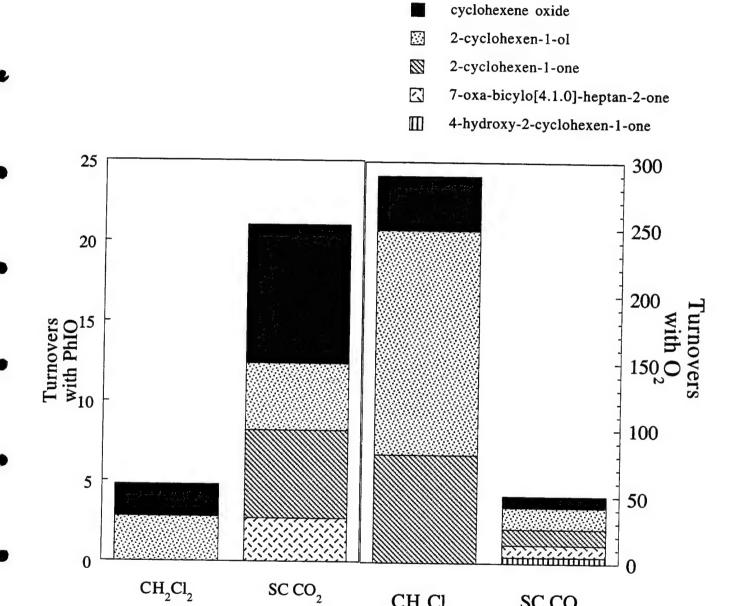


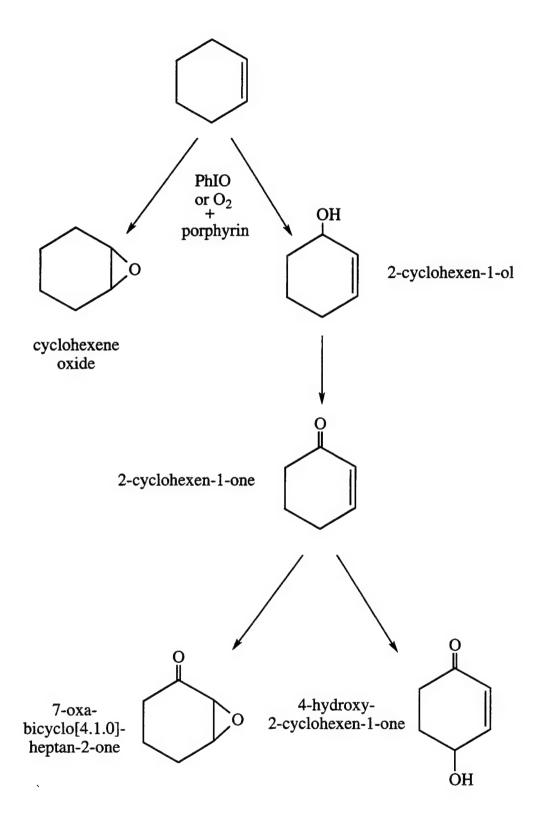
Figure 6.12 – Turnovers of cyclohexene observed in oxidation reactions with RuTFPPCl₈(CO) and either iodosobenzene (left) or dioxygen (right). PhIO data is after 4 hours, and the dioxygen results are at 24 hours (CH₂Cl₂) or 12 hours (SC CO₂) in the different solvents. Higher selectivity for epoxide formation is observed with PhIO in SC CO₂ relative to CH₂Cl₂. The dioxygen reactions are not as effective in the supercritical solvent.



CH₂Cl₂

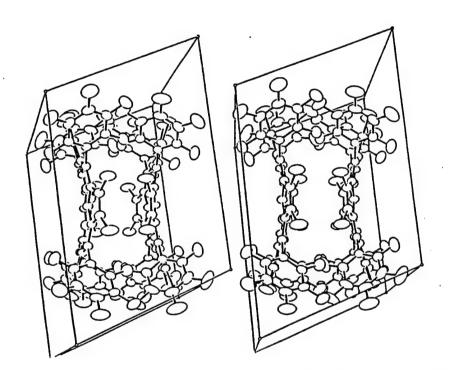
SC CO₂

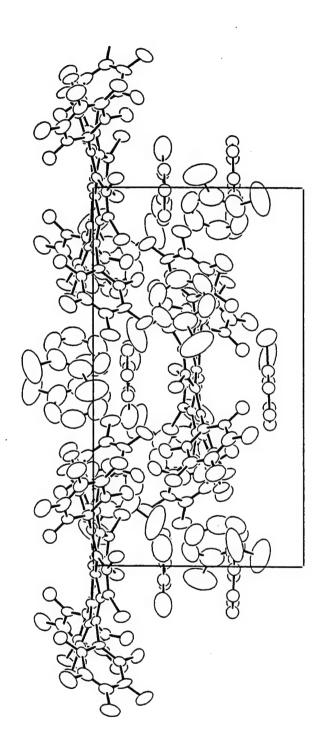
Figure 6.13 -- Partitioning mechanism to higher oxidation products.

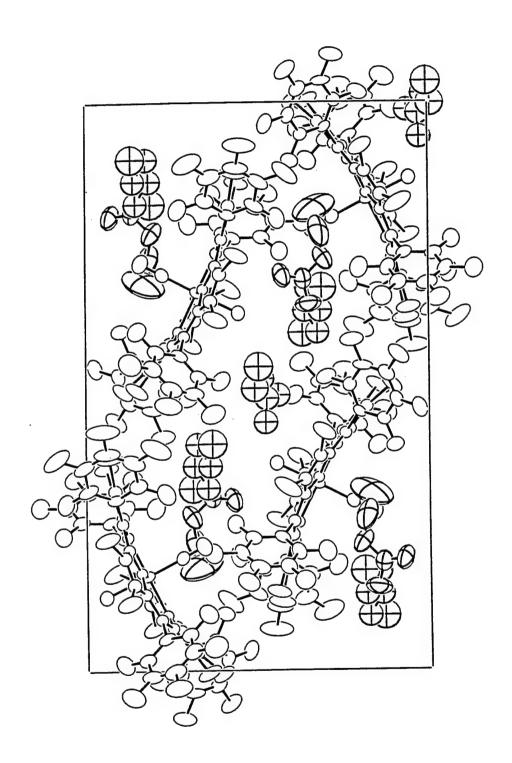


Appendix 2

Crystal Structure Data







•

•

•

•

•

•

Table 1. Final Heavy Atom Parameters for ${\bf Tetrakis(pentafluorophenyl)} \hbox{-} \beta\hbox{-}{\bf octachloroporphyrin}$

x, y, z and $U_{eq}^{a} \times 10^{4}$ U_{eq} Atom 8772(1) 7676(1) 3695(1) 599(2) Cl1 9105(1) 7909(1) 5768(1) 564(2) Cl2 7030(1) 6297(1) 9358(1) 649(3) C13 6863(1) 4203(1) 9784(1) 565(3) Cl4 666(1) 7251(1) 551(2) 8296(1) Cl5 388(1) 5189(1) 594(3) 8017(1) C16 5875(1) 3260(1) 2544(1) 610(2) C17 6089(1) 5349(1) 2107(1) 588(2) C18 N1 7751(2) 5801(2) 5404(2) 322(6) 7639(2) 4666(2) 7079(2) 303(6) N2 7448(2) 3089(2) 5970(2) 292(6) N3 7218(2) 4335(2) 4383(2) 311(6) **N4** 7855(3) 6171(2) 4534(2) 305(6) C1 8351(3) 6968(2) 4569(2) 347(7) C2 8477(3) 7076(2) 5450(2) 349(7) C3 8058(3) 6354(2) 6001(2) 318(7) C4 7890(3) 6276(2) 6972(2) 315(7) C5 5516(2) 7474(2) 305(7) C6 7600(3) 7306(3) 5446(2) 8484(2) 346(7) **C7** 7231(3) 4562(2) 8666(2) 335(7) C8

Table 1. (Cont.)

| Atom | z | \boldsymbol{y} | z | U_{eq} |
|------|---------|------------------|---------|----------|
| | | | | |
| C9 | 7464(3) | 4046(2) | 7771(2) | 295(7) |
| C10 | 7580(3) | 3079(2) | 7622(2) | 285(6) |
| C11 | 7659(3) | 2624(2) | 6766(2) | 287(6) |
| C12 | 7889(3) | 1611(2) | 6566(2) | 308(7) |
| C13 | 7771(3) | 1499(2) | 5684(2) | 318(7) |
| C14 | 7451(3) | 2439(2) | 5303(2) | 278(6) |
| C15 | 7112(3) | 2674(2) | 4449(2) | 298(7) |
| C16 | 6922(3) | 3579(2) | 4059(2) | 310(6) |
| C17 | 6483(3) | 3861(2) | 3212(2) | 349(7) |
| C18 | 6571(3) | 4745(2) | 3031(2) | 350(7) |
| C19 | 7080(3) | 5043(2) | 3756(2) | 304(7) |
| C20 | 7459(3) | 5865(2) | 3788(2) | 299(7) |
| C21 | 7988(3) | 7087(2) | 7529(2) | 313(7) |
| C22 | 6947(3) | 7927(2) | 7798(2) | 356(7) |
| C23 | 6998(3) | 8682(2) | 8311(2) | 417(9) |
| C24 | 8127(4) | 8587(2) | 8595(2) | 454(9) |
| C25 | 9175(3) | 7759(2) | 8359(2) | 444(8) |
| C26 | 9107(3) | 7027(2) | 7820(2) | 390(8) |
| C31 | 7581(3) | 2476(2) | 8462(2) | 287(6) |
| C32 | 8712(3) | 2034(2) | 8757(2) | 346(7) |
| | | | | |

Table 1. (Cont.)

| Atom | x | y | z | U_{eq} |
|------|----------|---------|----------|----------|
| | | | | |
| C33 | 8719(3) | 1485(2) | 9522(2) | 412(8) |
| C34 | 7567(4) | 1361(2) | 10009(2) | 491(10) |
| C35 | 6431(3) | 1784(2) | 9738(2) | 465(9) |
| C36 | 6446(3) | 2343(2) | 8980(2) | 368(7) |
| C41 | 7026(3) | 1869(2) | 3882(2) | 313(7) |
| C42 | 8108(3) | 1325(2) | 3209(2) | 388(7) |
| C43 | 8109(4) | 554(2) | 2699(2) | 516(9) |
| C44 | 7008(4) | 292(2) | 2873(3) | 572(10) |
| C45 | 5909(4) | 799(3) | 3536(3) | 573(9) |
| C46 | 5909(3) | 1603(2) | 4018(2) | 426(8) |
| C51 | 7431(3) | 6472(2) | 2950(2) | 306(6) |
| C52 | 8481(3) | 6277(2) | 2166(2) | 387(8) |
| C53 | 8433(4) | 6815(3) | 1389(2) | 478(9) |
| C54 | 7343(4) | 7583(3) | 1397(2) | 488(9) |
| C55 | 6295(3) | 7816(2) | 2163(3) | 454(9) |
| C56 | 6344(3) | 7253(2) | 2920(2) | 357(7) |
| F22 | 5813(2) | 8012(1) | 7569(1) | 587(5) |
| F23 | 5974(2) | 9491(1) | 8548(2) | 679(6) |
| F24 | 8193(2) | 9314(1) | 9096(1) | 721(6) |
| F25 | 10283(2) | 7663(2) | 8629(2) | 740(6) |

Table 1. (Cont.)

| Atom | æ | y | z | U_{eq} |
|------|----------|---------|----------|----------|
| F26 | 10183(2) | 6251(1) | 7549(2) | 661(6) |
| F32 | 9855(2) | 2125(1) | 8267(1) | 526(5) |
| F33 | 9839(2) | 1063(1) | 9778(1) | 670(6) |
| F34 | 7552(2) | 820(2) | 10752(1) | 833(7) |
| F35 | 5305(2) | 1658(2) | 10213(2) | 825(7) |
| F36 | 5305(2) | 2795(1) | 8753(1) | 560(5) |
| F42 | 9238(2) | 1523(2) | 3072(1) | 628(6) |
| F43 | 9185(2) | 56(2) | 2043(2) | 916(7) |
| F44 | 7005(3) | -470(2) | 2384(2) | 1022(8) |
| F45 | 4818(3) | 549(2) | 3707(2) | 985(7) |
| F46 | 4808(2) | 2121(2) | 4628(2) | 765(7) |
| F52 | 9591(2) | 5562(1) | 2157(1) | 677(6) |
| F53 | 9461(2) | 6597(2) | 639(1) | 827(7) |
| F54 | 7293(3) | 8122(2) | 650(2) | 864(7) |
| F55 | 5208(2) | 8568(1) | 2179(2) | 750(6) |
| F56 | 5271(2) | 7458(1) | 3637(1) | 627(6) |

 $[^]a$ $U_{eq}=\frac{1}{3}\sum_i\sum_j[U_{ij}(a_i^*a_j^*)(\vec{a}_i\cdot\vec{a}_j)]$

Table 2. Selected Distances and Angles for ${\bf Tetrakis(pentafluorophenyl)} \hbox{-}\beta\hbox{-}{\bf octachloroporphyrin}$

| Dis | stance(Å) | Dis | stance(Å) |
|----------|-----------|----------|-----------|
| Cl1 -C2 | 1.706(3) | C4 -C5 | 1.400(4) |
| Cl2 -C3 | 1.705(3) | C5 -C6 | 1.404(4) |
| Cl3 -C7 | 1.708(3) | C6 -C7 | 1.449(4) |
| C14 -C8 | 1.708(3) | C7 -C8 | 1.341(4) |
| Cl5 -C12 | 1.702(3) | C8 -C9 | 1.453(4) |
| Cl6 -C13 | 1.706(3) | C9 -C10 | 1.396(4) |
| Cl7 -C17 | 1.708(3) | C10 -C11 | 1.402(4) |
| Cl8 -C18 | 1.706(3) | C11 -C12 | 1.445(4) |
| N1 -C1 | 1.372(4) | C12 -C13 | 1.350(4) |
| N1 -C4 | 1.372(4) | C13 -C14 | 1.446(4) |
| N2 -C6 | 1.366(4) | C14 -C15 | 1.399(4) |
| N2 -C9 | 1.370(4) | C15 -C16 | 1.407(4) |
| N3 -C11 | 1.373(4) | C16 -C17 | 1.448(4) |
| N3 -C14 | 1.377(4) | C17 -C18 | 1.346(4) |
| N4 -C16 | 1.373(4) | C18 -C19 | 1.450(4) |
| N4 -C19 | 1.369(4) | C19 -C20 | 1.400(4) |
| C1 -C2 | 1.446(4) | | |
| C1 -C20 | 1.404(4) | | |
| C2 -C3 | 1.350(4) | | |
| C3 -C4 | 1.445(4) | | |

Table 2. (Cont.)

| Angle | (°) | An | igle(°) |
|--------------|----------|---------------|----------|
| C4 -N1 -C1 | 109.9(2) | C6 -C7 -Cl3 | 129.5(2) |
| C9 -N2 -C6 | 109.4(2) | C8 -C7 -C13 | 122.2(2) |
| C14 -N3 -C11 | 109.5(2) | C8 -C7 -C6 | 108.3(3) |
| C19 -N4 -C16 | 109.1(2) | C7 -C8 -C14 | 122.6(2) |
| C2 -C1 -N1 | 106.8(2) | C9 -C8 -C14 | 129.8(2) |
| C20 -C1 -N1 | 125.4(3) | C9 -C8 -C7 | 107.6(3) |
| C20 -C1 -C2 | 127.6(3) | C8 -C9 -N2 | 107.4(2) |
| C1 -C2 -Cl1 | 129.4(2) | C10 -C9 -N2 | 125.4(3) |
| C3 -C2 -Cl1 | 122.5(2) | C10 -C9 -C8 | 127.1(3) |
| C3 -C2 -C1 | 108.1(3) | C11 -C10 -C9 | 126.0(3) |
| C2 -C3 -C12 | 122.7(2) | C10 -C11 -N3 | 125.1(3) |
| C4 -C3 -C12 | 129.2(2) | C12 -C11 -N3 | 107.2(2) |
| C4 -C3 -C2 | 108.0(3) | C12 -C11 -C10 | 127.6(3) |
| C3 -C4 -N1 | 106.9(2) | C11 -C12 -Cl5 | 129.2(2) |
| C5 -C4 -N1 | 125.9(3) | C13 -C12 -C15 | 122.7(2) |
| C5 -C4 -C3 | 127.0(3) | C13 -C12 -C11 | 108.1(2) |
| C6 -C5 -C4 | 125.6(3) | C12 -C13 -C16 | 121.5(2) |
| C5 -C6 -N2 | 125.1(3) | C14 -C13 -Cl6 | 130.4(2) |
| C7 -C6 -N2 | 107.3(2) | C14 -C13 -C12 | 108.0(3) |
| C7 -C6 -C5 | 127.4(3) | C13 -C14 -N3 | 107.1(2) |

Table 2. (Cont.)

Angle(°)

| C15 -C14 -N3 | 125.5(2) |
|---------------|----------|
| C15 -C14 -C13 | 127.3(3) |
| C16 -C15 -C14 | 125.8(3) |
| C15 -C16 -N4 | 125.5(3) |
| C17 -C16 -N4 | 107.5(2) |
| C17 -C16 -C15 | 126.9(3) |
| C16 -C17 -C17 | 129.1(2) |
| C18 -C17 -C17 | 122.9(2) |
| C18 -C17 -C16 | 107.9(3) |
| C17 -C18 -C18 | 122.2(2) |
| C19 -C18 -C18 | 130.0(2) |
| C19 -C18 -C17 | 107.8(3) |
| C18 -C19 -N4 | 107.6(2) |
| C20 -C19 -N4 | 125.3(3) |
| C20 -C19 -C18 | 127.0(3) |
| C19 -C20 -C1 | 125.6(3) |

Table S1. Anisotropic Displacement Parameters for Tetrakis(pentafluorophenyl)- β -octachloroporphyrin

| Atom | U_{11} | U_{22} | U_{33} | <i>U</i> ₁₂ | U_{13} | U_{23} |
|------|----------|----------------|----------|------------------------|----------|----------|
| Cli | 990(8) | 710(6) | 410(5) | -647(6) | -262(5) | 235(4) |
| C12 | 906(7) | 624 (6) | 459(5) | -589(5) | -259(5) | 119(4) |
| C13 | 1245(9) | 425(5) | 309(5) | -384(5) | -93(5) | -55(4) |
| Cl4 | 1022(8) | 439(5) | 247(4) | -315(5) | -78(4) | 41(4) |
| C15 | 979(7) | 284(4) | 484(5) | -179(4) | -401(5) | 126(4) |
| C16 | 1110(8) | 252(4) | 520(5) | -199(5) | -417(5) | 35(4) |
| C17 | 1028(8) | 488(5) | 657(6) | -422(5) | -616(6) | 178(4) |
| C18 | 1017(8) | 492(5) | 554(6) | -402(5) | -552(5) | 253(4) |
| N1 | 476(16) | 288(13) | 286(14) | -200(12) | -150(12) | 53(11) |
| N2 | 421(15) | 286(13) | 235(13) | -146(11) | -102(12) | 13(11) |
| N3 | 399(15) | 245(13) | 269(13) | -126(11) | -127(11) | 41(11) |
| N4 | 459(16) | 271(13) | 275(14) | -164(12) | -166(12) | 43(11) |
| C1 | 385(18) | 312(16) | 283(16) | -166(14) | -133(14) | 53(13) |
| C2 | 443(19) | 359(17) | 320(17) | -226(15) | -118(15) | 81(13) |
| C3 | 436(19) | 323(16) | 384(18) | -220(15) | -147(15) | 52(14) |
| C4 | 408(18) | 283(16) | 327(17) | -171(14) | -134(14) | 49(13) |
| C5 | 385(18) | 282(16) | 328(17) | -146(14) | -132(14) | 21(13) |
| C6 | 364(18) | 274(16) | 307(16) | -118(13) | -118(14) | 12(13) |
| C7 | 468(19) | 310(17) | 261(16) | -126(14) | -89(14) | -21(13) |
| C8 | 427(19) | 333(17) | 255(16) | -138(14) | -85(14) | 40(13) |
| C9 | 369(18) | 302(16) | 236(15) | -129(13) | -93(13) | 40(13) |
| C10 | 329(17) | 293(16) | 262(16) | -121(13) | -106(13) | 65(12) |
| C11 | 301(16) | 286(16) | 296(16) | -111(13) | -98(13) | 60(13) |
| C12 | 367(17) | 250(15) | 338(17) | -113(13) | -131(14) | 82(13) |
| C13 | 382(18) | 258(15) | .344(17) | -117(13) | -129(14) | 11(13) |
| C14 | 318(17) | 250(15) | 286(16) | -100(13) | -102(13) | 12(12) |
| C15 | 327(17) | 279(16) | 311(16) | -122(13) | -91(13) | -2(13) |
| C16 | 393(18) | 311(16) | 287(16) | -159(14) | -135(14) | 25(13) |
| C17 | 453(19) | 343(17) | 334(17) | -158(15) | -213(15) | 23(13) |
| C18 | 451(19) | 325(17) | 346(17) | -152(15) | -200(15) | 100(13) |
| C19 | 376(18) | 302(16) | 280(16) | -142(14) | -126(14) | 49(13) |
| C20 | 326(17) | 299(16) | 286(16) | -108(13) | -99(13) | 64(12) |
| C21 | 425(19) | 281(16) | 295(16) | -172(14) | -128(14) | 44(13) |
| C22 | 386(19) | 362(18) | 404(18) | -200(15) | -150(15) | 80(14) |
| C23 | 540(22) | 253(17) | 422(19) | -137(16) | -41(17) | 10(14) |
| C24 | 740(26) | 390(20) | 363(19) | -338(19) | -166(18) | 10(15) |
| C25 | 546(22) | 522(22) | 432(20) | -299(19) | -264(17) | 94(16) |
| C26 | 484(21) | 316(17) | 391(18) | | -158(16) | 36(14) |
| C31 | 399(18) | 260(15) | 243(15) | -139(13) | -116(14) | 42(12) |

Table S1. (Cont.)

| Atom | U_{11} | U_{22} | U_{33} | U_{12} | U_{13} | U_{23} |
|------|----------|----------|----------|-----------------|----------------|----------|
| C32 | 411(20) | 330(17) | 319(17) | -135(15) | -112(15) | 13(14) |
| C33 | 522(22) | 367(18) | 347(18) | -51(16) | -239(17) | 36(14) |
| C34 | 745(27) | 373(19) | 293(18) | -116(18) | -116(18) | 140(15) |
| C35 | 490(22) | 441(20) | 406(20) | -181(17) | 29(17) | 128(16) |
| C36 | 385(19) | 330(17) | 401(19) | -107(15) | -135(16) | 76(14) |
| C41 | 413(19) | 298(16) | 300(16) | -157(14) | -169(15) | 45(13) |
| C42 | 460(21) | 385(18) | 381(18) | -145(16) | -207(16) | 2(15) |
| C43 | 599(24) | 436(20) | 461(21) | 17(19) | -279(19) | -124(17) |
| C44 | 871(31) | 346(20) | 657(26) | -228(21) | -437(24) | -20(18) |
| C45 | 745(28) | 633(25) | 678(26) | -512(23) | -420(23) | 217(21) |
| C46 | 450(21) | 481(20) | 416(19) | -219(17) | -145(17) | 55(16) |
| C51 | 389(18) | 301(16) | 285(16) | -169(14) | -112(14) | 45(13) |
| C52 | 387(19) | 396(18) | 395(19) | -131(16) | -123(16) | 28(15) |
| C53 | 566(23) | 618(23) | 307(19) | -332(20) | -22(17) | 37(17) |
| C54 | 789(28) | 526(22) | 377(20) | -421(21) | -299(20) | 215(17) |
| C55 | 559(23) | 300(18) | 625(24) | -154(17) | -359(20) | 105(16) |
| C56 | 381(19) | 335(17) | 376(18) | -122(15) | -124(16) | 25(14) |
| F22 | 486(12) | 505(12) | 829(15) | -148(10) | -287(11) | 16(10) |
| F23 | 746(15) | 350(11) | 807(15) | -90(11) | -59(12) | -71(10) |
| F24 | 1212(19) | 508(12) | 648(13) | -470(13) | -342(13) | -83(10) |
| F25 | 833(16) | 822(15) | 872(16) | -431(13) | -559(13) | 86(12) |
| F26 | 543(13) | 518(12) | 906(16) | -45(10) | -317(12) | -74(11) |
| F32 | 403(11) | 650(13) | 584(12) | -227(10) | -160(10) | 108(10) |
| F33 | 760(15) | 639(13) | 603(13) | -28(11) | -433(12) | 82(10) |
| F34 | 1148(19) | 766(15) | 455(12) | -179(14) | -165(12) | 367(11) |
| F35 | 685(15) | 841(16) | 814(16) | -298(13) | 111(13) | 347(13) |
| F36 | 402(11) | 624(12) | 681(13) | -178(10) | -181(10) | 186(10) |
| F42 | 434(12) | 861(15) | 598(13) | -242(11) | -87(10) | -140(11) |
| F43 | 807(17) | 874(17) | 819(16) | 178(14) | -324(14) | -470(14) |
| F44 | 1617(25) | 521(14) | 1228(21) | -413(15) | -803(19) | -154(13) |
| F45 | 1173(21) | 1190(20) | 1143(20) | -981(18) | -508(17) | 282(16) |
| F46 | 526(14) | 1098(18) | 679(15) | -393(13) | 21(12) | -121(13) |
| F52 | 472(12) | 650(13) | 701(14) | 4(11) | -17(10) | 13(11) |
| F53 | 941(17) | 1098(18) | 423(13) | | 142(12) | 7(12) |
| F54 | 1436(22) | 877(16) | 590(14) | | -494(14) | 462(12) |
| F55 | 817(16) | 459(12) | 1065(18) | | -575(14) | 203(11) |
| F56 | 442(12) | 663(13) | 621(13) | -62(10) | -7 (11) | 5(10) |
| | | | | | | |

 $U_{i,j}$ values have been multiplied by 10^4 The form of the displacement factor is: $\exp{-2\pi^2(U_{11}h^2a^{*2} + U_{22}k^2b^{*2} + U_{33}\ell^2c^{*2} + 2U_{12}hka^*b^* + 2U_{13}h\ell a^*c^* + 2U_{23}k\ell b^*c^*)}$

Table S2. Hydrogen Atom Parameters for ${\bf Tetrakis}({\bf pentafluorophenyl}) \hbox{-} \beta\hbox{-}{\bf octachloroporphyrin}$

 $x, y \text{ and } z \times 10^4$

| Atom | £ | y | z | В |
|----------|----------------------|----------------------|----------------------|------------|
| H1 | 7559(53) | 5227(40) | 5567(38) | 3.0 |
| H2 H3 | 7773(55) 7317(51) | 4537(41) 3747(40) | 6517(41) 5918(37) | 2.9 2.8 |
| H4 | 7414(55) | 4351(40) | 4900(40) | 2.9 |

All atoms have a population factor of one-half.

Table S3. Complete Distances and Angles for Tetrakis(pentafluorophenyl)- β -octachloroporphyrin

| akis(pentai | Idol opiicii | j 1)-ρ-000a0111 | ,roporping |
|----------------------|----------------------|----------------------|----------------------|
| Dis | $tance(ilde{A})$ | Dis | tance(A) |
| Cl1 -C2 | 1.706(3) | C15 -C41 | 1.496(4) |
| Cl2 -C3 | 1.705(3) | C16 -C17 | 1.448(4) |
| Cl3 -C7 | 1.708(3) | C17 -C18 | 1.346(4) |
| Cl4 -C8 | 1.708(3) | C18 -C19 | 1.450(4) |
| Cl5 -C12 | 1.702(3) | C19 -C20 | 1.400(4) |
| Cl6 -C13 | 1.706(3) | C20 -C51 | 1.506(4) |
| Cl7 -C17 | 1.708(3) | C21 -C22 | 1.373(4) |
| Cl8 -C18 | 1.706(3) | C21 -C26 | 1.381(4) |
| N1 -C1 | 1.372(4) | C22 -C23 | 1.372(4) |
| N1 -C4 | 1.372(4) | C22 -F22 | 1.343(4) |
| N1 -H1 | 0.94(6) | C23 -C24 | 1.375(5) |
| N2 -C6 | 1.366(4) | C23 -F23 | 1.331(4) |
| N2 -C9 | 1.370(4) | C24 -C25 | 1.361(5) |
| N2 -H2 | 0.82(6) | C24 -F24 | 1.335(4) |
| N3 -C11 | 1.373(4) | C25 -C26 | 1.375(5) |
| N3 -C14 | 1.377(4) | C25 -F25 | 1.342(4) |
| N3 -H3 | 0.93(6) | C26 -F26 | 1.337(4) |
| N4 -C16 | 1.373(4) | C31 -C32 | 1.380(4) |
| N4 -C19 | 1.369(4) | C31 -C36 | 1.373(4) |
| N4 -H4 | 0.84(6) | C32 -C33 | 1.370(4) |
| C1 -C2 | 1.446(4) | C32 -F32 | 1.342(3) |
| C1 -C20 | 1.404(4) | C33 -C34 | 1.369(5) |
| C2 -C3 | 1.350(4) | C33 -F33 | 1.335(4) |
| C3 -C4 | 1.445(4) | C34 -C35 | 1.363(5) |
| C4 -C5 | 1.400(4) | C34 -F34 | 1.336(4) |
| C5 -C6 | 1.404(4) | C35 -C36 | 1.368(5) |
| C5 -C21 | 1.500(4) | C35 -F35 | 1.340(4) |
| C6 -C7 | 1.449(4) | C36 -F36 | 1.343(4) |
| C7 -C8 | 1.341(4) | C41 -C42 | 1.374(4) |
| C8 -C9 | 1.453(4) | C41 -C46 | 1.380(4) 1.365(5) |
| C9 -C10 | 1.396(4) | C42 -C43 C42 -F42 | 1.341(4) |
| C10 -C11 | 1.402(4) | C42 -F42 C43 -C44 | 1.359(5) |
| C10 -C31 | 1.503(4) | C43 -C44 C43 -F43 | 1.339(4) |
| C11 -C12 C12 -C13 | 1.445(4) 1.350(4) | C44 -C45 | 1.362(6) |
| C12 -C13 | 1.446(4) | C44 -C43 C44 -F44 | 1.338(5) |
| C14 -C15 | 1.399(4) | C45 -C46 | 1.385(5) |
| C14 -C15 | 1.407(4) | C45 -F45 | 1.337(5) |
| 019 -010 | 1.401(4) | 040 -1 40 | 2.001(0) |

Table S3. (Cont.)

| | Distance(Å) | A | ngle(°) |
|--|--|--|--|
| C46 -F46 C51 -C52 C51 -C56 C52 -C53 C52 -F52 C53 -C54 C54 -C55 C54 -F54 C55 -F56 C56 -F56 | 1.329(4) 1.382(4) 1.377(4) 1.377(5) 1.331(4) 1.357(5) 1.336(4) 1.362(5) 1.341(4) 1.373(5) 1.341(4) | A C4 -N1 -C1 H1 -N1 -C1 H1 -N1 -C1 H1 -N1 -C4 C9 -N2 -C6 H2 -N2 -C6 H2 -N2 -C9 C14 -N3 -C11 H3 -N3 -C11 H3 -N3 -C14 C19 -N4 -C16 H4 -N4 -C16 H4 -N4 -C19 C2 -C1 -N1 C20 -C1 -N1 C20 -C1 -C2 C1 -C2 -C1 C3 -C2 -C1 C3 -C2 -C1 C3 -C2 -C1 C3 -C2 -C1 C4 -C3 -C1 C4 -C3 -C1 C5 -C4 -N1 C5 -C4 -C3 C6 -C5 -C4 C21 -C5 -C6 C5 -C6 -N2 C7 -C6 -N2 C7 -C6 -C5 C6 -C7 -C13 C8 -C7 -C13 C8 -C7 -C6 C7 -C6 | ngle(°) 109.9(2) 125.9(35) 124.1(35) 109.4(2) 125.7(42) 124.9(42) 109.5(2) 123.1(35) 127.4(35) 109.1(2) 123.6(40) 127.3(41) 106.8(2) 125.4(3) 127.6(3) 129.4(2) 122.5(2) 108.1(3) 122.7(2) 108.0(3) 106.9(2) 125.9(3) 127.0(3) 127.0(3) 127.0(3) 127.0(3) 127.1(2) 125.1(3) 107.3(2) 117.1(2) 125.1(3) 107.3(2) 127.4(3) 129.5(2) 108.3(3) 129.5(2) 108.3(3) 129.5(2) |
| · | | C7 -C8 -C14 C9 -C8 -C14 C9 -C8 -C7 C8 -C9 -N2 C10 -C9 -N2 | 122.6(2) 129.8(2) 107.6(3) 107.4(2) 125.4(3) |

Table S3. (Cont.)

| C10 -C9 -C8 127.1(3) F22 -C22 -C21 118.9 | (3) |
|--|-----|
| C11 -C10 -C9 126.0(3) F22 -C22 -C23 118.0 | |
| C31 -C10 -C9 117.0(2) C24 -C23 -C22 118.8 | |
| C31 -C10 -C11 116.9(2) F23 -C23 -C22 121.3 | (3) |
| C10 -C11 -N3 125.1(3) F23 -C23 -C24 119.9 | |
| C12 -C11 -N3 107.2(2) C25 -C24 -C23 120.1 | |
| C12 -C11 -C10 127.6(3) F24 -C24 -C23 119.6 | |
| C11 -C12 -C15 129.2(2) F24 -C24 -C25 120.3 | (3) |
| C13 -C12 -C15 122.7(2) C26 -C25 -C24 119.7 | (3) |
| C13 -C12 -C11 108.1(2) F25 -C25 -C24 120.5 | |
| C12 -C13 -C16 121.5(2) F25 -C25 -C26 119.8 | (3) |
| C14 -C13 -Cl6 130.4(2) C25 -C26 -C21 122.2 | (3) |
| C14 -C13 -C12 108.0(3) F26 -C26 -C21 119.7 | |
| C13 -C14 -N3 107.1(2) F26 -C26 -C25 118.1 | |
| C15 -C14 -N3 125.5(2) C32 -C31 -C10 122.1 | |
| C15 -C14 -C13 127.3(3) C36 -C31 -C10 121.4 | |
| C16 -C15 -C14 125.8(3) C36 -C31 -C32 116.5 | |
| C41 -C15 -C14 116.5(2) C33 -C32 -C31 122.4 | |
| C41 -C15 -C16 117.7(2) F32 -C32 -C31 119.1 | |
| C15 -C16 -N4 125.5(3) F32 -C32 -C33 118.5 | |
| C17 -C16 -N4 107.5(2) C34 -C33 -C32 119.0 | |
| C17 -C16 -C15 126.9(3) F33 -C33 -C32 120.4 | |
| C16 -C17 -C17 129.1(2) F33 -C33 -C34 120.6 | |
| C18 -C17 -C17 122.9(2) C35 -C34 -C33 120.3 | |
| C18 - C17 - C16 107.9(3) F34 - C34 - C33 120.1 C17 - C18 - C18 122.2(2) F34 - C34 - C35 119.6 | • • |
| | |
| | |
| C19 -C18 -C17 107.8(3) F35 -C35 -C34 120.2 C18 -C19 -N4 107.6(2) F35 -C35 -C36 120.2 | |
| C20 -C19 -N4 125.3(3) C35 -C36 -C31 122.2 | |
| C20 -C19 -C18 127.0(3) F36 -C36 -C31 119.0 | |
| C19 -C20 -C1 125.6(3) F36 -C36 -C35 118.7 | |
| C51 -C20 -C1 117.4(2) C42 -C41 -C15 120.2 | |
| C51 -C20 -C19 117.0(2) C46 -C41 -C15 123.3 | |
| C22 -C21 -C5 121.4(3) C46 -C41 -C42 116.5 | |
| C26 -C21 -C5 122.5(3) C43 -C42 -C41 122.5 | |
| C26 -C21 -C22 116.1(3) F42 -C42 -C41 119.3 | |
| C23 -C22 -C21 123.1(3) F42 -C42 -C43 117.8 | |

Table S3. (Cont.)

Angle(°)

| C44 -C43 -C42 | 119.1(3) |
|---------------|----------|
| F43 -C43 -C42 | 120.6(3) |
| F43 -C43 -C44 | 120.3(3) |
| C45 -C44 -C43 | 120.6(4) |
| F44 -C44 -C43 | 119.6(3) |
| F44 -C44 -C45 | 119.9(4) |
| C46 -C45 -C44 | 119.4(4) |
| F45 -C45 -C44 | 121.0(4) |
| F45 -C45 -C46 | 119.6(3) |
| C45 -C46 -C41 | 121.4(3) |
| F46 -C46 -C41 | 119.8(3) |
| F46 -C46 -C45 | 118.8(3) |
| C52 -C51 -C20 | 122.2(3) |
| C56 -C51 -C20 | 121.6(3) |
| C56 -C51 -C52 | 116.2(3) |
| C53 -C52 -C51 | 122.0(3) |
| F52 -C52 -C51 | 119.9(3) |
| F52 -C52 -C53 | 118.1(3) |
| C54 -C53 -C52 | 119.5(3) |
| F53 -C53 -C52 | 120.3(3) |
| F53 -C53 -C54 | 120.1(3) |
| C55 -C54 -C53 | 120.5(3) |
| F54 -C54 -C53 | 120.1(3) |
| F54 -C54 -C55 | 119.4(3) |
| C56 -C55 -C54 | 119.2(3) |
| F55 -C55 -C54 | 121.2(3) |
| F55 -C55 -C56 | 119.6(3) |
| C55 -C56 -C51 | 122.6(3) |
| F56 -C56 -C51 | 119.4(3) |
| F56 -C56 -C55 | 118.1(3) |
| | |

Table S4. Observed and Calculated Structure Factors for Tetrakis(pentafluorophenyl)- β -octachloroporphyrin

The columns contain, in order, ℓ , $10F_{obs}$, $10F_{calc}$ and $10\sigma F_{obs}$. A minus sign preceding F_{obs} indicates that F_{obs}^2 is negative.

| Tetraki | s (pen | taflu | oroj | phenyl) | -bet | a-oct | ach | loropor | phyr | in | | | 1 | Page | 1 |
|------------------|------------------|------------------|----------|-------------|-------------------------|------------------|---------|-------------|-------------------|-------------------|-------------|----------|-------------------------|-----------------|-------------|
| -10 | 1 | 1 | | 6 | 117 | 115 1 | 5 | 5 6 7 | 47 99 102 | 8 105 111 | 9 6 6 | 1 2 | 251 142 | 257 145 | 4 |
| 1 | 182 | 227 | 5 | - 8 | 4 | _ | | - | | | ٠ | 3 | 94 | 145 78 | 5 |
| 3 | -14 | 47 | 16 | 1 | 132 | 125 | 5 | -7 | 6 | 1 | | 5 | 131 10 | 122 10 | 4 19 |
| 3 | 42 | | 8 | 3 | 132 48 220 203 | 39 237 203 | 8 | 1 | 120 | 118 | 5 | 6 | 51 | 34 | 8 |
| -10 | 2 | 1 | | 5 | 203 79 | 203 61 | 5 6 | 2 3 | 96 | 17 87 | 9 | 7 | 20 37 | 35 48 | 15 11 |
| 1 | 39 | 41 | 10 | _ | | | ٠ | 4 | 208 | 200 | 5 | _ | | | |
| 2 | 16 | 28 | 18 | -8 | 5 | 1 | | 5 6 | 162 116 | 160 109 | 5 5 | -6 | 6 | 1 | |
| -10 | 3 | 1 | | 1 | 60 | 48 | 7 | | 7 | 1 | - | 1 | 36 133 | 17 139 | 4 |
| 1 | 80 | 63 | 6 | 3 | 53 188 | 29 189 | 8 5 | -7 | _ | _ | | 2 3 | 93 | 93 | 5 |
| | | | • | 4 | 65 | 62 | 7 | 1 2 | 79 232 | 87 240 | 6 | 5 | 285 46 | 271 27 | 9 |
| -9 | 1 | 1 | | -8 | 6 | 1 | | 3 | 98 | 98 | 6 | 6 | 46 125 73 | 139 | 5 |
| 1 2 | 117 56 | 104 31 | 5 7 | 1 | 129 | 128 | 5 | 4 | 61 | 58 | 7 | 7 | | 72 | 7 |
| 3 | 142 | 132 | 5 | 3 | 149 76 | 149 57 | 5 | - 7 | 8 | 1 | | - 6 | 7 | 1 | |
| 4 5 | 142 -21 11 | 1 ⁸ | 14 21 | 2 | | 57 | 7 | 1 | -21 | 7 | 14 | 1 2 | 249 | 261 | 10 |
| ĕ | 73 | 42 | 7 | - 8 | 7 | 1 | | 2 | 61 58 | 88 77 | 7 | 2 | - 29 | 50 1 | 10 9 |
| -9 | 2 | 1 | | 1 | 115 | 117 | 5 | | | | • | 3 4 | 33 -29 237 121 | 245 117 | 4 |
| 1 | 50 | 31 | 7 | -7 | 1 | 1 | | -6 | 1 | 1 | | 5 6 | 46 | 43 | 4 5 7 |
| 2 3 | 23 | 46 | 13 | | | | 10 | 1 | 343 | 362 | 4 | - 6 | 8 | 1 | |
| 3 4 | 60 61 | 65 67 | 7 | 1 2 | 26 46 | 17 59 | 10 7 | 2 3 4 | 347 199 | 349 185 | 4 | | | | _ |
| 4 5 | 156 | 151 | 5 | 3 | 84 | 76 7 | 5 | 4 5 | 184 66 | 183 44 | 6 | 1 2 | 113 75 | 113 92 | 5 6 |
| -9 | 3 | 1 | | 5 | 33 145 137 | 141 | 4 | 6 | 73 | 68 | 6 | 3 | 31 | 37 | 11 |
| 1 | 84 | 81 | 6 | 6 7 | 137 | 141 137 75 | 5 8 | 8 | 209 121 | 213 112 | 5 | 4 5 | 43 53 | 39 21 | 8 |
| 2 3 | 54 | 47 71 | 8 | 8 | 54 73 | 81 | 7 | 9 10 | 37 119 | 23 112 | 11 5 | - 6 | 9 | 1 | |
| 3 | 71 60 | 71 | 7 | 9 | -38 | 10 | 10 | | | | 3 | - | _ | | _ |
| -9 | 4 | 1 | | -7 | 2 | 1 | | -6 | 2 | 1 | | 1 2 | 105 57 | 124 61 | 5 8 8 |
| | | | _ | 1 | 111 | 108 | 4 | 1 2 | 264 | 272 120 212 | 4 | 3 | -43 | 6 | 8 |
| 1 2 | 65 36 | 88 29 | 7 11 | 3 | 42 284 | 27 296 | 8 | 3 | 106 206 | 212 | 4 | - 6 | 10 | 1 | |
| 3 | 38 | 17 | 11 | 5 | 50 141 | 51 139 | 6 | 4 5 | 99 39 | 107 | 8 | 1 | 80 | 58 | 6 |
| -9 | 5 | 1 | | 6 | 94 | 104 | 5 | 6 | 264 | 268 | 4 | - 5 | 1 | 1 | _ |
| 1 | 110 | 97 | 5 | 7 8 | 161 | 140 | 7 | 7 8 | 76 78 | 61 | 6 | _ | _ | _ | |
| | | 1 | - | 9 | 29 | 11 | 13 | 9 10 | 257 47 | 257 58 | 5 9 | 1 2 | 159 278 | 157 272 | 3 3 |
| - 8 | _ | _ | | -7 | 3 | 1 | | | | | 3 | 3 | 521 539 | 517 | 5 |
| 1 | 931 278 | 921 278 | 8 | 1 | 192 | 194 | 4 | -6 | 3 | 1 | | 5 | 73 | 534 55 | 5 5 |
| 2 3 4 5 | 55 | 47 | 7 | 2 | 97 | 92 | 5 | 1 2 | 200 193 | 199 192 | 4 | 6 7 | 134 287 | 126 277 | 4 |
| 5 | 119 40 | 122 24 155 | 5 8 | 3 4 5 | 105 192 | 112 190 | 4 | 3 | 125 | 125 236 | 4 | 8 9 | - 12 | 3 | 17 |
| 6 7 | 40 152 98 | 155 97 | 5 6 | 5 6 | 170 | 29 162 | 9 | 4 5 | 125 233 111 | 236 132 | 5 | 10 | 328 68 | 328 71 75 | 5 |
| ė. | 5 | 15 | 26 | 7 | 170 31 | 5 | 11 | 6 | 166 | 177 | 4 | 11 12 | 84 107 | 75 100 | 6 |
| -8 | 2 | 1 | | 8 | 116 | 110 | 5 | 7 8 | 179 25 | 176 34 | 13 | | | | |
| | | 86 | | -7 | 4 | 1 | | 9 10 | 174 14 | 160 28 | 5 20 | - 5 | 2 | 1 | |
| 1 2 | 116 206 | 201 | 4 | 1 | 116 | 126 | 4 | | | | 20 | 1 | 396 | 399 | 4 |
| 3 | 139 65 | 122 59 | 7 | 3 | 162 50 | 180 36 | 8 | -6 | 4 | 1 | | 3 | 135 447 230 | 130 450 | 5 |
| 5 | 12 | 16 | 19 | 4 | 198 | 208 | 4 | 1 | 50 | 26 17 | 6 | 5 | 230 | 228 | 4 |
| 6 7 | 196 130 | 192 129 | 5 | 5 6 | 161 158 | 162 161 | 5 | 2 3 | 59 151 | 148 | 4 | 6 7 | 289 | 282 | 4 |
| | | 1 | _ | 7 | 53 | 56 | 8 | 5 | 50 221 | 41 222 | 4 | 7 | 32 248 | 33 248 | 10 |
| - 8 | | | | - 7 | 5 | 1 | | 6 | 40 | 27 74 | 9 | 9 | 136 | 129 | 5 |
| 1 2 | 288 261 | 284 276 | 4 | 1 | 39 | 11 | 9 | 7 8 | 84 136 | 154 | 6 | 10 11 | 71 | 71 | 22 |
| 3 | 174 | 172 | 4 | 2 | 189 | 187 158 | 4 | 9 | 46 | 29 | 8 | - 5 | 3 | 1 | |
| 4 5 | 100 68 | 57 | 7 | 4 | 143 70 | 53 | 6 | -6 | 5 | 1 | | - 0 | • | - | |

| Tetrakis | (pen | taflu | oropl | henyl) | -bet | a-oct | achl | oropor | phyr | in | | | | Page | 2 |
|-------------|------------|------------|---------|----------|------------------|------------------|-------------|-------------|------------|------------------|-------------|-------------|------------|------------|-------------|
| 1 | 432 43 | 441 | 6 | 6 | 94 | 100 | 6 | 3 | 27 415 | 0 436 | 9 | 1 | 423 | 423 | 4 |
| 3 | 84 | 35 87 | 4 | - 5 | 10 | 1 | | 5 | 205 77 | 436 209 83 | 5 | 2 | 883 660 | 872 632 | 7 |
| -5 | 230 229 | 227 225 | 4 | 1 | 110 | 124 | 5 | 7 | 160 | 158 170 | 4 | 5 | 54 1223 | 1209 | 10 |
| 6 7 | 245 110 | 240 107 | 5 | 3 | 75 -14 | 72 43 81 | 18 | 9 | 167 -21 | 5 | 13 | 6 | 95 | 94 | 4 |
| 8 9 | 75 60 | 69 71 | 6 | 4 | 80 | 81 | 6 | 10 11 | 108 37 | 94 11 | 5 11 | 7 8 | 161 120 | 164 130 | 4 |
| 10 11 | 74 56 | 76 65 | 7 | - 5 | 11 | 1 | | -4 | 6 | 1 | | 9 10 | 180 113 | 177 | 5 13 |
| | 4 | 1 | · | 1 2 | 53 66 | 51 64 | 7 | 1 | 187 | 183 | 3 | 11 | 26 - 55 | 49 14 | 13 |
| -5 | | - | | - | | 1 | • | 3 | 354 | 350 48 | 4 5 | 12 13 | 207 | 207 | 5 |
| 1 2 | 208 113 | 207 124 | 3 | -4 | 1 | | _ | 4 | 95 | 87 | 4 | -3 | 2 | 1 | |
| 3 | 68 380 | 52 367 | 5 4 | 1 2 | 522 359 | 509 347 | 4 | 5 6 | 99 314 | 107 311 | 4 | 1 | 533 | 533 | 5 |
| 5 6 | 16 | 21 | 7 14 | 3 | 63 98 | 59 105 | 4 | 7 8 | - 20 | 66 8 | 7 14 | 2 3 | 254 493 | 255 504 | 4 |
| 7 8 | 52 | 48 | 6 | 5 | 211 89 | 207 88 | 3 | 9 10 | 125 81 | 113 63 | 5 6 | 4 5 | 401 170 | 399 142 | 3 |
| 9 | -39 30 | 16 51 | 12 | 7 | 332 139 | 328 | 4 | | 7 | | • | 6 | 78 44 | 64 | 4 7 |
| 10 | -24 | 12 | 14 | 8 | 272 | 134 279 | 4 | -4 | | 1 | | 8 | 141 | 160 | 4 |
| -5 | 5 | 1 | | 10 11 | 155 183 | 157 171 | 5 | 1 2 | 84 78 | 80 92 | 5 | 10 | 200 379 | 194 378 | 4 5 5 |
| 1 2 | 79 313 | 73 311 | 4 | 12 13 | 70 -16 | 79 11 | 7 18 | 3 | 67 269 | 70 272 | 4 | 11 12 | 124 161 | 123 153 | 5 |
| 3 | 419 179 | 415 179 | 5 | -4 | 2 | 1 | | 5 6 | 151 71 | 154 70 | 6 | 13 | 83 | 83 | 6 |
| 4 5 | 245 | 248 | 10 | | 977 | 994 | 8 | 7 8 | 130 326 | 132 319 | 5 | - 3 | 3 | 1 | |
| 6 7 | 36 29 | 52 47 | 12 | 1 2 | 430 | 446 | 4 | ğ | 133 | 130 | 5 | . 1 | 791 | 792 53 | 7 |
| 8 9 | 92 | 24 92 | 24 6 | 3 4 | 352 165 | 356 156 | 3 | -4 | 8 | 1 | | 3 | 55 188 | 183 | 3 |
| 10 | 71 | 72 | 7 | 5 6 | 151 175 | 155 168 | 3 | 1 | 162 | 172 | 4 | 5 | 159 835 | 161 827 | 3 7 |
| - 5 | 6 | 1 | | 7 8 | 336 208 | 334 194 | 4 | 3 | 129 31 | 131 | 10 | 6 7 | - 28 20 | 13 | |
| · 1 | 249 134 | 242 136 | 4 | 9 10 | 150 179 | 150 177 | 4 | 4 5 | 87 | 96 85 | 5 | 8 9 | -37 266 | 259 | 7 |
| 3 | 331 | 332 | 4 | 11 12 | 88 | 92 27 | 6 | 6 | 168 59 | 157 62 | 4 | 10 | 327 145 | 314 138 | 5 |
| 4 5 | 80 38 | 84 22 | 8 | | -30 | | 12 | 8 | 165 | 167 | 5 | 11 | 214 | 207 | 5 |
| 6 7 | 123 | 16 134 | 9 5 | -4 | 3 | 1 | | -4 | 9 | 1 | | 13 | 192 | 196 | . 5 |
| 8 9 | 16 86 | 10 86 | 17 6 | 1 2 | 591 353 | 597 360 | 5 | 1 | 272 | 265 | 4 | - 3 | | 1 | |
| -5 | 7 | 1 | | 3 | 58 306 | 33 304 | 5 | 3 | 178 -2 | 168 40 | 25 | 1 2 | 137 171 | 135 166 | 3 |
| | 24 | 31 | 11 | 5 | 335 | 330 307 | 4 | 4 5 | 189 188 | 185 188 | 4 | 3 | 70 61 | 73 51 | 4 |
| 1 2 | - 22 | 1 | 11 | 7 | 369 | 365 | 4 | 6 | 166 168 | 178 183 | 5 | 4 5 6 | 247 125 | 237 129 | 3 4 |
| 3 4 | 86 | 61 | 6 | 8 9 | 136 125 | 138 126 33 | 5 | | | | 3 | 7 | 130 | 143 | 4 |
| 5 6 | 53 150 | 49 155 | 8 5 | 10 11 | -42 112 | 120 | 8 5 | -4 | 10 | 1 | _ | 8 | 309 | 313 | 4 |
| 7 8 | 142 62 | 141 54 | 5 8 | 12 | 29 | 25 | 13 | 1 2 | 41 50 | 38 16 | 9 8 5 | 10 11 | 133 336 | 118 331 | 5 5 |
| -5 | | 1 | | -4 | 4 | 1 | | 3 | 96 106 | 83 94 | 5 5 | 12 | 142 | | 5 |
| 1 | -23 | | 12 | 1 | 167 191 | 166 209 | 3 | 5 | 232 | 245 35 | 5 10 | -: | 5 | 1 | |
| 2 3 | -30 57 | 14 2 | 10 | 3 | 94 | 82 78 | 3 4 4 | -4 | | 1 | | 1 2 | 527 197 | 527 190 | 5 |
| 4 | 108 | 107 | 5 | 4 5 | 80 427 139 | 432 | 5 | | | | | 3 | 57 45 | 65 | 5 |
| 5 6 | 80 10 | 93 | 6 21 | 6 | 33 | 145 30 139 | 9 | 1 2 3 | 18 183 | 167 | 16 | 5 | 154 | 161 | 4 |
| 7 | 107 | 115 | 6 | 8 | 146 54 | 51 | 8 | 3 | 88 92 | 81 96 | 6 | 6 7 | 68 121 | 128 | 4 |
| - 5 | 9 | 1 | | 10 | 17 -39 | 1 | 16 | -4 | | 1 | | 8 9 | 39 164 | 154 | 7 |
| 1 2 | 99 -40 | 103 23 | 5 8 | -4 | 5 | 1 | - | 1 | 57 | 62 | 7 | 10 11 | 70 200 | 196 | 5 5 |
| 2 3 4 | 116 -28 | 116 31 | - 5 | | 615 | 619 | 6 | 2 | 95 | 88 | 6 | 11 12 | 51 | 42 | |
| 5 | 145 | 131 | 5 | 1 2 | 58 | 67 | 5 | - 3 | 1 | 1 | | - : | 3 6 | 1 | |

| Tetrakis (penta | fluorophenyl)-be | ta-octachloropo | orphyrin | Page 3 |
|---|--|---|--|--|
| 2 159 1 3 84 4 234 2 5 410 4 6 151 1 7 72 8 170 1 | 718 6 -3 13 167 3 1 207 168 4 1 207 132 4 100 4 -2 1 153 4 -2 1 153 6 1 125 187 4 2 145 187 4 3 104 | 7 206 5 9 10 11 11 12 12 13 14 10 13 14 55 10 | 297 291 4 51 74 6 210 214 4 96 88 5 57 64 7 66 79 7 232 233 5 21 7 16 | 1 108 120 5 2 67 64 6 3 63 50 55 5 226 220 4 6 44 15 8 279 260 5 |
| 9 249 2 10 135 1 | 20 5 4 143 | | | -2 12 l |
| -3 7 1 1 388 3 2 108 1 3 -12 | 6 309 | 320 4 2 399 4 3 9 104 4 4 9 81 5 5 3 307 4 6 1 108 6 7 | 307 306 3 83 78 4 552 546 5 448 450 4 57 53 5 300 298 4 143 142 4 40 21 8 | 1 145 150 4 2 146 145 5 3 89 104 6 4 91 86 6 5 42 34 10 6 50 65 9 |
| 5 59 | 52 6 13 2 | 49 13 9 | 47 43 8 135 133 5 | -2 13 l |
| 7 87 8 139 1 9 54 10 32 | 47 8 51 12 1 23 | 2 1 11 3 219 3 -3 | 106 114 5 11 4 21 | 1 82 80 6 2 44 27 9 3 101 83 6 4 241 222 5 |
| 11 66 | 68 7 2 57- 3 49 | 5 504 4 1 | 46 38 6 | -1 1 l |
| 2 108 1 3 208 2 | | 2 372 4 2 5 255 3 3 2 36 5 4 4 576 5 5 0 383 4 6 | 92 87 4 146 142 3 181 181 3 230 227 4 232 230 4 205 211 4 | 1 380 367 3 2 729 715 6 3 186 190 2 4 422 432 4 5 41 0 4 |
| 5 281 2 6 73 7 50 8 193 1 9 41 | 274 4 10 -1 60 6 11 24 50 6 12 14 181 4 13 7 67 9 14 22 | 1 11 18 8 2 228 4 9 6 143 5 10 5 71 7 11 | 248 251 4 136 116 5 101 107 5 207 191 5 | 4 422 432 4 5 411 0 4 6 163 163 3 7 53 86 5 8 454 465 5 9 53 52 6 10 430 433 5 11 59 58 6 |
| | -2 | 3 1 | | 12 144 139 4 13 -46 6 7 |
| 2 173 1 3 167 1 4 183 1 | 1 67 265 4 2 6 169 4 3 10 168 4 4 8 197 4 5 30 | 1 51 4 3 6 115 3 4 5 93 3 5 8 298 3 6 | 66 72 5 119 112 4 260 261 4 67 54 5 449 433 5 | 14 90 96 6 15 107 107 6 -1 2 l |
| 6 -11 7 66 8 115 1 | 192 4 6 18 30 19 7 7 65 7 8 4 107 5 9 13 108 6 10 7 | 8 70 4 8 0 37 7 9 0 141 4 10 7 84 6 11 7 181 4 | 30 12 11 400 404 5 219 221 4 56 49 8 90 80 6 | 1 122 125 2 2 425 408 4 3 152 138 2 4 783 795 7 5 12 4 12 6 399 387 4 |
| -3 10 1 | 11 17 1 12 15 13 19 | 1 152 5 - 4 191 5 | | 7 95 105 4 8 803 798 7 |
| 2 107 1 3 310 3 4 159 1 5 130 1 6 84 | 250 4 107 5 -2 307 4 132 4 1 9 116 5 2 8 77 6 3 19 | 1 1 2 8 99 5 4 1 94 3 5 3 196 3 6 | 149 147 4 71 74 5 35 44 8 43 14 8 44 21 8 87 87 5 166 153 4 | 9 927 928 8 10 139 134 4 11 280 289 4 12 307 295 4 13 70 87 7 14 91 92 6 |
| 7 14 8 65 | 12 18 4 16 35 7 5 42 | 8 429 4 8 | 157 155 5 | -1 3 I |
| -3 11 1 | 1 6 20 | 8 44 7 10 | | 1 446 436 4 |
| I 189 | 184 4 9 4 | 0 48 8 - | 2 10 l | 2 207 212 2 3 214 212 3 |
| 2 203 1 3 34 4 58 5 32 | 199 4 10 -3 27 9 11 -3 33 7 12 -4 35 11 13 3 126 5 | 0 17 9 2 | 101 103 5 151 152 4 173 167 4 | 4 378 385 4 5 120 113 3 6 31 21 7 7 626 617 6 8 193 194 3 9 55 54 6 |
| -3 12 | 1 | 6 | 138 125 5 | 10 139 142 4 |
| 3 101 | 88 5 2 28 206 5 3 28 94 5 4 49 157 5 5 22 | 7 286 3 8 5 291 3 9 7 511 5 | -27 7 12 | 11 -36 16 9 12 318 323 5 13 200 202 5 14 201 198 5 |

| -1 4 1 | Tetraki | s (pe | ntaflu | oroph | enyl) | -beta | s-oct | achl | oropoi | phyri | in | | | | Page | 4 |
|---|----------|------------|----------------|-------|-------|------------|-------------|------|------------|------------|-------------|--------|--------------|------------|-------------|------------|
| 3 - 9 5 13 2 11 143 153 4 4 05 405 4 3 5 468 666 4 - 15 106 102 6 - 1888 2509 17 5 515 226 3 3 468 666 4 - 15 106 102 6 - 1888 2509 17 5 517 220 281 4 6 11 8 16 - 13 - 20 8 14 - 2 281 281 11 8 8 37 25 8 7 22 45 13 - 12 8 14 - 2 281 283 3 9 216 210 4 8 169 165 4 - 11 259 232 4 0 557 363 361 11 9 5 8 5 5 5 10 25 40 17 - 20 10 10 156 165 4 0 11 1 259 232 4 0 1 557 363 361 11 9 5 8 5 5 5 10 25 40 17 - 2 20 10 11 9 5 8 5 5 5 10 10 25 40 17 - 2 20 10 10 156 165 4 - 11 1 1 1 1 1 1 1 1 1 1 1 1 1 1 1 1 | | | _ | | | | | | 13 | | 337 | 5 | | 639 408 | 635 423 | |
| 3 -9 5 13 | 1 | 595 | 605 | 5 | | _ | _ | 2 | 15 | 72 | 64 | 7 | - 8 | - 6 | 29 | 17 |
| \$\begin{array}{c c c c c c c c c c c c c c c c c c c | 3 | - 9 | 5 | 13 | 2 | 111 | 101 | 4 | 0 | 1 | 1 | | -6 | 885 | 853 2009 | 17 |
| 9 2500 2333 4 6 6 11 8 16 -13 -20 8 14 -2 281 283 38 8 77 25 8 7 22 45 13 -12 81 89 6 -1 58 67 3 9 210 210 4 8 169 165 4 -11 239 232 4 0 552 343 3 8 9 210 210 4 8 169 165 4 -11 239 232 4 0 552 343 3 10 155 165 165 4 9 172 171 4 -9 1576 160 2 4 1 219 50 5 8 11 23 30 47 11 11 74 72 7 - 220 251 3 4 1 291 505 8 14 84 82 7 -1 10 1 -0 151 154 3 5 429 451 4 1 213 13 215 207 5 1 10 1 -5 215 154 3 5 429 451 4 1 213 13 215 207 5 1 1 1 1 74 72 7 - 220 251 3 4 3 233 339 3 3 4 1 84 82 7 -1 10 1 -5 215 124 204 2 8 209 217 3 1 2 248 251 4 -5 241 204 2 8 209 217 3 1 2 2 248 251 4 -5 241 204 2 8 209 217 3 1 2 2 2 2 2 2 2 2 2 2 2 2 2 2 2 2 2 2 | 5 | 315 | 326 | 3 | 4 | 382 | 386 | 4 | | | 102 | | -4 | 1298 | 1311 | 11 |
| 0 2 10 2 10 4 8 169 165 4 -11 239 232 4 0 352 343 1 191 55 8 101 150 165 4 9 172 171 4 -10 137 130 4 1 1971 955 8 111 95 87 5 10 172 171 4 -10 137 130 4 1 1971 955 8 112 30 47 11 11 74 72 7 -8 347 351 4 3 1280 1292 11 13 215 207 5 -1 10 1 -6 168 619 5 6 23 139 305 3 14 84 82 7 -1 10 1 -6 168 619 5 6 638 635 5 4 1 1 1 1 1 1 1 1 1 1 1 1 1 1 1 1 1 | 7 | 290 | 283 | 4 | 6 | 11 | 8 | 16 | -13 | - 20 | 8 | 14 | - 2 | 281 | 283 | 3 |
| 12 30 47 11 11 74 72 7 8 347 351 4 321 328 329 3 14 84 82 7 -1 10 1 -6 151 154 3 5 429 431 | 8 9 | 37 216 | 25 210 | 4 | 8 | 169 | 165 | 4 | -11 | 239 | 232 | 4 | Ö | 352 | 343 | 3 |
| 12 30 47 11 11 74 72 7 -8 341 331 4 3 120 121 11 13 125 207 5 1 1 | | 156 95 | 165 87 | 5 | | 25 | 43 | 14 | -9 | 596 | 602 | 6 | 2 | 319 | 305 | . 3 |
| -1 5 1 | 12 | 30 | 47 | | 11 | | | 7 | - 7 | 220 | 203 | 3 | 4 | 323 | 339 | 3 |
| 1 369 368 4 | | | | 7 | -1 | 10 | 1 | | | | 154 219 | 3 | 6 | 356 | 355 | 4 |
| 1 369 368 4 | - | 1 5 | 1 | | | | 24 251 | | - 3 | 214 | 602 204 | 2 | 8 | 209 | 112 217 | 3 |
| \$ \$ \$ \$ \$ \$ \$ \$ \$ \$ \$ \$ \$ \$ \$ \$ \$ \$ \$ | 1 | | | 4 | 3 | 401 | 3 99 | 5 | | 201 52 | 14 | 3 | | | 117 259 | 4 |
| 1 | 3 | 362 | 379 | 4 | 5 | 374 | 368 | 5 | 1 | 193 | 204 | 2 | 11 | 356 287 | 357 281 | 4 |
| 7 144 144 4 9 -33 710 5 1108 1103 9 15 351 352 5 8 140 130 4 10 89 85 6 6 798 798 7 9 292 284 4 -11 11 1 8 2 46 8 10 -15 37 16 -1 11 1 8 9 91 83 4 -15 126 132 5 13 66 85 7 2 100 96 5 11 638 640 6 -13 166 165 5 13 66 85 7 3 36 28 8 12 364 365 5 -12 93 100 5 -1 6 1 4 631 627 6 13 388 392 5 -11 199 203 4 1 214 227 3 6 177 175 4 15 115 132 5 -9 86 90 4 1 214 227 3 6 177 175 4 15 115 132 5 -9 86 90 4 1 214 227 3 6 177 175 4 15 115 132 5 -9 86 90 4 1 214 227 3 6 177 175 4 15 115 132 5 -9 86 90 4 1 214 227 3 6 177 175 4 15 115 132 5 -9 86 90 4 2 189 192 3 7 -35 1 9 2 160 148 5 -15 230 221 5 -5 338 331 332 11 3 5 331 328 4 -11 20 10 0 2 1 -7 116 114 36 33 332 11 4 5 331 328 4 -11 21 -14 336 336 5 -4 274 269 3 7 87 79 4 12 1 -14 336 336 5 -4 274 269 3 7 87 79 4 12 216 211 4 -11 436 426 5 -1 422 424 4 10 116 117 5 3 58 34 6 -10 697 707 6 0 0 230 230 2 11 227 232 4 7 75 83 6 -9 229 240 4 1 1080 1093 9 204 192 4 2 216 211 4 -11 436 426 5 -1 422 424 4 10 116 117 5 3 58 34 6 -10 697 707 6 0 0 230 230 2 11 227 232 4 7 75 83 6 -9 229 240 4 1 1080 1093 9 11 26 6 148 5 5 125 128 5 -8 49 42 6 2 1333 1331 11 13 117 118 6 6 -35 129 10 -7 213 199 3 3 1088 1077 9 11 26 6 148 5 5 125 128 5 -8 49 42 6 2 1332 1331 11 13 117 118 6 6 -35 129 10 -7 213 199 3 3 1088 1077 919 8 1 6 6 6 798 798 70 70 70 70 70 70 70 70 70 70 70 70 70 | 5 | 765 | 764 | 7 | 7 | 56 | 43 | 7 | 3 | 289 | 265 | 3 | 13 | 117 | 120 | 5 12 |
| 1 | 7 | 144 | 144 | 4 | 9 | - 33 | 7 | 10 | 5 | 1108 | 1103 | 9 | | 351 | 352 | 5 |
| 9 91 83 4 -15 126 132 5 112 777 92 6 1 | 9 | 292 | 284 | 4 | | | | ь | 7 | 242 | 247 | 3 | (| 4 | 1 | |
| 13 66 85 7 2 100 96 5 11 688 640 6 -13 166 165 5 -1 6 1 3 88 28 8 12 364 365 5 -12 93 100 5 -1 6 1 5 4 631 627 6 13 388 392 5 -11 199 203 4 1 214 227 3 6 177 175 4 15 115 132 5 -9 86 90 4 2 189 192 3 7 -55 1 9 | 11 | 17 | 26 | 14 | | | · . | _ | 9 | 91 | 83 | 4 | - 15 | | | 5 |
| -1 6 1 | 12 13 | | 92 85 | 7 | 2 | 100 | 96 | 5 | 11 | 638 | 640 | 6 | - 13 | 166 | 165 | 5 |
| 1 214 227 3 6 177 175 4 15 115 132 5 -9 86 90 4 2 189 192 3 7 -35 1 9 0 2 1 -7 116 114 3 4 584 592 5 9 180 148 5 9 180 148 5 -15 230 221 5 -5 338 332 13 5 5 331 328 4 -12 10 0 2 1 -6 1333 1332 11 5 333 13328 4 -12 10 10 1 14 356 356 5 -4 274 269 3 1332 11 1 1 1 1 1 1 1 1 1 1 1 1 1 1 1 | - | 1 6 | 3 1 | | 4 | 631 | 627 | 6 | 13 | 388 | 392 | 5 | - 11 | 199 | 203 | |
| \$\begin{array}{c c c c c c c c c c c c c c c c c c c | 1 | 214 | | 3 | 6 | 177 | 175 | 4 | 15 | | | 5 | - 9 | 86 | 90 | |
| 4 584 592 5 9 160 148 5 5 331 328 4 -15 230 221 5 -5 333 1332 13 6 26 10 9 -1 12 1 -14 336 336 5 -4 274 209 3 7 87 79 4 2 204 192 4 2 210 211 401 120 5 -2 195 205 2 2 204 192 42 2 210 211 436 426 5 -1 422 424 42 42 42 42 42 42 42 42 42 42 42 42 42 434 436 436 5 -2 229 240 4 1 1080 1093 9 11 25 128 5 12 5 8 4 6 2 1332 1331 11 11 11 8 <td< td=""><td>2</td><td>189 654</td><td>192</td><td></td><td></td><td>41</td><td>20</td><td>10</td><td>0</td><td>2</td><td>1</td><td></td><td>- 7</td><td>116</td><td>114</td><td>3</td></td<> | 2 | 189 654 | 192 | | | 41 | 20 | 10 | 0 | 2 | 1 | | - 7 | 116 | 114 | 3 |
| 6 26 10 9 -1 12 1 -14 350 350 5 -2 214 209 3 | 4 5 | 584 331 | 592 328 | | 9 | | | 5 | | 230 | 221 | | - 5 | 338 | 331 | 3 |
| 8 674 675 6 1 -6 5 22 -12 101 120 5 -2 195 205 2 4 2 216 211 4 -11 436 426 5 -1 422 424 4 10 116 117 5 3 58 34 6 -10 697 707 6 0 230 230 2 11 227 232 4 75 83 6 -9 229 240 4 1 1080 1093 9 12 156 148 5 5 125 128 5 -8 49 42 6 2 1332 1331 11 13 10 -7 213 199 3 3 1088 1077 9 1 10 120 4 10 1012 8 5 220 234 3 10 1012 8 5 220 234 3 10 11 10 -7 213 | 6 | . 26 | 3 10 | 4 | -1 | _ | | | - 13 | 93 | 101 | 5 | - 3 | 1184 | 1214 | 10 |
| 11 227 222 4 4 75 83 6 -9 229 240 4 1 1080 1093 9 12 156 148 5 5 125 128 5 -8 49 42 6 2 1332 1331 11 13 117 118 6 6 -35 19 10 -7 213 199 3 3 1088 1077 9 -1 7 1 | | 674 | 675 | | | | 211 | 4 | -12 -11 | 436 | 120 426 | 5 | -1 | 422 | 424 | 4 |
| 13 117 118 6 6 -35 19 10 -7 213 199 3 3 1068 1017 9 8 1 -1 7 1 | | 116 | 8 117 | | | 58 75 | 83 | 6 | -9 | 229 | 240 | 4 | 1 | 1080 | 1093 | 9 |
| 7 74 82 7 -6 809 303 3 4 901 919 8 -1 7 1 -1 13 1 -1 13 1 -1 13 1 -1 70 6 6 521 521 5 1 640 618 6 2 163 161 3 1 107 116 5 -2 255 633 5 7 66 658 3 249 241 3 2 133 123 5 -1 469 482 4 9 44 54 7 4 107 102 4 3 55 60 8 0 1133 120 9 10 76 82 5 5 51 56 6 4 36 32 8 1 66 47 3 11 90 72 5 6 138 138 4 5 65 67 7 2 633 615 5 12 437 421 5 7 359 354 4 6 56 60 8 3 238 245 2 13 -19 9 15 8 91 56 5 9 798 785 7 -1 14 1 5 5 453 464 10 33 33 11 1 60 58 7 7 29 29 29 39 11 74 80 6 1 6 5 5 8 7 7 29 29 29 39 12 -28 17 12 2 131 121 5 8 79 82 4 -15 197 193 5 11 297 290 4 1 297 290 4 2 101 1037 8 13 82 65 6 -10 115 77 563 6 2 71 78 4 2 1011 1037 8 13 82 65 6 -10 115 77 563 6 2 71 78 4 2 1011 1037 8 13 82 65 6 -10 115 77 563 6 2 71 78 4 2 1011 1037 8 13 82 65 6 -10 115 77 563 6 2 71 78 4 2 1011 1037 8 13 82 65 6 -10 115 77 563 6 2 71 78 4 2 1011 1037 8 13 82 65 6 -10 115 77 563 6 2 71 78 4 2 1011 1037 8 13 82 65 6 -10 115 77 563 6 3 178 171 4 8 67 68 5 5 7 8 8 -3 327 326 3 10 182 175 4 10 273 288 4 -13 -41 80 8 -2 762 774 6 11 162 158 5 11 139 133 4 -12 120 137 5 -1048 1058 9 | 12 | 150 | 8 148 7 118 | 5 | 5 | 125 | 128 19 | | -8 -7 | 213 | 199 | 3 | 3 | 1088 | 1077 | 9 |
| -1 13 1 | | | | | | 74 | 82 | 7 | - 6 | 1001 | 303 1012 | 3 8 | 5 | 220 | 234 | 3 |
| \$\begin{array}{cccccccccccccccccccccccccccccccccccc | | _ | | | -1 | 15 | 1 | | -4 | 754 655 | 770 | | 6 7 | | | 4 |
| 4 107 102 4 3 55 60 8 0 1133 1209 9 10 76 82 5 5 51 56 6 4 36 32 8 1 66 47 3 11 90 72 5 6 138 138 4 5 65 67 7 2 623 615 5 12 437 421 5 7 359 354 4 6 56 60 8 3 238 245 2 13 -19 9 15 8 97 98 785 7 -1 14 1 5 453 464 4 1115 1130 9 14 48 58 9 9 798 785 7 -1 14 1 5 453 464 4 1115 1130 9 14 48 58 9 9 798 785 7 -1 14 1 5 453 464 4 1115 1130 9 14 48 58 9 11 74 80 6 1 60 58 7 7 299 299 3 12 -28 17 12 2 131 121 5 8 79 82 4 -15 197 193 5 112 -28 17 12 2 131 121 5 8 79 82 4 -15 197 193 5 8 12 -28 17 12 2 131 121 5 8 79 82 4 -15 197 193 5 8 12 297 290 4 11 12 104 4 -13 81 88 8 6 12 271 78 4 2 1011 1037 8 13 82 65 6 -10 115 116 4 3 309 304 4 3 991 86 3 14 120 128 5 -9 224 239 4 1 123 133 4 4 651 661 5 15 91 105 6 -8 259 256 4 5 98 100 4 5 491 484 4 5 9 1 86 3 14 120 128 5 -9 224 239 4 1 1 129 196 196 4 7 104 80 3 8 178 171 4 8 177 198 5 -15 50 43 9 -4 206 199 3 9 260 259 4 9 -20 12 11 -14 55 78 8 -3 327 326 3 10 182 175 4 10 273 268 4 -13 -14 30 8 -2 762 774 6 11 162 158 5 11 139 133 4 -12 120 137 5 -1 1048 1058 9 | | 16 | 3 161 | 3 | 1 2 | | 116 | 5 | - 2 | 225 | 236 | 2 | 8 9 | 44 | 54 | 7 |
| 6 1 1 2 1 3 5 4 6 6 6 6 8 3 2 2 8 6 1 5 5 12 4 3 7 4 2 1 5 8 9 1 5 6 5 5 4 1 11 5 11 3 0 9 1 4 4 8 5 8 9 9 7 9 8 7 8 5 7 -1 1 4 1 5 4 5 3 3 6 6 1 6 1 2 6 1 | 9 | 10 | 7 102 | 4 | 3 | 55 | 60 | 8 | | 1133 | 1209 | 9 | 11 | 90 | 82 72 | 5 |
| \$ 91 56 5 7 -1 14 1 5 435 464 4 10 33 33 11 | (| 13 | 8 138 | 4 | 5 | 65 | 67 | 7 | 2 | 623 | 615 245 | 2 | 12 13 | 437 -19 | 9 | 15 |
| 10 | | 9 | 1 56 | 5 | _ | | | | 4 | 1115 | 1130 | 9 | 14 | 48 | 58 | 9 |
| 12 -28 17 12 2 151 121 5 8 79 82 4 -15 197 193 5 6 -1 8 1 10 10 12 104 4 -13 81 88 6 1 297 290 4 12 90 88 5 6 -11 577 563 6 2 71 78 4 2 1011 1037 8 13 82 65 6 -10 115 116 4 3 91 86 3 14 120 128 5 -9 224 239 4 4 13 91 86 3 14 120 128 5 -9 224 239 4 4 123 133 4 4 651 661 5 15 91 105 6 -8 259 256 4 <td>10</td> <td>3</td> <td>3 33</td> <td>11</td> <td></td> <td></td> <td>-</td> <td>7</td> <td>6</td> <td>124</td> <td>133</td> <td>3</td> <td></td> <td></td> <td></td> <td></td> | 10 | 3 | 3 33 | 11 | | | - | 7 | 6 | 124 | 133 | 3 | | | | |
| -1 8 1 | | | | | 2 | 131 | 121 | . 5 | 8 | 79 | 82 | 4 | - 15 - 14 | | 193 | 6 |
| 2 71 78 4 2 1011 1037 8 13 82 65 6 -10 115 110 4 3 309 304 4 3 91 86 3 14 120 128 5 -9 224 239 4 4 123 133 4 4 651 661 5 15 91 105 6 -8 259 256 4 5 98 100 4 5 491 484 4 -7 -26 6 8 6 16 3 14 6 580 571 5 0 3 1 -6 128 129 3 7 196 196 4 7 104 80 3 -5 603 570 5 8 178 171 4 8 177 198 3 -15 50 43 9 -4 206 199 3 9 260 259 4 9 -20 12 11 -14 55 78 8 -3 327 326 3 10 182 175 4 10 273 268 4 -13 -41 30 8 -2 762 774 6 11 162 158 5 11 139 133 4 -12 120 137 5 -1 1048 1058 9 | • | -1 | 8 1 | | | | | | 10 | 112 | 104 | 4 | - 13 | 81 | . 88 | - 6 - 5 |
| \$\begin{array}{cccccccccccccccccccccccccccccccccccc | | 29 | 7 290 | | | | | , B | 12 | 96 | 93 | 5 | -10 | 115 | 565 116 | 6 |
| 5 98 100 4 5 491 484 4 -7 -7 -26 6 8 6 16 3 14 6 580 571 5 0 3 1 -6 128 129 3 7 196 196 4 7 104 80 3 -5 603 570 5 8 178 171 4 8 177 198 3 -15 50 43 9 -4 206 199 3 9 260 259 4 9 -20 12 11 -14 55 78 8 -3 327 326 3 10 182 175 4 10 273 288 4 -13 -41 30 8 -2 762 774 6 11 162 158 5 11 139 133 4 -12 120 137 5 -1 1048 1058 9 | 1 | 3 30 | 9 304 | 4 | 3 | 91 | 86 | 3 | 14 | 120 | 128 | 5 | - 9 | 224 | 239 256 | 4 |
| 7 196 196 4 7 104 80 5 -5 603 570 5 8 178 171 4 8 177 198 3 -15 50 43 9 -4 206 199 3 9 260 259 4 9 -20 12 11 -14 55 78 8 -3 327 326 3 10 182 175 4 10 273 268 4 -13 -41 30 8 -2 762 774 6 11 162 158 5 11 139 133 4 -12 120 137 5 -1 1048 1058 9 | 1 | 5 9 | 8 100 | 4 | 5 | 491 | 484 | 4 | | | | - | -7 | -26 | 129 | 8 |
| 9 260 259 4 9 -20 12 11 -14 55 78 8 -3 327 326 3 10 182 175 4 10 273 268 4 -13 -41 30 8 -2 762 774 6 11 162 158 5 11 139 133 4 -12 120 137 5 -1 1048 1058 9 | | 7 19 | 6 196 | 4 | 7 | 104 | 80 | 3 | | 50 | 43 | 9 | - 5 | 603 | 570 199 | 5 |
| 11 162 158 5 11 139 133 4 -12 120 137 5 -1 1048 1058 9 | | 9 26 | 0 259 | 4 | 9 | -20 | 12 | 11 | -14 | 55 | 78 | 8 | - 3 - 2 | 327 762 | 326 774 | 3 |
| 12 193 175 5 12 278 270 4 -11 299 306 4 0 715 727 6 | 1. | 1 16 | 2 158 | 5 | | 139 278 | 133 | 4 | -12 -11 | 120 299 | 137 306 | | - 1 | . 1048 | 1058 | 9 |

| Tetrakis(pentafluor | ophenyl)-beta-octachlo | roporphyrin | Page 5 |
|---|--|--|--|
| 1 770 766 6 2 202 200 3 3 660 687 6 4 278 279 3 5 389 409 4 6 284 289 3 7 230 231 3 8 102 111 4 9 227 219 4 | -13 95 98 6 -12 -26 38 11 -11 122 129 5 -10 -38 17 8 -9 67 84 6 -8 258 257 4 -7 88 84 4 -6 526 531 5 -5 358 359 4 | 7 75 86 6 8 65 69 7 9 250 252 4 10 -38 12 9 11 54 68 8 0 11 I -11 196 191 5 -10 107 115 5 | -3 73 73 6 -2 80 88 6 -1 86 96 6 0 126 121 5 1 42 30 9 2 50 47 8 3 171 160 5 4 250 236 5 5 24 31 14 |
| 11 231 229 12 209 216 13 110 103 | -4 494 496 5 -3 85 90 4 -2 215 218 3 -1 29 38 7 | -9 -30 13 11 -8 174 188 4 -7 -27 39 11 -6 195 195 4 | -3 124 122 5 -2 391 376 5 |
| 14 25 50 14 0 6 1 | 0 417 426 4 1 15 27 12 2 55 44 5 | -5 31 52 10 -4 148 149 4 -3 38 48 8 | -1 50 67 9 0 -49 19 7 1 141 133 5 |
| -14 166 161 1 -13 134 133 | 3 425 416 4 4 466 472 5 | -2 229 235 4 -1 395 401 4 0 245 249 4 | 1 -14 l |
| -12 -14 23 1 -11 339 339 -10 529 530 -9 455 446 -8 37 76 -7 287 289 -6 60 50 | 6 379 369 4 7 263 254 4 8 351 352 4 9 101 104 5 10 139 125 5 11 149 154 5 12 94 80 6 | 1 15 35 13 2 71 71 71 3 280 287 4 4 249 245 4 5 133 122 4 6 258 256 4 7 128 136 5 | 0 249 238 5 1 25 27 13 2 108 112 5 3 -34 25 9 4 91 91 6 5 147 130 5 6 195 188 5 |
| -4 360 361 -3 435 419 | 0 9 1 | 8 370 348 5 9 49 14 7 10 56 37 8 | 1 -13 l |
| -1 514 513 0 348 345 1 473 484 2 302 316 3 219 230 4 220 233 5 50 18 6 529 530 7 50 56 | -13 128 140 5 -12 58 75 8 -11 -24 50 13 -10 -44 11 7 -9 51 64 10 -8 659 667 6 -7 92 90 5 -6 40 22 7 -5 268 268 4 -4 319 324 4 | 0 12 1 -10 235 229 5 -9 58 78 7 -8 116 121 5 -7 133 138 5 -6 189 188 4 -5 215 218 4 -4 404 406 5 | 0 183 184 4 1 214 220 5 2 143 150 5 3 178 166 4 4 214 215 5 6 157 147 5 7 464 456 8 8 7 95 6 |
| 9 165 153 10 73 84 11 239 238 12 155 163 13 90 93 | -3 254 253 4 -2 83 90 4 -1 27 6 9 0 163 155 3 1 307 298 4 2 260 264 4 3 347 344 4 4 434 434 5 5 487 489 5 | -3 416 420 5 -2 -24 38 11 -1 258 253 4 0 390 379 5 1 63 79 6 2 368 359 5 3 327 330 4 4 82 54 6 5 108 129 5 | 1 -12 1 0 47 25 8 1 247 246 4 2 377 380 5 3 349 336 5 4 212 199 4 5 290 299 4 6 305 294 4 |
| -13 137 142 -12 179 179 -11 116 116 -10 23 50 1 -9 908 911 -8 332 340 | 5 6 31 2 9 4 7 13 3 16 5 8 427 425 5 2 9 155 154 4 8 10 54 71 8 | 6 -30 9 10 7 175 166 5 8 117 109 5 0 13 1 | 7 215 219 4 8 11 55 20 9 -44 26 8 10 221 210 5 |
| -7 31 47 -6 581 585 -5 97 95 -4 406 412 -3 84 86 -2 98 119 -1 171 70 467 484 1 70 79 2 492 509 3 59 58 4 326 320 5 561 558 6 408 416 7 363 364 8 205 215 9 225 221 | 12 7 44 24 14 0 10 1 14 -12 225 208 5 13 -11 127 127 5 15 59 8 1 -9 64 66 7 14 -8 -49 5 6 5 -7 62 85 6 1 -6 611 602 6 1 -5 288 280 4 2 -5 288 280 4 3 459 457 5 4 -1 35 140 4 1 1 95 92 4 4 0 499 498 5 1 1 57 59 6 | -8 38 42 10 -7 190 174 5 -6 271 270 4 -5 67 78 78 -4 45 16 8 -3 345 350 5 -2 340 335 5 -1 34 22 10 0 194 191 4 1 224 221 4 2 305 309 4 3 250 239 4 4 124 135 5 -4 0 25 6 61 60 7 7 24 18 14 | 0 287 283 4 1 122 134 4 2 129 147 4 3 49 83 7 4 27 30 11 5 499 493 6 6 257 225 4 7 89 92 5 8 117 125 5 9 -49 6 6 10 102 101 5 11 172 161 5 1 -10 1 0 19 13 10 1 254 255 4 2 202 197 4 |
| 11 94 91 12 225 225 13 68 51 0 8 1 | 5 2 203 210 4 5 3 457 457 5 7 4 213 214 4 5 369 361 4 6 192 182 4 | -7 223 202 5 -6 123 134 5 -5 178 184 5 -4 170 163 5 | 3 308 309 4 4 136 130 4 5 -29 23 9 6 199 211 4 |

| Tetrakis (per | tafluor | ophenyl)-be | ta-octach | loroporphyrin | Page 6 |
|---|--|---|---|--|--|
| 7 444 8 118 9 -35 10 252 11 19 | 445 5 119 5 9 9 261 4 10 16 | 0 35 1 238 2 679 3 117 | 21 6 250 3 686 6 123 3 | 1 313 334 3 2 251 281 2 3 689 695 6 4 481 477 4 5 209 214 3 | 12 97 95 5 13 216 213 4 14 120 118 5 15 99 86 6 |
| 12 99 | 109 6 | 4 771 5 960 | 758 7 | 6 174 168 3 7 401 395 4 | 1 2 1 |
| 1 -9 | 1 | 6 20 7 567 | 4 10 | 8 209 212 3 9 538 539 5 | -15 272 266 5 -14 50 50 9 |
| 0 298 1 1022 2 78 3 194 4 441 5 549 6 118 7 126 8 121 | 295 4 1015 9 81 4 192 3 450 5 555 5 102 4 118 4 | 8 487 9 186 10 -36 11 172 12 93 13 115 14 108 15 239 | 483 5 185 4 1 7 175 4 108 5 125 5 106 6 | 10 474 470 5 11 37 39 7 12 317 320 4 13 75 79 6 14 379 378 5 15 109 105 6 | -13 45 56 9 -12 267 256 4 -11 131 119 4 -10 217 213 4 -9 180 175 4 -8 -24 4 9 -7 255 271 3 -6 772 765 7 -5 802 790 7 |
| 9 -32 10 38 | 48 9 27 9 | 1 -4 | 1 | -15 186 174 5 -14 -26 31 13 | -4 1506 1519 13 -3 665 641 6 |
| 11 -28 12 47 13 117 | 34 11 71 9 122 5 | 0 397 1 301 2 770 3 187 4 459 5 201 | 782 6 191 3 459 4 | -13 271 274 4 -12 -39 2 8 -11 77 72 5 -10 139 139 4 -9 205 207 4 -8 47 53 5 | -2 529 526 4 -1 570 580 5 0 748 756 6 1 -11 12 10 2 11 23 9 |
| 0 297 1 698 | 504 4 683 6 | 6 1110 7 369 | 358 4 | -7 399 402 4 -6 472 459 4 | 4 505 507 4 5 888 876 7 |
| 2 414 3 341 | 420 4 354 4 | 8 158 9 183 | 177 4 | -5 257 261 3 -4 232 224 3 | 6 297 285 3 7 400 399 4 |
| 4 38 5 70 | 43 7 73 5 | 10 57 11 57 | 72 6 | -3 43 48 5 -2 1104 1068 9 | 9 163 167 3 |
| 6 228 7 39 8 340 | 233 4 38 7 348 4 | 12 72 13 287 14 14 | 296 5 | -1 134 112 2 1 219 207 2 2 860 865 7 | 10 368 363 4 11 338 332 4 12 24 47 13 |
| 9 333 10 163 | 348 4 327 4 164 4 | 15 291 | 285 5 | 3 969 954 8 4 28 14 7 | 13 153 152 4 |
| 11 357 12 245 | 373 5 237 5 | 1 -3 | _ | 5 590 587 5 6 633 631 6 | 15 269 258 5 |
| 13 167 | 159 5 | 0 249 1 168 | 171 2 | 7 63 72 4 8 719 727 6 | 1 3 l |
| 1 -7 | 1 | 2 244 3 1852 | 1859 15 | 9 570 559 5 10 123 126 4 | -15 147 152 5 -14 250 255 5 |
| 0 402 1 101 2 254 | 417 4 82 3 257 3 | 4 227 5 565 6 475 | 236 3 569 5 466 4 | 11 65 67 6 12 60 82 6 13 416 410 5 | -13 22 36 13 -12 396 389 5 -11 299 290 4 |
| 3 210 4 167 | 209 3 153 3 | 7 646 8 118 | 667 6 | 14 222 220 4 15 295 290 5 | -11 299 290 4 -10 131 123 4 -9 52 28 6 |
| 5 152 6 51 | 149 3 30 6 | 9 472 | 462 5 | 1 1 1 | -8 288 294 4 -7 257 244 3 |
| 7 289 8 366 | 284 4 | 11 252 | 247 4 | -15 99 108 6 | -6 642 623 6 -5 566 572 5 |
| 9 87 10 136 | 79 5 147 4 | 13 351 14 -46 | 353 5 19 7 | -14 254 241 5 -13 313 304 5 | -4 1414 1408 12 -3 315 322 3 |
| 11 72 12 110 | 75 6 127 5 | 15 87 | 98 6 | -12 299 291 4 -11 125 115 4 | -1 755 704 6 |
| 13 -35 14 125 | 30 10 132 5 | | | -10 554 555 5 -9 129 130 4 | 0 885 869 7 1 542 536 4 2 369 365 3 |
| 1 -6 | 1 | 0 1175 1 698 2 243 | 683 6 | -8 138 137 3 -7 440 431 4 -6 228 240 3 | 3 495 492 4 |
| 0 206 1 20 2 509 3 334 4 391 | 193 3 1 9 511 5 335 4 403 4 | 3 812 4 298 5 419 6 166 7 156 | 796 7 277 3 434 4 165 3 159 3 | -5 770 765 7 -4 346 336 3 -3 734 725 6 -2 212 202 2 -1 26 23 6 | 5 124 121 3 6 633 609 6 7 173 193 3 8 557 573 5 9 268 264 4 |
| 5 394 6 321 7 -21 | 404 4 312 4 40 10 | 8 -39 9 497 | 501 5 | 0 252 256 2 1 42 0 3 | 10 572 566 6 11 131 129 4 |
| 8 79 9 157 | 60 4 153 4 | 10 430 11 502 12 -45 | 501 5 | 2 494 506 4 3 809 759 7 4 1322 1325 11 | 12 76 68 6 12 218 216 4 14 74 86 7 |
| 10 98 11 189 | 101 5 197 4 | 13 148 14 284 | 161 5 | 5 207 193 3 6 1113 1118 9 | 15 106 99 6 |
| 12 135 13 454 | 135 5 455 5 | 15 250 | 245 5 | 7 759 768 7 8 284 281 4 | 1 4 1 |
| 14 197 | 193 5 | 1 -1 | - | 9 413 413 4 10 142 139 4 | -15 -32 34 11 -14 54 58 8 |
| 1 -5 | 1 | 0 412 | 436 3 | 11 204 190 4 | -13 164 186 5 |

| Tetrakis (pentaf | fluorophenyl). | beta-octachl | oroporphyrin | Page 7 |
|---|--|---|---|---|
| -11 20 19 19 10 10 10 10 10 10 10 10 10 10 10 10 10 | 98 6 1 2 3 4 5 6 7 8 8 8 7 7 8 7 8 7 8 8 8 8 7 8 7 8 8 8 8 7 8 7 8 | 504 497 4 577 358 4 8895 875 8 8108 113 3 2433 432 4 1124 9 172 170 4 89 92 179 196 4 | -13 60 73 8 -12 -29 5 1 -11 -57 3 5 -10 111 103 9 -8 134 142 4 -7 35 35 35 -6 314 313 4 -6 314 313 4 -6 314 313 4 -7 35 35 35 -10 106 66 665 -3 476 487 5 -2 549 547 -1 -1 106 66 665 -3 476 403 3 -2 228 218 3 -4 403 3 -2 202 201 3 -4 148 141 4 -7 266 268 4 -7 266 268 4 -7 266 390 385 4 -7 266 390 385 4 -7 266 390 385 11 -1 10 1 -12 197 187 5 -10 498 19 19 -11 29 63 12 -1 138 75 -1 10 498 497 5 -9 -34 10 9 -9 -34 10 6 -7 108 175 5 -6 70 71 5 -5 403 407 4 -1 138 353 4 -2 127 132 4 -3 366 254 4 -3 366 254 5 -6 70 353 355 4 -1 138 39 7 -9 -34 10 9 -9 -35 366 5 -6 70 55 353 4 -1 138 39 7 -6 180 176 4 -5 191 204 4 -7 108 177 4 -7 58 39 7 -7 108 170 5 -9 -5 377 376 5 -6 180 174 4 -7 109 245 246 5 -7 377 378 5 -6 180 174 4 -7 109 245 246 5 -7 377 378 5 -6 180 174 4 -7 112 125 4 -7 3203 341 4 | 1 12 1 -10 55 56 8 -9 226 208 5 -8 -17 48 167 -6 220 203 4 -5 44 57 8 -4 165 165 4 -3 438 441 5 -2 98 91 5 -1 44 44 57 -6 220 234 4 2 288 287 4 2 288 287 4 2 288 287 5 -1 44 45 5 -1 14 5 5 6 200 193 4 7 253 255 42 5 5 109 193 4 7 253 255 85 5 -7 109 107 5 -6 119 138 5 -5 175 168 4 -3 15 168 16 -1 14 19 496 5 -1 14 14 96 5 -1 14 14 96 5 -1 14 14 96 5 -1 14 14 96 5 -1 14 14 96 5 -1 14 18 15 -1 14 18 15 -1 14 18 15 -1 14 18 15 -1 15 15 168 4 -2 123 15 168 5 -1 14 18 15 -1 14 18 15 -1 15 15 168 5 -1 15 15 168 5 -1 15 15 15 168 5 -1 15 15 15 15 168 5 -1 15 15 15 15 168 5 -1 15 15 15 15 168 5 -1 15 15 15 15 168 5 -1 15 15 15 15 168 5 -1 15 15 15 15 168 5 -1 15 15 15 15 168 5 -1 15 15 15 15 168 5 -1 15 15 15 168 5 -1 15 15 15 168 5 -1 15 15 15 167 5 -1 15 15 15 167 5 -1 15 15 167 5 -1 15 15 167 5 -1 15 15 168 5 -1 15 15 167 5 -1 15 15 167 5 -1 15 15 167 5 -1 15 15 167 5 -1 15 15 167 5 -1 15 15 168 5 -1 15 15 167 5 -1 15 15 167 5 -1 15 15 167 5 -1 15 164 15 7 -1 15 15 164 164 15 7 -1 15 15 164 164 15 7 -1 15 15 164 164 15 7 -1 15 15 164 164 15 7 -1 15 15 164 164 15 7 -1 15 15 164 164 15 7 -1 15 164 164 164 164 164 164 164 164 164 164 |
| -14 113 1 -13 151 151 12 -63 151 152 153 151 159 159 159 159 159 159 159 159 159 | 1 0 107 6 2 | 17 27 9 152 150 3 64 35 5 552 341 4 101 87 4 211 203 4 134 132 4 130 115 4 220 224 4 130 187 4 188 180 5 85 84 6 | -6 180 174 4 -5 191 204 4 -4 112 125 4 -3 203 205 4 | 1 15 1 |

| Tetrakis (pentaf | luoropheny l |)-beta-octach | loroporphyrin | Page 8 |
|---|-----------------------------------|--|--|--|
| 3 268 26 2 -13 l | 5 | 467 458 5 545 551 5 210 209 4 | 10 326 327 4 11 33 56 9 12 -11 38 19 | -3 543 541 5 -2 1345 1337 11 -1 1372 1340 11 |
| 0 176 16 1 90 8 2 39 4 | 269 | 92 88 4 30 48 8 163 165 4 156 161 4 | 13 217 225 4 14 -38 17 9 15 -35 4 11 | 0 1956 1966 16 1 293 284 3 2 387 340 3 3 84 84 3 |
| 3 265 25 4 136 11 | 3 5 11 8 5 12 | -21 17 14 169 177 5 | 2 -3 1 | 4 184 174 2 5 207 204 3 |
| 5 108 9 6 41 2 7 84 6 | 3 10 | 53 58 8 -7 1 | 0 956 944 8 1 497 500 4 2 72 63 3 | 7 100 66 3 8 179 185 3 |
| 2 -12 l | 0 | 275 274 3 572 583 5 | \$ 628 622 5 4 952 916 8 5 553 567 5 | 9 594 599 6 10 -41 15 6 11 20 32 12 |
| 0 128 12 1 205 19 | 0 5 2 0 4 3 | 390 385 4 485 475 5 | 6 911 873 8 7 25 25 8 | 12 -47 4 6 13 387 389 5 |
| 2 -4 2 3 46 5 4 227 22 | 785 | 267 257 3 139 135 3 549 555 5 | 8 109 119 4 9 276 279 4 10 26 13 10 | 14 163 171 5 15 205 206 5 16 91 95 6 |
| 5 96 10 6 24 4 | 4 5 7 | 6 27 19 155 157 4 | 11 245 244 4 12 262 262 4 | 2 1 l |
| 7 302 29 8 163 15 9 291 26 | 5 5 10 | 417 405 5 128 121 4 -36 0 9 | 13 258 263 4 14 110 108 5 15 55 64 7 | -14 -20 26 13 -13 225 231 4 -12 122 102 5 |
| 2 -11 1 | 5 11 12 13 14 | 112 114 5 244 248 5 150 146 5 | 2 -2 1 | -11 71 73 6 |
| 0 41 5 1 330 32 | 3 9 4 4 2 | -6 l | 0 2153 2167 18 1 91 84 3 | -Q 388 38Q A |
| 4 85 9 | 5 7 0 4 5 1 | 78 86 4 354 355 4 279 262 3 | 2 565 353 3 3 900 892 7 4 1253 1245 10 | -6 81 77 4 -5 555 582 5 |
| 5 299 28 6 129 12 7 76 7 | 8 4 2 3 5 3 | 25 18 8 | 5 863 851 7 6 246 237 3 7 314 318 3 | |
| 8 148 14 9 44 5 | 4 5 5 7 9 6 | 530 534 5 511 516 5 | 8 -18 34 11 9 93 99 4 | -1 438 432 4 0 22 11 7 |
| 10 52 4 2 -10 l | 8 9 | 221 219 3 653 641 6 353 358 4 | 10 304 309 4 11 650 644 6 12 39 56 9 | 1 144 154 2 2 288 270 3 3 183 160 2 |
| 0 392 38 1 73 6 | 9 4 11 9 5 12 | 211 198 4 -34 21 9 -4 50 24 | 13 54 91 8 14 166 167 5 15 -30 38 12 | 3 183 160 2 4 163 160 2 5 604 619 5 6 1114 1128 9 |
| 2 -11 2 3 133 14 | 5 16 13 5 4 14 | 61 61 7 38 46 10 | 2 -1 1 | 7 175 187 3 8 597 607 5 |
| 4 139 14 5 17 2 6 44 4 | 0 15 2 | -5 l | 0 1525 1490 13 1 61 45 3 | 9 637 625 6 10 18 34 12 11 197 202 4 |
| 7 301 29 | 6 4 0 0 10 1 8 5 2 1 5 3 | 271 278 3 468 455 4 361 354 4 | 2 341 330 3 3 300 273 3 | 12 325 338 4 13 -34 24 9 |
| 10 153 15 11 297 29 | 1 5 3 | 210 208 3 227 245 3 | 5 986 983 8 6 371 360 4 | 14 125 126 5 15 267 269 5 16 44 49 10 |
| 12 77 7 2 -9 1 | 6 7 | 58 71 4 322 321 4 154 148 3 | 7 605 582 5 8 133 146 3 9 244 255 4 | 2 2 I |
| 0 -28 1 158 15 | 2 8 9 8 4 10 | 270 277 4 445 442 5 265 272 4 | 10 178 184 4 11 99 109 4 12 276 282 4 | -14 291 285 5 -13 138 125 5 -12 125 120 5 |
| 1 158 15 2 287 29 3 193 19 4 93 10 | 2 4 11 7 4 12 2 4 13 | 533 524 5 99 117 5 | 13 168 185 4 14 72 74 6 | -11 205 216 4 -10 458 455 5 |
| 5 336 32 6 537 54 | 8 4 14 3 5 15 | -15 26 17 -22 45 14 122 115 6 | 16 66 62 8 | -8 500 486 5 -7 82 81 4 |
| 7 160 16 8 192 18 9 109 11 | 3 4 2 | -4 1 | 2 0 l -14 208 182 5 | -6 135 132 3 -5 258 262 3 -4 976 968 8 |
| 10 265 25 11 326 31 12 -13 1 | 5 4 0 | 266 262 3 465 481 4 653 659 6 | -13 209 202 5 -12 -30 13 11 | -3 640 631 5 -2 1174 1144 10 |
| 2 -8 1 | 3 4 | 906 926 8 1199 1217 10 | -10 27 40 11 -9 74 67 5 | 0 454 399 4 1 135 144 2 |
| 0 44 3 1 498 51 2 88 9 | 6 6 6 3 5 7 | 273 264 3 952 972 8 | -8 256 249 4 -7 462 441 5 -6 51 53 5 | 3 585 584 5 4 57 50 4 |
| 2 88 9 3 56 3 | 9 4 8 8 5 9 | 430 436 4 645 652 6 | -5 1037 1059 9 -4 455 469 4 | 5 91 87 3 6 340 331 3 |

| Totackie (nentafino | ophenyl)-beta-octach | loroporphyrin | Page 9 |
|---|--|--|---|
| 7 168 169 8 349 359 9 328 311 10 413 413 11 274 264 12 153 168 13 381 369 14 22 10 1 15 135 151 2 3 1 -14 307 296 -13 117 124 -12 291 290 | 3 -14 248 239 5 1 -13 34 54 11 1 -12 188 182 4 1 -11 79 85 6 1 -10 58 50 6 1 -9 312 314 4 2 -8 458 459 5 3 -7 605 615 6 5 -6 569 584 5 -5 620 594 6 -1 118 117 3 -2 848 852 7 -1 743 756 6 | 0 25 70 8 1 206 193 3 2 252 255 3 3 365 384 4 4 285 291 3 5 561 557 5 6 233 252 3 7 638 197 4 9 323 317 4 10 658 649 5 11 87 73 71 6 13 165 163 5 14 231 235 5 | -11 235 231 5 -10 84 81 6 -9 69 70 6 -8 121 129 5 -7 150 149 4 -6 380 378 4 -5 448 462 5 -4 -38 1 6 -3 173 171 4 -2 356 353 4 -1 154 154 3 0 64 80 5 1 185 179 3 91 93 4 3 903 917 8 4 60 62 5 |
| -11 545 539 -10 369 378 -9 261 263 -8 267 239 -7 368 377 -6 150 176 -5 267 283 -4 298 278 -3 1246 1238 -2 1351 1362 -1 210 198 0 157 144 1 271 281 2 1010 988 3 1283 1277 | 1 124 122 3 2 1150 1157 10 3 1840 1829 15 4 532 534 5 4 532 534 5 8 10 789 7 3 6 258 259 3 7 68 73 4 8 8 94 4 9 90 92 4 10 66 74 6 9 90 92 4 11 52 78 7 12 552 562 6 11 572 88 7 | 2 8 1 -13 100 105 6 -12 -42 7 8 -11 263 265 4 -10 131 131 5 -9 211 218 4 -8 319 324 4 -7 378 374 4 -6 247 238 4 -5 337 344 4 -6 46 33 6 -3 413 414 4 -2 114 117 3 -1 631 645 6 | 5 166 165 4 6 250 254 4 7 303 280 4 8 181 169 4 9 83 82 6 10 59 63 7 11 24 51 14 12 257 249 5 2 11 1 -11 124 105 5 -10 86 83 6 -9 77 81 6 -8 200 203 4 |
| 7 355 358 8 253 245 9 865 864 10 115 117 11 70 76 12 325 332 13 434 432 14 -17 6 | 9 2 6 1 64 -14 6 28 24 3 -15 160 174 5 8 -12 99 106 5 4 -11 227 220 4 6 -10 176 188 4 4 -9 612 608 6 5 -8 35 37 8 6 -7 48 19 6 1 -6 69 80 4 -5 300 301 3 -4 387 389 4 -3 565 546 5 | 0 315 319 3 1 -35 14 5 2 85 101 4 3 41 52 6 4 114 109 3 5 7 22 16 6 713 705 6 7 354 364 6 7 175 4 9 260 259 4 10 224 237 4 11 77 74 6 12 261 264 5 13 355 371 5 | -7 366 369 5 -6 326 327 -5 233 233 4 -4 61 49 6 -3 75 90 6 -1 105 95 45 -1 105 95 5 1 255 258 4 2 444 442 5 3 451 443 5 4 447 5 382 383 5 6 152 156 4 |
| -14 58 61 -13 116 102 -12 121 120 -11 91 104 -10 102 90 -9 369 377 -8 300 289 -7 575 575 | 8 -2 64 32 4 5 -1 1090 1110 9 5 0 556 557 5 5 1 84 93 3 5 2 67 62 4 4 3 708 687 6 4 4 1794 1778 15 5 770 756 7 | 2 9 1 -12 34 47 11 -11 103 111 5 -10 -38 12 8 -9 -33 7 8 -8 415 417 5 -7 140 131 4 | 7 231 236 4 8 508 504 5 9 261 264 4 10 82 74 6 11 68 73 7 2 12 1 |
| -6 73 87 -5 552 516 -4 1405 1399 -3 638 658 -2 625 622 -1 326 332 0 482 484 1 688 694 2 1085 1093 3 1598 1604 4 164 162 5 63 79 6 343 341 | 4 6 347 345 4 5 7 189 211 3 12 8 393 392 4 5 9 667 674 6 5 10 551 551 6 11 -26 6 1 4 12 105 95 5 6 13 62 82 7 9 14 146 152 8 13 2 7 1 4 -13 151 146 5 3 -12 410 394 | -6 527 532 5 -5 73 71 5 -4 63 73 5 -3 244 250 3 -2 542 525 5 -1 579 556 4 0 970 975 8 1 270 270 270 3 2 -43 3 5 3 45 52 6 4 797 818 7 | -9 98 105 6 -8 -39 17 8 -7 120 103 5 -6 -44 12 7 -5 429 448 5 -4 263 274 4 -3 120 130 4 -2 216 224 4 -1 324 332 4 -1 324 332 4 -1 52 223 4 2 154 167 468 4 |
| 7 207 219 8 50 28 9 213 210 10 276 268 11 122 140 12 264 260 13 90 96 14 210 198 15 58 49 | 8 -11 102 105 4 4 -10 118 110 4 4 -9 63 48 4 4 -8 287 281 4 -7 605 601 6 6 -6 160 170 5 -5 -34 21 248 -4 231 248 -3 355 343 | 7 387 387 4 8 201 193 4 9 -34 24 9 10 160 152 4 11 118 125 5 12 41 56 10 13 28 29 14 | 4 \$02 \$00 4 5 71 80 6 6 -17 35 15 7 174 183 4 8 89 91 6 9 90 95 6 10 123 125 5 |
| 2 5 1 | | -12 -37 25 10 | -9 153 155 5 |

| Tetrakis (pent | afluorophenyl) | -beta-octachloroporphyrin | Page 10 |
|--|---|--|--|
| -8 -41 -7 -19 -6 35 -5 368 -4 13 -3 329 -2 597 -1 597 0 122 1 595 2 44 | 2 8 6 25 15 7 313 5 8 363 5 9 23 17 10 324 4 5 585 6 3 42 7 124 4 0 597 6 1 50 8 2 | 104 120 5 4 310 305 4 -15 1 17 5 131 139 3 -31 2 10 6 203 222 3 149 151 5 7 132 126 4 209 198 5 8 347 333 4 9 527 536 5 -10 1 10 177 159 4 11 252 242 4 12 61 85 7 372 368 5 13 55 66 8 7 372 368 5 13 55 66 8 | 7 \$25 \$24 4 8 240 243 3 9 8 17 17 10 195 194 4 11 560 557 6 12 108 115 5 13 -34 30 9 14 225 215 5 15 260 251 5 |
| 6 -44 7 161 8 83 2 14 | 5 8 3 184 4 5 34 7 6 165 5 7 108 6 8 1 10 | 171 186 4 -38 6 8 3 -5 1 30 15 11 215 195 4 0 1296 1282 11 103 96 5 1 256 234 3 -34 32 9 2 470 478 4 179 182 4 3 180 189 3 69 81 6 4 654 652 6 40 8 10 5 600 596 5 | 0 608 608 5 1 1164 1156 10 2 798 797 7 3 37 3 5 4 717 720 6 5 13 26 11 6 131 137 3 7 157 161 3 |
| -7 50 -6 127 -5 227 -4 223 -3 44 -2 99 -1 25 0 221 1 48 2 217 | 63 9 1229 5 3 2222 4 0 5 5 7 6 5 5 7 5 7 7 6 7 7 7 6 7 7 6 7 7 6 7 7 7 6 7 | -9 1 7 372 366 4 3 33 7 356 347 4 9 43 33 7 245 239 4 10 304 309 4 175 178 4 11 298 292 4 168 171 4 12 100 103 5 111 105 4 13 8 46 21 144 138 4 14 103 95 6 521 504 5 15 147 138 5 | 8 467 469 5 9 479 479 5 10 215 208 4 11 -28 6 9 12 88 99 5 13 84 95 6 14 33 46 11 15 330 324 5 16 252 234 5 |
| 3 372 4 211 5 64 6 306 7 48 2 15 | \$7\$ 5 7 220 4 8 74 7 9 286 5 10 27 9 11 1 25 14 | 34 13 9 54 55 7 3 -4 1 407 413 5 69 66 6 0 95 103 3 183 194 5 1 291 302 3 167 164 5 2 155 160 3 3 520 521 5 -8 1 4 506 522 5 5 283 292 3 | -14 47 22 10 -13 -38 15 9 -12 281 285 5 -11 251 252 4 -10 166 159 4 -9 192 197 4 -8 88 91 4 |
| -4 252 -3 71 -2 53 0 63 1 2483 3 62 4 174 | 255 5 0 67 7 1 59 7 2 10 11 3 47 7 4 241 5 5 88 6 6 30 7 7 178 5 8 | 101 103 4 6 115 124 3 178 177 4 7 556 569 5 94 114 4 8 362 369 4 218 216 4 9 91 91 4 57 63 6 10 -21 0 11 583 590 6 11 321 324 4 56 40 6 12 60 89 7 468 470 5 13 206 211 4 81 89 5 14 98 99 6 409 589 5 15 557 345 5 | -7 116 125 4 -6 348 345 4 -5 360 356 4 -4 46 38 5 -3 830 821 7 -2 54 45 4 -1 46 6 4 0 152 145 2 1 2457 2456 2 2 384 374 3 |
| 3 -13 0 124 1 241 2 170 3 204 4 166 5 334 | 1 10 11 113 5 12 241 5 13 165 5 13 156 5 3 156 5 3 11 2 | 218 216 4 141 143 5 3 -3 1 229 27 11 231 211 5 0 605 591 5 1 853 864 7 -7 1 2 20 6 8 5 161 159 3 50 51 6 4 228 223 3 40 0 7 5 750 788 6 9 9 16 6 448 455 4 | 4 301 503 5 5 818 810 7 6 445 445 4 7 169 183 3 8 762 774 7 9 230 238 4 10 138 124 4 11 106 103 4 12 65 93 6 |
| 0 49 1 215 2 208 3 129 4 82 5 211 6 29 7 54 8 21 | 48 8 4 5 2011 4 6 129 5 7 83 6 8 201 4 9 15 12 10 46 8 11 1 5 12 1 1 15 12 1 1 15 12 1 1 15 12 1 1 15 12 1 1 15 12 1 1 15 12 1 1 15 12 1 1 15 1 1 1 1 | -12 2 13 7 107 108 3 50 45 6 8 27 34 9 42 44 7 9 30 11 7 359 359 4 10 461 459 5 762 7 287 291 4 12 100 98 5 110 110 5 13 86 96 6 409 402 5 14 167 154 5 172 175 4 15 -40 27 8 259 276 4 108 122 5 3 -2 1 | 13 164 158 4 14 62 59 7 15 -40 16 9 16 85 79 6 3 1 1 -14 263 260 5 -13 224 211 5 -12 275 260 5 -11 212 208 4 -10 8 27 20 |
| 3 -11 0 185 1 129 2 129 3 129 4 308 5 147 | 1 14 173 4 3 133 5 139 5 0 18 10 1 314 4 2 148 4 3 | 190 185 5 -6 1 1 409 411 4 2 300 297 3 138 134 3 3 188 192 3 124 129 3 4 747 758 6 29 38 6 5 357 372 4 103 100 3 6 125 144 3 | -9 -12 8 16 -8 27 29 10 -7 115 106 4 -6 212 211 3 -5 358 365 4 -4 67 53 4 -3 323 321 3 |

| Tetrakis (pentafluo | ophenyl)-beta-octachloroporphy | rin Page 11 |
|--|--|---|
| -2 227 230 -1 1947 1987 1 0 1856 1838 1 1 503 484 2 666 653 3 134 125 4 255 259 5 718 696 6 39 16 7 941 954 8 72 57 | 13 341 330 5 -6 95 14 27 6 13 -5 263 15 186 182 5 -4 127 -3 150 | 338 5 6 214 216 3 90 6 7 56 52 6 184 4 8 9 28 17 417 5 9 243 252 4 367 4 10 35 51 10 90 4 11 23 37 12 261 3 12 65 81 7 114 3 13 236 227 5 146 3 9 1 551 4 4 8 9 1 |
| 9 \$55 \$37 10 247 240 11 234 228 12 279 279 13 402 599 14 201 194 15 57 71 16 62 59 3 2 1 | -14 -22 41 15 0 127 -13 -20 18 15 1 11 -12 23 36 12 2 257 -11 62 45 6 3 541 -10 392 390 5 4 446 -9 555 548 6 5 179 -8 241 248 4 6 590 -7 533 543 5 7 679 -6 363 580 4 8 153 -5 907 918 8 9 476 -4 116 119 3 10 331 -3 200 209 3 11 78 | 114 5 -12 178 181 5 13 12 -11 156 175 5 265 3 -10 147 153 5 519 5 -9 134 137 4 430 4 -8 11 18 179 3 -7 684 689 6 578 5 -6 216 211 4 682 6 -5 306 312 4 162 4 -4 320 319 4 465 5 -3 285 295 4 522 4 -2 238 227 3 97 6 -1 238 234 3 89 6 0 461 463 5 |
| -12 191 183 -11 124 119 -10 231 234 -9 534 533 -8 201 211 -7 312 303 -6 547 559 -5 249 246 -4 184 187 -3 15 59 1 -2 712 713 -1 224 224 0 95 86 1 681 653 2 1035 1004 | -1 22 23 8 13 208 0 97 98 3 14 186 1 360 367 3 2 1819 1805 15 5 7 3 611 613 5 4 554 549 5 -13 70 5 70 65 4 -12 43 6 64 74 4 -11 475 7 2 44 19 -10 186 8 462 460 5 -9 79 9 460 463 5 -8 160 10 31 28 9 -7 235 11 -12 55 17 -6 219 12 132 137 5 -5 113 13 304 303 5 -4 528 | 209 S 1 410 416 4 175 5 2 237 238 3 3 678 669 6 1 4 68 81 5 1 5 187 202 3 97 7 6 244 243 4 0 10 7 258 255 4 468 5 8 108 120 4 142 4 9 178 173 4 83 5 10 44 61 8 166 4 11 45 70 9 249 4 12 125 122 5 204 2 13 269 267 5 116 4 520 5 3 10 1 |
| 4 642 638 5 1252 1249 1 6 250 273 7 125 124 8 342 339 9 222 217 | 15 252 252 5 -2 27 1 836 3 5 1 0 366 1 -13 35 54 10 2 60 1 -12 247 256 5 3 570 1 1 1 1 1 1 1 1 2 2 1 3 7 5 4 1 88 1 -10 166 181 4 5 4 1 -9 212 208 4 6 289 1 -8 561 555 5 7 93 1 -7 117 88 4 8 296 1 -8 739 735 7 9 240 1 -6 739 735 7 9 240 1 -6 739 735 7 9 240 1 -7 154 158 3 10 262 -4 95 108 3 11 167 -3 23 21 8 12 129 | 29 8 -11 72 68 7 843 7 -10 39 51 10 843 4 -9 -15 43 17 607 6 -8 19 35 14 50 4 -7 155 164 4 599 5 -6 220 231 4 183 3 -5 108 100 4 23 18 -4 108 107 4 294 4 -3 446 438 5 92 4 -2 569 563 5 294 4 -1 208 198 3 235 4 0 -31 9 7 275 4 1 239 231 4 173 4 2 301 309 4 124 5 3 132 126 4 |
| -14 85 78 -13 36 59 1 -12 77 78 -11 100 87 -10 383 384 -9 404 420 -8 211 211 -7 252 260 -6 792 793 -5 64 52 -4 448 445 -3 32 2 | 0 -1 905 884 8 14 41 0 716 711 6 1 693 693 6 3 8 2 624 609 5 5 2 98 303 3 -12 15 6 4 288 283 3 -11 105 6 518 531 5 -9 187 7 7 225 248 3 -8 378 8 418 425 4 -7 -11 9 59 56 5 -6 577 10 37 45 8 | 51 10 5 160 155 4 6 209 204 4 1 7 48 31 7 8 366 356 5 108 5 10 233 246 4 39 19 11 58 52 8 188 4 12 55 54 8 21 16 3 11 1 578 5 93 4 -11 221 213 5 |
| -2 102 96 -1 846 835 0 98 89 1 723 705 2 209 210 3 1858 1832 1 4 150 149 5 254 264 6 524 501 7 577 564 | 7 12 197 203 4 -3 331 13 103 102 5 -2 242 3 14 -23 8 14 -1 191 2 15 98 111 6 0 473 | 445 4 -10 193 186 5 330 4 -9 28 47 12 240 3 -8 195 197 4 183 3 -7 212 211 4 490 4 -6 96 101 5 92 4 -5 70 72 6 5 8 -4 16 47 14 64 5 -3 252 263 4 170 3 -2 883 371 4 |

| Tetrakis (pentafluorophenyl) - beta-octachloroporphyrin Page 12 | | | | | | | | | | | | | | | |
|---|--------------------|-------------------|---------|-------------|------------------|------------------|--------------|----------------|------------------|-------------------|-------------|----------------|----------------|-------------------|-------------|
| 0 | 143 102 | 130 103 | 4 | - 5 | 31 | 36 | 12 | 5 6 | 130 -15 | 127 14 | 13 | 14 15 | 193 165 | 192 176 | 5 5 |
| 2 3 | 269 191 | 267 183 | 4 | -4 | -18 -55 | 20 | 16 | 8 | 223 643 93 | 219 636 | 6 | 4 | - 3 | 1 | |
| 5 | 204 409 | 197 408 | 5 | -2 -1 | 107 381 | 110 391 70 | 5 5 7 | 9 10 | 238 142 | 100 231 135 | 4 5 | 0 | 101 149 | 99 149 | 3 |
| 6 | 235 211 | 245 200 | 4 | 0 | 70 172 187 | 160 | 5 | 11 12 | 93 | 90 | ĕ | 2 3 | 63 | 54 170 | 4 |
| 8 9 | - 26 305 | 27 288 | 11 5 | 3 | 353 | 170 349 | 5 | 4 | -7 | 1 | | 4 5 | 377 | 371 59 | 4 |
| 10 11 | 208 79 | 208 87 | 6 | 5 | 117 -29 | 121 27 | 5 12 | ō | 455 310 | 450 312 | 5 4 | 6 | 305 213 | 288 210 | 4 |
| 3 | 12 | 1 | | 3 | 16 | 1 | | 1 2 3 | 71 56 | 68 73 | 5 5 | 8 | 185 581 | 189 588 | 8 |
| -10 -9 | 45 149 | 136 | 10 5 | -1 0 | -30 | 54 | 8 11 | 5 | -31 41 | 3 44 | 8 | 10 11 | 89 | 47 72 | 20 |
| -8 -7 | 64 | 46 | 7 | ĭ | 93 | 87 | 6 | 6 | 73 337 | 70 330 | 5 | 12 13 | 158 105 | 170 111 | 4 5 |
| -6 -5 | 146 | 152 19 | 16 | 4 | -12 | 1 | | 8 | 163 224 | 148 233 | 4 | 14 15 | 172 279 | 182 266 | 5 5 |
| -4 -3 | 31 -38 | 41 30 | 8 | 0 | 49 83 | 70 86 | 8 | 10 11 | 179 30 | 167 42 | 12 | 4 | - 2 | 1 | |
| - 2 - 1 | 535 310 | 541 321 | 5 | 3 | 57 101 | 107 | 8 5 | 12 13 | 153 305 | 155 300 | 5 5 | 0 | 416 | 408 | 4 |
| 0 | 145 59 | 158 61 | 6 | 4 5 | 290 46 | 293 38 | 5 9 | 4 | - 6 | 1 | | 1 2 | 410 12 | 419 | 11 |
| 3 | -25 143 | 19 148 | 10 | 6 | 132 | 128 | 5 | 0 | 175 | 175 | 3 | 3 4 | 283 379 | 284 383 | 3 |
| 4 5 | 41 181 | 73 179 | 8 | 4 | -11 | 1 | _ | 1 2 | -26 52 | 34 | 8 | 5 6 | 298 243 | 308 239 | 3 3 |
| 6 | -10 93 | 46 122 | 19 5 | 1 | 241 174 | 26 254 | 9 | 3 | 321 560 | 313 547 | 5 | 7 8 | 125 183 | 126 185 | 3 3 7 |
| 8 | 350 201 | 340 212 | 5 | 3 | 162 | 169 160 | 4 | 5 6 | 278 222 | 273 219 | 4 | 10 | 386 375 | 385 373 | 4 5 |
| 10 | 238 | 235 | 5 | 5 | 251 169 | 257 171 | 5 | 7 8 9 | 176 54 79 | 177 51 82 | 4 6 5 | 11 12 13 | -34 38 | 5 6 5 5 | 9 |
| 3 | 13 | 1 | _ | 6 | 98 107 | 91 112 | 5 | 10 | 177 379 | 181 404 | 4 5 | 14 15 | 65 202 | 70 201 | 7 5 |
| -9 -8 | 115 72 193 | 105 81 | 5 7 | 8 9 | -22 70 | 23 78 | 14 7 | 11 12 13 | - 32 | 29 119 | 8 | 4 | -1 | 1 | Ü |
| -7 -6 -5 | 266 | 184 255 140 | 5 | 4 | -10 | 1 | | 14 | 125 386 | 374 | 5 | 0 | 369 | 344 | 4 |
| -4 | 143 -36 | 300 | 9 | 0 | 100 237 | 96 238 | 5 | 4 | - 5 | 1 | | 1 2 | 426 652 | 430 | 4 |
| -3 -2 -1 | 305 - 22 564 | 14 556 | 13 | 1 2 3 | 47 | 55 22 | 4 7 10 | 0 | 42 227 | 19 224 | 8 | 3 | 190 593 | 185 598 | 3 |
| 0 | 143 | 152 208 | 4 | 4 5 | 116 131 | 119 128 | 5 | 3 | 718 729 | 224 707 738 | 6 | 4 5 6 | 412 | 418 54 | 4 |
| 2 3 | 68 | 72 259 | 6 | ĕ 7 | 126 261 | 131 | 5 | 4 5 | 226 | 214 32 | 13 | 7 8 | 538 419 | 522 424 | 4 |
| 4 5 | 19 106 | 28 116 | 14 | 8 9 | 81 36 | 91 38 | 11 | 6 | 144 210 | 148 | 3 | 10 | 380 211 | 372 216 | 4 |
| 6 7 | 190 170 | 200 169 | 4 5 | 10 | 93 | 102 | 6 | 8 | 330 271 | 221 331 272 | 4 | 11 12 13 | 290 386 | 284 397 | 4 5 |
| 8 | 151 | 148 | 5 10 | 4 | - 9 | 1 | | 10 11 | 43 -18 | 45 34 | 8 15 | 14 | 425 135 | 423 142 270 | 5 5 |
| 3 | 14 | 1 | | 0 | 32 60 | 33 62 | 10 5 | 12 13 | 160 -37 | 174 28 | 9 | 15 | 279 | | 5 |
| -7 | 44 | 57 | 9 | 3 | 440 54 | 430 58 | 5 7 | 14 | -33 | . 5 | 11 | 4 | | 1 | |
| -6 -5 | 242 103 | 238 111 | 5 5 | 5 | 18 57 | 10 38 | 12 | 4 | _ | 1 | _ | -13 -12 | 234 198 | 234 | 5 |
| -4 | -34 79 | 82 | 6 | 6 | 766 93 | 777 | 5 | 0 | 118 26 | 123 16 | 8 | -11 -10 | -15 -6 | 14 23 | 23 |
| -2 -1 | 167 313 | 155 310 | 4 | 8 | 176 268 | 182 275 | 4 | 3 | 79 161 | 81 152 | 3 | -9 -8 | 135 | 31 140 209 | 4 |
| 0 | 36 249 | 49 244 | 4 | 10 11 | 14 | 36 21 | 9 18 | 4 5 | 485 527 | 509 516 | 5 | -7 -6 | 213 511 | 524 | 5 |
| 2 | 362 62 | 362 54 | 7 | 4 | - 8 | 1 | | 6 | 165 425 | 166 | 4 | -5 -4 -3 | 53 26 38 | 20 | 8 8 |
| 5 | 94 131 | 102 131 | . 5 | o | 117 | 122 237 | 4 | 9 | 462 407 | 461 395 521 | 5 4 5 | - 2 | 733 572 | 725 575 | 6 |
| 6 7 | 111 89 | 105 | | 1 2 | 70 | 75 | 5 | 10 11 | 523 103 | 104 | 5 | -1 0 1 | 1019 648 | 1018 | 3 9 |
| | 15 | 1 | | 3 | 141 143 | 137 153 | | 12 13 | -57 182 | 190 | 5 | 2 | 82 | 9 | |

| Tetrakis (pen | tafluorophenyl |)-beta-octa | chloroporphyrin | | Page 13 |
|---|---|--|--|--|--|
| \$ 225 4 127 5 52 6 605 | 221 3 15 134 3 16 60 5 606 5 4 | 37 24 1 | 1 -4 271 264 6 -3 161 174 -2 147 137 -1 514 529 | 3 12 103 7 3 13 248 9 5 14 -7 | 426 5 71 5 234 5 30 23 |
| 7 73 8 105 | 83 4 113 4 -13 | | 7 1 238 258 | 3 3 4 8 | 1 |
| 9 134 10 564 11 175 12 113 13 213 14 128 15 -41 16 -25 | 126 4 -12 551 5 -10 170 4 -10 120 5 -9 230 4 -8 122 5 -7 6 7 -6 31 13 -5 1 -3 | 80 103 549 555 121 119 140 147 100 112 71 73 260 254 437 445 233 225 153 157 214 221 | 6 3 388 40: 5 4 43 1: 4 5 568 53: 4 6 221 22: 5 7 -10 1: 4 8 475 48: 9 250 25: 3 10 408 40: 3 12 442 44: | 2 4 -12 29 3 5 -11 136 2 5 -10 460 3 -9 85 7 15 -8 49 4 5 -7 572 4 -6 258 9 5 -5 294 4 -4 555 1 5 -3 16 | 37 13 133 5 455 5 71 6 24 8 577 6 256 4 302 4 555 5 17 12 39 9 |
| -13 -39 -12 -19 | 29 9 -1 17 15 0 | 139 125 77 87 | 3 13 280 28 3 14 165 17 3 15 -33 1 | 3 5 -1 37 | 30 6 412 4 |
| -11 166 -10 58 -9 171 | 170 5 1 64 7 2 164 4 3 | 11 27 1 126 132 511 499 | 5 4 6 l | 1 411 2 175 | 426 4 173 3 |
| -8 -25 -7 127 | 25 10 4 107 4 5 | 538 561 136 144 | 5 3 -13 116 12 | 3 93 1 6 4 191 8 16 5 453 | 193 3 |
| -6 446 -5 130 -4 278 | 457 5 6 119 3 7 263 3 8 | 100 101 162 168 221 220 | 3 -11 166 18 3 -10 222 22 | 4 5 6 150 9 4 7 366 | 126 3 372 4 |
| -\$ 101 -2 29 | 107 3 9 11 7 10 | 306 310 644 628 | 4 -9 107 9 6 -8 22 2 | 8 11 9 137 | 292 4 147 4 100 5 |
| -1 717 0 304 1 607 | 712 6 11 278 3 12 616 5 13 | 157 165 -53 41 80 76 | 6 -6 36 4 | 2 7 11 329 0 3 12 -44 | 339 5 49 8 |
| 2 696 3 261 | 691 6 14 264 3 15 | 78 78 | 6 -4 280 27 18 -3 326 30 | 0 4 14 115 | 31 8 124 6 |
| 4 44 5 576 6 285 | 34 4 582 5 310 3 | 4 1 | -1 316 33 0 576 57 | 4 3 4 9 | |
| 7 76 8 136 | 86 4 -13 134 3 -12 | 73 72 65 87 304 305 | 7 1 326 32 7 2 413 38 5 3 766 72 | 7 4 -10 164 | 162 5 |
| 9 580 10 317 11 48 | 320 4 -10 61 7 -9 | 171 168 435 428 | 4 4 714 69 5 5 59 5 | 9 6 -8 100 5 4 -7 43 | 111 5 37 7 |
| 12 295 13 415 14 320 | 419 5 -7 | 15 27 3 -30 3 111 109 | 15 6 419 40 8 7 587 59 4 8 211 20 | 1 5 -5 101 18 4 -4 133 | 97 4 135 4 |
| 15 242 16 -38 | 247 5 -5 11 10 -4 | 348 344 666 677 | 4 9 290 28 6 10 454 45 | 7 5 -2 574 | 573 5 |
| 4 2 | 1 -3 -2 -1 | 384 376 218 208 442 449 | 3 12 -35 4 4 13 144 12 | 1 9 0 289 28 5 1 677 | 288 4 680 6 |
| -13 76 -12 110 -11 138 | 121 5 1 | 879 898 162 160 924 911 | 7 14 47 3 15 -37 | 38 9 2 425 25 10 3 43 4 31 | 37 6 36 8 |
| -10 34 -9 -11 | 15 10 3 25 18 4 | 451 428 1423 1427 | 4 4 7 1 | 5 246 6 194 34 11 7 887 | 191 4 |
| -8 125 -7 418 -6 407 | 411 4 6 | 331 320 482 483 446 450 | 5 -11 274 27 | 73 5 8 204 89 6 9 126 | 204 4 |
| -5 405 -4 351 | 401 4 8 343 4 9 | 641 638 676 672 | 6 -9 459 44 6 -8 362 37 9 -7 312 31 | | 21 5 |
| -3 364 -2 63 -1 63 | 60 4 11 | -30 11 114 118 | 9 -6 192 195 -5 63 | 91 4 13 241 84 5 | 234 5 |
| 0 435 1 834 2 254 | 835 5 14 | -20 44 | 15 -3 102 1 | 10 3 16 3 -11 152 | 2 146 5 |
| 3 83 4 904 | 71 3 894 8 | 4 5 1 | -1 86 0 -18 | 89 4 -10 29 12 10 -9 11 19 3 -8 -3 | 54 12 3 120 5 |
| 5 142 6 528 7 263 | 3 520 5 -13 2 275 3 -12 | 171 170 | 8 2 423 4 5 3 22 | 12 4 -7 -8 23 9 -6 30 | 38 20 2 305 4 |
| 8 93 9 487 | 87 4 -11 7 479 5 -10 | 151 148 276 266 | 5 4 747 7- 4 5 579 5 | 46 7 -5 190 62 5 -4 -23 59 4 -3 700 | 3 26 10 0 697 6 |
| 10 267 11 -29 12 -38 | 23 9 -8 3 15 8 -7 | 228 233 334 337 | 4 7 -37 4 8 136 1 | 0 6 -2 8 49 4 -1 53 | 7 97 4 5 540 5 |
| 13 171 14 57 | 175 4 -6 | | 3 9 -17 4 10 -41 | 34 13 0 31 11 7 1 43 | |

| Tetrakis (pentafluoro | phenyl)-beta-octachl | oroporphyrin | Page 14 |
|---|---|--|--|
| 2 473 474 5 3 110 107 4 4 63 57 5 5 255 248 4 | 8 35 45 11 9 52 66 8 4 14 1 | 9 28 60 12 10 162 159 5 5 -8 1 | 6 317 319 4 7 282 284 4 8 382 395 4 9 467 455 5 |
| 6 460 458 5 7 225 251 4 8 -37 36 8 9 293 284 4 | -7 100 116 6 -6 122 131 5 -5 45 57 9 | 0 226 221 4 1 114 101 4 2 354 362 4 | 11 339 326 5 12 -33 38 9 13 100 111 6 |
| 10 70 86 6 11 44 60 9 12 248 237 5 | -4 227 235 4 -3 53 43 6 -2 203 198 4 | 3 89 86 5 4 334 327 4 5 156 172 4 | 14 185 191 5 5 -\$ 1 |
| 4 11 1 | -1 54 74 7 0 -42 10 7 1 112 124 5 | 6 559 340 4 7 144 146 4 8 6 5 21 9 -35 17 9 | 0 557 554 5 1 344 350 4 2 193 174 3 |
| -10 290 279 5 -9 80 83 6 -8 187 198 4 | 3 103 143 4 4 -40 53 8 | 9 -35 17 9 10 357 345 5 11 87 95 6 12 128 132 5 | 3 231 231 3 4 21 16 9 5 140 142 3 |
| -7 113 115 5 -6 104 97 5 -5 469 486 5 -4 10 7 18 | 5 9 43 20 6 248 239 5 7 111 102 5 8 56 56 8 | 5 -7 1 | 6 121 117 4 7 456 454 5 8 390 403 4 9 491 493 5 |
| -3 183 197 4 -2 115 118 4 -1 70 69 5 | 4 15 1 | 0 97 98 4 1 219 216 4 2 222 233 4 | 10 229 235 4 |
| 0 197 190 4 1 107 111 4 2 690 698 6 3 296 296 4 | -5 24 29 14 -4 135 131 5 -3 33 26 11 -2 -40 13 8 | 3 -17 27 12 4 200 204 4 5 91 86 5 6 172 174 4 | 12 98 91 5 13 248 252 5 14 99 112 6 15 19 19 17 |
| 4 43 44 7 5 106 114 4 6 177 185 4 | -1 130 139 5 0 63 74 7 1 45 44 8 | 7 86 75 5 8 69 65 6 9 -30 3 8 | 5 -2 1 |
| 7 100 105 5 8 415 411 5 9 327 346 5 | 2 188 176 5 3 121 113 5 4 300 288 5 5 8 15 22 | 10 30 25 11 11 314 315 5 12 106 111 6 | 0 316 308 4 1 308 321 3 2 168 163 3 3 352 343 4 |
| 10 99 95 5 11 117 114 5 | 5 8 15 22 6 216 211 5 | 5 -6 l 0 226 223 4 | 4 242 237 3 5 83 87 4 |
| -9 249 254 5 -8 118 121 5 | -1 92 93 6 0 -54 6 6 | 1 133 120 4 2 325 324 4 3 168 171 4 | 8 335 333 4 9 294 302 4 |
| -7 86 91 6 -6 243 252 4 -5 456 459 5 -4 40 30 8 | i 80 62 6 5 -11 I | 4 29 26 8 5 166 170 4 6 115 117 4 7 487 471 5 | 11 188 188 4 12 440 440 5 13 477 462 5 |
| -3 179 186 4 -2 154 160 4 -1 256 267 4 | 0 104 107 5 1 92 79 6 2 107 115 5 | 8 60 59 6 9 132 139 4 10 75 81 6 | 15 110 124 6 |
| 0 162 166 4 1 263 289 4 2 54 57 6 3 303 299 4 | \$ 104 99 5 4 67 81 7 5 87 84 6 6 \$5 29 10 | 11 138 129 5 12 11 27 20 13 179 180 5 | 5 -1 1 0 167 166 3 1 692 724 6 |
| 4 131 123 4 5 74 89 6 6 97 106 5 | 7 94 99 6 5 -10 l | 5 -5 l 0 198 193 3 | 2 1019 1035 9 3 68 81 4 4 373 369 4 |
| 7 226 242 4 8 117 126 5 9 205 187 5 10 71 74 7 | 0 81 92 6 1 72 65 6 2 34 26 11 | 1 272 257 4 2 35 24 7 3 324 320 4 4 285 282 4 | 5 538 540 5 6 27 14 8 7 473 464 5 8 -23 27 10 |
| 4 13 1 | 3 42 45 9 4 50 51 8 5 33 12 9 | 5 329 331 4 6 118 116 4 7 -12 27 14 | 9 35 50 8 10 72 88 5 11 110 123 5 |
| -8 285 274 5 -7 286 276 5 -6 70 37 6 -5 64 63 6 | 6 -15 3 17 7 -26 30 12 8 48 62 9 9 187 177 5 | 8 506 494 5 9 183 185 4 10 199 188 4 11 142 142 5 | 12 34 24 10 13 239 243 4 14 46 58 9 15 67 78 7 |
| -4 259 251 4 -3 206 205 4 -2 100 105 5 | 5 -9 1 | 11 142 142 5 12 159 173 5 13 -30 2 11 14 -53 11 7 | 5 0 1 |
| -1 111 101 5 0 115 119 5 1 301 303 4 2 -41 9 6 | 0 139 156 4 1 123 124 5 2 36 41 10 3 -3 14 24 | 5 -4 l 0 528 516 5 | -12 17 48 18 -11 44 39 9 -10 52 50 8 -9 48 50 8 |
| 3 259 268 4 4 445 434 5 5 31 69 11 | 4 -3 15 25 5 126 119 5 6 138 125 5 | 1 233 239 3 2 67 66 4 3 40 51 5 | -8 21 45 14 -7 96 83 5 -6 205 201 4 |
| 6 45 37 8 7 160 160 5 | 7 340 339 5 8 63 65 7 | 4 110 105 4 5 278 281 4 | -5 533 530 5 -4 42 16 6 |

| Tetrakis (pentafluorophenyl) -beta-octachloroporphyrin |
|--|
| 0 0 35 6 6 6 5 5 7 1 1 245 240 3 1 150 140 5 1 247 240 3 1 1 237 228 4 281 3 2 3 1 17 6 -11 150 140 5 1 2 2 3 1 17 6 -11 150 140 5 1 2 3 1 2 3 1 2 3 1 1 7 6 -11 150 140 5 1 2 3 1 1 1 1 1 1 1 1 1 1 1 1 1 1 1 1 1 |
| 1 237 222 3 5 3 1 2 3851 17 7 -10 280 277 5 5 2 84 281 3 |
| \$\begin{array}{c c c c c c c c c c c c c c c c c c c |
| \$ 184 189 \$ \$ -10 \$ 378 \$ \$80 \$ \$ 6 \$ 220 \$ 221 \$ \$ -7 \$ 687 \$ 640 \$ 6 \$ 6 \$ 219 \$ 212 \$ \$ -9 \$ 43 \$ 611 \$ 9 \$ 7 \$ 220 \$ 214 \$ 3 \$ -6 \$ 248 \$ 218 \$ 4 \$ 7 \$ 32 \$ 29 \$ 8 \$ -8 \$ 206 \$ 214 \$ 8 \$ 123 \$ 115 \$ 4 \$ -5 \$ 256 \$ 253 \$ 4 \$ 8 \$ 363 \$ 354 \$ 4 \$ -7 \$ 192 \$ 185 \$ 4 \$ 9 \$ 164 \$ 155 \$ 4 \$ -4 \$ -28 \$ 0 \$ 8 \$ 363 \$ 354 \$ 4 \$ -7 \$ 192 \$ 185 \$ 4 \$ 10 \$ 213 \$ 217 \$ 4 \$ -3 \$ 45 \$ 43 \$ 6 \$ 9 \$ 66 \$ 65 \$ -6 \$ 114 \$ 118 \$ 4 \$ 10 \$ 213 \$ 217 \$ 4 \$ -3 \$ 45 \$ 6 \$ 6 \$ 10 \$ 218 \$ 219 \$ 4 \$ -5 \$ 87 \$ 93 \$ 4 \$ 11 \$ 248 \$ 250 \$ 4 \$ -2 \$ 551 \$ 564 \$ 5 \$ 11 \$ 64 \$ 55 \$ 6 \$ -4 \$ 62 \$ 45 \$ 5 \$ 12 \$ 334 \$ 340 \$ 5 \$ -1 \$ 96 \$ 100 \$ 4 \$ 12 \$ 438 \$ 435 \$ 5 \$ -3 \$ 91 \$ 88 \$ 4 \$ 13 \$ 238 \$ 234 \$ 4 \$ 0 \$ 111 \$ 127 \$ 3 \$ 13 \$ 124 \$ 132 \$ 5 \$ -2 \$ 589 \$ 583 \$ 5 \$ 14 \$ 200 \$ 194 \$ 5 \$ 1 \$ 296 \$ 302 \$ 4 \$ 14 \$ 276 \$ 273 \$ 5 \$ -1 \$ 38 \$ 44 \$ 6 \$ 15 \$ -59 \$ 14 \$ 6 \$ 2 \$ -19 \$ 24 \$ 9 \$ 14 \$ 276 \$ 273 \$ 5 \$ -1 \$ 38 \$ 44 \$ 6 \$ 15 \$ -59 \$ 14 \$ 6 \$ 2 \$ -19 \$ 24 \$ 9 \$ 14 \$ 276 \$ 273 \$ 5 \$ 1 \$ 24 \$ 31 \$ 8 \$ 5 \$ 6 \$ 1 \$ 4 \$ 50 \$ 377 \$ 5 \$ 1 \$ 24 \$ 31 \$ 8 \$ 5 \$ 6 \$ 1 \$ 4 \$ 50 \$ 377 \$ 5 \$ 1 \$ 24 \$ 212 \$ 2 \$ 2 \$ 2 \$ 2 \$ 2 \$ 2 \$ 2 \$ 2 \$ |
| 6 219 212 3 -9 43 61 9 7 220 115 4 -5 256 253 4 8 563 354 4 -7 192 185 4 9 164 155 4 -4 -28 0 8 9 66 66 5 -6 114 118 4 10 213 217 4 -3 45 43 6 10 218 219 4 -5 87 93 4 11 248 240 5 -1 96 100 4 11 64 55 6 -4 62 245 5 12 334 340 5 -1 96 100 4 112 438 435 5 -3 91 88 4 13 238 234 4 0 111 127 3 13 124 132 5 -2 589 583 5 14 200 194 5 1 296 302 4 14 276 273 5 -1 58 446 6 15 -59 14 6 2 -19 24 9 14 276 273 5 -1 58 446 6 15 -59 14 6 2 -19 24 9 15 194 181 5 0 129 125 3 3 37 60 7 15 194 181 5 0 129 125 3 3 341 333 4 -12 130 149 5 6 270 289 4 1-12 121 132 5 4 263 262 3 -11 93 81 6 7 349 354 4 1-12 121 132 5 4 263 262 3 -11 93 81 6 7 349 354 4 1-13 -5 24 10 5 142 148 3 -10 -31 15 11 8 435 431 5 1-10 -66 81 7 6 430 410 4 -9 12 22 18 9 636 639 6 1-9 274 273 4 7 -23 24 9 -8 167 169 4 10 17 50 15 1-8 137 144 4 8 90 86 4 -7 520 511 5 11 339 348 5 1-7 128 128 4 9 162 160 4 -6 67 57 5 12 -35 41 10 1-6 443 448 5 10 594 590 6 -5 205 199 4 13 32 31 10 1-6 443 448 5 10 594 590 6 -5 205 199 4 13 32 31 10 1-5 265 262 4 11 -465 146 14 6 -4 18 9 10 14 63 75 8 1-2 346 351 4 14 215 204 5 -1 73 59 4 1 382 391 4 5 4 12 38 282 5 5 833 838 10 -7 245 229 4 1 382 391 4 5 4 12 38 282 5 5 833 838 10 -7 245 229 4 1 382 391 4 5 4 1 288 282 5 5 833 838 10 -7 245 229 4 1 382 391 4 5 4 1 288 282 5 5 833 838 10 -7 245 229 4 1 382 391 4 5 4 1 288 282 5 5 833 838 10 -7 245 229 4 1 382 391 4 5 4 1 288 282 5 5 833 838 10 -7 245 229 4 1 382 391 4 5 4 1 288 282 5 5 833 838 10 -7 245 229 4 1 383 37 38 4 5 4 14 215 204 5 -1 73 59 4 5 5 5 5 5 5 5 5 5 5 5 5 5 5 5 5 5 |
| 10 |
| 10 218 219 4 -5 87 93 4 11 248 250 5 -1 96 100 4 11 24 35 4 35 5 -4 62 45 5 12 354 340 5 -1 96 100 4 11 27 31 12 438 435 5 -3 91 88 4 13 238 234 4 0 111 127 3 13 124 132 5 -2 589 583 5 14 200 194 5 1 296 302 4 14 276 273 5 -1 38 44 6 15 -59 14 6 2 -19 24 9 15 15 194 181 5 0 129 125 3 |
| 12 438 433 5 -2 589 583 5 14 200 194 5 1 296 302 4 14 276 273 5 -1 38 44 6 15 -59 14 6 2 -19 24 9 7 15 194 181 5 0 129 125 3 5 1 24 31 8 5 6 1 4 50 37 60 7 15 194 181 5 1 24 31 8 5 6 1 4 50 37 60 7 15 194 181 5 1 24 31 8 5 6 1 4 50 37 60 7 15 194 181 5 1 24 31 8 5 6 1 5 531 331 4 15 11 -35 24 10 5 142 148 3 -10 -31 15 11 8 435 431 5 -10 66 81 7 6 430 410 4 -9 12 22 18 9 638 639 6 10 10 17 50 15 -9 274 273 4 7 -23 24 9 -8 167 169 4 10 17 50 15 -8 137 144 4 8 90 86 4 -7 520 511 5 11 339 348 5 -7 128 128 4 9 162 160 4 -6 67 57 5 12 -35 41 10 -5 265 262 4 11 -46 14 6 -4 18 9 10 14 63 75 8 -4 26 53 9 12 393 387 5 -3 376 373 4 -2 105 104 4 13 291 290 4 -2 77 64 4 5 9 1 14 63 75 8 -1 193 183 3 15 153 145 5 0 494 486 5 -11 57 60 8 10 37 5 8 -1 12 38 291 290 4 -2 77 64 4 6 -1 10 38 351 10 13 582 391 4 5 4 1 2394 396 4 -9 120 121 5 5 6 6 6 6 7 7 7 1108 1109 9 -8 0 117 26 8 421 426 5 -3 258 259 4 6 135 121 3 -9 153 145 5 0 494 486 5 -11 57 60 8 8 421 426 5 -3 258 267 4 11 10 101 108 4 0 9 -8 0 17 26 8 421 426 5 -3 258 267 4 11 119 143 4 -4 165 164 3 12 86 90 6 133 132 24 245 5 -1 331 332 24 11 119 143 4 -4 165 164 3 12 86 90 6 133 132 5 -3 258 267 4 11 119 143 4 -4 165 164 3 12 86 90 6 133 132 5 -3 363 373 4 11 119 143 4 -4 165 164 3 11 119 143 4 -4 165 164 3 11 119 143 4 -4 165 164 3 11 119 143 4 -4 165 164 3 11 119 143 4 -4 165 164 3 11 119 143 4 -4 165 164 3 11 119 143 4 -4 165 164 3 11 119 143 4 -4 165 164 3 11 119 143 4 -4 165 164 3 11 119 143 4 -4 165 164 3 11 119 143 4 -4 165 164 3 11 119 143 4 -4 165 164 3 11 119 143 4 -4 165 164 3 11 119 143 5 -2 193 195 3 145 5 7 1 108 103 9 105 5 15 15 15 15 15 15 15 15 15 15 15 15 |
| 15 194 181 5 0 129 125 3 8 5 6 1 4 50 37 5 5 1 1 2 24 31 8 5 6 1 4 50 37 5 5 1 1 2 21 4 129 3 5 331 331 4 1 121 132 5 4 263 262 3 -11 93 81 6 7 333 331 3 4 1 11 -35 24 10 5 142 148 3 -10 -31 15 11 8 435 431 5 1 10 66 81 7 6 430 410 4 -9 12 22 18 9 636 639 6 1 9 274 273 4 7 -23 24 9 -8 167 169 4 10 17 50 15 15 1 1 339 348 5 1 1 1 37 144 4 8 90 86 4 -7 520 511 5 11 339 348 5 1 1 1 337 144 4 8 90 86 4 -7 520 511 5 11 339 348 5 1 1 1 2 2 2 2 2 2 2 2 2 2 2 2 2 2 2 2 |
| 5 1 1 2 124 129 3 5 331 331 4 5 4 121 130 149 5 6 270 289 4 4 11 -35 24 10 5 142 148 3 -11 93 81 6 7 349 354 4 1-11 -35 24 10 5 142 148 3 -10 -31 15 11 8 435 431 5 10 66 81 7 6 430 410 4 -9 12 22 18 9 636 639 6 639 6 135 121 3 144 4 8 90 86 4 -7 520 511 5 11 339 348 5 10 594 590 6 -5 205 511 5 11 339 348 5 10 594 590 6 -5 205 199 4 13 32 31 10 -5 265 262 4 11 -46 14 6 -4 18 9 10 14 63 75 8 1-2 50 104 4 13 291 290 4 -2 77 64 4 5 9 1 14 63 75 8 1 15 104 4 13 291 290 4 -2 77 64 4 5 9 1 1 2 348 35 1 1 1 1 2 38 2 39 1 4 1 2 204 5 -1 73 59 4 1 1 2 38 2 391 4 5 4 1 2 204 5 -1 73 59 4 1 1 3 382 391 4 5 4 1 2 204 5 -1 73 59 4 1 1 3 382 391 4 5 4 1 2 2 394 396 4 -9 120 121 5 1 2 394 396 4 -9 120 121 5 1 2 394 396 4 -9 120 121 5 1 2 394 396 4 -9 120 121 5 1 2 394 396 4 -9 120 121 5 1 2 394 396 4 -9 120 121 5 1 2 394 396 4 -9 120 121 5 1 2 394 396 4 -9 120 121 5 1 2 394 396 4 -9 120 121 5 1 2 394 396 4 -9 120 121 5 1 2 394 396 4 -9 120 121 5 1 2 394 396 4 -9 120 121 5 1 2 394 396 4 -9 120 121 5 1 2 394 396 4 -9 120 121 5 1 2 394 396 4 -9 120 121 5 1 2 394 396 4 -9 120 121 5 1 2 394 396 4 -9 120 121 5 1 2 394 396 4 -9 120 121 5 1 2 394 396 4 -9 120 120 121 5 1 2 394 396 4 -9 120 120 121 5 1 2 394 396 4 -9 120 120 120 120 120 120 120 120 120 120 |
| -12 121 132 5 4 263 262 3 -11 -35 15 11 8 435 431 5 -10 -66 81 7 6 430 410 4 -9 12 22 18 9 636 639 6 -9 274 273 4 7 -23 24 9 -8 167 169 4 10 17 50 15 7 -8 137 144 4 8 90 86 4 -7 520 511 5 11 339 348 5 -7 128 128 4 9 162 160 4 -6 67 57 5 12 -35 41 10 -6 443 448 5 10 594 590 6 -5 5 205 199 4 13 32 31 10 -5 265 262 4 11 -46 14 6 -4 18 9 10 14 63 75 8 -2 26 53 9 12 393 387 5 -3 376 373 4 -2 26 53 9 12 393 387 5 -3 376 373 4 -2 26 53 9 12 393 387 5 -3 376 373 4 -2 346 351 4 14 215 204 5 -1 73 59 4 -2 346 351 4 14 215 204 5 -1 73 59 4 -2 346 351 4 14 215 204 5 -1 73 59 4 -1 193 183 3 15 153 145 5 0 492 486 5 -11 57 60 8 1 382 591 4 5 4 1 23 32 32 292 3 -8 274 279 4 3 4 614 597 5 -11 238 252 5 5 833 838 7 -7 245 229 4 4 614 597 5 -11 238 252 5 5 833 838 7 -6 115 107 4 4 6 14 597 5 -11 238 252 5 5 833 838 7 -6 115 107 4 5 5 25 0 9 -10 48 68 8 6 90 89 4 -5 35 32 9 6 135 121 3 -9 153 145 4 7 14 27 13 -4 48 50 7 7 1108 1109 9 -8 0 17 26 8 421 426 5 -3 258 267 4 10 101 108 4 -5 14 13 14 11 103 112 5 0 60 55 5 11 119 143 4 -4 165 164 3 12 86 90 6 1 318 322 4 11 191 143 4 -4 165 164 3 12 86 90 6 1 318 322 4 11 191 143 4 -4 165 164 3 12 86 90 6 1 318 322 4 11 191 143 4 -4 165 164 3 12 86 90 6 1 318 322 4 11 119 143 4 -4 165 164 3 12 86 90 6 1 318 322 4 11 191 143 4 -4 165 164 3 12 86 90 6 1 318 322 4 11 119 143 4 -4 165 164 3 12 86 90 6 1 318 322 4 11 119 143 4 -4 165 164 3 12 86 90 6 1 318 322 4 11 119 143 4 -4 165 164 3 12 86 90 6 1 318 322 4 11 119 143 4 -4 165 164 3 12 86 90 6 1 318 322 4 11 119 143 4 -4 165 164 3 12 86 90 6 1 318 322 4 11 119 143 147 7 -1 1401 1386 12 15 227 209 5 4 567 565 5 115 313 297 5 0 97 98 3 14 301 292 5 3 98 85 4 13 13 127 5 -2 193 195 3 14 301 292 5 3 98 85 4 13 13 13 127 5 -2 193 195 3 14 301 292 5 3 98 85 4 13 149 147 3 5 7 108 103 4 14 14 14 14 14 14 14 14 14 14 14 14 1 |
| -10 66 81 7 6 450 410 4 -9 12 22 18 9 636 639 6 -9 274 273 4 7 -23 24 9 -8 167 169 4 10 17 50 15 -8 137 144 4 8 90 86 4 -7 520 511 5 11 339 348 5 -7 128 128 4 9 162 160 4 -6 67 57 5 12 -35 41 10 -6 443 448 5 10 594 590 6 -5 205 199 4 13 32 31 10 -5 265 262 4 11 -46 14 6 -4 18 9 10 14 63 75 8 -4 26 53 9 12 393 387 5 -3 376 373 4 -3 105 104 4 13 291 290 4 -2 77 64 4 5 9 1 -2 346 351 4 14 215 204 5 -1 73 59 4 -1 193 183 3 15 153 145 5 0 494 486 5 -11 57 60 8 0 472 469 4 1 382 591 4 5 4 1 2 394 396 4 -9 120 121 5 2 691 697 6 3 84 78 3 -12 51 68 9 4 17 13 10 -7 245 29 4 4 614 597 5 -11 238 232 5 5 833 838 7 -7 245 29 4 4 614 597 5 -11 238 232 5 5 833 838 7 -6 115 107 4 5 25 0 9 -10 48 68 8 6 90 89 4 -5 35 32 9 6 135 121 3 -9 153 145 4 7 14 27 13 -4 48 50 7 7 1108 1109 9 -8 0 17 26 8 421 426 5 -3 258 267 4 9 771 794 7 -6 148 148 4 10 491 490 5 -1 331 332 4 10 101 108 4 -5 14 13 14 11 103 112 5 0 60 55 5 11 119 143 4 -4 165 164 3 12 86 90 6 1 318 322 4 11 313 127 5 -2 193 195 3 14 301 292 5 3 98 85 4 12 313 297 5 0 97 98 5 13 131 127 5 -2 193 195 3 14 301 292 5 3 98 85 4 14 61 41 7 -1 1401 1386 12 15 227 209 5 4 567 565 5 15 313 297 5 0 97 98 5 1 149 147 3 5 7 1 68 98 103 5 5 2 1 2 318 313 3 5 242 241 3 -12 34 74 6 8 98 103 5 |
| -8 137 144 4 8 90 86 4 -7 520 511 5 11 389 348 5 -7 128 128 4 9 162 160 4 -6 67 57 5 12 -35 41 10 6 67 57 5 12 -35 41 10 6 67 57 5 12 -35 41 10 6 7 5 265 262 4 11 -46 14 6 -4 18 9 10 14 63 75 8 6 7 5 8 7 5 105 104 4 13 291 290 4 -2 77 64 4 5 9 1 7 10 10 10 10 10 10 10 10 10 10 10 10 10 |
| -7 128 128 4 5 10 594 590 6 -5 205 199 4 13 52 51 10 -5 265 262 4 11 -46 14 6 -4 18 9 10 14 63 75 8 -4 28 53 9 12 335 387 5 -3 376 373 4 -5 105 104 4 13 291 290 4 -2 77 64 4 5 9 1 -2 546 351 4 14 215 204 5 -1 73 59 4 -1 193 183 3 15 153 145 5 0 494 486 5 -11 57 60 8 10 472 469 4 1 382 391 4 5 4 1 23 394 396 4 -9 120 121 5 2 691 697 6 3 84 78 3 -12 51 68 9 4 17 13 10 -7 245 229 4 614 597 5 -11 238 232 5 5 833 838 7 -6 115 107 4 6 8 367 376 4 -7 55 48 6 9 17 181 4 27 13 -4 48 50 7 7 1108 1109 9 -8 0 17 26 8 421 426 5 -3 258 267 4 8 367 376 4 -7 55 48 6 9 177 181 4 -2 456 467 5 9 771 794 7 -6 148 148 4 10 491 490 5 -1 331 332 4 11 19 143 4 -4 165 164 3 12 86 90 6 1 318 322 4 11 19 143 4 -4 165 164 3 12 86 90 6 1 318 322 4 11 19 143 4 -4 165 164 3 12 86 90 6 1 318 322 4 11 19 143 4 -4 165 164 3 12 86 90 6 1 318 322 4 11 19 143 4 -4 165 164 3 12 86 90 6 1 318 322 4 11 19 143 4 -4 165 164 3 12 86 90 6 1 318 322 4 11 19 143 4 -4 165 164 3 12 86 90 6 1 318 322 4 11 19 143 4 -4 165 164 3 12 86 90 6 1 318 322 4 11 119 143 4 -4 165 164 3 12 86 90 6 1 318 322 4 11 119 143 4 -4 165 164 3 12 86 90 6 1 318 322 4 11 119 143 4 -4 165 164 3 12 86 90 6 1 318 322 4 11 119 143 7 -1 1401 1386 12 15 227 209 5 3 98 85 4 14 801 41 7 -1 1401 1386 12 15 227 209 5 4 567 565 5 115 313 297 5 0 97 98 3 5 143 301 292 5 3 98 85 4 14 801 41 7 -1 1401 1386 12 15 227 209 5 4 567 565 5 115 313 297 5 0 97 98 3 5 143 301 292 5 3 98 85 4 14 801 41 7 -1 1401 1386 12 15 227 209 5 4 567 565 5 115 313 297 5 0 97 98 3 5 143 301 292 5 3 98 85 4 14 801 41 7 -1 1401 1386 12 15 227 209 5 4 567 565 5 115 313 297 5 0 97 98 5 1 149 147 3 5 7 1 108 103 4 1 11 103 112 5 1 108 103 4 1 11 103 112 5 1 108 103 4 1 11 103 112 5 1 108 103 4 1 11 103 112 5 1 108 103 4 1 11 103 112 5 1 108 103 4 1 11 103 112 5 1 108 103 4 1 11 103 112 5 1 108 103 4 1 11 103 112 5 1 108 103 4 1 11 103 112 5 1 108 103 4 1 11 103 112 5 1 108 103 4 1 11 103 112 5 1 108 103 4 1 11 103 112 5 1 108 103 4 1 11 103 112 5 1 108 103 4 1 11 103 112 5 1 108 103 4 1 11 103 112 5 1 108 103 4 1 11 103 11 |
| -5 265 262 4 11 393 387 5 -3 376 373 4 5 9 1 -3 105 104 4 13 291 290 4 -2 77 64 4 5 9 1 -2 346 351 4 14 215 204 5 -1 73 59 4 -1 193 183 3 15 153 145 5 0 494 486 5 -11 57 60 8 -1 193 183 3 15 153 145 5 0 494 486 5 -11 57 60 8 -1 193 183 3 15 153 145 5 0 494 486 5 -11 57 60 8 -1 193 183 3 15 153 145 5 0 494 486 5 -11 57 60 8 -1 193 183 3 15 153 145 5 0 494 486 5 -11 57 60 8 -1 2 394 396 4 -9 120 121 5 -1 3 82 391 4 5 4 1 2 394 396 4 -9 120 121 5 -1 3 84 78 3 -12 51 68 9 4 17 13 10 -7 245 229 4 -1 3 84 78 3 -12 51 68 9 4 17 13 10 -7 245 229 4 -1 4 614 597 5 -11 238 232 5 5 833 838 7 -6 115 107 4 -1 5 25 0 9 -10 48 68 8 6 90 89 4 -5 35 32 9 -1 10 101 108 1109 9 -8 0 17 26 8 421 426 5 -3 258 267 4 -3 367 376 4 -7 55 48 6 9 177 181 4 -2 456 462 5 -9 367 376 4 -7 55 48 6 9 177 181 4 -2 456 462 5 -9 367 376 4 -7 55 48 6 9 177 181 4 -2 456 462 5 -9 367 376 4 -7 55 48 6 9 177 181 4 -2 456 462 5 -9 367 376 4 -7 55 48 6 9 177 181 4 -2 456 462 5 -9 367 376 4 -7 55 48 6 9 177 181 4 -2 456 462 5 -9 367 376 4 -7 55 48 6 9 177 181 4 -2 456 462 5 -9 367 376 4 -7 55 48 6 9 177 181 4 -2 456 462 5 -9 367 376 4 -7 55 48 6 9 177 181 4 -2 456 462 5 -9 367 376 4 -7 55 48 6 9 177 181 4 -2 456 462 5 -9 367 376 4 -7 55 48 6 9 177 181 4 -2 456 462 5 -9 367 376 4 -7 55 48 6 9 177 181 4 -2 456 462 5 -9 367 376 4 -7 55 48 6 9 177 181 4 -2 456 462 5 -9 367 376 4 -7 55 48 6 9 177 181 4 -2 456 462 5 -9 367 376 4 -7 55 48 6 9 177 181 4 -2 456 462 5 -11 119 143 4 -4 165 164 3 112 86 90 6 1 318 322 4 -11 119 143 4 -4 165 164 3 112 86 90 6 1 318 322 4 -11 149 147 3 5 7 1 6 8 98 103 5 -11 149 147 3 5 7 1 6 8 98 103 5 -11 149 147 3 5 7 1 6 8 98 103 5 -11 149 147 3 7 1 1401 1386 12 15 227 209 5 4 567 565 5 -11 149 147 3 7 1 1401 1386 12 15 227 209 5 5 3 98 88 10 35 5 -1 149 147 3 7 1 12 347 327 5 9 66 77 6 |
| -3 105 104 4 12 15 204 5 -1 73 59 4 -1 193 183 3 15 153 145 5 0 494 486 5 -11 57 60 8 |
| -1 193 185 3 15 185 125 2 1 2 394 396 4 -9 120 121 5 1 2 2 394 396 4 -9 120 121 5 1 2 2 394 396 4 -9 120 121 5 1 2 3 2 394 396 4 -9 120 121 5 1 2 3 2 394 396 4 -9 120 121 5 1 2 3 2 3 2 3 2 3 2 3 2 3 2 3 2 3 2 3 2 |
| 3 84 78 3 -12 51 68 9 4 17 13 10 -7 245 229 4 4 614 597 5 -11 238 232 5 5 833 838 7 -6 115 107 4 5 25 0 9 -10 48 68 8 6 90 89 4 -5 35 32 9 6 135 121 3 -9 153 145 4 7 14 27 13 -4 48 26 -7 245 266 62 5 -8 21 17 181 4 -2 456 462 5 -3 258 267 4 7 1108 1109 9 -8 0 17 181 4 -2 456 462 5 9 771 181 4 -2 456 462 5 9 771 181 4 -2 456 462 5 9 771 181 4 -2 456 462 5 9 771 181 4 -2 <t< td=""></t<> |
| \$\begin{array}{cccccccccccccccccccccccccccccccccccc |
| 6 135 121 3 -9 153 145 4 7 14 27 13 -4 48 50 7 7 1108 1109 9 -8 0 17 26 8 421 426 5 -3 258 267 4 8 367 376 4 -7 55 48 6 9 177 181 4 -2 456 462 5 9 771 794 7 -6 148 148 4 10 491 490 5 -1 331 332 4 10 101 108 4 -5 14 13 14 11 103 112 5 0 60 55 5 11 119 143 4 -4 165 164 3 12 86 90 6 1 318 322 4 12 38 34 8 -3 417 421 4 13 165 148 5 2 150 150 3 13 131 127 5 -2 193 195 3 14 301 292 5 3 98 85 4 14 61 41 7 -1 1401 1386 12 15 227 209 5 4 567 565 5 15 313 297 5 0 97 98 3 5 365 373 4 14 301 292 5 3 98 85 4 14 61 41 7 -1 1401 1386 12 15 227 209 5 5 365 373 4 14 301 292 5 3 365 |
| 8 367 376 4 -7 55 48 6 9 177 181 4 -2 456 462 5 9 771 794 7 -6 148 148 4 10 491 490 5 -1 331 332 4 10 101 108 4 -5 14 13 14 11 103 112 5 0 60 55 5 11 119 143 4 -4 165 164 3 12 86 90 6 1 318 322 4 12 38 34 8 -3 417 421 4 13 165 148 5 2 150 150 3 13 131 127 5 -2 193 195 3 14 301 292 5 3 98 85 4 14 61 41 7 -1 1401 1386 12 15 227 209 5 4 567 565 5 15 313 297 5 0 97 98 3 5 149 147 3 5 7 1 6 33 30 9 5 2 1 2 318 313 3 5 7 108 103 4 5 2 150 150 3 4 5 150 150 3 150 150 150 150 150 150 150 150 150 150 |
| 9 71 194 1 -5 14 13 14 11 103 112 5 0 60 55 5 1 11 119 143 4 -4 165 164 3 12 86 90 6 1 318 322 4 12 88 34 8 -3 417 421 4 13 165 148 5 2 150 150 3 13 131 127 5 -2 193 195 3 14 301 292 5 3 98 85 4 14 81 41 7 -1 1401 1386 12 15 227 209 5 4 567 565 5 15 313 297 5 0 97 98 3 5 1 6 33 30 9 1 149 147 3 5 7 1 6 33 30 9 1 149 147 3 5 7 1 6 33 30 9 1 149 147 3 5 7 1 6 8 98 103 5 1 1 149 147 3 5 7 1 1 149 147 3 1 1 1 1 1 149 147 3 1 1 1 1 1 149 147 3 1 1 1 1 1 1 1 1 1 1 1 1 1 1 1 1 1 1 |
| 12 38 34 8 -3 417 421 4 13 165 148 5 2 150 150 3 13 131 127 5 -2 193 195 3 14 301 292 5 3 98 85 4 14 61 41 7 -1 1401 1386 12 15 227 209 5 4 567 565 5 15 313 297 5 0 97 98 3 5 365 373 4 15 313 297 5 0 149 147 3 5 7 1 6 33 30 9 5 2 1 2 318 313 3 7 108 103 4 5 2 1 2 318 313 3 -12 94 74 6 8 98 103 5 3 242 241 3 -12 94 74 6 8 98 103 5 |
| 13 14 61 41 7 -1 1401 1386 12 15 227 209 5 4 567 565 5 15 313 297 5 0 97 98 3 5 365 373 4 15 313 297 5 0 97 98 3 5 365 373 4 149 147 3 5 7 1 6 33 30 9 5 2 1 2 318 313 3 7 108 103 4 3 242 241 3 -12 94 74 6 8 98 103 5 3 242 241 3 -12 94 74 6 8 98 103 5 4 74 6 8 98 103 5 5 11 347 327 5 9 66 77 6 |
| 15 313 297 5 1 149 147 3 5 7 1 6 53 30 9 5 2 1 2 318 313 3 7 108 103 4 3 242 241 3 -12 94 74 6 8 98 103 5 3 242 241 3 -12 94 74 6 8 98 103 5 |
| 3 242 241 3 -12 94 74 6 8 98 103 5 3 242 241 3 -12 94 74 6 8 98 103 5 10 170 150 5 4 508 508 5 -11 347 327 5 9 66 77 6 |
| |
| -11 -22 25 14 5 374 374 4 -10 97 109 6 10 -45 14 7 |
| -9 143 143 4 7 104 102 4 -8 52 45 7 12 145 152 5 -9 143 143 4 7 104 102 4 -8 52 45 7 12 145 152 5 |
| -7 202 208 4 9 265 266 4 -6 572 590 6 8 130 131 4 10 -19 6 13 -5 286 274 4 5 10 1 |
| -5 142 143 4 11 38 63 8 -4 -24 9 8 -10 112 105 5 |
| -3 365 337 4 13 127 140 5 -2 867 878 8 -9 23 06 14 -2 1050 1050 9 14 286 289 5 -1 778 774 7 -8 117 125 5 |
| -1 468 447 4 15 172 165 5 0 211 216 3 -4 31 11 11 |
| 1 173 172 5 5 5 1 2 299 289 3 -5 296 263 4 2 195 187 3 5 5 1 3 262 261 3 -4 200 200 4 |
| 3 48 39 5 -12 35 28 12 4 937 947 8 -3 101 190 4 4 648 652 6 -11 172 162 5 5 234 228 3 -2 175 190 4 |
| 5 120 135 3 -10 156 166 5 6 287 300 4 -1 303 310 4 6 341 323 4 -9 10 23 20 7 469 462 5 0 185 185 4 |
| 8 38 14 7 -7 188 191 4 9 -38 25 7 2 234 240 4 |
| 10 200 212 4 -5 468 475 5 11 402 400 5 4 182 184 4 |
| 11 259 263 4 -4 153 121 3 12 -27 20 10 5 305 301 4 12 150 147 4 -3 44 33 4 13 85 86 6 6 175 178 4 |

| Tetrakis | (pent | afluc | roph | nyl) | -bet | a-oct | ach | loropor | phyr | in | | | : | Page | 16 |
|------------------------------|--|---|--|--|---|---|---------------------------------------|--------------------------------------|---|---|----------------------------|---|--|---|-------------------------------|
| 10 11 12 | 46 38 237 400 89 -47 | 51 55 225 408 99 16 | 7 7 4 5 6 8 | -4 -3 -2 -1 0 1 2 3 | 372 252 254 225 49 83 193 68 | 369 239 242 227 51 92 174 82 32 | 5 4 4 6 6 4 6 25 | 6 7 8 9 10 11 | 251 42 143 92 108 236 | 248 41 146 110 97 229 | 4 9 5 6 5 5 | 0 1 2 3 4 5 6 7 8 | 394 143 15 388 77 533 97 153 -15 | 394 134 392 72 527 93 169 20 | 12 14 4 5 4 14 |
| -8 -7 -6 -5 | -30 204 215 257 156 426 85 | 25 1 203 218 259 140 427 84 | 1444455 | 5 6 7 8 | 80 85 206 103 | 74 95 199 96 | 6 5 6 | 0 1 2 3 4 5 | 287 214 119 74 226 82 258 | 291 205 130 68 238 89 257 | 4445454 | 9 10 11 12 13 14 | 185 83 251 485 68 70 | 184 89 254 484 67 65 | 4 5 7 7 |
| -2 -1 0 1 2 3 | 220 189 80 220 419 625 134 | 214 199 87 214 420 641 151 | 4 5 4 5 6 4 | -4 -3 -2 -1 0 1 | 76 265 142 91 121 336 311 | 80 262 134 93 110 321 302 | 7556555 | 7 8 9 10 11 12 | 69 287 167 67 140 -31 | 64 284 154 69 136 | 6 4 7 5 11 | 6 0 1 2 3 | -1 23 376 492 87 445 | 28 385 484 81 454 | 9 |
| 6 7 8 9 | 714 237 -12 -23 -15 75 190 | 715 242 47 44 21 102 198 | 7 4 18 12 17 6 5 | 3 4 5 6 5 | 26 32 -2 147 16 | 38 36 19 138 1 | 13 12 25 5 | 6 0 1 2 3 4 5 | -5 37 199 142 248 197 230 | 35 196 141 245 194 230 | 84444444 | 5 6 7 8 9 10 11 12 | 491 484 226 176 261 -35 -19 425 | 485 475 230 175 257 7 5 435 | 5 4 4 4 8 12 |
| -7 | 12 49 319 270 345 | 65 331 258 330 | 9555 | 6 0 1 2 | -10 15 87 | 1 27 83 20 | 18 6 11 | 6 7 8 9 10 | 27 179 272 372 300 77 | 34 182 268 385 290 89 | 10 4 4 5 4 6 | 13 14 15 | 196 22 129 0 | 186 16 120 1 | 5 15 5 |
| -5 -4 -3 -2 -1 | 228 332 159 -21 357 175 | 235 349 158 5 354 192 | 13 | 3 4 5 6 7 | 32 133 -44 110 -15 57 | 127 7 116 43 63 | 5 8 5 17 8 | 12 13 6 | -44 -31 -4 257 | 0 50 1 250 | 8 11 | -11 -10 -9 -8 -7 -6 | 120 44 80 114 79 196 | 109 57 95 113 84 189 | 5 9 6 5 6 4 |
| 1 2 3 4 5 | 357 78 221 35 98 171 -50 77 | 349 81 216 39 102 168 0 94 35 | 4 5 4 9 5 4 6 6 25 | 6 0 1 2 3 4 5 6 | -9 291 264 97 56 160 182 -22 | 270 258 98 56 154 172 14 | 5 4 5 7 5 4 13 | 1 2 3 4 5 6 7 8 | 223 92 202 668 327 -31 79 69 | 218 74 205 695 323 11 87 69 434 | 4 4 6 4 8 4 6 5 | -5 -4 -3 -2 -1 0 1 2 | 232 40 232 245 187 214 229 876 103 | 250 242 249 179 206 226 866 85 | 3 3 3 8 3 |
| 10 5 -7 -6 | 174 13 126 18 | 163 1 134 | 5 5 16 | 7 8 9 | 124 94 -8 | 59 115 107 1 | 9 5 6 | 10 11 12 13 14 | 440 272 79 142 -27 | 447 278 94 144 23 | 5 6 5 13 | 4 5 6 7 8 9 | 102 112 309 141 67 223 | 85 104 315 134 80 232 | 3 4 4 5 |
| -2 -1 0 | 262 50 265 447 203 365 | 248 61 268 440 206 363 | 7 4 5 4 5 | 012345 | 99 59 -31 85 41 168 | 100 58 6 91 46 162 | 5 7 10 5 8 | 6 0 1 2 3 | -3 245 198 34 118 | 1 243 201 37 124 | 3744 | 10 11 12 13 14 15 | 443 177 288 268 254 -14 | 437 173 287 268 262 22 | 5 4 5 5 |
| 1 2 3 4 5 6 | 193 68 123 281 -37 462 120 | 199 81 131 287 13 465 127 | 4 6 5 4 8 5 5 | 6 7 8 9 10 | 236 73 115 92 283 | 237 59 111 68 266 | 6 5 6 5 | 5 6 7 8 9 | 112 -11 204 125 114 62 48 | 118 22 199 135 116 72 56 | 15 4 4 6 8 | -11 -10 -9 -8 | 117 106 -27 -28 | 1 113 92 9 50 | 12 11 |
| 8 9 5 - 6 - 5 | 52 70 14 42 193 | 58 79 1 72 179 | 8 7 9 5 | 0 1 2 3 4 5 | 76 139 40 143 -34 93 | 74 134 37 151 21 83 | 9495 | 11 12 13 14 | 124 39 62 331 -2 | 122 35 53 329 | 5 9 7 5 | -7 -6 -5 -4 -3 -2 | 67 127 27 83 109 85 209 | 50 120 22 82 116 65 206 | 10 5 4 |

| Tetrakis | (pent | taflu | oroj | phenyl) | -bet | a-oct | ach | loropor | phyr | in | | | 1 | Page | 17 |
|---|---|--|--|---|---|--|--|--|--|--|--|--|---|---|--|
| 0 1 2 3 4 4 5 6 7 8 9 10 11 11 12 13 | 521 691 145 135 103 5189 274 -32 108 | 535 240 710 107 141 1498 595 252 260 583 | 536343456440555 | -11 -10 -8 -6 -5 -10 -12 | 667 923 1632 2838 4245 1688 1793 | 67 39 86 166 24 278 14 384 413 168 190 170 592 | 78640 104844333435 | 6 7 8 9 10 11 12 13 14 6 | 71 439 43 154 378 328 104 44 118 7 | 94 437 16 163 364 321 82 52 134 1 | 557455595 | 0 1 2 3 4 5 6 7 8 9 10 11 12 13 | 161 121 514 492 97 663 285 326 -31 640 244 304 | 161 125 520 44 480 91 672 283 321 28 74 237 303 | 44565464486855 |
| 14 15 | 166 195 | 173 187 | 5 5 | 3 | 478 168 | 470 163 | 5 | - 8 - 7 | 297 336 | 304 326 | 4 | 6 | 10 | 1 | |
| 6 | 2 | 1 | | 5 6 | 160 340 | 152 330 | 3 | -6 -5 | 144 | 140 153 | 4 | -9 -8 -7 | 98 | 105 60 | 8 6 7 |
| -11 -10 -8 -7 -6 -5 -4 -3 -2 | -16 64 127 139 203 453 239 100 269 311 918 680 | 15 64 117 151 212 452 237 103 274 299 902 685 | 18 7 5 4 5 4 4 4 4 8 6 | 7 8 9 10 11 12 13 14 15 | 266 173 119 229 461 220 290 327 214 | 261 165 127 222 466 230 283 320 220 | 444454555 | 432101234567 | 271 -25 357 403 342 472 284 447 443 129 | 271 17 369 396 334 463 278 228 433 40 129 162 | 494444545574 | -76-54-52-1012345 | 61 444 213 34 381 105 533 168 221 191 184 344 203 | 442 203 387 387 325 1025 179 179 211 | 10 4 4 4 4 4 4 4 4 4 4 4 4 4 4 4 4 4 4 4 |
| 1 2 3 | 79 350 237 | 49 327 225 | 4 3 | -11 -10 -9 | 153 -16 236 | 145 14 239 | 17 4 | 8 9 10 | 148 350 315 | 353 322 | 4 | 6 | 240 212 | 233 212 | 4 |
| 5 6 7 8 | 471 61 504 213 148 | 451 72 497 216 158 | 5 5 4 4 | -8 -7 -6 -5 | 142 175 190 205 113 | 149 168 188 212 111 | 5 4 4 4 4 | 11 12 13 14 | 5 250 39 | 0 60 248 42 | 23 7 5 11 | 8 9 10 11 12 | -31 130 209 -45 52 | 20 121 209 12 61 | 10 5 4 6 9 |
| 9 10 | 304 114 | 310 95 | 4 | -3 -2 | 191 30 | 184 | \$ 8 | -10 | 8 119 | 1 115 | 5 | 6 | 11 | 1 | |
| 11 12 13 14 15 | 517 223 52 36 | 76 303 220 39 22 | 6 5 4 8 11 | -1 0 1 2 3 | 60 47 155 257 433 256 | 29 41 168 248 438 238 | 553343 | -9 -8 -7 -6 | 102 107 559 117 119 | 89 93 554 116 120 | 5 6 5 | -9 -8 -7 -6 | 60 90 95 124 374 | 72 70 99 116 381 | 8 6 5 5 |
| 6 | 3 | 1 | | 5 6 | 277 253 | 270 244 | 4 | -4 -3 | 228 122 | 227 128 572 | 4 | -4 -3 | 440 296 | 434 306 | 5 4 5 |
| -11 -10 -9 -8 -7 -6 -5 -4 -3 -10 | -17 127 295 130 48 234 431 259 254 52 107 453 | 11 132 291 130 52 229 440 270 251 48 21 110 | 17555845445453 | 7 8 9 10 11 12 13 14 15 | 195 748 298 97 253 208 161 214 -30 | 197 756 306 102 257 213 153 205 44 1 | 4 7 4 5 4 4 5 5 1 2 | -2 -1 0 1 2 3 4 5 6 7 8 9 | 568 44 -24 365 26 200 351 527 623 84 187 73 | 9 12 360 4 202 363 529 620 77 189 77 | 5694954565461 | -2 -10 12 34 56 78 90 | 108 -22 25 552 308 121 -19 354 -43 176 | 106 16 31 21 545 320 106 40 212 38 360 14 | 11 11 15 4 8 4 14 5 8 5 |
| 3 | 49 492 | 31 483 | 5 | -10 -9 | 85 207 | 89 193 | 6 | 11 12 13 | 236 -27 97 | 237 4 90 | 12 6 | 11 6 | 91 12 | 92 1 | 6 |
| 10 11 12 13 14 15 | 582 183 186 349 91 318 178 242 361 35 171 30 | 575 191 176 339 318 170 247 353 51 164 | 3 4 4 4 5 11 5 | -87 -54 -32 -01 23 45 | 76 223 129 124 108 4241 258 291 157 576 411 | 65 213 135 128 100 418 244 161 292 60 180 567 4215 | 6444433453544 | -10 -9 -8 -7 -6 -5 -4 -3 -2 | | 1 45 29 210 69 81 58 121 168 72 522 | 9 11 4 5 6 7 4 4 5 | -8 -7 -6 -5 -4 -2 -10 12 3 | 144 109 111 511 207 81 193 559 438 164 177 118 | 141 103 263 33 195 68 180 578 446 169 170 | 19 84 64 65 44 |

| Tetrakis (pentaf | luorophenyl |)-bets-oct | tachloropoz | phyrin | | Page 18 |
|---|---|--|--|---|---|---|
| 4 100 10 5 134 14 6 - 40 7 27 3 8 180 16 9 173 18 | 4 4 7 0 8 7 12 0 2 4 1 2 5 2 | -7 l 174 166 87 86 110 124 80 110 | 13 7 6 0 5 1 6 2 | -2 l 47 61 97 108 | 5 1 36 2 121 3 284 4 106 7 5 337 4 6 243 5 7 562 | 33 7 120 3 291 4 93 4 331 4 250 4 578 5 |
| 6 13 1 -7 33 3 -6 27 4 -5 332 33 | 2 12 7 1 13 8 | 57 47 143 145 52 58 254 252 112 118 25 25 | 7 3 4 8 5 4 6 5 7 12 8 | 108 105 237 240 214 202 -27 12 69 72 128 125 | 4 8 204 4 9 254 4 10 381 9 11 208 5 12 137 4 13 173 | 373 5 198 4 148 5 179 5 |
| -4 113 11 -3 17 2 | 0 16 | 150 142 -6 l | 5 9 10 11 | 218 220 171 167 24 8 1 | 4 14 118 4 2 7 2 | |
| -2 100 10 -1 44 4 0 98 8 | 0 8 | 193 193 | 4 13 | 116 106 | 5 5 -10 71 | 74 7 |
| 1 98 10 2 62 6 | 1 5 1 4 7 2 0 11 3 | 50 37 59 68 67 86 90 83 | 8 14 7 6 7 | 246 242 -1 l | 5 -9 -16 -8 61 -7 32 -6 57 | 58 6 52 11 70 7 |
| 5 20 3 6 47 5 | 9 14 5 7 8 6 | 133 115 71 76 | 6 1 | 106 108 180 181 35 43 | 4 -5 81 3 -4 117 7 -3 174 | 117 4 |
| 7 198 19 8 114 11 9 186 18 | 2 5 8 | 245 248 -17 30 188 196 | 14 3 | 51 20 65 63 | 7 -2 180 5 -1 21 | 187 4 27 9 |
| 6 14 1 | 10 11 | 3 40 108 101 | 26 5 | 51 62 -4 41 2 239 246 | 6 0 69 0 1 63 4 2 120 | 62 4 |
| -4 215 22 | 9 6 0 | -5 1 205 206 33 47 | 8 9 8 4 10 | 245 246 | 4 3 43 0 4 320 4 5 103 | 34 6 316 4 84 4 |
| -1 229 22 0 345 33 1 201 21 | 8 4 2 7 5 3 3 4 4 | -2 27 105 96 38 16 | 24 12 5 13 9 14 | 102 111 127 128 185 167 | 5 7 161 5 8 140 5 9 39 | 132 4 32 8 |
| 3 -36 4 137 14 5 117 12 6 7 | 2 6 5 5 9 6 6 5 7 0 5 8 3 23 9 8 6 10 | 61 58 260 253 128 119 102 106 64 28 149 155 -20 20 | 4 7 4 5 -9 3 7 -8 5 -7 | 101 100 127 148 | 11 389 12 278 6 13 246 5 14 129 13 15 356 | 9 391 5 8 286 4 3 228 5 5 145 5 8 343 5 |
| 6 15 l | 12 | 76 73 | 3 7 -5 | 159 161 32 4 48 51 | 9 | 3 l 3 126 5 |
| -3 169 15 -2 47 -1 352 3 0 250 24 1 108 12 2 287 27 3 109 11 4 379 3 5 142 14 | 10 9 0 1 1 1 1 1 1 1 1 1 1 1 1 1 1 1 1 1 | 7 -4 1 50 33 89 98 77 61 339 350 42 34 61 56 296 302 101 242 | 5 5 0 1 4 1 2 4 8 3 6 4 5 6 5 6 | 62 78 118 110 | 6 -10 12: 5 -9 8: 4 -8 8: 10 -7 22: 4 -6 -1: 5 -5 8: 3 -4 32: 4 -3 30: 4 -2 3: 4 -1 27: 7 0 12: | 5 88 6 70 6 8 216 4 8 13 15 1 83 5 7 319 4 5 307 4 9 261 4 |
| 0 97 9 1 59 9 2 53 0 3 216 2 4 21 5 | 93 6 10 12 8 11 32 8 12 13 5 13 39 15 4 13 7 | 263 269 340 359 47 64 -17 29 341 328 | 9 4 8 9 5 9 4 9 10 9 14 11 | 414 408 290 296 -15 52 149 139 253 264 19 47 | 5 1 22 4 2 5 15 3 2 4 4 80 4 5 25 15 6 20 15 7 38 | 1 218 4 8 32 7 7 33 10 3 805 7 2 235 4 2 197 4 0 377 4 |
| 7 -8 1 | 0 | 95 88 19 27 | 7 12 | | 9 3 10 15 | 3 29 10 6 167 4 |
| 1 66 2 133 1 3 64 4 59 5 181 1 | 55 6 3 56 6 4 50 5 5 86 7 6 85 7 7 80 5 8 | 32 15 121 95 508 514 115 112 33 1 73 73 272 274 117 120 | 5 4 -9 4 5 -8 2 4 -7 1 9 -6 2 5 -5 4 4 -4 | 61 87 108 127 30 45 64 60 130 130 17 16 61 74 | 10 11 33 8 12 6 5 13 12 12 14 3 7 15 17 4 7 | 7 57 7 5 126 5 5 9 11 |
| 7 -20 8 59 | 20 15 10 49 8 11 42 9 12 | 93 93 160 153 29 3 | 3 5 -2 3 5 -1 | 135 141 341 342 132 131 | 4 -10 -3 | 7 91 6 |

| Tetrakis (pentafl | uorophenyl |)-beta-oc | tachlo | ropor | phyri | in | | | F | age | 19 |
|---|---|--|---|---|---|--|--|--|---|---|--|
| -7 201 191 -6 114 130 -5 168 161 -4 126 123 -3 98 94 -2 45 38 -1 251 236 0 397 395 1 223 228 2 168 168 | 4 -10 4 -9 7 -8 4 -7 4 -6 3 -5 | 7 1 102 117 110 107 25 30 102 84 44 72 38 34 | 6 6 12 5 8 9 | 12 13 7 -8 -7 -6 -5 -4 -3 | 87 28 10 -26 129 108 18 50 | 94 | 6 12 13 5 5 14 8 9 | 0 1 2 3 4 5 6 7 8 9 | 94 178 482 59 107 -32 77 -25 88 -22 | 114 162 471 67 126 37 99 29 80 3 | 5 6 5 10 6 13 6 |
| 3 136 146 4 23 24 5 570 556 | 3 -3 10 -2 5 -1 | 132 135 327 350 217 210 | 4 | -2 -1 | 461 156 | 467 158 | 5 | 7 | 14 | 1 | |
| 6 341 343 7 169 157 8 278 271 9 -25 13 10 137 137 11 37 13 12 245 250 13 -33 18 209 223 | 4 0 4 1 4 2 11 3 4 4 9 5 4 6 | 213 219 425 469 295 294 220 225 53 60 234 227 113 88 750 760 185 187 | 4 7 5 4 6 4 6 4 7 4 6 | 0 1 2 3 4 5 6 7 8 9 10 | 127 -34 25 679 473 121 427 168 -39 163 88 | 143 20 11 687 473 116 417 168 32 163 106 | 4 8 11 6 5 4 5 4 8 4 6 | -3 -3 -10 12 3 4 5 6 | 139 190 50 99 113 -12 93 118 242 84 335 | 130 190 22 109 120 2103 110 246 70 324 | 55855965565 |
| -10 29 34 | 12 12 | 52 72 30 5 | 12 | 11 12 | 113 33 | 121 8 | 5 12 | 7 | 243 | 225 1 | 5 |
| -9 207 201 | . 5 13 | 326 315 127 123 | 5 | 7 | 11 | 1 | | -1 | 15 29 | 41 | 12 |
| -8 124 116 -7 122 116 -6 211 256 -5 84 56 -4 91 79 -3 90 87 -2 451 434 -1 263 257 | 4 7 5 -9 5 -8 5 -7 | 59 60 171 175 185 201 90 80 | 5 | -8 -7 -6 -5 -4 | 317 92 186 122 76 335 | 295 85 180 115 76 345 | 5 6 5 6 4 | 0 1 2 3 4 | 91 14 214 197 144 | 98 27 217 181 143 | 18 5 5 5 |
| 0 348 347 1 631 641 | 4 -5 | 217 207 199 193 | 4 | -2 -1 | 370 175 | 363 170 | 5 4 | 8 | - 8 | 1 | |
| 2 285 280 3 209 210 | 3 -3 | 416 403 259 267 | 7 4 | 0 | 155 | 151 26 | 10 | 3 | 92 55 | 93 32 52 | 6 7 7 |
| 4 85 91 5 386 381 6 37 44 | 4 -1 | 152 161 238 233 180 180 | 5 4 | 3 4 | -31 191 157 | 15 183 160 | 9 | 4 8 | 60 -7 | 1 | ' |
| 7 550 564 8 376 372 9 47 56 | 5 2 2 4 3 3 8 4 | 600 60: 277 28: 491 49: 72 5: | 6 8 4 5 5 | 5 6 7 8 | 96 72 294 182 | 92 47 296 173 | 5 6 4 | 0 1 2 | 153 48 26 | 140 52 31 | 5 9 11 |
| 11 539 537 12 81 99 | 7 6 6 | 245 244 298 310 | 4 4 | 9 10 | 261 99 | 270 115 | 6 | 34 | 84 60 66 | 107 66 73 | 6 7 7 |
| 13 38 38 14 62 83 7 6 1 | | 71 6: 92 8: 48 6: 98 11: | 5 5 5 8 | 11 7 | 284 12 | 268 1 | 5 | 6 7 8 | 167 76 51 | 160 84 66 | 5 6 9 |
| -10 53 | 5 12 13 | 24 1 133 12 | 7 14 | -7 -6 | 97 123 | 86 131 | 5 | 8 | -6 | 1 | , |
| -9 108 10: -8 81 10: -7 120 10: -6 207 19: -5 52 5: -4 64 7: -3 394 40: -2 114 11: -1 410 40: 0 299 28: 1 63 5: 2 454 45: | 8 6 6 7 8 8 4 9 9 9 9 9 9 9 9 9 9 9 9 9 9 9 9 9 | 7 9 1 137 13 79 8 90 9 224 22 32 2 126 13 43 1 229 13 | 4 5 1 6 1 4 1 10 4 4 9 7 | -5 -4 -3 -2 -1 0 1 2 3 4 5 6 | -26 215 150 182 -30 186 496 419 -25 -50 -27 | 1 226 146 187 13 191 499 412 6 86 | - 6 | 0 1 2 3 4 5 6 7 8 9 | 189 162 66 17 266 76 68 50 82 | 184 163 69 18 270 81 71 54 84 | 5 7 16 4 6 7 8 6 6 |
| 3 242 24 4 -22 | 040 | 200 19 179 18 | 5 4 | 7 8 | 291 139 | 296 136 | 5 | 8 | | 1 33 | 7 |
| 5 208 20 6 152 15 | 3 4 3 | 423 42 76 6 143 14 | 75 | 9 10 | -34 33 | 20 45 | | 0 1 2 | 35 239 | Q | 10 |
| 7 292 29 8 452 45 9 565 56 | 1 5 5 | 143 14 446 44 54 4 | 75 | 7 | | 1 | | 3 | 51 52 | 228 27 23 | 8 |
| 10 206 19 11 105 11 | 6 4 7 | 292 28 359 35 | 7 5 | - 5 - 4 | 73 91 | 65 78 | 6 | 5 6 | 109 109 | 89 90 51 | 5 |
| 12 629 60 13 120 11 14 -17 2 | 9 5 10 | 72 8 -42 1 30 3 | 6 6 1 8 9 12 | -3 -2 -1 | 49 57 280 | 43 284 | 6 | 7 8 9 | 5328 -24 | 345 26 | 5 |
| | | | | | | | | | | | |

| 10 | Tetrakis (pen | tafluoroph | enyl)-beta-oc | ctachloropo | phyrin | Page 20 |
|--|---|---|---|--|---|--|
| 8 - 4 2 157 165 4 0 301 284 4 -3 180 142 4 180 142 4 180 142 4 180 142 4 180 142 180 142 180 142 180 | 10 40 | 8 10 | -1 169 165 0 106 109 1 268 267 | 5 4 -3 9 4 -2 7 4 -1 | 341 342 4 257 266 4 28 10 11 | -5 85 82 6 -4 109 112 5 |
| 0 88 91 5 4 385 376 4 2 78 81 5 -1 133 127 4 1 38 22 9 5 288 296 4 7 131 107 107 188 6 3 51 13 67 2 325 325 4 6 39 29 7 4 110 127 4 4 1 2 33 1 18 6 1 90 130 5 5 8 27 24 29 7 4 110 127 4 4 1 2 33 1 18 6 1 90 130 5 5 8 27 28 5 5 8 124 1 116 1 15 5 9 8 18 6 6 222 22 22 4 1 117 5 9 9 218 222 4 7 113 106 4 4 141 138 4 7 242 246 4 11 116 115 5 9 80 88 6 6 2222 222 4 8 2255 220 4 12 256 243 5 9 10 39 12 8 7 115 5 4 8 255 220 4 12 256 243 5 9 10 39 12 8 7 115 5 4 9 357 14 9 11 14 47 34 10 11 2 98 114 8 5 11 27 14 13 8 -3 1 -8 41 62 10 8 4 1 12 12 12 14 18 5 11 27 14 13 8 -3 1 -8 41 62 10 8 4 1 12 12 12 12 14 18 5 11 27 14 13 8 -3 1 -8 41 62 10 8 4 1 112 12 12 14 18 5 11 27 14 13 8 -3 1 -8 41 62 10 8 4 1 112 12 12 14 18 5 11 27 14 13 1 10 6 4 4 9 -8 83 7 85 6 -9 18 1 21 29 8 114 14 14 14 14 14 14 14 14 14 14 14 14 | 8 -4 | 1 | 2 157 165 3 95 82 | 5 4 0 | 200 202 4 | -3 150 142 4 -2 113 111 4 |
| 8 -5 -8 41 62 10 8 4 1 13 13 139 144 5 0 64 49 -7 37 50 11 1 134 138 4 -5 356 334 5 -8 1 221 29 2 37 6 9 -4 67 59 6 -7 110 111 5 -8 27 8 14 3 199 194 4 -3 144 155 4 -6 184 190 4 -7 25 17 14 4 165 155 4 -2 573 377 4 -5 138 133 5 -6 275 283 5 5 192 191 4 -1 514 317 4 -4 45 9 9 -5 151 151 4 6 -33 6 9 0 83 80 5 -3 225 271 4 -4 76 6 76 5 7 145 142 4 1 117 121 4 -2 354 335 4 -5 252 255 4 8 110 105 5 2 126 128 4 -1 197 197 4 -2 192 255 4 8 110 105 5 2 126 128 4 -1 197 197 4 -2 192 3 16 10 54 38 8 4 63 58 4 1 4 30 30 7 1 -2 12 3 16 11 18 8 -2 1 8 194 190 4 5 85 90 6 2 152 153 4 8 -2 1 8 194 190 4 5 85 90 6 2 152 153 4 8 -2 1 8 194 190 4 5 85 74 5 4 5 8 8 4 8 8 8 8 8 8 8 9 10 10 10 10 10 10 10 10 10 10 10 10 10 | 1 38 2 325 3 100 4 399 5 119 6 93 7 242 8 233 9 37 10 35 11 82 | 28 9 325 4 5 1111 5 5 117 5 5 1100 5 4 220 4 4 129 11 85 | 4 385 376 5 288 296 6 39 297 7 294 298 8 87 88 9 218 221 11 116 111 12 256 244 13 107 107 14 47 56 | 6 4 2 6 9 7 4 5 6 5 6 7 6 5 5 8 7 6 5 5 9 7 6 11 4 10 12 | 132 127 4 120 124 4 151 147 4 70 88 6 113 106 4 124 121 4 80 88 6 -39 12 8 90 89 6 96 114 5 | 0 38 15 7 1 47 38 7 2 33 1 8 3 51 138 4 5 124 135 4 6 228 232 4 7 115 95 4 8 71 59 5 9 85 65 65 10 77 61 6 |
| 0 64 49 6 -6 83 78 6 -9 108 96 6 8 7 1 1 134 138 4 -5 356 354 5 -8 1 21 29 2 137 6 6 9 -4 67 59 6 -7 110 111 5 -8 27 8 14 3 199 194 4 -3 144 155 4 -6 184 190 4 -7 25 17 14 4 165 155 4 -2 373 377 4 -5 138 133 5 -6 275 263 5 5 192 191 4 -1 314 317 4 -4 45 9 9 -5 151 151 4 8 10 105 5 2 126 128 4 -1 197 197 4 -2 195 193 4 8 110 105 5 2 126 128 4 -1 197 197 4 -2 195 193 4 11 180 195 5 3 377 382 4 0 307 308 4 -1 -12 3 16 10 54 38 8 4 63 58 4 1 44 0 7 0 245 240 4 11 180 195 5 5 128 119 4 2 308 308 4 1 111 101 4 12 -8 32 23 6 88 103 5 3 586 590 6 2 152 153 4 8 -2 1 8 194 190 4 5 85 74 5 4 38 44 8 0 155 160 4 10 156 155 4 7 88 77 5 8 6 -9 10 220 226 13 10 13 3 177 5 5 8 1 137 161 4 11 76 64 6 8 212 208 4 7 41 35 3 164 173 4 1 138 194 190 4 5 85 74 5 4 38 44 8 1 138 194 190 4 5 85 74 5 4 38 44 8 1 138 194 190 4 5 85 74 5 4 38 44 8 1 138 194 190 4 5 85 74 5 4 38 44 8 1 138 194 190 4 5 85 74 5 4 38 44 8 1 138 194 190 4 5 85 74 5 4 38 44 8 1 138 194 190 4 5 85 74 5 4 38 44 8 1 138 194 190 4 5 85 74 5 4 38 44 8 1 138 194 190 4 5 85 74 5 4 38 44 8 1 138 194 190 4 5 8 15 15 15 10 10 10 10 10 10 10 10 10 10 10 10 10 | | | | | | 12 54 57 8 |
| 1 134 138 4 -5 356 354 5 -8 1 21 29 2 37 6 9 -4 67 59 6 -7 110 111 5 -8 27 8 14 3 199 194 4 -3 144 155 4 -6 184 190 4 -7 25 17 14 4 165 155 4 -2 373 377 4 -5 138 133 5 -6 275 263 5 5 192 191 4 -1 314 317 4 -4 45 9 9 -5 151 151 4 6 -33 6 9 0 83 80 5 -3 285 271 4 -4 76 76 5 7 145 142 4 1 117 121 4 -2 354 353 4 -3 252 255 4 8 110 105 5 2 126 128 4 -1 197 197 4 -2 195 193 4 9 361 337 5 3 377 382 4 0 307 308 4 -1 -12 516 10 5 4 38 8 4 63 58 4 1 44 0 7 0 -245 240 4 11 180 195 5 5 128 119 4 2 308 308 4 1 111 101 4 12 -8 32 23 6 88 103 5 3 586 590 6 2 152 153 4 8 -2 1 8 194 190 4 6 85 51 5 3 164 173 4 8 -2 1 8 194 190 4 6 8 51 5 3 164 173 4 8 -2 1 8 194 190 4 5 85 74 5 4 38 44 8 0 155 160 4 10 156 155 4 6 8 212 208 4 7 4 18 60 7 6 25 262 262 4 0 1 137 161 4 11 76 64 8 212 208 4 7 4 16 107 5 3 139 114 4 13 49 47 9 5 9 146 128 4 7 4 16 107 5 3 139 114 4 13 49 47 9 5 9 146 128 4 7 4 16 107 5 3 139 114 4 13 49 47 9 5 9 146 128 4 7 4 10 6 18 18 19 11 1 1 1 1 1 1 1 1 1 1 1 1 1 1 | | | -7 37 30 | 0 11 | | |
| 9 8 10 21 -8 39 31 11 8 5 1 8 8 1 10 431 424 5 -7 191 201 5 11 148 157 5 -6 285 285 5 -9 51 69 8 -8 -11 16 21 12 105 117 6 -5 68 42 6 -8 13 30 20 -7 51 67 9 13 67 61 7 -4 134 133 5 -7 59 38 7 -6 110 111 5 -3 104 88 5 -6 110 114 5 -5 37 40 9 8 -1 1 -2 80 70 5 -5 13 30 16 -4 43 55 8 -1 108 113 4 -4 29 34 11 -3 225 228 4 0 204 206 4 0 233 230 4 -3 110 112 5 -2 378 377 5 1 256 269 4 1 35 4 -2 203 207 4 -1 250 252 4 2 264 270 4 2 136 135 4 -1 49 33 7 0 103 97 4 3 3551 361 4 3 175 173 4 0 135 143 4 1 129 125 4 4 44 1 7 4 63 47 5 1 244 235 4 2 24 10 10 5 189 188 4 5 224 221 4 2 49 7 5 3 86 99 5 6 32 45 9 6 312 306 4 3 334 31 4 4 526 523 5 7 65 65 65 6 7 192 193 4 4 391 386 4 5 255 244 4 8 162 157 4 8 409 416 5 5 265 270 4 6 412 405 5 9 141 142 4 9 118 120 5 6 -29 11 9 7 313 313 4 10 74 86 6 10 111 131 5 7 149 147 4 8 359 360 5 11 232 226 4 11 -15 16 17 8 46 30 7 9 103 100 5 12 56 66 8 12 11 15 18 9 252 241 4 10 10 45 5 13 165 163 5 13 -22 22 15 10 390 371 5 11 80 84 6 -7 57 73 8 -9 159 147 5 -8 116 113 6 -8 31 55 12 8 6 1 -8 82 65 7 -6 81 78 6 -8 31 55 12 8 6 1 -8 82 65 7 -7 219 233 5 -8 116 113 5 -7 103 94 6 -7 57 73 8 -9 159 147 5 -6 81 78 6 -8 31 55 12 8 6 1 -8 82 65 7 -7 219 233 5 -6 117 189 5 | 1 134 2 2 379 4 1652 5 1652 6 -333 7 1410 9 3611 110 180 12 -8 8 -2 0 1555 1 137 2 298 3 139 4 825 5 34 | 138 4 194 4 155 4 195 4 105 5 337 5 338 5 195 2 1 160 4 161 4 161 4 161 4 161 4 161 4 161 4 161 7 | -6 83 77 -5 356 35 -3 144 31 -2 373 37 -2 373 37 1 117 12 1 126 12 3 377 38 5 128 11 6 88 10 7 115 11 8 194 13 10 156 15 11 78 194 12 12 124 12 13 49 4 8 2 1 | 8 6 -98 -76 -76 -76 -76 -76 -76 -76 -76 -76 -76 | 1 21 29 110 111 5 1184 190 4 1388 133 5 45 9 9 285 271 4 354 353 4 197 197 4 307 308 4 44 0 7 308 308 4 44 0 7 308 508 4 586 590 6 68 51 5 85 74 5 158 165 4 68 72 6 68 72 6 68 122 208 4 148 158 4 220 228 4 -24 25 13 34 38 16 | -8 27 8 14 -7 25 263 5 -5 151 151 4 -4 76 76 5 -3 252 255 4 -1 195 193 4 -1 195 193 4 -1 111 101 4 2 152 240 4 1 111 101 4 2 152 153 4 3 164 173 4 3 164 173 4 4 38 458 4 6 632 622 6 7 41 35 8 8 116 107 5 10 106 118 5 10 106 118 5 11 33 39 16 |
| 11 148 157 5 -6 285 285 5 -9 51 69 8 -8 -11 16 21 12 105 117 6 -5 68 42 6 -8 13 30 20 -7 51 67 9 13 67 61 7 -4 134 133 5 -7 59 38 7 -6 110 111 5 | 9 8 | 10 21 | -8 39 3 | 31 11 8 | 5 1 | 8 8 1 |
| -7 57 73 8 -9 159 147 5 -6 81 78 6 -8 31 55 12 8 6 1 -8 82 65 7 -5 128 113 5 -7 103 94 6 -7 219 233 5 -4 99 108 5 -8 67 58 6 -9 47 49 10 -6 171 189 5 | 11 148 12 105 13 67 8 -1 0 204 1 256 2 264 3 351 4 44 5 189 6 32 7 6 65 9 141 10 74 11 232 12 56 13 165 | 157 5 117 6 61 7 1 206 4 269 4 270 4 361 4 1 7 188 9 65 6 157 4 142 4 86 6 8 163 5 | -6 285 28 -6 28 -6 -5 68 4 -6 -5 68 8 4 -7 -7 -1 108 11 0 233 23 1 25 136 3 175 17 4 63 4 26 312 30 7 192 9 118 12 11 -15 11 11 11 -15 11 113 -22 14 354 32 | 85 5 -9 842 6 -8 85 5 -6 13 4 -3 13 4 -3 14 7 5 1 12 16 2 5 6 16 17 8 17 18 9 18 19 19 19 19 19 19 19 19 19 19 19 19 19 | 13 | -6 110 111 5 -5 37 40 9 -4 43 55 8 -3 225 228 4 -2 378 377 5 -1 250 252 4 0 103 97 1 1 129 125 4 2 24 10 10 3 86 99 5 4 528 523 5 5 255 244 405 5 7 313 313 4 8 359 360 5 10 144 150 5 11 261 270 5 13 -26 24 13 |
| | -7 57 -6 81 -5 128 -4 99 -3 139 | 73 8 78 6 113 5 108 5 153 4 | -8 31 5 -7 103 9 -6 67 5 -5 83 7 | 47 5 55 12 8 94 6 58 6 -9 73 6 -8 | 3 6 l· 47 49 10 | -8 82 65 7 -7 219 233 5 -6 171 189 5 -5 198 196 4 |

| Tetrakis(pentafluoro | phenyl)-beta-octachloroporphyrin | Page 21 |
|---|---|---|
| -3 91 89 5 -2 75 60 6 -1 20 214 4 0 52 44 6 1 233 229 4 2 33 27 9 3 52 32 7 4 34 12 9 5 74 67 6 6 278 291 4 7 208 208 4 8 500 511 5 9 208 219 4 10 37 55 10 11 98 6 12 12 27 21 | -4 82 91 6 0 119 106 5 -3 176 160 5 1 409 430 5 -2 15 3 17 2 96 86 5 -1 8 30 21 3 206 216 4 0 122 122 5 4 5 52 7 1 65 47 7 5 104 112 5 2 67 51 6 211 225 4 3 305 300 5 7 26 43 10 4 64 66 7 8 100 99 5 5 50 59 8 9 50 55 8 6 58 52 8 10 55 52 8 7 375 368 5 11 125 110 5 8 228 218 5 9 -1 1 | -7 36 32 11 -8 125 117 5 -5 57 45 8 -4 148 166 5 -3 181 182 4 -1 169 161 4 -1 93 70 5 0 115 99 4 1 222 218 4 2 374 364 4 3 144 145 4 4 197 197 4 5 49 57 7 6 165 161 4 7 442 443 5 8 81 75 6 9 -34 9 10 |
| 8 10 l | 2 177 161 5 1 241 246 4 | 9 -34 9 10 10 123 131 5 11 262 257 5 |
| -7 134 113 5 -6 68 76 6 -5 152 165 5 -4 146 136 5 -3 82 98 6 -2 118 128 5 -1 -7 0 20 0 225 226 4 1 156 157 4 2 52 44 6 | 1 1 2 2 3 2 165 156 4 0 247 245 5 3 54 36 7 1 69 83 7 4 182 179 4 2 267 263 5 5 260 252 4 3 339 346 5 6 83 50 6 4 -27 23 12 7 373 376 5 189 177 5 8 95 100 5 6 204 202 5 9 -8 33 22 9 -6 1 11 32 44 12 12 266 267 5 | 12 -14 35 19 13 281 275 5 9 3 1 -7 141 134 5 -6 74 77 7 -5 6 9 24 -4 147 140 5 -3 85 70 6 |
| 72 61 6 4 45 13 8 5 311 299 4 6 157 147 4 7 139 145 4 8 -25 1 12 9 127 132 5 10 126 111 5 11 294 290 5 | 1 79 68 6 2 40 40 10 9 0 1 3 28 18 13 4 86 81 6 -6 55 74 8 5 41 26 10 -5 -5 0 24 6 143 136 5 -4 -24 6 13 -3 194 189 4 9 -5 1 -2 56 7 7 0 84 101 6 0 114 78 5 | -2 28 4 12 -1 79 81 6 0 256 256 4 1 216 215 4 2 51 14 7 3 272 283 4 4 266 251 4 5 25 35 12 6 118 109 5 7 23 11 14 |
| 8 11 1 -6 55 61 8 -5 152 168 5 -4 103 102 5 -3 173 164 4 -2 33 37 10 -1 46 57 8 0 77 79 6 | 2 19 5 15 2 125 116 4 3 105 88 5 5 4 91 86 6 4 36 10 9 5 140 148 5 5 41 57 8 6 82 95 6 6 246 261 4 7 70 60 7 7 83 69 5 8 51 53 8 57 66 6 9 5 8 51 53 8 9 -16 18 15 | 8 38 25 10 9 -27 4 12 10 44 38 9 11 89 90 6 12 261 248 5 13 234 228 5 |
| 1 292 289 4 2 101 86 5 3 352 349 5 4 172 177 4 5 77 96 6 441 448 7 501 306 5 8 113 110 5 9 143 166 5 10 265 263 5 8 12 1 -5 54 9 11 -4 248 224 5 -3 117 123 5 -2 69 69 6 | 9 -4 1 10 25 13 14 10 27 11 11 -12 9 20 11 2 39 48 11 11 -12 9 20 11 2 39 48 11 11 -12 11 2 11 2 11 2 11 2 11 2 11 | -6 111 125 6 -5 -19 9 16 -4 81 77 6 -3 206 198 4 -2 21 7 15 -1 148 133 4 0 141 100 4 1 58 12 7 2 133 139 7 3 82 62 5 4 281 287 4 5 55 3 43 7 6 153 153 4 7 280 284 4 8 104 99 25 9 11 26 298 5 |
| -1 | 1 132 113 5 4 256 250 4 2 171 160 4 5 168 171 4 3 187 190 4 6 120 122 5 4 104 121 5 7 28 22 11 5 24 8 11 8 109 92 5 6 -20 33 13 9 344 380 5 7 27 4 12 10 105 124 5 8 91 98 6 11 462 450 5 9 -11 7 17 12 110 122 6 10 52 53 8 13 95 83 6 11 52 56 8 9 2 1 | 11 83 88 6 12 55 38 8 13 173 165 5 9 5 1 -7 88 104 6 -6 79 68 7 -5 95 87 6 -4 179 183 5 -3 280 281 4 -2 42 28 9 |

| trakis(| 07 | 209 | | 8 | 275 | 270 | 4 | - | | | | 7 | 292 | Page 286 | 5 |
|-----------------|------------------|------------|---------------|----------------|------------------|-----------------------|---------|------------|------------------|------------|-------------|------------|------------------|-----------------|------------------------|
| 0 1 | 57 28 | 164 114 | 4 | 9 10 | 52 | 32 151 31 85 | 8 | 9 | 13 | 1 | | 8 | 106 | 106 72 | 5 6 5 |
| 2 3 | 38 | 339 | 4 | 11 | 141 -24 90 | 31 | 14 | - 2 | 61 174 | 64 173 | 8 5 | 10 11 | 82 163 82 | 164 81 | 5 |
| 3 4 | 42 78 | 75 | 8 | 12 | | | 6 | - <u>1</u> | 172 | 165 | 5 | | | | Ü |
| 5 1 | 31 19 | 141 | 14 | 9 | 9 | 1 | | 1 2 | 75 27 | 71 18 1 | 6 | 10 | 1 | 1 | |
| 7 1 | 06 | 28 123 | 5 11 | - 6 - 5 | 55 57 | 65 51 | 7 | 3 | 85 -21 | 86 | 6 | -4 -3 | 94 76 | 107 52 | 6 |
| 8 9 3 | 32 | 326 | 5 | -4 | 40 | 36 | 8 | 5 | 152 | 165 | 5 | - 2 | 72 | 74 | 6 |
| | 26 89 | 35 176 | 13 5 | -3 -2 | 116 302 | 130 309 | 4 | 6 | 199 | 202 | 5 | -1 | 218 286 | 235 292 | 4 5 |
| 12 | 67 | 63 133 | 7 | - <u>1</u> | 37 16 | 30 10 | 9 16 | 9 | 14 | 1 | | 1 2 | 335 183 | 348 186 | 5 4 |
| | | | 3 | 1 | 107 | 106 | 5 | 2 | 28 | | 13 | 3 | 72 | 86 | ē |
| 9 | 6 | 1 | | 3 | 97 487 | 97 487 | 5 | 5 | 64 | 59 | 7 | 4 5 | 71 90 | 71 73 | 6 5 5 |
| -7 | 46 | 45 | 8 | 4 5 | 230 179 | 232 173 | 4 | 10 | - 4 | 1 | | 6 | 53 208 | 51 204 | 8 |
| - 5 | 39 | 21 | 10 10 | 6 | 54 | 44 72 | 7 | 2 | -36 | . 8 | 9 | 8 | 67 | 72 | 7 |
| -4 1 -3 | 83 | 154 73 | 5 | 7 8 | 100 291 | 283 | 5 5 | 3 | 66 52 61 | 51 70 | 7 8 7 | 9 10 | 38 219 70 | 53 216 56 | 10 5 |
| -2 2 | 104 | 268 86 | 4 5 | 9 10 | 260 121 | 265 127 | 5 5 | 5 6 | 61 55 | 50 37 | 7 | 11 | 70 | 56 | 6 |
| 0 | 39 | 45 58 | 9 | îĭ | 206 | 194 | 5 | | -3 | | • | 10 | 2 | 1 | |
| 2 | 57 77 | 76 | 6 5 | 9 | 10 | 1 | | 10 | | 1 | | - 5 | 51 | 46 | 9 |
| 3 4 1 | 91 134 | 91 127 | 5 4 | - 5 | -30 | 3 | 11 | 0 | - 9 45 | 43 | 21 8 | -4 -3 | 168 61 | 146 38 | 9 5 7 |
| 5 1 | 200 | 149 182 | 4 | -4 -3 | 86 78 | 102 74 | 6 | 3 | 56 128 | 112 | 8 5 | -2 -1 | 160 121 | 162 116 | 5 5 7 |
| 7 3 | 364 | 361 | 5 | - 2 | 21 | 5 | 13 | 4 | 134 | 112 131 | 5 | . 0 | 62 | 48 | 7 |
| 9 1 | 553 191 | 555 186 | 4 | 0 | 122 30 | 117 28 | 9 | 5 | 116 86 | 121 111 | 5 6 | 1 2 | 163 286 | 151 286 | 4 |
| 10 2 11 | 213 48 | 211 | 5 | 1 2 3 | 206 195 | 211 183 | 4 | 7 8 | 33 54 | 13 | 1 <u>1</u> | 3 | 310 84 | 305 81 | - 5 |
| 2 1 | 158 | 166 | 5 | 3 | 490 149 | 501 | 5 | 10 | - 2 | 1 | • | 5 | 40 204 | 28 205 | - 5 |
| 9 | 7 | 1 | | 5 | 287 | 123 303 | 3 | | _ | _ | | 7 | 105 | 91 | 5 |
| 7 | 84 | 80 | 7 | 6 | 95 82 22 | 100 97 | 6 | 0 | -21 12 | 3.1 | 14 19 | 8 9 | 84 147 | 78 137 | 6 5 |
| 6 5 1 | 29 194 | 37 187 | 13 5 | 8 | 22 -1 | 9 33 | | 3 | 27 54 | 9 27 | 12 | 10 11 | 3 9 85 | 25 80 | 11 6 |
| 4 | 63 | 72 274 | .7 | 10 | 178 | 170 | 5 | 5 | 146 219 | 131 219 | 5 | 10 | | 1 | |
| 2 | 59 | 34 | 6 | 9 | 11 | 1 | | 6 | 44 | 30 | 9 | | | | |
| 0 1 | 310 113 | 301 109 | 5 | - 5 | 134 | 131 | 5 | 7 8 | 116 120 94 | 112 128 | 5 5 | -5 -4 | 100 58 | 85 53 | 8 |
| 1 1 2 3 1 | 114 | 98 | 15 | -4 | 123 292 | 127 295 | 5 | 9 | 94 | 87 | 6 | - 3 - 2 | 118 80 | 101 81 | 5 6 |
| § 1 | 114 | 123 72 | 6 | -3 -2 -1 | 313 | 300 | 5 | 10 | -1 | 1 | | - <u>1</u> | 29 187 | 175 | 12 |
| 4 | 66 29 | 20 | 11 | 0 | -31 271 | 270 | 4 | 0 | 46 | 3 | 9 | 1 | 313 | 312 | 6 12 4 4 5 |
| 7 | 105 159 | 85 160 | 5 | 1 2 3 | 164 227 | 163 214 | 4 | 1 2 | 117 177 | 138 174 | 4 | 3 | 133 118 | 107 129 | 5 |
| 8 | 67 290 | 72 285 | 7 | 3 | 48 242 | 68 254 | | 3 | 94 | 69 15 | 5 11 | 5 | 90 207 | 85 220 | 5 4 7 |
| 10 | 105 | 115 | 5 | 5 | 316 | 318 | 5 | 5 | 31 43 | 21 | 9 | 6 7 | 57 153 | 57 160 | 7 |
| $\frac{11}{12}$ | 63 56 | 57 9 | 8 | 6 7 | 289 66 | 289 62 | 6 | 6 7 | 29 131 | 141 | 12 5 | 8 | 110 | 108 | 5 |
| 9 | 8 | 1 | | 8 | 132 19 | 138 | | 8 | 78 26 | 76 19 | 6 14 | 10 | -6 181 | 18 188 | 5 |
| -6 | 13 | 9 | 20 | 9 | 12 | 1 | | 10 | -40 | 5 | 9 | 11 | - 15 | 56 38 | 9 19 |
| - 5 | 58 | 32 | 8 | | | | | 10 | 0 | 1 | | | | | 13 |
| -4 -3 | 51 46 | 51 25 | 8 | -3 -2 | 48 62 | 46 | 9 | -4 | 60 | 31 | 8 | 10 | | 1 | _ |
| - 2 | 72 178 | 38 181 | 6 | -1 0 | 170 58 | 171 50 | . 5 | -3 | 38 33 | 64 39 | 11 11 | -5 -4 | 58 118 | 62 135 | 8 5 |
| 0 | 66 | 58 | 6 | 1 | 151 | 148 | | - 1 | 51 | 19 | 8 | - 3 | 90 | 88 | 6 |
| 1 2 | 262 214 43 | 274 220 | 4 | 3 | 84 21 | 90 28 | 12 | 0 | 89 168 | 54 181 | 4 | -2 -1 | 42 72 | 15 72 | 7 |
| 3 | 43 19 | 19 | 8 14 | 5 | 49 - 28 | 61 | 8 | 2 | 63 76 | 62 57 | 7 6 | 0 | 49 191 | 48 186 | 4 |
| 5 | 16 | 7 | 15 | 6 | 24 | 110 | 14 | 4 5 | 55 104 | 54 93 | 7 | 2 3 | 138 305 | 114 300 | 4 |
| 6 | 48 196 | 43 198 | 8 | á | 103 117 | 120 | 5 | 6 | 128 | 138 | 5 | i | 148 | 140 | |

| rakis | (pent | aflu | oropl | aenyl) | -beta | -oct | achlo | ropor | phyri | n | | | age 23 |
|---|---|--|---|--|--|--|---|--|--|--|--|--|--|
| 5 6 7 8 9 10 11 12 10 | 87 122 137 84 96 -20 188 75 | 76 125 111 83 100 14 196 87 1 | 6 5 6 6 15 7 | 2 3 4 5 6 7 8 9 10 | 70 350 165 221 144 110 47 -18 -18 | 60 356 154 228 135 108 48 16 12 | 5 4 4 5 7 16 17 | 11 0 1 2 3 4 5 6 7 8 | 0 43 32 72 54 165 26 135 56 | 1 | 5 6 7 | 52 34 88 43 149 71 76 64 154 103 106 124 -23 | 60 9 \$8 12 79 6 20 8 158 5 59 7 49 6 135 5 98 6 108 6 122 6 122 15 |
| -4 -3 | -31 21 | 6 | 12 16 | -4 | 111 40 90 | 126 22 | 5 10 | 11 | 1 | 1 | | | |
| -21-0123456789011 | 193 54 47 51 101 175 2312 186 186 196 29 | 157 33 101 37 41 78 161 65 309 182 191 88 197 | 15 15 15 15 15 15 15 15 15 15 15 15 15 1 | -\$2 -10 12 5 4 5 6 7 8 9 10 | 90 46 112 329 60 42 127 68 47 202 143 78 | 22 84 77 5 122 330 47 137 73 47 200 153 70 | 6685569579557 | -1 0 1 2 3 4 5 6 7 8 9 | 84 89 54 62 87 194 40 96 37 104 45 | 83 6 17 6 44 8 43 7 89 6 189 5 16 10 93 6 12 10 96 6 28 10 | 11 -32 -10123456789 | 117 160 74 37 35 64 101 347 72 32 77 | 1 122 6 5 7 7 9 35 11 7 7 7 41 7 98 5 5 7 7 1 31 12 7 7 31 12 7 |
| 10 | 6 | 1 | | 10 | 10 | 1 85 | 6 | -2 -1 | 119 46 | 111 5 43 9 | 11 | 7 | 1 |
| 5432101234567 | 26 106 91 55 90 128 239 32 259 258 48 233 120 | 52 115 75 44 89 125 125 25 25 25 25 25 25 25 25 25 25 25 25 2 | 13 6 6 7 6 5 4 10 4 4 8 4 5 | | 80 106 226 42 80 117 82 248 76 55 483 97 189 | 101 226 38 105 115 253 41 454 490 186 | 549656468665 | 0 12 3 4 5 6 7 8 9 | 36 -21 142 96 47 37 64 -12 30 | 35 11 0 14 116 5 78 5 36 9 30 10 79 7 44 20 24 12 84 6 | -2 -1 0 1 2 3 4 5 6 7 8 9 | 42 36 21 30 34 61 119 58 157 56 46 -10 | 29 9 37 11 57 13 27 12 24 11 31 7 124 5 42 8 143 5 31 7 54 10 27 21 |
| 8 | 90 145 | 96 152 13 | 6 | 10 | | | 6 | -1 | 27 32 | 30 13 | 11 | 8 | 1 |
| 10 11 10 -5 -4 -3 -2 -1 0 | 25 38 121 277 115 119 114 | 256 1 32 43 114 279 110 114 | 14 11 5 5 5 5 5 | -2 -10 12 34 56 78 | 88 -20 70 172 193 10 -6 50 236 163 203 | 66 11 47 169 198 18 51 238 161 196 | 13 5 5 20 23 8 5 5 | 1 2 3 4 5 6 7 8 9 | 186 90 112 72 -18 107 116 208 42 25 | 101 12 169 5 86 6 119 5 11 16 101 5 116 5 203 9 26 15 | -2 -10 12 34 56 78 | 110 47 82 72 78 240 68 175 41 160 68 | 85 6 42 8 88 6 86 7 70 6 243 4 66 6 171 5 51 10 145 5 64 7 |
| 2 | 288 175 | 279 165 | 4 | 10 | | _ | 7 9 | -3 | _ | | 11 | . 9 | 1 |
| 5 6 7 8 9 10 11 | 58 346 85 61 286 -16 39 230 | 10 351 84 10 291 29 224 | 5 6 7 1 5 17 | -1 0 1 2 3 4 5 6 | 244 244 36 135 109 -20 64 103 | 256 123 123 123 13 103 103 | 5 11 5 5 13 7 | -2 -1 0 1 2 3 4 5 | 204 230 193 81 155 51 154 78 | 231 5 191 5 76 7 150 5 43 8 43 7 154 5 41 10 | -1 0 1 2 3 4 5 6 7 | -14 157 51 106 -24 -3 77 61 68 | |
| - 5 | 69 | 66 | 3 6 | 1 2 | 65 | 5 | 1 7 | 7 8 | -16 | 4 18 | 8 1 | | |
| -4 -3 -2 -1 0 | 56 56 59 68 142 110 | 5 3 15 | 8 8 2 11 1 7 8 6 4 5 | 2 3 4 5 6 7 | 117 78 240 72 73 76 | 120 7 25 7 7 | 5 5 9 7 5 7 | 10 1 -3 | 131 69 1 5 88 | 53 8 | 0 1 2 3 | 86 59 -6 | 98 6 56 8 27 24 |

| Tetraki: | s (pen | tafl | 1010 | phenyl) | -bet | a-oc1 | achl | огороз | phyr | in | • | | | Page | 24 |
|----------|-----------|-----------|---------|---------|----------|----------|------|--------|-----------|-----------|----|-----|------------|------------|--------|
| 4 | 20 130 | 5 132 | 15 | 3 | 44 | 41 91 | 9 | 12 | 5 | 1 | | 4 5 | 222 139 | 228 125 | 5 5 |
| 6 | 49 | 21 | 5 | 5 | 94 39 | ī | 10 | 2 | 25 83 | 17 90 | 15 | 6 | - 6 | 3 | 25 |
| 11 | 11 | 1 | | 12 | 4 | 1 | | 4 5 | 39 182 | 19 185 | 12 | 12 | 7 | 1 | |
| 2 | 138 25 | 132 10 | 5 14 | 2 | 68 59 | 82 14 | 7 | 6 | 110 | 118 | 6 | 3 | 152 108 | 154 93 | 5 6 |
| 4 | 30 | | 12 | 4 5 | 50 29 | 51 29 | 13 | 12 | 6 | 1 | | 5 | 86 | 74 | 6 |
| 12 | 3 | 1 | | 6 | 13 | - 5 | 17 | 2 | 62 | 53 | 7 | | | | |

 $\label{Table 1. Final Heavy Atom Parameters for} Tetrakis (pentafluorophenyl) octachloroporphina to Zinc(II) \cdot 6 (C_6H_4Cl_2).$

x,y,z and $U_{eq}{}^a imes 10^4$

| Atom | x | y | z | U_{eq} or B | Pop |
|------|---------|----------|-----------|-----------------|-----|
| Zn | 0 | 0 | 0 | 291(4) | |
| N | 1015(4) | 231(4) | 95(9) | 268(20) | |
| C1 | 2135(5) | 108(6) | 626(10) | 286(26) | |
| C2 | 1542(5) | -246(5) | 180(10) | 297(26) | |
| C3 | 1475(5) | -943(5) | -120(11) | 264(25) | |
| C4 | 1296(6) | 861(6) | 338(10) | 287(28) | |
| C5 | 1989(6) | 776(6) | 720(10) | 326(28) | |
| Cl1 | 2909(2) | -235(2) | 1075(3) | 484(8) | |
| C12 | 2544(2) | 1359(2) | 1352(3) | 506(9) | |
| C6 | 2123(5) | -1340(6) | -259(11) | 325(30) | |
| C7 | 2322(6) | -1829(6) | 564(11) | 346(29) | |
| F7 | 1935(4) | -1938(4) | 1575(7) | 547(20) | |
| C8 | 2900(7) | -2243(7) | 393(14) | 524(39) | |
| F8 | 3050(4) | -2723(4) | 1207(8) | 714(24) | |
| C9 | 3288(7) | -2138(8) | -611(14) | 513(39) | |
| F9 | 3850(4) | -2525(5) | -810(8) | 767(27) | |
| C10 | 3140(6) | -1612(7) | -1458(14) | 533(41) | |
| F10 | 3529(4) | -1512(5) | -2431(8) | 743(25) | |
| C11 | 2554(6) | -1232(5) | -1240(12) | 329(28) | |
| F11 | 2406(4) | -770(4) | -2088(7) | 549(20) | |

Table 1. (Cont.)

| Atom | x | y | ż | U_{eq} or | В | Pop [†] |
|------|----------|----------|----------|-------------|---|------------------|
| C13 | 4428(9) | 6030(8) | 1705(11) | 1957(66) | | 0.50 |
| Cl4 | 3904(6) | 4528(8) | 1753(12) | | | 0.50 |
| C15 | 5339(3) | 910(4) | 74(9) | 2172(35) | | |
| C16 | 4712(11) | 1149(11) | 2927(13) | 2586(92) | | 0.47 |
| C17 | 4300(10) | 2220(11) | -277(23) | 3762(115) |) | 0.53 |
| C31 | 4769 | 1516 | 620 | 1226 | | 0.47 |
| C32 | 4520 | 1628 | 1741 | 1229 | | 0.47 |
| C33 | 4060 | 2202 | 1935 | 1230 | | 0.47 |
| C34 | 3895 | 2612 | 964 | 1226 | | 0.47 |
| C35 | 4159 | 2490 | -201 | 1229 | | 0.47 |
| C36 | 4608 | 1930 | -396 | 1230 | | 0.47 |
| C41 | 4845 | 1295 | 1233 | 1225 | | 0.53 |
| C42 | 4449 | 1874 | 964 | 1229 | | 0.53 |
| C43 | 4104 | 2128 | 2010 | 1230 | | 0.53 |
| C44 | 4173 | 1816 | 3130 | 1225 | | 0.53 |
| C45 | 4602 | 1219 | 3265 | 1229 | | 0.53 |
| C46 | 4933 | 976 | 2264 | 1230 | | 0.53 |
| C14 | 5068 | 5371 | 1677 | 3.5 | • | 0.75 |
| C15 | 4797 | 4709 | 1695 | 3.5 | • | 0.75 |
| C16 | 5239 | 4163 | 1670 | 3.5 | • | 0.75 |

Table 1. (Cont.)

| Popt | U_{eq} or B | z | $oldsymbol{x} oldsymbol{y}$ | | Atom |
|------|-----------------|------|-----------------------------|------|------|
| 0.75 | 3.5 * | 1626 | 4262 | 5961 | C17 |
| 0.75 | 3.5 • | 1609 | 4923 | 6215 | C18 |
| 0.75 | 3.5 * | 1634 | 5469 | 5773 | C19 |
| 0.25 | 3.5 * | 1727 | 5072 | 4657 | C21 |
| 0.25 | 3.5 * | 1716 | 5782 | 4555 | C22 |
| 0.25 | 3.5 | 1726 | 6237 | 5106 | C23 |
| 0.25 | 3.5 * | 1746 | 5977 | 5775 | C24 |
| 0.25 | 3.5 * | 1756 | 5255 | 5863 | C25 |
| 0.25 | 3.5 * | 1746 | 4818 | 5311 | C26 |

 $^{^{}a}$ $U_{eq} = \frac{1}{3} \sum_{i} \sum_{j} [U_{ij}(a_{i}^{*}a_{j}^{*})(\vec{a}_{i} \cdot \vec{a}_{j})]$

^{*} Isotropic displacement parameter, B

[†] Population Parameter, if different from 1.0

 $\label{eq:Table 2. Anisotropic Displacement Parameters for $$ Tetrakis(pentafluorophenyl)octachloroporphinato $Zinc(II) \cdot 6(C_6H_4Cl_2)$. }$

| Atom | <i>U</i> ₁₁ | U_{22} | U_{33} | U_{12} | U_{13} | U_{23} |
|------------|------------------------|-----------|-----------|------------|------------|-----------|
| Zn | 246(8) | 246(8) | 381(15) | 0 | 0 | 0 |
| N | 262(45) | 193(44) | 348(55) | -13(38) | -37(47) | 31(47) |
| C1 | 265(59) | 302(70) | 290(62) | 30(52) | -71(51) | -5(53) |
| C2 | 214(54) | 337(62) | 341(72) | 12(47) | 82(54) | 104(56) |
| C3 | 299(61) | 255(59) | 239(64) | 55(49) | 52(58) | 46(55) |
| C4 | 337(68) | 274(64) | 251(71) | -58(52) | -36(51) | -9(51) |
| C5 | 317(68) | 269(63) | 393(72) | -40(56) | -23(58) | -8(56) |
| Cl1 | 325(17) | 409(18) | 719(23) | 64(14) | -208(17) | -66(17) |
| C12 | 378(18) | 370(18) | 769(25) | 10(15) | -259(19) | -79(18) |
| C6 | 181(55) | 290(61) | 503(85) | 31(48) | 30(57) | -65(59) |
| C7 | 336(69) | 372(70) | 329(71) | 42(58) | -33(58) | -11(59) |
| F 7 | 509(48) | 603(51) | 529(45) | 31(38) | 27(41) | 112(41) |
| C8 | 469(86) | 385(80) | 718(113) | 121(71) | -235(82) | -134(74) |
| F8 | 797(59) | 461(48) | 885(65) | 288(45) | -309(53) | 66(47) |
| C9 | 315(74) | 569(97) | 654(99) | 161(72) | -90(74) | -204(84) |
| F9 | 407(46) | 766(60) | 1128(75) | 328(45) | -143(46) | -271(57) |
| C10 | 272(71) | 624(94) | 702(109) | -27(69) | 196(75) | -262(88) |
| F10 | 529(52) | 879(64) | 822(59) | -3(45) | 305(50) | -253(54) |
| C11 | 272(63) | 260(63) | 455(74) | -66(53) | -46(63) | -31(60) |
| F11 | 586(50) | 543(48) | 519(48) | -5(43) | 156(41) | 18(42) |
| C13 | 3244(222) | 1771(143) | 855(85) | 799(149) | 664(122) | -94(89) |
| Cl4 | 901(81) | 2158(150) | 1174(90) | -365(93) | 261(71) | -130(98) |
| C15 | 1313(57) | 1979(76) | 3224(114) | -271(55) | 510(69) | -1399(84) |
| C16 | 3216(276) | 3402(265) | 1139(111) | -2200(230) | -667(138) | 947(142) |
| C17 | 2496(199) | 3595(275) | 5194(352) | -1801(195) | -2386(228) | 3455(273) |
| C31 | 1002 | 925 | 1751 | 260 | 5 | -205 |
| C32 | 1368 | 1214 | 1105 | -116 | -302 | 437 |
| C33 | 1272 | 1561 | 857 | -193 | 286 | -264 |
| C34 | 1002 | 925 | 1751 | 260 | 5 | -205 |
| C35 | 1368 | 1214 | 1105 | -116 | -302 | 437 |
| C36 | 1272 | 1561 | 857 | -193 | 286 | -264 |

Table 2. (Cont.)

| Atom | U_{11} | U_{22} | U_{33} | U_{12} | U_{13} | U_{23} |
|------|----------|----------|----------|----------|----------|----------|
| C41 | 1156 | 1426 | 1093 | -67 | 334 | -410 |
| C42 | 1426 | 1368 | 893 | -222 | -200 | 377 |
| C43 | 1060 | 867 | 1763 | 250 | -162 | 16 |
| C44 | 1156 | 1426 | 1093 | -67 | 334 | -410 |
| C45 | 1426 | 1368 | 893 | -222 | -200 | 377 |
| C46 | 1060 | 867 | 1763 | 250 | -162 | 16 |

 $U_{i,j}$ values have been multiplied by 10^4 The form of the displacement factor is: $\exp{-2\pi^2(U_{11}h^2a^{*^2}+U_{22}k^2b^{*^2}+U_{33}\ell^2c^{*^2}+2U_{12}hka^*b^*+2U_{13}h\ell a^*c^*+2U_{23}k\ell b^*c^*)}$

 $\label{eq:Table 3. Complete Distances and Angles for $$ Tetrakis(pentafluorophenyl)octachloroporphinato $Zinc(II) \cdot 6(C_6H_4Cl_2).$$

| Dista | ance(Å) | Dista | Distance(Å) | | | | |
|----------------------|----------------|----------|-------------|--|--|--|--|
| Zn -N | 2.032 | C23 -C24 | 1.401 | | | | |
| N -C2 | 1.390(13) | C24 -C25 | 1.419 | | | | |
| N -C4 | 1.371(14) | C25 -C26 | 1.373 | | | | |
| C1 -C2 | 1.431(15) | Cl5 -C31 | 1.728 | | | | |
| C1 -C5 | 1.337(15) | Cl5 -C41 | 1.758 | | | | |
| C1 -Cl1 | 1.722(11) | Cl6 -C32 | 1.640 | | | | |
| C2 -C3 | 1.405(15) | C17 -C42 | 1.541 | | | | |
| C3 -C6 | 1.490(15) | C31 -C32 | 1.334 | | | | |
| C3 -C4 | 1.401(16) | C31 -C36 | 1.407 | | | | |
| C4 -C5 | 1.423(16) | C32 -C33 | 1.449 | | | | |
| C5 -C12 | 1.716(12) | C33 -C34 | 1.367 | | | | |
| C6 -C7 | 1.365(16) | C34 -C35 | 1.393 | | | | |
| C6 -C11 | 1.378(16) | C35 -C36 | 1.416 | | | | |
| C7 -F7 | 1.354(14) | C41 -C42 | | | | | |
| C7 -C8 | 1.399(18) | C41 -C46 | | | | | |
| C8 -F8 | 1.324(16) | C42 -C43 | | | | | |
| C8 -C9 | 1.35(2) | C43 -C44 | | | | | |
| C9 -F9 | 1.349(17) | C44 -C45 | | | | | |
| C9 -C10 | 1.41(2) | C45 -C46 | 1.355 | | | | |
| C10 -F10 | 1.320(16) | | | | | | |
| C10 -C11 | 1.381(18) | | | | | | |
| C11 -F11 | 1.324(14) | | | | | | |
| Cl3 -C14 | 1.792 | | | | | | |
| Cl3 -C26 | | | | | | | |
| Cl4 -C15 | 1.779 | | | | | | |
| Cl4 -C21 | 1.813 | | | | | | |
| C14 -C15 | 1.395 | | | | | | |
| C14 -C19 | 1.389 | | | | | | |
| C15 -C16 | | | | | | | |
| C16 -C17 C17 -C18 | 1.422 1.381 | | | | | | |
| C17 -C18 | | | | | | | |
| C16 -C19 | | | | | | | |
| C21 -C22 | 1.368 | | | | | | |
| C21 -C26 | 1.308 | | | | | | |
| UZZ -UZ3 | 1.033 | | | | | | |

Table 3. (Cont.)

| Angle | ·(°) | An | gle(°) | | |
|---------------|-----------|---------------|-----------|--|--|
| N -Zn -N | 90.2 | C10 -C11 -C6 | 123.8(11) | | |
| N -Zn -N | 174.1 | F11 -C11 -C6 | 121.0(10) | | |
| Zn -N -C2 | 125.2 | F11 -C11 -C10 | 115.2(11) | | |
| Zn -N -C4 | 42.4 | C15 -C14 -Cl3 | 113.5 | | |
| C4 -N -C2 | 106.9(8) | C19 -C14 -Cl3 | 126.2 | | |
| C5 -C1 -C2 | 108.8(10) | C19 -C14 -C15 | 120.2 | | |
| Cl1 -C1 -C2 | 128.2(8) | C14 -C15 -Cl4 | 123.8 | | |
| Cl1 -C1 -C5 | 122.9(9) | C16 -C15 -C14 | 117.5 | | |
| C1 -C2 -N | 107.4(9) | C16 -C15 -C14 | 118.7 | | |
| C3 -C2 -N | 124.2(9) | C17 -C16 -C15 | 121.2 | | |
| C3 -C2 -C1 | 128.4(10) | C18 -C17 -C16 | 118.8 | | |
| C6 -C3 -C2 | 116.5(9) | C19 -C18 -C17 | 120.0 | | |
| C4 -C3 -C2 | 126.5(10) | C18 -C19 -C14 | 121.1 | | |
| C4 -C3 -C6 | 116.9(10) | C22 -C21 -C14 | 117.6 | | |
| C3 -C4 -N | 122.4(10) | C26 -C21 -Cl4 | 122.9 | | |
| C5 -C4 -N | 109.4(9) | C26 -C21 -C22 | 119.5 | | |
| C5 -C4 -C3 | 128.0(10) | C23 -C22 -C21 | 121.3 | | |
| C4 -C5 -C1 | 107.1(10) | C24 -C23 -C22 | 119.1 | | |
| Cl2 -C5 -C1 | 122.9(9) | C25 -C24 -C23 | 118.3 | | |
| Cl2 -C5 -C4 | 129.7(9) | C26 -C25 -C24 | 121.3 | | |
| C7 -C6 -C3 | 122.5(10) | C21 -C26 -Cl3 | 128.3 | | |
| C11 -C6 -C3 | 121.2(10) | C25 -C26 -Cl3 | 111.2 | | |
| C11 -C6 -C7 | 116.4(11) | C25 -C26 -C21 | 120.4 | | |
| F7 -C7 -C6 | 119.2(10) | C32 -C31 -Cl5 | 131.5 | | |
| C8 -C7 -C6 | 123.0(11) | C36 -C31 -C15 | 105.3 | | |
| C8 -C7 -F7 | 117.8(11) | C36 -C31 -C32 | 123.2 | | |
| F8 -C8 -C7 | 119.8(12) | C31 -C32 -Cl6 | 123.2 | | |
| C9 -C8 -C7 | 118.2(13) | C33 -C32 -Cl6 | 117.8 | | |
| C9 -C8 -F8 | 121.9(13) | C33 -C32 -C31 | 119.1 | | |
| F9 -C9 -C8 | 120.1(13) | C34 -C33 -C32 | 119.0 | | |
| C10 -C9 -C8 | 121.9(13) | C35 -C34 -C33 | 121.4 | | |
| C10 -C9 -F9 | 118.0(12) | C36 -C35 -C34 | 119.8 | | |
| F10 -C10 -C9 | 121.1(12) | C35 -C36 -C31 | 117.5 | | |
| C11 -C10 -C9 | 116.5(12) | C42 -C41 -C15 | 119.7 | | |
| C11 -C10 -F10 | 122.3(12) | C46 -C41 -Cl5 | 110.3 | | |
| | | | | | |

Table 3. (Cont.)

Angle(°)

| C46 -C41 -C42 | 129.9 |
|---------------|-------|
| C41 -C42 -C17 | 129.9 |
| C43 -C42 -C17 | 117.8 |
| C43 -C42 -C41 | 112.1 |
| C44 -C43 -C42 | 121.2 |
| C45 -C44 -C43 | 120.4 |
| C46 -C45 -C44 | 118.5 |
| C45 -C46 -C41 | 118.0 |

Table 4. Intermolecular Distances Less Than 3.5 Å for Tetrakis(pentafluorophenyl)octachloroporphinato $Zinc(II) \cdot 6(C_6H_4Cl_2)$.

| Dista | ance(Å) | Distance(Å) | | | | |
|----------------------|-----------|-------------|-------|--|--|--|
| C2 -C14 | 3.487(17) | C24 -C34 | 2.952 | | | |
| C4 -C17 | | | | | | |
| Cl1 -F10 | 3.122(9) | | | | | |
| Cl2 -C33 | 3.441 | | | | | |
| Cl2 -C43 | 3.467 | | | | | |
| Cl2 -F8 | | | | | | |
| C7 -F10 | | | | | | |
| F7 -C24 | 3.463 | | | | | |
| F7 -C33 | | | | | | |
| F7 -C34 | 3.257 | | | | | |
| F7 -C43 | 3.133 | | | | | |
| F7 -C44 | 3.268 | | | | | |
| F7 -F9 | 3.408(11) | | | | | |
| F7 -F10 | 3.344(11) | | | | | |
| C8 -F10 | | | | | | |
| | 3.401 | | | | | |
| F8 -C35 | 3.199 | | | | | |
| F8 -C10 | 3.125(16) | | | | | |
| F8 -F10 | 2.985(12) | | | | | |
| F8 -C11 | 3.165(14) | | | | | |
| F8 -F11 | 2.970(11) | | | | | |
| F9 -C24 | | | | | | |
| F9 -Cl4 | | | | | | |
| F9 -C36 | | | | | | |
| F10 -C46 | | | | | | |
| F11 -Cl6 | 3.49(2) | | | | | |
| F11 -C32 | | | | | | |
| F11 -C44 | | | | | | |
| | 3.014(17) | | | | | |
| F11 -C22 | | | | | | |
| F11 -C23 | | | | | | |
| C17 -C35 | | | | | | |
| C18 -C35 | | | | | | |
| C23 -C33 C23 -C34 | | | | | | |
| 023 -034 | 3.001 | | | | | |

 $\label{eq:Table 5. Observed and Calculated Structure Factors for $$ Tetrakis(pentafluorophenyl)octachloroporphinato Zinc(II) \cdot 6(C_6H_4Cl_2). $$$

The columns contain, in order, h, $10F_{obs}$, $10F_{calc}$ and $10\sigma F_{obs}$. A minus sign preceding F_{obs} indicates that F_{obs}^2 is negative.

| Tetrakis (C6F5) - | Octachloroporpl | inato Zinc | 6 (C6H4C12) | Page | 1 |
|---|--|--|--|---|---|
| h 0 0 2 221 23 4 1480 142 6 504 48 8 1446 144 10 845 79 | 15 15 16 15 17 16 15 17 18 17 18 17 18 18 18 18 18 18 18 18 18 18 18 18 18 | 76 189 16 57 141 18 11 323 13 74 273 15 10 163 14 | 9 292 356 10 315 308 11 336 330 12 26 63 13 142 193 14 143 121 15 211 188 16 564 480 | 10 13 -69 11 14 377 11 15 50 45 16 276 18 17 249 19 18 210 15 19 120 | 98 31 325 14 115 36 291 13 255 14 175 16 114 24 |
| | 5 31 21 1 | 74 160 18 80 40 50 | 17 -106 16 18 285 315 | 22 h 13 | 0 |
| 16 -115 4 18 487 56 20 237 14 22 94 10 | 8 17 6 13 h 6 14 2 27 4 25 5 6 | 4 0 31 2483 26 70 620 8 | 19 217 252 20 97 43 21 183 160 22 -43 26 | 15 13 186 26 14 144 18 15 107 44 16 180 17 131 | 40 25 187 18 133 23 177 17 103 21 104 65 |
| h 1 0 | 7 60 | 00 625 9 | h 8 0 | 18 10 19 144 | 104 65 183 21 |
| | 7 9 10 18 11 10 18 18 11 11 11 12 13 7 12 5 12 7 13 16 8 14 8 16 4 9 15 2 18 10 16 15 5 22 17 | 75 80 20 172 16 173 172 16 173 227 15 173 227 15 175 598 11 175 822 12 175 822 14 175 822 14 | 8 1230 1226 9 972 949 10 38 41 11 20 86 13 943 904 14 252 221 15 21 31 16 454 398 17 -35 4 | 17 12 h 14 36 48 14 -97 13 15 -77 13 16 124 14 17 140 55 18 -93 13 42 h 15 | 0 10 30 61 28 56 22 105 21 18 25 |
| 11 481 61 12 712 78 13 231 31 14 245 20 | 33 11 19 3 15 12 20 - | 14 241 12 56 133 35 35 113 21 | 19 57 100 20 293 284 21 92 24 | 36 15 461 14 16 292 28 17 -64 | 424 17 288 14 34 34 |
| 15 192 15 16 -88 | 5 15 22 2 2 23 | 13 203 16 | h 9 0 | h 16 | 0 |
| 17 360 24 18 88 11 | 19 13 h 10 29 | 5 0 | 9 107 22 | 26 16 412 | 433 18 |
| 19 121 6 20 221 19 21 23 25 22 141 1 23 25 h 2 0 | 54 20 5 11 91 15 6 14 22 15 7 4 37 21 8 10 91 56 9 4 10 1 10 1 11 5 12 3 | 67 1486 14 60 453 9 66 1029 12 94 501 9 56 116 13 09 469 10 63 374 11 | 10 291 238 11 419 309 12 -98 41 13 352 301 14 53 47 15 484 503 16 -82 132 17 193 199 | 12 11 h 0 20 12 1 1588 36 2 48 13 3 1174 28 4 581 15 5 531 | 1 1641 12 41 13 1085 9 561 6 534 6 |
| 3 464 4 4 659 6 5 437 4 6 244 2 7 -54 6 8 591 6 9 276 2 | 52 6 14 1 25 7 15 3 56 7 16 - 90 8 17 6 31 21 18 | 99 236 14 28 165 19 45 337 12 28 183 48 03 567 13 64 25 36 24 83 21 56 160 19 79 413 12 | 19 225 204 20 206 178 21 198 152 h 10 0 | 18 6 496 15 7 1182 16 8 485 17 9 692 10 404 11 499 12 72 16 13 686 11 14 -60 | 500 6 1156 10 495 6 687 7 399 7 494 7 92 17 644 8 48 22 |
| 11 48 12 344 3 13 -65 14 110 1 15 593 6 16 141 1 | 67 29 22 2 17 10 97 25 h 89 21 52 12 6 5 76 19 7 - | 79 413 12 14 180 16 6 0 70 647 12 69 11 19 12 109 16 | 12 145 139 13 150 121 14 214 205 15 447 477 16 -41 54 17 101 90 | 18 15 496 19 16 -84 16 17 291 13 18 121 29 19 131 24 20 213 15 21 121 | 440 8 35 17 248 10 107 17 90 14 227 11 153 16 |
| 18 546 5 19 117 1 | $\begin{array}{cccccccccccccccccccccccccccccccccccc$ | 67 280 10 40 638 10 | 20 -116 12 | 25 22 193 20 23 148 | 221 12 126 15 |
| 21 67 | 11 33 12 4 | 50 301 11 93 473 11 | h 11 0 | h 1 | 1 |
| 23 -85 | 2 28 14 4 15 2 0 16 2 | 21 414 11 02 342 12 38 244 14 07 206 16 44 76 44 | 11 145 251 12 -38 84 13 477 319 | 12 4 1079 | 808 7 1050 9 |
| 5 359 3 6 431 2 7 1796 18 8 -100 1 9 140 1 | 56 12 19 2 73 7 20 5 08 8 21 1 26 16 22 -1 97 16 96 13 h | 44 76 44 84 368 13 31 211 14 69 366 13 31 122 23 09 13 23 | 15 144 115 16 -54 87 3 17 103 177 2 18 126 110 2 19 -57 65 20 -31 11 | 21 6 1281 34 7 538 24 8 475 22 9 233 36 10 593 51 11 320 12 692 | 1289 10 591 6 491 6 3 212 7 513 7 257 7 2 715 8 |
| 11 -53 | 36 34 39 26 7 59 10 8 | 31 553 1 90 29 1 | | 13 445 14 435 5 21 15 -39 | 3 428 8 |

| Tetrakis (C6F5 | 5)-Octachl | oroporphin | ato Zinc | 6 (C6H4Cl2) | Page | 2 |
|---|---|--|---|--|--|--|
| 16 193 17 -78 18 -79 19 30 20 350 21 -91 22 157 23 40 | 217 11 30 20 58 21 70 36 358 9 22 18 170 14 44 36 | 6 268 7 597 8 347 9 806 10 676 11 -19 12 529 13 479 14 479 15 148 | 230 6 526 7 370 7 746 8 705 8 16 36 564 8 112 23 509 8 125 13 | 15 247 241 16 434 396 17 54 56 18 318 288 19 71 71 20 260 226 21 78 69 h 10 1 | 11 12 47 10 13 -79 26 14 332 9 15 252 24 16 107 10 17 449 24 18 181 19 159 20 -9 21 -90 | 23 24 39 16 303 8 232 10 142 17 457 9 201 13 141 12 47 52 57 18 |
| 3 384 | 361 5 | 16 470 17 -49 | 461 9 55 30 | 11 308 372 12 254 271 | 9 22 97 10 | 94 20 |
| 6 1003 7 545 8 470 9 604 10 135 11 731 | 771 7 1233 10 904 9 502 6 425 6 601 7 144 10 759 8 545 8 | 18 399 19 212 20 432 21 155 22 183 h 6 7 218 | 403 8 204 10 410 9 155 14 178 13 | 13 334 348 14 206 186 15 165 151 16 70 81 17 245 231 18 150 160 19 -5 78 20 88 110 | 9 h 1 12 1 1160 22 2 493 10 3 951 14 4 772 57 5 720 21 6 162 7 1957 | 2 1091 11 518 5 913 8 739 7 758 7 152 7 1983 16 |
| 13 595 14 47 6 | 561 8 396 8 | 8 588 9 387 | 658 7 400 7 | h 11 1 | 8 323 9 1034 | 304 6 966 9 |
| 15 -33 16 107 17 501 18 141 19 493 20 119 21 242 22 -61 23 -66 | 60 33 139 17 506 9 60 15 499 8 90 16 240 10 19 26 54 34 | 10 380 11 759 12 189 13 260 14 253 15 279 16 -64 17 187 18 148 19 462 | 381 7 792 9 247 10 250 9 256 10 280 10 18 24 213 13 210 13 464 8 | 12 141 137 13 65 101 14 205 301 15 113 171 16 194 221 17 -63 44 18 217 206 19 62 73 20 193 168 | 14 10 462 25 11 885 12 12 641 18 13 550 11 14 341 24 15 442 11 16 214 27 17 226 13 18 -66 | 470 7 814 9 603 8 551 8 356 8 440 9 240 11 246 11 67 25 |
| h 3 | 1 | 20 -46 21 131 | 70 31 162 16 | h 12 1 | 19 285 20 85 21 180 | 286 9 85 20 174 12 |
| 5 1346 1 6 776 7 1048 1 | 1041 9 1350 11 811 7 1112 9 596 7 | 22 -64 h 7 | 83 26 | 13 370 362 14 120 160 15 359 316 16 126 158 | 10 22 122 17 8 h 2 15 | 140 17 2 |
| 9 411 10 411 11 107 12 525 13 220 14 607 | 411 7 379 7 122 12 441 8 233 9 630 8 | 8 802 9 462 10 642 11 438 12 302 13 183 14 306 | 763 8 468 7 577 8 440 8 305 8 215 11 237 9 | 17 239 254 18 95 96 19 211 186 h 13 1 14 -53 106 | 10 2 115 20 3 499 12 4 975 5 1246 6 575 7 791 25 8 125 | 222 11 541 5 972 8 1329 10 578 6 832 8 164 10 |
| 15 371 16 138 17 239 18 502 19 -87 20 211 21 87 22 -51 | 375 9 152 14 271 11 513 9 49 17 228 11 68 21 | 15 152 16 263 17 167 18 193 19 -87 20 240 21 140 | 178 13 300 10 192 14 219 11 39 18 249 10 105 15 | 15 146 123 16 173 182 17 126 176 18 142 143 19 140 120 h 14 1 | 13 9 188 12 10 334 16 11 221 15 12 390 16 13 177 14 494 15 212 | 151 8 323 7 250 8 350 8 123 10 470 8 184 11 |
| 22 -51 h 4 | 23 30 1 | 22 -76 h 8 | 53 31 | 15 201 217 16 226 251 | 16 263 11 17 210 11 18 161 | 256 10 231 12 198 14 |
| 5 603 6 1198 1 7 1166 1 8 824 | 551 6 1138 10 1138 10 881 8 | 9 -36 10 234 11 415 12 436 | 98 27 283 9 462 8 | 17 79 35 18 107 122 h 15 1 | 23 19 331 19 20 413 21 138 22 174 | 333 9 428 9 138 15 183 13 |
| 9 206 10 782 | 301 8 756 8 | 13 321 14 279 | 459 8 323 9 273 10 | 16 401 398 17 171 120 | 9 h 3 | 2 |
| 11 -22 12 12 554 14 279 15 247 16 183 17 470 18 156 20 162 21 422 22 103 | 169 34 220 9 5298 9 272 10 221 12 464 9 167 15 155 13 148 13 82 19 | 15 471 16 213 17 78 18 -80 19 222 20 139 21 129 h 9 | 451 9 236 12 82 20 45 19 276 11 131 15 146 16 1 | h 0 2 0 2468 2461 1 848 810 2 74 32 3 641 555 4 1238 1198 5 733 762 6 37 297 7 158 149 | 3 2365 4 1316 5 1676 17 6 564 7 7 422 11 8 1195 6 9 360 10 10 535 7 11 343 6 12 272 8 13 589 | 2372 21 1274 11 1624 13 468 6 366 6 1216 10 355 7 476 7 378 7 277 8 6022 8 |
| h 5 | 1 | 11 392 12 401 13 681 14 495 | 403 8 387 8 698 9 527 9 | 8 562 501 9 316 350 10 846 868 11 99 98 | 7 14 409 7 15 328 8 16 185 13 17 394 | 380 8 320 9 169 12 393 9 |

| Tetrakis (C6F5)-O | ctachloropo | rphina | to Zi | nc 6 | (C6H40 | C12) | | | Pag | e | 3 | |
|--|------------------------|-------------------|-------------------|----------------|----------------|-------------------|--------------------|----------------|----------------|-------------------|-------------------|----------------|
| 18 86 110 | 22 14 8 15 | | 211 96 | 11 19 | 19 | 88 | 79 | 22 | Ъ | 2 | 3 | |
| 19 386 369 20 105 94 21 157 170 | 18 16 14 17 | 233 | 243 272 | 11 10 | h | 13 | 2 | | 3 | 440 379 | 423 415 | 6 |
| 22 -69 36 | 24 18 | 164 | 126 284 | 12 10 | 13 14 | 105 122 | 201 116 | 24 15 | 5 | 235 168 | 246 207 | 6 |
| h 4 2 | 20 21 | 284 | 260 128 | 10 15 | 15 16 | 122 289 -91 | 297 46 | 9 18 | 7 8 | 505 492 | 482 563 | 77 |
| 4 1785 1774 5 1106 1040 | 16 9 h | | 2 | | 17 18 | -51 115 | 79 107 | 29 18 | 9 10 | 611 379 | 613 374 | 7 8 7 |
| 8 1360 1250 7 883 843 | 11 8 8 | 757 | 726 | 11 | h | 14 | 2 | | 11 12 | 460 179 | 437 238 | 10 |
| 8 633 670 9 498 480 | 7 9 7 10 | 661 | 297 702 | 8 | 14 | 338 | 329 | 12 | 13 14 | 195 213 | 243 179 | 10 10 9 |
| 10 230 257 11 28 120 | 8 11 31 12 8 13 | 331 | 389 315 | 8 9 9 | 15 16 17 | 343 208 114 | 307 205 129 | 11 18 | 15 16 17 | 396 281 132 | 418 257 162 | 10 16 |
| 12 345 360 13 166 163 14 540 509 | 8 13 11 14 8 15 | 325 | 374 325 364 | 9 10 | 18 | 148 | 170 | 15 | 18 19 | 122 | 90 182 | 14 10 |
| 15 340 371 16 330 344 | 9 16 9 17 | 114 92 | 137 96 | 18 18 | h | 15 | 2 | | 20 21 | 119 -73 | 138 | 16 22 |
| 17 317 303 18 370 389 | 10 18 8 19 | 329 23 | 341 | 43 | 15 16 | 292 73 | 324 108 | 14 24 | 22 | 96 | 121 | 20 |
| 19 219 191 20 324 330 | 10 20 9 21 | 267 180 | 260 196 | 10 13 | 17 | 38 | 81 | 37 | h | 3 | 3 | |
| 21 19 40 22 92 108 | 46 21 h | 9 | 2 | | h | 16 | 2 | | 5 | 682 | 436 714 403 | 6 7 8 |
| h 5 2 | 9 | 1043 43 | 959 85 | 13 28 | 16 h | 262 0 | 262 3 | 15 | 6 7 8 | 376 129 400 | 70 492 | 107 |
| 5 1236 1130 6 481 498 | 12 11 6 12 | 452 449 | 398 458 | 8 9 | | 2683 | 2563 | 21 | 9 10 | 367 289 | 371 | 8 |
| 7 523 601 8 414 463 | 7 13 7 14 | 323 184 | 336 176 | 9 12 | | 2509 290 | 2369 311 | 18 | 11 12 | 143 691 | 108 658 | 11 |
| 9 422 386 10 399 352 | 7 15 7 16 | 284 160 | 340 210 | 10 14 | 5 | 449 25 | 476 80 | 6 26 | 13 14 | 374 -70 | 372 95 | 8 20 |
| 11. 310 303 12 346 300 | 8 17 8 18 | 386 75 | 386 69 | 22 | 6 | 590 124 | 612 98 | 7 10 | 15 16 | 633 | 68 | 32 |
| 13 530 549 14 194 149 15 41 75 | 8 19 11 20 31 21 | 134 100 125 | 180 110 153 | 15 19 19 | 8 9 10 | -6 1406 131 | 14 1395 155 | 42 12 11 | 17 18 19 | 166 186 183 | 231 177 135 | 14 11 12 |
| 15 41 75 16 368 384 17 365 380 | 9 | | 2 | 19 | 11 12 | 409 496 | 418 471 | 7 8 | 20 21 | 466 | 398 57 | 34 |
| 18 101 93 19 255 253 | 17 | 395 | 328 | 12 | 13 14 | 518 52 | 554 43 | 8 26 | 22 | 105 | 133 | 19 |
| 20 156 112 21 356 318 | 13 11 9 12 | 346 215 | 357 275 | 9 11 | 15 16 | 104 | 117 65 | 17 49 | h | 4 | 3 | |
| 22 24 79 h 6 2 | 44 13 14 15 | 234 414 99 | 243 435 89 | 11 9 20 | 17 18 19 | 151 159 389 | 88 80 313 | 14 12 8 | 5 6 7 | 772 416 315 | 817 452 275 | 8 6 7 |
| h 6 2 6 435 459 | 16 | 282 116 | 255 116 | 9 16 | 20 21 | 423 | 380 160 | 9 14 | 8 | 511 727 | 514 695 | 7 7 8 |
| 7 314 223 8 252 252 | 7 18 | 174 81 | 183 | 12 22 | 22 | 139 | 120 | 15 | 10 11 | 602 496 | 813 435 | 8 |
| 9 234 248 10 878 857 | 8 20 9 | 262 | 216 | 11 | h | | 3 | | 12 13 | 463 352 | 473 363 | 8 |
| 11 145 188 12 497 494 | 8 | h 11 | 2 | | 3 | 2875 450 | 2782 415 228 | 20 6 6 | 14 15 16 | 178 92 340 | 252 155 | 12 19 10 |
| 13 116 133 14 473 440 15 316 243 | 9 12 | 753 173 523 | 725 188 520 | 12 12 9 | 4 5 6 | 208 563 893 | 533 970 | 6 | 17 18 | 280 230 | 323 279 191 | 11 |
| 16 242 214 17 -55 96 | 11 14 | -51 253 | 67 296 | 30 | 7 8 | 475 425 333 | 480 | 6 | 19 20 | 537 184 | 518 158 | 8 12 |
| 18 275 286 19 171 187 | 9 16 12 17 | -49 225 | 18 222 | 28 11 | 10 | 422 | 323 476 | 7 | 21 22 | 92 79 | 86 82 | 20 23 |
| 20 183 193 21 187 193 | 12 18 12 19 | 178 94 | 150 124 | 12 20 | 11 12 | 211 356 | 194 381 | 8 | h | 5 | 3 | |
| 22 113 133 h 7 2 | | 47 | 33 2 | 33 | 13 14 15 | 431 443 68 | 458 477 156 | 8 8 23 | 6 | 269 493 | 263 517 | 7 |
| n 7 2 | | h 12 64 | 66 | 34 | 16 17 | 432 174 | 415 157 | 9 13 | 8 | 1156 265 | 1173 284 | 10 8 |
| 8 656 589 9 633 609 | 8 13 7 8 14 | 79 51 | 95 147 | 34 23 27 | 18 | 360 186 | 335 186 | 8 11 | 10 11 12 | 350 269 | 378 256 | 8 8 |
| 10 145 11° 11 344 33° | 7 11 15 1 8 16 | 171 250 | 149 246 | 12 10 | 20 21 | -45 180 | 48 181 | 31 12 | 13 | 738 191 | 677 164 193 | 9 11 11 |
| 12 389 419 13 473 53 | | 107 155 | 97 180 | 18 14 | 22 | 158 | 173 | 14 | 14 15 | 210 262 | 293 | 10 |

| Tetrak | c i s | (C6F | 5)-Oc | tach | loropo | phin | ato Z | inc | 6 (C6H4 | C12) | | | Page | 4 | |
|--|----------------------------|--|--|---|--|--|--|---|---|---|---|--|---|--|---|
| 16 17 18 19 20 21 | 8 9 1 | 344 78 206 253 161 -91 74 | 331 95 199 218 168 4 89 | 10 23 11 10 13 18 45 | 14 15 16 17 18 19 20 | 46 447 187 186 -38 -20 92 | 138 367 176 188 65 74 127 | 32 8 11 12 34 46 21 | 4 5 6 7 8 9 10 | 190 952 783 392 83 694 199 316 | 190 916 696 330 37 630 150 276 | 8 9 8 7 14 8 9 | 15 172 16 519 17 72 18 314 19 71 20 372 21 118 | 528 86 302 40 2 361 | 13 9 21 9 23 9 |
| | h | 6 | 3 | | h | 11 | 3 | | 12 13 | 704 371 | 688 347 | 9 | h 5 | 4 | |
| 7 8 9 10 11 12 13 14 15 | 1 2 3 4 5 5 5 | 375 352 754 -28 204 285 438 224 192 218 | 408 377 792 152 146 266 456 247 213 173 | 7 8 32 10 9 8 10 12 12 | 12 13 14 15 16 17 18 19 | 455 145 73 154 196 239 133 -39 | 395 173 104 181 209 238 153 59 | 9 15 25 13 11 10 15 35 | 14 15 16 17 18 19 20 21 | -69 205 34 42 -76 185 214 95 46 | 90 171 47 48 20 201 229 89 70 | 21 11 37 34 19 12 11 20 38 | 5 656 6 446 7 765 8 361 9 319 10 233 11 225 12 246 13 103 14 273 | 3 431 5 808 1 313 9 330 8 240 5 238 3 194 5 151 | 10 7 8 7 8 9 9 9 17 |
| 17 18 | | 86 - 40 | 141 26 | 19 31 | 13 | -72 | 112 | 23 | h | 2 | 4 | | 15 332 16 171 | 298 | 10 |
| 19 20 21 |) | 189 -22 137 | 184 64 143 | 12 43 15 | 14 15 16 17 18 | 172 91 228 159 -59 | 190 47 197 95 | 12 19 11 13 27 | 2 3 4 5 | 741 142 263 500 758 | 739 155 303 479 718 | 9 7 7 8 | 17 -73 18 86 19 258 20 92 21 -46 | 22 3 101 3 274 2 119 | 20 20 10 20 32 |
| 8 | 8 | 630 | 593 | 8 | 19 | 187 | 158 | 13 | 6 7 8 | 259 908 | 283 881 | 7 | h (| | - |
| 10 | 9 | 438 629 | 404 585 | 8 | h | 13 | 3 | | 9 10 | 470 256 | 433 248 | 7 | 6 788 | | 11 |
| 11 12 13 14 15 16 | 1 2 3 4 5 7 | 208 384 268 307 227 -46 185 | 240 312 224 281 171 118 180 | 10 8 10 9 11 32 11 | 14 15 16 17 18 | 197 110 205 90 -80 | 165 91 175 103 36 | 11 17 11 21 21 | 11 12 13 14 15 16 | 493 265 262 138 87 428 -29 | 441 286 227 155 69 441 43 | 8 9 14 20 9 | 7 138 8 689 9 473 10 343 11 233 12 276 13 146 | 3 203 612 8 442 2 320 2 191 3 220 187 | 10 8 8 8 10 9 |
| 18 19 20 | 9 | 353 148 193 | 351 132 195 | 9 14 12 | 15 16 | 405 218 | 384 198 | 9 11 | 18 19 20 | 134 227 105 | 84 187 103 | 14 10 18 | 14 299 15 276 16 329 | 3 291 | 10 |
| 21 | i | -82 | 52 | 21 | 17 | 168 | 168 | 14 | 21 | 120 | 119 | 17 | 17 3 18 10 | 2 58 2 158 | 10 35 18 |
| | h | 8 | 3 | | h | 15 | 3 | | h | . 3 | 4 | | 19 110 20 179 | 8 91 | 17 |
| 10 11 12 |) 1 2 | 166 180 820 100 | 206 129 836 122 | 10 10 9 | 16 h | 74 | 102 | 24 | . 5 6 | 668 565 937 234 | 703 546 914 272 | 9 7 9 7 | 21 5: | 1 45 7 4 | 31 |
| 13 14 15 16 17 18 19 20 21 | 4 5 6 7 8 9 | 125 225 386 87 72 107 270 -28 133 | 128 193 380 115 91 13 269 17 144 | 15 11 9 22 22 14 10 41 16 | 3 4 5 6 7 8 | 525 748 1660 680 639 257 380 158 253 | 515 788 1612 754 618 270 335 177 279 | 8 7 13 7 7 6 9 | 7 8 9 10 11 12 13 14 15 | 166 266 291 310 73 582 326 38 563 | 132 237 314 272 98 592 526 112 540 207 | 9 7 8 8 19 8 9 52 9 | 7 78 8 44 9 84 10 20 11 53 12 25 13 17 14 26 15 13 | 2 520 7 819 8 219 1 523 8 241 9 213 4 232 7 158 | 11 8 9 10 8 10 12 10 16 |
| | h | 9 | 3 | | 9 10 | 416 214 | 457 238 | 7 | 16 17 | 259 114 | 97 | 11 18 | 16 18 17 21 | 1 217 | 11 |
| 11 | 1 2 | 395 367 37 110 | 382 379 94 92 | 8 9 33 17 | 11 12 13 14 15 | 392 687 57 464 44 | 341 698 153 476 92 | 8 24 9 31 | 18 19 20 21 | 78 521 115 173 | 97 535 132 183 | 21 9 17 13 | 18 16 19 30 20 2 | 0 289 | 13 10 44 |
| 1 | 4 | 317 281 | 325 234 | 10 | 16 17 | 361 221 | 359 253 | 9 12 | 1 | 4 | 4 | | 8 49 | | 11 |
| 111111111111111111111111111111111111111 | 6 7 8 9 | 306 135 207 -105 55 | 281 149 219 39 | 14 11 15 29 | 18 19 20 21 22 | 392 117 198 -37 287 | 381 128 182 27 271 | 16 12 36 12 | 4 5 6 7 8 | 986 380 778 545 364 | 897 371 800 561 314 | 11 7 8 7 | 9 48 10 86 11 42 12 32 13 23 | 7 492 2 894 3 457 4 350 | 10 9 9 |
| | h | 10 | 3 | | h | 1 | 4 | | 9 10 | 290 60 | 286 117 | 21 | 14 29 15 -6 | 1 289 0 83 | 10 27 |
| 1 | 1 | 211 | 281 | 11 | 1 | 284 | 259 | 8 | 11 | 143 | 200 1160 | 12 11 | 16 19 17 16 | 0 224 5 147 | 11 12 |
| 1 | | 287 712 | 231 607 | 10 10 | 3 | 545 225 | 483 224 | 6 | 13 14 | 454 226 | 421 237 | 10 | 18 31 19 -7 | 6 309 | 22 |

| Tetraki | s (C6F | 5)-Oct | achle | oropor | phina | ato Zi | inc | 6 (0 | C6H40 | 212) | | | Pag | e | 5 | |
|----------------|-------------------|-------------------|----------------|----------------|-------------------|-------------------|----------------|------|----------------|-------------------|-------------------|---------------|----------------|-------------------|-------------------|---------------|
| 20 | 63 | 81 | 27 | 5 | 608 | 658 | 7 | | 17 | 292 363 | 282 354 | 9 | 9 | 479 | 461 | 8 |
| h | 9 | 4 | | 6 | 189 371 | 204 383 | 8 7 9 | | 18 19 20 | 143 271 | 125 267 | 14 10 | 10 11 | 158 492 | 149 | 12 |
| 9 | 526 | 509 | 11 | 8 | 191 748 | 162 644 30 | 8 | | 21 | 112 | 129 | 18 | 12 13 | -47 256 | 49 240 | 29 11 |
| 10 11 | 76 141 | 119 56 | 20 14 | 10 11 | - 48 298 | 192 | 24 | | h | 4 | 5 | | 14 15 | 253 137 | 260 129 | 11 |
| 12 13 | 441 362 | 411 335 | 9 | 12 | 522 659 | 494 553 | 8 | | 5 | 509 459 | 486 478 | 7 | 16 17 | 205 213 | 226 219 | 11 11 |
| 14 15 | 381 178 | 380 168 | 10 11 | 14 15 | 202 -60 | 190 20 | 11 25 35 | | 6 7 8 | 243 | 223 416 | 8 | 18 19 | 39 164 | 37 146 | 35 |
| 16 17 | 183 324 | 155 334 | 9 | 16 17 18 | 40 167 -57 | 51 170 69 | 12 25 | | 9 10 | 270 383 | 251 395 | 8 | h | 9 | 5 | •• |
| 18 19 | 150 112 | 123 | 14 18 12 | 19 20 | 296 -49 | 299 | 10 | | 11 12 | 479 154 | 511 149 | 8 13 | 10 | 304 | 295 | 9 |
| 20 | 202 | 216 | 12 | 21 | 177 | 199 | 13 | | 13 14 | 127 141 | 141 | 15 14 | 11 12 | 390 199 | 367 230 | 9 12 |
| h 10 | | 245 | 14 | h | 1 | 5 | | | 15 16 | 395 380 | 415 | 10 | 13 14 | -69 401 | 123 410 | 24 |
| 11 12 | 228 299 192 | 307 | 12 | 2 | 298 553 | 355 618 | 7 | | 17 18 | 139 285 | 322 170 278 | 14 | 15 16 | 193 294 | 209 298 | 11 9 17 |
| 13 14 | -48 201 | 59 209 | 31 12 | 4 5 | 274 681 | 214 715 | 7 8 | | 19 20 | 501 94 | 460 97 | 20 | 17 18 | 108 87 | 61 95 | 21 |
| 15 16 | 92 463 | 133 465 | 18 | 6 | 854 | 845 383 | 9 | | 21 | 73 | 82 | 34 | 19 | 19 | 62 | 47 |
| 17 18 | 115 | 119 114 | 17 23 | 8 | 321 773 598 | 747 640 | 8 | | h | 5 | 5 | 6 | h | 10 | 5 | |
| 19 | -70 | 54 | 24 | 10 11 | 292 252 | 271 234 | 8 | | 6 7 | 524 432 | 474 426 386 | 7 | 11 12 | 153 117 | 137 180 | 14 |
| 1 | | 4 | | 12 13 | 480 161 | 481 190 | 12 | | 8 | 461 341 | 334 | 8 | 13 | 205 232 | 222 193 | 12 10 8 |
| 11 12 | 393 170 | 401 201 | 13 13 | 14 15 | -86 | 123 38 | 19 | | 10 11 | 298 282 | 249 261 | 9 | 15 16 | 468 155 226 | 447 156 231 | 13 |
| 13 14 | 202 196 | 210 171 | 12 11 | 16 17 | 235 -46 | 234 10 | 11 28 | | 12 13 | 202 376 | 243 371 | 11 9 15 | 17 18 | 244 | 211 | 11 |
| 15 16 | 247 390 | 278 376 | 10 | 18 19 | 90 -19 | 126 85 91 | 19 45 27 | | 14 15 16 | 142 235 200 | 163 264 217 | 11 10 | h | 11 | 5 | |
| 17 18 19 | 207 114 251 | 181 133 253 | 11 17 11 | 20 21 | 62 97 | 63 | 20 | | 17 18 | -71 84 | 69 102 | 21 21 | 12 13 | 361 229 | 399 235 | 10 10 |
| 15 | | 4 | 11 | h | 2 | 5 | | | 19 20 | 62 149 | 88 144 | 26 15 | 14 15 | 103 114 | 143 132 250 | 17 17 |
| 12 | 409 | 448 | 13 | 3 | 596 537 | 605 485 | 7 | | h | 6 | 5 | | 16 17 | 264 125 | 86 | 10 16 |
| 13 | 107 59 | 148 86 | 16 25 | 5 6 | 928 207 | 929 213 | 9 8 | | 7 | 132 | 151 | 12 | 18 | 224 | 211 | 12 |
| 14 15 16 | -51 104 | 53 117 | 28 18 | 7 8 | 705 345 | 671 299 | 8 | | 8 | 484 289 | 413 304 | 8 | h | 12 52 | 5 | 28 |
| 17 18 | - 53 - 63 | 43 31 | 29 26 | 10 | 606 210 | 633 201 | 8 | | 10 11 | 291 380 | 281 364 | 9 9 10 | 13 14 15 | 144 -79 | 145 180 95 | 14 20 |
| | h 13 | 4 | | 11 12 | 354 231 | 356 224 | 10 9 | | 13 | 282 177 166 | 296 188 | 12 13 | 16 17 | 160 | 127 129 | 14 20 |
| 13 | 134 -72 | 158 35 | 20 21 | 13 14 15 | 469 232 | 462 228 375 | 11 9 | | 14 15 16 | 289 96 | 216 257 147 | 10 18 | ı. | | 5 | |
| 14 15 16 | 198 70 | 216 99 | 12 25 | 16 17 | 418 37 181 | 75 143 | 37 11 | | 17 18 | 197 | 231 | 11 | 14 | 241 | 271 | 10 |
| 17 | 182 | 206 | 13 | 18 19 | 187 180 | 183 213 | 12 | | 19 20 | 208 69 | 214 | 12 25 | 15 16 | 102 191 | 103 201 | 19 12 |
| | h 14 | 4 | | 20 21 | 157 117 | 116 119 | 14 18 | Į. | | h 7 | 5 | | 17 | 37 | 39 | 48 |
| 14 15 | 523 92 | 478 79 | 12 20 | ŀ | 3 | 5 | | | 8 | 85 | 87 | 17 | 1 | | 5 | ., |
| 16 | 201 | 187 | 12 26 | 4 | 396 | 387 | 7 | | 9 10 | 128 472 393 | 100 448 | 13 | 15 16 | 150 183 | 162 186 | 14 13 |
| | h 15 | 4 | | .5 6 | 456 467 | 480 481 | 7 | r | 11 12 | 450 | 348 455 | 9 | 1 | h 0 | в | |
| 15 | -97 | | 24 | 7 8 | 271 432 | | 2 | 7 | 13 | 112 432 -42 | 100 426 77 | 17 9 29 | 0 | 1466 691 | 1440 627 | 10 8 |
| 16 | | | 12 | 9 10 11 | 315 337 435 | 373 | | 8 | 15 16 17 | 103 | 130 114 | 17 17 | 2 3 | 1081 365 | 1032 390 | 10 |
| 3 | | | 6 | 12 13 | 703 | 667 | 9 | 9 | 18 19 | 355 | 342 | 18 | 4 5 | 77 151 | 46 58 | 16 10 |
| | 381 | 327 | 6 | 14 15 | 205 186 | 175 | 11 | 1 | 20 | | 219 | 11 | 6 7 | 46 92 | 159 | 15 |
| | | 233 | 8 | 16 | 449 | 442 | 10 | ő | | h 8 | 5 | | 8 | 282 | 355 | 8 |

| Tetrakis | (C6I | 75)-Oc | tach | loropor | phin | ato Z | inc | 6 (C6H46 | C12) | | | Pa | ge | 6 | |
|-----------------------|--|---|-----------------------------|--------------------------------|--|--|----------------------------|----------------------------|---------------------------------|--------------------------------|---------------------------|----------------------------------|--|--|----------------------------------|
| 10 11 12 13 | 121 238 284 229 104 | 141 284 329 300 86 | 14 10 9 10 | h 4 5 | 361 108 | 6 351 44 | 10 13 | 12 13 14 15 16 | 376 192 268 -18 235 | 349 164 234 18 250 | 10 13 9 45 10 | 16 17 18 19 | -59 -66 31 140 | 71 60 17 167 | 25 23 39 15 |
| 15 | $\frac{114}{195}$ | 58 213 | 17 13 | 6 7 | 333 132 | 349 72 | 8 12 | 17 18 | -16 63 | 33 70 | 48 27 | h | 1 | 7 | |
| 17 18 19 | 119 185 -89 -28 233 | 156 201 51 30 189 | 15 12 18 40 11 | 8 9 10 11 12 13 | 600 168 195 174 351 219 | 587 170 147 127 297 220 | 8 11 11 12 9 | h 9 10 11 | 9 685 50 171 | 711 46 123 | 12 50 13 | 2 3 4 5 6 7 | 160 424 550 216 384 340 | 193 378 584 237 396 328 | 10 8 8 9 8 |
| h | 1 | 6 | | 14 15 | 332 272 | 294 317 | 10 | 12 13 | 305 233 | 285 216 | 10 10 | 8 | 360 275 | 374 290 | 8 |
| 2 3 4 5 6 | 454 446 349 605 341 271 | 1444 446 351 554 321 261 | 10 7 7 8 7 8 | 16 17 18 19 20 | 202 265 237 94 109 | 193 310 198 40 142 | 11 10 11 20 19 | 14 15 16 17 18 | 237 256 125 404 80 | 188 232 142 381 77 | 10 10 16 9 23 | 10 11 12 13 14 15 | 157 67 246 282 196 59 | 194 125 318 264 202 | 13 23 11 10 10 25 |
| 8 | 526 335 | 479 289 | 8 | h | 5 | 6 | | h | 10 | 6 | | 16 17 | 112 | 116 | 17 |
| 10 11 | 561 94 391 -24 | 563 110 386 | 17 9 | 5 6 7 | 862 150 237 | 894 181 256 | 12 11 9 | 10 11 12 | 97 154 189 | 88 125 179 | 27 14 11 | 18 19 | 81 132 | 69 71 118 | 23 22 16 |
| 13 14 | 148 | 59 168 23 | 14 | 8 9 10 | 86 294 | 182 320 | 18 | 13 14 | 253 183 | 230 157 | 10 12 | h | 2 | 7 | |
| 15 16 17 | 378 121 -90 | 345 142 105 | 21 10 15 17 | 11 12 13 | 148 238 191 360 | 145 267 192 349 | 13 10 12 9 | 15 16 17 | 97 146 19 | 122 130 61 | 19 14 47 | \$ 4 5 6 | 648 238 147 52 | 643 230 205 56 | 8 9 12 25 |
| 18 19 | 72 232 | 188 | 23 11 | 14 15 | 71 230 | 34 235 | 25 10 | h | 11 | 6 | | . 7 | 224 156 | 200 206 | 10 |
| 20 h | 35 2 | 83 6 | 38 | 16 17 18 19 | -55 106 103 142 | 97 103 152 | 26 17 18 15 | 11 12 13 | 486 172 134 | 443 181 137 | 11 12 14 | 9 10 11 | 218 -80 567 | 240 17 522 | 10 18 . 9 |
| | 337 321 | 1262 329 | 14 | та | 6 | 6 | 15 | 14 15 | 138 294 95 | 152 264 | 10 | 12 | 171 379 | 170 403 | 13 10 |
| 4 | 107 422 | 107 | 12 | 6 | 268 | | 12 | 16 17 | 163 | 113 158 | 20 14 | 14 15 | 189 117 | 191 | 11 15 |
| 6 | 264 342 | 242 317 | 8 | 7 8 | 325 188 | 341 350 217 | 8 | h | 12 | 6 | | 16 17 | 214 181 | 181 149 | 11 12 13 |
| 8 | 805 477 | 827 506 | 9 | 9 10 | 299 525 | 292 505 | 9 | 12 13 | 253 189 | 231 | 14 | 18 19 | 163 153 | 153 160 | 15 |
| 10 | 122 213 | 140 221 | 14 10 | 11 12 | 342 314 | 350 307 | 9 | 14 15 | 177 | 194 125 231 | 12 12 | h | 3 | 7 | |
| 12 | 539 112 | 537 118 | 9 17 | 13 14 | 63 305 | 59 303 | 26 10 | 16 | 224 132 | 119 | 11 16 | 4 | 280 | 257 | 8 |
| | -73 42 | 66 | 22 35 | 15 16 | 297 269 | 283 289 | 9 | h | 13 | 6 | | 5 6 7 | 246 419 | 245 390 | 9 8 9 |
| 16 | 81 -57 | 67 36 | 20 26 | 17 18 | -40 159 | 32 158 | 33 | 13 14 | 383 127 | 327 135 | 13 16 | 8 | 255 233 110 | 213 240 87 | 10 16 |
| 18 | 315 293 | 280 303 | 10 | 19 | 257 | 232 | ii | 15 | 69 | 100 | 25 | 10 11 | 163 155 | 145 153 | 13 13 11 |
| | 184 | 183 | 13 | h | 7 | 6 | | h | 14 | 6 | | 12 13 | 255 | 274 79 | 11 |
| h | 3 | 6 | | 7 8 | 332 132 | 296 84 | 12 14 | 14 15 | 114 80 | 138 101 | 24 32 | 14 15 | 33 397 157 | 365 162 | 8 |
| 4 | 419 450 | 458 441 | 10 | 9 10 | 390 90 | 368 49 | 19 | h | 0 | 7 | | 16 17 | -38 369 | 96 339 | 33 |
| 5 6 | 452 70 | 460 36 | 7 18 | 11 12 | 316 170 | 280 145 | 9 13 | 1 | 424 | 385 | 7 | 18 19 | 366 192 | 359 186 | 13 |
| 7 8 | 293 199 | 336 179 | 10 | 13 14 | 378 195 | 390 158 | 10 11 | 3 | 300 118 | 310 139 | 8 13 | h | 4 | 7 | |
| 10 | 379 267 | 375 232 | 9 | 15 16 | 126 49 | 168 95 | 15 30 | 5 | 146 152 | 192 162 | 11 | 5 | 352 | 303 | 8 |
| 11 12 | 319 281 | 325 292 | 10 | 17 18 | -49 134 | 59 114 | 29 15 | 6 | 67 923 | 28 911 | 20 10 | 6 | 212 469 | 218 521 | 10 |
| 13 14 15 | 454 83 191 | 430 102 | 9 22 13 | 19 | 226 | 200 | 11 | 8 | 416 175 | 338 146 | 12 | 8 | 235 237 | 204 250 | 10 10 |
| 16 17 | 148 | 212 228 270 | 13 | h | 8 | 6 | | 10 11 | 188 172 | 188 121 | 11 12 | 10 11 | 239 | 100 239 | 20 11 |
| 18 19 | 294 211 259 | 175 201 | 9 11 10 | 9 | 323 -52 257 | 393 47 | 13 26 | 12 13 | -55 48 | 18 86 | 27 32 | 12 | 88 111 | 130 56 | 21 18 |
| 20 | 129 | 107 | 16 | 10 11 | 95 | 291 138 | 10 19 | 14 15 | -35 202 | 51 195 | 33 11 | 14 15 | 64 226 | 35 206 | 23 10 |

| Tetrakis (| C6F5)-Oct | achloropo | rphin | ato Zi | nc 6 | (C6H4C | 212) | | | Pag | e | 7 | |
|--|--|---|--|--|---------------------------------|----------------------------------|--|--|----------------------------------|---------------------------------------|--|--|---|
| 18 10 | 74 264 03 83 91 85 | 11 14 10 15 19 16 24 h | 86 176 54 11 98 | 51 148 26 7 109 91 | 21 13 30 18 16 | 13 14 15 16 17 18 | 134 206 173 66 78 282 | 153 195 132 67 90 294 | 14 11 12 25 23 10 | 9 10 11 12 13 14 15 | 277 134 375 162 21 133 147 67 | 233 137 382 187 36 155 164 88 | 11 13 8 12 44 15 14 26 |
| 7 3: | 20 306 32 209 | 9 14 10 15 | 124 231 33 | 237 85 | 11 | 3 | 118 | 188 | 20 | h | 8 | 8 | |
| 9 16 10 43 11 23 12 13 13 16 | 32 191 32 425 34 198 85 118 82 133 | 13 16 9 11 h 13 14 13 | 47 12 218 165 | 97 7 250 153 | 33 11 13 | 4 5 6 7 8 9 | 124 139 241 534 214 263 | 136 155 256 531 205 261 | 14 13 10 9 11 10 | 8 9 10 11 12 | 428 93 74 138 194 | 418 78 137 162 204 | 13 21 21 14 11 |
| 15 16 16 2 17 16 | 86 145 08 74 15 188 67 136 80 172 | 12 14 17 15 11 13 h | 207 | 187 7 | 12 | 10 11 12 13 | 102 195 139 252 | 96 203 138 284 | 19 13 13 10 | 12 13 14 15 16 | 244 215 158 197 | 254 209 108 209 | 10 11 14 12 |
| h | 6 7 | 14 | 168 | 176 | 14 | 14 15 | - 56 28 | 34 78 | 26 40 | h | 9 | 8 | |
| 7 3 | 50 365 | 9 h | 0 | 8 | | 16 17 | 198 263 | 182 277 | 12 10 | 9 | 312 | 316 | 12 19 |
| 9 | 04 113 99 110 | 17 0 18 1 11 2 | 276 -38 104 | 380 13 17 | 12 29 16 | 18 h | 38 | 3.5 8 | 48 | 10 11 12 | -76 243 126 | 43 225 122 | 10 |
| 11 50 12 2 13 2 | 40 281 08 557 16 217 48 249 | 9 3 12 4 9 5 | -60 122 183 | 55 106 206 | 22: 14 11 | 4 5 | 113 | 99 237 | 22 11 | 13 14 15 | 167 46 137 | 122 170 35 113 | 13 32 16 |
| 15 | 26 129 61 114 | 15 6 26 7 | 394 -39 | 400 2 623 | 31 9 | 6 7 8 | 320 83 230 | 287 72 239 | 9 20 11 | h | 10 | 8 | |
| 17 | 74 32 55 85 18 149 | 21 8 29 9 17 10 | 615 69 69 -77 | 7 96 18 | 23 24 21 | 9 10 11 | -89 292 117 | 66 273 86 | 18 10 18 | 10 11 12 13 | 233 73 63 | 258 98 96 | 14 23 26 |
| h | 7 7 | 12 13 | 156 -35 | 126 32 | 15 33 | . 12 13 14 | 231 138 275 | 225 141 291 | 10 14 10 | 13 14 15 | -31 20 109 | 101 92 132 | 38 46 19 |
| 9 | 48 433 99 100 57 132 | 9 14 18 15 28 16 | 110 11 -41 | 146 79 13 | 16 51 33 | 15 | 176 101 | 146 | 12 19 | h | 11 | 8 | 10 |
| 11 1 12 5 13 | 25 108 32 490 31 73 87 62 | 17 17 10 18 36 18 1 | 84 133 | 38 78 8 | 22 16 | 17 h | 201 | 216 8 | 12 | 11 12 13 | 184 47 250 | 204 31 226 | 17 31 11 |
| 15 | 70 117 84 198 | 24 12 1 | 149 | 169 | 17 | 5 6 | 213 137 | 229 132 | 15 14 | 14 | 89 | 81 | 21 |
| 17 1 18 | 28 148 28 76 | 16 2 42 3 | 78 238 | 69 278 | 19 10 | 7 8 | 177 259 | 160 279 | 12 10 | h | 12 | 8 | 0.1 |
| h | 8 7 | 4 5 6 | 214 170 201 | 208 169 205 | 10 12 11 | 9 10 11 | 200 119 234 | 219 140 227 | 12 17 11 | 12 13 | 143 78 | 180 59 | 21 23 |
| | 61 664 35 138 | 9 7 16 8 | 438 | 427 253 | 9 10 | 12 13 | 164 209 | 143 226 | 12 11 | h | 0 | 9 | |
| 11 2 12 2 13 1 14 - | 277 251 270 245 137 153 145 53 167 187 | 11 9 9 10 14 11 30 12 13 13 | 240 377 282 315 255 148 | 328 274 277 267 103 169 | 9 10 10 11 13 12 | 14 15 16 17 | 96 102 162 245 | 73 76 127 240 | 19 18 13 11 | 1 2 3 4 5 | 762 187 677 138 229 | 726 126 646 76 229 76 | 9 12 9 14 11 19 |
| 16 17 1 | 57 49 159 144 | 28 14 14 15 16 | 177 139 121 | 118 107 | 14 16 | 6 | 196 | 208 | 16 | 7 8 | 564 236 | 604 239 | 11 |
| h | 9 7 | 17 18 | 113 | 94 35 | 18 37 | 7 | 63 50 | 65 80 | 25 30 | 10 | -48 152 | 20 91 | 31 12 |
| 11 | 189 196 183 203 | | h 2 | 8 | | 10 10 | 56 246 | 214 | 29 11 23 | 11 12 13 | 230 167 48 | 208 164 99 | 10 12 30 |
| 13 | 231 253 253 244 148 116 | 10 10 2 14 3 | 256 362 | 220 368 | 13 8 | 11 12 13 | 84 381 27 | 373 27 | 8 39 | 14 15 | 165 83 | 169 77 | 13 22 |
| 15 | 181 162 | 12 4 10 5 | 324 155 | 313 213 | 12 | 14 15 | 83 30 | 85 48 | 21 39 | 16 | 112 | 100 | 18 |
| | 50 84 | 31 6 | 250 514 | 272 465 | 10 | 16 17 | 161 115 | 160 112 | 14 18 | 1 2 | 451 | 9 463 | 9 |
| h 11 | 10 7 381 372 | 8 9 8 10 | 86 171 306 | 54 153 310 | 20 13 10 | 1 | h 7 | 8 | | 3 | 193 257 | 224 190 | 11 |
| 12 | -67 62 235 230 | 22 11 10 12 | 155 | 142 400 | 14 | , 7 8 | 334 -24 | | 13 43 | 5 6 | 258 275 | 289 299 | 10 10 10 |

| Tetrakis | (C6F | 5)-Oc | tach | loropo | phin | ato Z | inc | 6 (C6H40 | 212) | | | Pag | ge | 8 | |
|---|--|---|--|---|---|---|---|---|---|---|--|--|---|---|--|
| 7 8 | 108 290 | 36 289 | 18 10 | 11 12 | 374 276 | 362 234 | 9 10 | h | 2 | 10 | | h | 8 | 10 | |
| 9 10 11 12 13 14 15 | 45 249 44 105 138 157 96 | 60 242 67 144 132 155 94 | 33 9 30 17 14 13 20 | 13 14 15 h | 137 48 59 7 152 | 171 34 96 9 | 15 31 28 | 2 3 4 5 6 7 | 171 83 120 169 228 165 | 206 124 154 99 258 145 | 19 22 17 14 10 12 | 8 9 10 11 12 | 195 125 261 75 72 | 248 126 249 54 77 | 16 16 10 24 25 |
| 16 | 93 | 47 | 21 | 9 10 | 155 279 | 149 304 | 13 | 8 9 | 145 157 | 156 166 | 13 13 | h | 9 | 10 | |
| h 3 | 2 193 | 9 171 173 | 11 | 11 12 13 | 122 27 232 | 96 38 220 | 16 41 11 | 10 11 12 13 | 191 43 -79 | 174 16 79 | 12 32 21 | 9 10 11 | 86 71 77 | 95 45 106 | 29 25 24 |
| 4 5 6 | 208 147 97 | 173 151 73 | 11 14 19 | 14 15 | 164 54 | 145 91 | 14 30 | 13 14 | -41 135 | 47 134 | 33 16 | h | 10 | 10 | |
| 7 8 | 360 96 | 371 137 | 10 20 | h | 8 | 9 | | h | 3 | 10 | | 10 | 124 | 107 | 23 |
| 9 10 11 12 13 14 | 209 184 316 6 91 81 100 | 175 145 297 45 176 62 | 12 11 9 55 20 22 19 | 9 10 11 12 13 14 | 232 173 129 168 163 156 | 249 119 113 154 142 153 | 10 12 15 13 14 14 | 3 4 5 6 7 8 9 | 310 118 206 92 181 199 153 | 302 98 198 99 182 177 149 | 14 18 10 18 11 11 | h 1 2 3 4 | 29 -52 239 250 172 | 11 13 67 234 262 149 26 | 37 27 10 10 |
| 16 h | 67 | 52 9 | 26 | h 10 | 9 -75 | 9 49 | 21 | 10 11 12 | 103 174 78 | 149 191 53 | 18 13 23 | 6 7 8 | -76 95 76 | 26 133 95 | 21 19 23 |
| 4 5 6 7 | 344 150 334 62 | 318 149 310 78 | 9 14 10 26 | 11 12 13 14 | 94 120 88 136 | 87 129 75 133 | 20 17 21 22 | 13 14 h | 197 62 4 | 164 53 | 12 28 | 10 11 12 | 100 50 186 90 | 60 82 158 34 | 19 31 13 21 |
| 8 9 | 125 201 | 121 147 | 17 13 | h | 10 | 9 | | 4 5 | 121 -48 | 123 27 | 22 27 | h | 1 | 11 | |
| 10 11 12 13 14 15 | 368 122 80 -57 144 126 102 | 371 94 98 41 135 166 105 | 8 15 21 26 14 16 20 | 11 12 13 h | 49 91 174 11 | 51 42 142 9 | 31 21 13 | 6 7 8 9 10 11 12 | -63 28 109 16 173 82 202 | 84 44 110 7 164 113 198 | 22 38 17 47 12 22 12 | 2 3 4 5 6 7 8 | 197 135 194 209 270 146 103 | 202 70 193 199 258 154 124 | 11 14 11 11 10 14 18 |
| h | 4 | 9 | | h | 0 | 10 | | 13 | 84 125 | 87 129 | 22 17 | 9 10 | 115 201 | 107 189 | 17 |
| 5 6 | 119 167 | 125 192 | 16 13 | 0 | -21 -32 | 39 13 | 57 38 | h | 5 | 10 | | 11 12 | 75 73 | 93 53 | 24 25 |
| 7 8 9 10 11 12 13 14 15 | 289 147 168 199 87 127 176 68 -43 175 | 348 135 189 143 91 186 155 98 135 | 10 15 12 11 20 15 12 25 33 | 2 3 4 5 6 7 8 9 10 111 12 | 327 10217 10217 1187 1445 1195 1197 1197 | 423 445 215 298 172 160 125 191 181 | 9 19 12 10 14 11 13 18 10 12 22 | 5 6 7 8 9 10 11 12 13 | 144 42 144 -54 102 -28 133 94 202 | 191 130 130 39 84 45 134 186 | 18 31 13 27 18 40 15 20 12 | h 5 4 5 6 7 8 9 10 | 103 68 57 95 233 129 134 108 76 | 11 66 82 56 39 235 163 122 88 69 | 17 23 27 19 11 15 15 18 24 |
| h | 5 | 9 | | 13 14 | 79 -19 | 10 60 | 23 47 | 6 | 132 156 | 144 | 20 | 12 | -50 | 57 | 35 |
| 6 7 8 | 202 42 219 | 196 63 187 | 12 34 12 | h | 1 | 10 | | 7 8 9 | 156 152 93 | 168 133 112 | 13 13 19 | h 4 | 204 | 11 220 | 11 |
| 10 11 12 13 14 15 | 49 309 76 79 65 199 83 | 103 263 48 77 22 212 82 | 28 9 22 22 25 12 22 | 1 2 3 4 5 6 7 8 | 215 40 186 260 192 72 374 134 | 208 18 190 251 155 50 372 91 | 17 35 13 11 13 21 8 | 10 11 12 13 | 260 138 92 80 | 259 150 29 60 10 | 10 15 21 23 | 5 6 7 8 9 10 | 111 26 123 170 172 163 56 | 69 94 94 164 198 147 | 17 41 16 13 13 14 29 |
| h | | 9 | | 9 10 | -78 -66 | 77 68 | 19 23 | 8 | 283 -27 170 | 28 213 | 40 13 | H | | 11 | |
| 7 8 9 10 | 312 159 37 132 | 356 168 48 169 | 10 12 33 14 | 11 12 13 14 | 178 96 220 55 | 186 88 189 38 | 12 19 11 29 | 10 11 12 13 | 112 226 176 117 | 73 203 115 75 | 17 11 13 25 | 5 6 7 8 | 131 70 105 43 | 95 30 74 62 | 15 24 18 33 |

| Tetr | akis | (C6F | 5)-Oc | tach | loropo | rphin | ato Z | linc | 6 (C6H4C | 12) | | | Pag | ge | 9 | |
|------|------|------|-------|------|--------|-------|-------|------|----------|-----|-----|----|-----|------|-----|----|
| | 9 | 159 | 149 | 14 | 8 | 148 | 132 | 15 | 1 | 287 | 299 | 14 | 4 | -23 | 46 | 44 |
| | 10 | -73 | 50 | 23 | 9 | 102 | 103 | 19 | 2 | 69 | 9 | 24 | 5 | - 37 | 46 | 36 |
| | īĭ | 205 | 199 | 12 | 10 | 192 | 205 | 18 | 3 | 179 | 150 | 13 | 6 | 127 | 139 | 16 |
| | | 200 | 100 | | | | | | ž | 100 | 103 | 19 | 7 | 136 | 131 | 16 |
| | h | 5 | 11 | | h | 8 | 11 | | 5 | 122 | 138 | 16 | 8 | 103 | 104 | 19 |
| | п | Ð | TT | | и | | 11 | | ĕ | 88 | 30 | 21 | - | | 201 | |
| | ~ | | | | | | 101 | 4.4 | 7 | 95 | 109 | 20 | ь | 4 | 12 | |
| | 6 | -45 | 29 | 31 | 9 | 159 | 194 | 14 | | | | | п | • | 1.2 | |
| | 7 | 120 | 125 | 16 | | _ | | | 8 | 93 | 29 | 21 | - | | | |
| | 8 | 90 | 125 | 20 | h | 0 | 12 | | | _ | | | 4 | 207 | 179 | 16 |
| | 9 | 123 | 96 | 16 | | | | | h | 2 | 12 | | 5 | 57 | 29 | 28 |
| | 10 | 126 | 97 | 16 | 0 | 77 | 145 | 31 | | | | | в | 85 | 95 | 22 |
| | īĭ | 86 | 53 | 22 | 1 | 30 | 37 | 39 | 2 | 245 | 234 | 15 | 7 | 113 | 120 | 18 |
| | | • | | | 2 | 330 | 332 | 9 | 3 | 88 | 57 | 21 | | | | |
| | h | 6 | 11 | | • | 68 | 5 | 25 | Ä | 82 | 82 | 22 | h | 5 | 12 | |
| | | U | | | ã | 84 | 25 | 22 | 5 | 126 | 126 | 16 | - | - | | |
| | - | | | | 5 | 244 | 264 | īī | ě | 109 | 105 | 18 | 5 | -42 | 51 | 44 |
| | 7 | 205 | 203 | 12 | | 269 | 233 | 10 | 7 | 115 | 71 | 18 | ĕ | 56 | 106 | 29 |
| | 8 | 69 | 27 | 25 | 6 | | | | 8 | 126 | 128 | 17 | 7 | 91 | 74 | 21 |
| | 9 | 167 | 130 | 13 | 7 | 156 | 125 | 14 | ۰ | 120 | 120 | 14 | | 91 | 19 | 21 |
| | 10 | 81 | 31 | 23 | 8 | 75 | 33 | 24 | | _ | | | , | | • • | |
| | | | | | | | | | h | 3 | 12 | | h | 6 | 12 | |
| | h | 7 | 11 | | h | 1 | 12 | | | | | | - | | | |
| | | | | | | | | | 3 | 197 | 174 | 17 | 6 | 131 | 137 | 23 |

Table 1. Final Refined Parameters for Aquo, Carbonyl Tetrakis(Pentafluorophenyl)octachloroporphyrin Ruthenium(II).

x,y,z and $U_{eq}^{\ a} \times 10^4$ Ueg or B y Atom 2126(.5) 1763(.5) 1683(.3) 291(2) Ru Cl1 2662(2) 3927(2) -61(1)647(9) C1 2188(6) 3188(6) 328(3) 2.8(2) * 2635(6) 2714(6) 722(3) 2.3(2) * C2 N1 1953(5) 2315(4) 990(3) 2.1(1) * 795(3) 2.5(2) * 3597(6) 2573(6) C3 3997(6) 2.3(2) * C4 2090(5) 1169(3) 1785(5) 1581(3) 2.1(1) * N2 3546(5) 1202(4) 3.1(2) * 4960(6) 1836(6) C5 773(1) 748(11) C125843(2) 1956(2) C6 5069(7) 1380(6) 1619(4) 3.4(2) * 876(3) 1761(1) 992(14) C13 6082(2) 2.8(2) * 1364(6) 1874(4) **C7** 4191(6) 2.8(2) * **C**8 4026(6) 1052(6) 2355(4) 1023(6) 2593(4) 2.7(2) * C9 3163(6) 1189(5) 2367(3) 2.4(2) * N3 2306(5) C10 2978(7) 796(6) 3109(4) 3.2(2) * 695(10) Cl4 3744(2) 581(2) 3587(1) 3.1(2) * C11 2051(7) 828(6) 3186(4) 663(3) 813(12) 3763(1)

Cl5

1570(2)

Table 1. (Cont.)

| Atom | x | y | z | U_{eq} or B |
|------|----------|---------|---------|-----------------|
| | | | | |
| C12 | 1613(6) | 1046(6) | 2710(4) | 2.8(2) * |
| C13 | 659(6) | 1038(6) | 2602(3) | 2.5(2) * |
| C14 | 261(6) | 1224(6) | 2135(3) | 2.5(2) * |
| N4 | 715(5) | 1586(4) | 1736(3) | 2.1(1) * |
| C15 | -708(7) | 1098(6) | 1993(4) | 3.3(2) * |
| C16 | -1575(2) | 602(2) | 2313(1) | 767(11) |
| C16 | -798(7) | 1367(6) | 1519(4) | 3.4(2) * |
| C17 | -1825(2) | 1228(3) | 1192(1) | 805(11) |
| C17 | 82(6) | 1708(6) | 1360(3) | 2.5(2) * |
| C18 | 263(6) | 2147(6) | 908(3) | 2.5(2) * |
| C19 | 1108(6) | 2475(6) | 757(3) | 2.3(2) * |
| C20 | 1280(6) | 3034(6) | 342(4) | 2.8(2) * |
| C18 | 500(2) | 3514(2) | -50(1) | 718(10) |
| C21 | 4245(6) | 2982(6) | 425(4) | 309(24) |
| C22 | 4358(7) | 2698(7) | -51(4) | 460(30) |
| C23 | 4973(8) | 3078(8) | -388(4) | 532(39) |
| C24 | 5459(7) | 3762(8) | -242(5) | 494(34) |
| C25 | 5369(7) | 4056(7) | 223(4) | 418(31) |
| C26 | 4771(6) | 3684(6) | 558(4) | 347(26) |
| C31 | 4834(6) | 696(7) | 2634(4) | 390(29) |

Table 1. (Cont.)

| | Atom | x | y | z | Ueq or B |
|---|------|----------|----------|---------|----------|
| | C32 | 4985(7) | -153(7) | 2647(4) | 460(30) |
| | C33 | 5726(7) | -491(8) | 2911(4) | 521(32) |
| | C34 | 6323(7) | 34(9) | 3166(4) | 564(41) |
| | C35 | 6179(7) | 870(8) | 3155(4) | 497(34) |
| | C36 | 5457(7) | 1178(7) | 2890(4) | 485(33) |
| | C41 | 14(6) | 853(7) | 3025(4) | 375(30) |
| | C42 | -182(7) | 60(9) | 3185(4) | 548(36) |
| | C43 | -756(8) | -63(10) | 3598(5) | 655(40) |
| | C44 | -1151(9) | 600(13) | 3840(5) | 801(57) |
| | C45 | -984(9) | 1377(11) | 3683(5) | 758(46) |
| | C46 | -419(7) | 1509(8) | 3273(4) | 544(34) |
| | C51 | -564(6) | 2279(7) | 567(4) | 403(29) |
| • | C52 | -1167(7) | 2958(7) | 633(4) | 472(32) |
| | C53 | -1943(7) | 3056(8) | 342(5) | 581(38) |
| | C54 | -2128(7) | 2515(10) | -26(5) | 613(48) |
| | C55 | -1549(8) | 1857(9) | -110(4) | 626(38) |
| | C56 | -765(7) | 1723(8) | 184(4) | 487(30) |
| | F22 | 3874(5) | 2015(4) | -195(2) | 706(20) |
| | F23 | 5056(5) | 2762(5) | -849(3) | 832(25) |
| | F24 | 6020(5) | 4122(5) | -576(3) | 818(22) |

| T_{2} | ble | 1. | (Cont.) |
|---------|-----|----|---------|
| | | | |

| Atom | x | \boldsymbol{y} | z | U_{eq} or B |
|------|----------|------------------|---------|-----------------|
| | | | | |
| F25 | 5857(4) | 4728(4) | 369(3) | 648(19) |
| F26 | 4692(4) | 4006(4) | 1018(2) | 581(18) |
| F32 | 4412(4) | -675(4) | 2400(3) | 665(19) |
| F33 | 5841(5) | -1327(4) | 2922(3) | 768(21) |
| F34 | 7021(4) | -306(5) | 3428(3) | 789(23) |
| F35 | 6777(4) | 1349(4) | 3402(3) | 763(22) |
| F36 | 5338(4) | 2009(4) | 2890(3) | 741(22) |
| F42 | 198(5) | -592(4) | 2962(3) | 776(23) |
| F43 | -939(5) | -852(6) | 3747(3) | 1120(29) |
| F44 | -1711(5) | 483(7) | 4237(3) | 1269(38) |
| F45 | -1382(6) | 2026(7) | 3920(3) | 1343(35) |
| F46 | -259(5) | 2311(5) | 3120(3) | 886(24) |
| F52 | -994(4) | 3506(4) | 1002(3) | 714(21) |
| F53 | -2506(5) | 3710(5) | 414(3) | 969(27) |
| F54 | -2872(4) | 2604(5) | -321(3) | 936(29) |
| F55 | -1730(5) | 1297(5) | -476(3) | 996(26) |
| F56 | -218(5) | 1070(4) | 112(3) | 801(22) |
| C61 | 2044(7) | 2772(7) | 1999(4) | 380(27) |
| O61 | 1983(6) | 3394(5) | 2200(3) | 727(27) |
| 01 | 2165(4) | 550(4) | 1319(3) | 455(18) |

Table 1. (Cont.)

| Atom | æ | $oldsymbol{y}$ | z | U _{eq} or E | \$ |
|------|----------|----------------|----------|----------------------|----|
| C71 | 6734(14) | 1512(12) | 8525(6) | 1339(72) | |
| C72 | 7369(10) | 1351(10) | 8083(6) | 810(47) | |
| O2 | 7836(7) | 727(6) | 8029(4) | 1052(36) | |
| О3 | 7307(8) | 1937(6) | 7730(5) | 1123(39) | |
| C73 | 7799(23) | 1823(15) | 7264(11) | 2118(126) | |
| C74 | 7208(30) | 1689(27) | 6858(12) | 3385(205) | |

 $[^]a$ $U_{eq}=\frac{1}{3}\sum_i\sum_j[U_{ij}(a_i^*a_j^*)(\vec{a}_i\cdot\vec{a}_j)]$

 $^{^{}st}$ Isotropic displacement parameter, B

Table 2. Assigned Parameters for Aquo, Carbonyl Tetrakis(Pentafluorophenyl)octachloroporphyrin Ruthenium(II).

x,y,z and $U_{eq}^{a} \times 10^{4}$

| Atom | x | y | z | В | |
|------|------|------|------|------|---|
| C81 | 2113 | 608 | 117 | 10.0 | * |
| C82 | 3110 | 277 | 177 | 10.0 | * |
| O4 | 3395 | 244 | 596 | 10.0 | * |
| O5 | 3902 | 140 | -172 | 10.0 | * |
| C83 | 4801 | -74 | 1 | 13.5 | * |
| C84 | 5482 | 37 | -378 | 15.0 | * |
| C91A | 4182 | 1901 | 8228 | 15.0 | * |
| C92A | 3256 | 1464 | 8232 | 10.0 | * |
| C93A | 2614 | 1851 | 8622 | 10.0 | * |
| C94A | 1677 | 1396 | 8619 | 10.0 | * |
| C95A | 1024 | 1765 | 9002 | 10.0 | * |
| C96A | 98 | 1328 | 9006 | 15.0 | * |
| C91B | 4073 | 2287 | 8474 | 15.0 | * |
| C92B | 3311 | 1674 | 8335 | 10.0 | * |
| C93B | 2440 | 1827 | 8656 | 10.0 | * |
| C94B | 1666 | 1226 | 8527 | 10.0 | * |
| C95B | 806 | 1382 | 8845 | 10.0 | * |
| C96B | 44 | 784 | 8715 | 15.0 | * |
| C91C | 3801 | 2164 | 8479 | 15.0 | * |
| C92C | 3028 | 1549 | 8341 | 10.0 | * |
| C93C | 2156 | 1671 | 8645 | 10.0 | * |
| C94C | 1405 | 1091 | 8521 | 10.0 | * |
| C95C | 545 | 1247 | 8840 | 10.0 | * |
| C96C | -240 | 644 | 8712 | 15.0 | * |
| H71A | 6799 | 1075 | 8765 | 10.0 | * |
| H71B | 6886 | 2030 | 8677 | 10.0 | * |
| H71C | 6100 | 1528 | 8413 | 10.0 | * |
| H73A | 8214 | 1373 | 7293 | 10.0 | * |
| H73B | 8120 | 2321 | 7183 | 10.0 | * |
| H74A | 7585 | 1586 | 6569 | 10.0 | * |
| H74B | 6889 | 1151 | 6928 | 10.0 | * |
| | | | | | |

Table 2. (Cont.)

| Atom | x | $oldsymbol{y}$ | Z | В | |
|------|------|----------------|------|------|---|
| H74C | 6796 | 2099 | 6818 | 10.0 | * |
| H81A | 1811 | 602 | 432 | 10.0 | * |
| H81B | 2131 | 1164 | -8 | 10.0 | * |
| H81C | 1780 | 265 | -113 | 10.0 | * |
| H83A | 4956 | 271 | 279 | 10.0 | * |
| H83B | 4801 | -643 | 103 | 10.0 | * |
| H84A | 6077 | -112 | -249 | 10.0 | * |
| H84B | 5335 | -308 | -657 | 10.0 | * |
| H84C | 5489 | 605 | -480 | 10.0 | * |
| H91A | 4572 | 1652 | 7983 | 10.0 | * |
| H91B | 4093 | 2474 | 8150 | 10.0 | * |
| H91C | 4467 | 1853 | 8549 | 10.0 | * |
| H91D | 4606 | 2185 | 8274 | 10.0 | * |
| H91E | 3859 | 2841 | 8419 | 10.0 | * |
| H91F | 4233 | 2219 | 8818 | 10.0 | * |
| H91G | 4331 | 2059 | 8277 | 10.0 | * |
| H91H | 3589 | 2719 | 8423 | 10.0 | * |
| H91I | 3963 | 2098 | 8822 | 10.0 | * |
| H92A | 3349 | 891 | 8309 | 10.0 | * |
| H92B | 2975 | 1512 | 7910 | 10.0 | * |
| H92D | 3528 | 1121 | 8391 | 10.0 | * |
| H92E | 3154 | 1742 | 7991 | 10.0 | * |
| H92G | 3250 | 998 | 8396 | 10.0 | * |
| H92H | 2877 | 1619 | 7997 | 10.0 | * |
| H93A | 2518 | 2424 | 8546 | 10.0 | * |
| H93B | 2892 | 1803 | 8945 | 10.0 | * |
| H93D | 2227 | 2381 | 8600 | 10.0 | * |
| H93E | 2600 | 1759 | 8999 | 10.0 | * |
| H93G | 1937 | 2224 | 8590 | 10.0 | * |
| H93H | 2311 | 1603 | 8989 | 10.0 | * |
| H94A | 1777 | 823 | 8695 | 10.0 | * |

Table 2. (Cont.)

| Atom | x | y | z | В | |
|------|------|------|------|------|---|
| H94B | 1403 | 1444 | 8295 | 10.0 | * |
| H94D | 1878 | 672 | 8582 | 10.0 | * |
| H94E | 1505 | 1293 | 8183 | 10.0 | * |
| H94G | 1616 | 537 | 8577 | 10.0 | * |
| H94H | 1243 | 1158 | 8178 | 10.0 | * |
| H95A | 927 | 2338 | 8926 | 10.0 | * |
| H95B | 1301 | 1717 | 9325 | 10.0 | * |
| H95D | 593 | 1936 | 8790 | 10.0 | * |
| H95E | 967 | 1314 | 9189 | 10.0 | * |
| H95G | 334 | 1801 | 8784 | 10.0 | * |
| H95H | 708 | 1180 | 9183 | 10.0 | * |
| H96A | -292 | 1577 | 9251 | 10.0 | * |
| H96B | -187 | 1376 | 8685 | 10.0 | * |
| H96C | 187 | 755 | 9084 | 10.0 | * |
| H96D | -483 | 893 | 8918 | 10.0 | * |
| H96E | -122 | 850 | 8372 | 10.0 | * |
| H96F | 252 | 228 | 8771 | 10.0 | * |
| H96G | -762 | 759 | 8918 | 10.0 | * |
| H96H | -410 | 708 | 8370 | 10.0 | * |
| H96I | -36 | 87 | 8769 | 10.0 | * |
| | | | | | |

Population Parameters: C91A to C96A, 0.302; C91B to C96B, 0.298; C91C to C96C, 0.236. Hydrogen atoms have same population as attached carbon atom; hydrogen atoms A, B and C are on 'A' carbon atoms, D, E and F on 'B' carbon atoms and G, H and I on 'C' carbon atoms. C81, C82, C83, C84 O4 and O5 have population parameter 0.5.

Table 3. Anisotropic Displacement Parameters for Aquo, Carbonyl Tetrakis(Pentafluorophenyl)octachloroporphyrin Ruthenium(II).

| Atom | <i>U</i> ₁₁ | U_{22} | U_{33} | U_{12} | U_{13} | U_{23} |
|------|------------------------|-----------|----------|----------------|----------|----------|
| Ru | 172(4) | 413(5) | 289(4) | -13(4) | -3(3) | 76(4) |
| Cl1 | 392(16) | 884(24) | 664(21) | -5(16) | 37(15) | 444(18) |
| C12 | 327(16) | 1175(30) | 744(22) | 194(17) | 208(15) | 461(21) |
| C13 | 358(18) | 1677(40) | 944(28) | 362(21) | 171(18) | 729(28) |
| C14 | 400(17) | 1312(30) | 373(17) | 47(18) | -99(13) | 225(18) |
| C15 | 468(19) | 1627(37) | 343(17) | -69(21) | 11(14) | 200(20) |
| C16 | 333(16) | 1384(32) | 585(21) | -289(18) | -35(14) | 397(21) |
| C17 | 341(16) | 1413(34) | 659(22) | -267(19) | -130(15) | 389(22) |
| C18 | 350(16) | 1152(29) | 650(21) | 17(17) | -67(14) | 526(20) |
| C21 | 266(53) | 354(63) | 308(59) | 38(45) | -4(44) | 123(47) |
| C22 | 519(70) | 408(71) | 453(75) | -24(57) | -35(59) | -16(58) |
| C23 | 464(70) | 910(105) | 223(62) | 222(70) | 90(52) | 87(65) |
| C24 | 286(62) | 606(86) | 590(86) | 28(59) | 60(59) | 193(70) |
| C25 | 226(56) | 415(70) | 613(83) | -21(51) | -39(54) | 117(61) |
| C26 | 244(54) | 421(66) | 374(65) | 27(49) | -64(47) | 36(53) |
| C31 | 261(58) | 562(76) | 347(64) | -15(54) | 17(47) | 126(56) |
| C32 | 314(60) | 643(85) | 421(68) | -79(60) | -48(51) | 73(61) |
| C33 | 414(71) | 536(82) | 612(81) | 238(62) | 51(61) | 180(65) |
| C34 | 243(62) | 976(112) | 473(76) | 62(69) | -74(54) | 155(74) |
| C35 | 263(62) | 645(87) | 581(79) | -54(61) | -104(56) | 75(67) |
| C36 | 290(62) | 505(79) | 660(82) | -35(58) | -21(58) | 134(65) |
| C41 | 230(53) | 626(79) | 268(60) | -47(53) | -1(45) | 91(56) |
| C42 | 323(66) | 863(103) | 458(75) | -84(67) | -36(55) | 299(73) |
| C43 | 458(77) | 947(115) | 560(91) | -146(77) | -133(67) | 361(85) |
| C44 | 494(87) | 1562(174) | 348(83) | -291(103) | 55(66) | 90(93) |
| C45 | 473(82) | 1218(137) | 583(94) | 11(87) | 136(70) | -257(95) |
| C46 | 355(65) | 759(98) | 517(78) | -95(63) | 49(57) | 90(70) |
| C51 | 231(54) | 608(77) | 371(65) | 21(53) | 6(47) | 209(58) |
| C52 | 312(63) | 629(85) | 477(74) | -37(57) | 62(55) | 100(62) |
| C53 | 339(69) | 747(102) | 656(89) | 148(66) | -20(63) | 183(75) |
| C54 | 186(60) | 1063(115) | 590(88) | 76(71) | -90(60) | 235(82) |
| C55 | 540(79) | 955(106) | 380(71) | -247(82) | -187(60) | 63(74) |
| C56 | 410(65) | 628(80) | 423(69) | -6(64) | -71(53) | 100(66) |

Table 3. (Cont.)

| Atom | U_{11} | U_{22} | U_{33} | U_{12} | U_{13} | U_{23} |
|------|-----------|-----------|-----------|------------|-----------|------------|
| F22 | 679(45) | 876(56) | 565(44) | -213(40) | 65(35) | -180(39) |
| F23 | 767(50) | 1276(67) | 454(45) | 40(46) | 170(37) | -103(43) |
| F24 | 640(46) | 968(57) | 849(55) | -34(41) | 372(41) | 453(45) |
| F25 | 495(39) | 514(43) | 934(54) | -152(34) | 45(36) | 178(38) |
| F26 | 571(41) | 698(46) | 474(42) | -144(34) | 35(32) | -85(35) |
| F32 | 564(43) | 638(47) | 790(51) | 8(36) | -206(38) | 0(39) |
| F33 | 645(47) | 747(53) | 910(56) | 247(40) | -110(40) | 54(43) |
| F34 | 435(40) | 1121(61) | 809(52) | 162(39) | -250(37) | 254(45) |
| F35 | 466(41) | 945(56) | 874(55) | -133(38) | -276(38) | -16(44) |
| F36 | 493(42) | 722(53) | 1007(59) | -118(36) | -222(39) | 97(43) |
| F42 | 705(51) | 603(49) | 1021(62) | 54(41) | 119(44) | 131(44) |
| F43 | 807(58) | 1426(79) | 1125(70) | -334(54) | -101(49) | 810(63) |
| F44 | 741(55) | 2569(118) | 500(50) | -408(65) | 317(43) | 118(61) |
| F45 | 1057(70) | 1987(108) | 989(70) | 72(69) | 472(57) | -628(71) |
| F46 | 876(57) | 758(57) | 1028(63) | 22(46) | 263(48) | -212(49) |
| F52 | 466(40) | 839(54) | 835(53) | 186(36) | -48(37) | -165(43) |
| F53 | 533(46) | 1258(69) | 1115(67) | 474(48) | -72(44) | 168(54) |
| F54 | 385(40) | 1701(81) | 718(52) | 63(46) | -247(37) | 208(52) |
| F55 | 813(56) | 1311(73) | 859(60) | -68(50) | -386(47) | -240(54) |
| F56 | 776(51) | 780(53) | 844(56) | 201(44) | -269(42) | -226(43) |
| C61 | 310(59) | 389(69) | 442(70) | 27(53) | 3(50) | 66(56) |
| O61 | 807(64) | 587(63) | 787(66) | 50(49) | 51(50) | -143(51) |
| 01 | 438(43) | 417(44) | 511(47) | -6(35) | -44(35) | 3(36) |
| C71 | 1856(192) | 1558(179) | 601(107) | 552(146) | -273(118) | -139(112) |
| C72 | 777(107) | 679(106) | 974(127) | 5(86) | -104(92) | 35(100) |
| 02 | 1119(87) | 724(72) | 1314(95) | 293(65) | 222(72) | 231(67) |
| O3 | 1238(94) | 876(85) | 1255(100) | 194(68) | -35(78) | 386(75) |
| C73 | 3124(411) | 1029(170) | 2221(315) | 292(215) | 2029(317) | 446(201) |
| C74 | 4265(600) | 4101(521) | 1808(322) | -2050(429) | 1958(371) | -1157(350) |
| | | | | | | |

 $U_{i,j}$ values have been multiplied by 10^4 The form of the displacement factor is: $\exp{-2\pi^2(U_{11}h^2a^{*2} + U_{22}k^2b^{*2} + U_{33}\ell^2c^{*2} + 2U_{12}hka^*b^* + 2U_{13}h\ell a^*c^* + 2U_{23}k\ell b^*c^*)}$

Table 4. Complete Distances and Angles for Aquo, Carbonyl Tetrakis(Pentafluorophenyl)octachloroporphyrin Ruthenium(II).

| Di | stance(Å) | Dis | Distance(Å) | | |
|----------|------------|----------|-------------|--|--|
| Ru -N1 | 2.063(7) | C15 -Cl6 | 1.711(10) | | |
| Ru -N2 | 2.060(7) | C15 -C16 | 1.340(14) | | |
| Ru -N3 | 2.059(7) | C16 -C17 | 1.724(11) | | |
| Ru -N4 | 2.052(7) | C16 -C17 | 1.443(13) | | |
| Ru -C61 | 1.828(10) | C17 -C18 | 1.420(13) | | |
| Ru -01 | 2.172(7) | C18 -C19 | 1.384(12) | | |
| Cl1 -C1 | 1.717(10) | C18 -C51 | 1.507(13) | | |
| C1 -C2 | 1.446(13) | C19 -C20 | 1.448(13) | | |
| C1 -C20 | 1.327(13) | C20 -C18 | 1.710(10) | | |
| C2 -N1 | 1.373(11) | C21 -C22 | 1.359(14) | | |
| C2 -C3 | 1.411(13) | C21 -C26 | 1.400(13) | | |
| N1 -C19 | 1.385(11) | C22 -C23 | 1.404(16) | | |
| C3 -C4 | 1.385(13) | C22 -F22 | 1.350(13) | | |
| C3 -C21 | 1.510(13) | C23 -C24 | 1.354(16) | | |
| C4 -N2 | 1.368(11) | C23 -F23 | 1.335(13) | | |
| C4 -C5 | 1.444(13) | C24 -C25 | 1.334(16) | | |
| N2 -C7 | 1.384(12) | C24 -F24 | 1.336(13) | | |
| C5 -Cl2 | 1.724(10) | C25 -C26 | 1.377(14) | | |
| C5 -C6 | 1.340(14) | C25 -F25 | 1.341(12) | | |
| C6 -Cl3 | 1.705(11) | C26 -F26 | 1.338(11) | | |
| C6 -C7 | 1.437(14) | C31 -C32 | 1.376(15) | | |
| C7 -C8 | 1.398(13) | C31 -C36 | 1.363(15) | | |
| C8 -C9 | 1.396(13) | C32 -C33 | 1.384(16) | | |
| C8 -C31 | 1.489(14) | C32 -F32 | 1.342(12) | | |
| C9 -N3 | 1.393(12) | C33 -C34 | 1.378(16) | | |
| C9 -C10 | 1.452(14) | C33 -F33 | 1.349(13) | | |
| N3 -C12 | 1.374(12). | C34 -C35 | 1.354(16) | | |
| C10 -C14 | 1.714(10) | C34 -F34 | 1.336(14) | | |
| C10 -C11 | 1.349(14) | C35 -C36 | 1.345(16) | | |
| C11 -Cl5 | 1.710(10) | C35 -F35 | 1.324(13) | | |
| C11 -C12 | 1.456(13) | C36 -F36 | 1.341(13) | | |
| C12 -C13 | 1.398(13) | C41 -C42 | 1.370(15) | | |
| C13 -C14 | 1.400(13) | C41 -C46 | 1.391(15) | | |
| C13 -C41 | 1.493(13) | C42 -C43 | 1.393(18) | | |
| C14 -N4 | 1.379(11) | C42 -F42 | 1.321(14) | | |
| C14 -C15 | 1.455(13) | C43 -C44 | 1.37(2) | | |
| N4 -C17 | 1.365(11) | C43 -F43 | 1.352(16) | | |

Table 4. (Cont.)

| Distance(Å) | | | $\operatorname{Distance}(\mathbf{\mathring{A}})$ | | |
|-------------|-------|-----------|--|---------|----------------|
| C44 - | -C45 | 1.33(2) | C91C | -C92C | 1.528 |
| | F44 | 1.347(18) | | -C93C | 1.507 |
| | -C46 | 1.382(19) | | -C94C | 1.461 |
| C45 - | -F45 | 1.345(17) | C94C | -C95C | 1.524 |
| C46 - | -F46 | 1.367(14) | C95C | -C96C | 1.520 |
| C51 - | -C52 | 1.402(15) | C71 | -H71A | 0.953 |
| C51 - | -C56 | 1.384(15) | C71 | -H71B | 0.948 |
| C52 - | -C53 | 1.365(16) | C71 | -H71C | 0.957 |
| C52 - | -F52 | 1.340(13) | C73 | -H73A | 0.938 |
| C53 - | -C54 | 1.333(18) | C73 | -H73B | 0.947 |
| C53 - | -F53 | 1.338(14) | C74 | -H74A | 0.959 |
| C54 - | -C55 | 1.360(18) | C74 | -H74B | 0.993 |
| C54 - | -F54 | 1.333(15) | C74 | -H74C | 0.890 |
| C55 - | -C56 | 1.387(17) | C81 | -H81A | 0.950 |
| C55 - | -F55 | 1.351(15) | C81 | -H81B | 0.950 |
| C56 - | -F56 | 1.323(13) | C81 | -H81C | 0.950 |
| C61 - | -061 | 1.134(13) | C83 | -H83A | 0.950 |
| C71 · | -C72 | 1.52(2) | C83 | -H83B | 0.950 |
| C72 | -O2 | 1.213(19) | C84 | -H84A | 0.950 |
| C72 | -O3 | 1.331(19) | C84 | -H84B | 0.950 |
| О3 | -C73 | 1.44(3) | C84 | -H84C | 0.950 |
| C73 | -C74 | 1.39(5) | | -H91A | 0.950 |
| C81 | -C82 | 1.535 | | -H91B | 0.950 |
| C82 | -04 | 1.191 | | -H91C | 0.950 |
| C82 | -O5 | 1.490 | | -H92A | 0.950 |
| O5 | -C83 | 1.411 | | -H92B | 0.950 |
| | -C84 | 1.421 | | -H93A | 0.950 |
| | -C92A | 1.503 | | -Н93В | 0.950 |
| | -C93A | 1.526 | | -H94A | 0.950 |
| | -C94A | 1.530 | | -H94B | 0.950 |
| | -C95A | 1.512 | | 4 -H95A | 0.950 |
| | -C96A | 1.503 | | A -H95B | 0.950 |
| | -C92B | 1.515 | | A -H96A | 0.950 |
| | -C93B | 1.539 | | A -H96B | 0.950 |
| | -C94B | 1.507 | | A -H96C | 0.950 0.950 |
| | -C95B | 1.524 | | B -H91D | 0.950 |
| C95B | -C96B | 1.494 | C91 | B-H91E | 0.950 |

Table 4. (Cont.)

| Distance(Å) | | An | gle(°) |
|-------------|-------|----------------------------|----------------------|
| C91B -H91F | 0.950 | N1 -Ru -N2 | 89.3(3) |
| C92B -H92D | 0.950 | N1 -Ru -N3 | 178.8(3) |
| C92B -H92E | 0.950 | N1 -Ru -N4 | 90.4(3) |
| C93B -H93D | 0.950 | N1 -Ru -C61 | 91.6(4) |
| C93B -H93E | 0.950 | N1 -Ru -O1 | 89.2(3) |
| C94B -H94D | 0.950 | N2 -Ru -N3 | 90.3(3) |
| C94B -H94E | 0.950 | N2 -Ru -N4 | 172.2(3) |
| C95B -H95D | 0.950 | N2 -Ru -C61 | 96.4(4) |
| C95B -H95E | 0.950 | N2 -Ru -O1 | 85.9(3) |
| C96B -H96D | 0.950 | N3 -Ru -N4 | 89.8(3) |
| C96B -H96E | 0.950 | N3 -Ru -C61 | 89.6(4) |
| C96B -H96F | 0.950 | N3 -Ru -O1 | 89.7(3) |
| C91C -H91G | 0.950 | N4 -Ru -C61 | 91.4(4) |
| C91C -H91H | 0.950 | N4 -Ru -O1 | 86.3(3) |
| C91C -H91I | 0.950 | C61 -Ru -O1 | 177.6(4) |
| C92C -H92G | 0.950 | Ru -C61 -O61 | 178.9(9) |
| C92C -H92H | 0.950 | Ru -N1 -C2 | 125.7(6) |
| C93C -H93G | 0.950 | Ru -N1 -C19 | 125.6(6) |
| C93C -H93H | 0.950 | Ru -N2 -C4 | 125.8(6) |
| C94C -H94G | 0.950 | Ru -N2 -C7 | 125.2(6) |
| C94C -H94H | 0.950 | Ru -N3 -C9 | 125.0(6) |
| C95C -H95G | 0.950 | Ru -N3 -C12 | 125.2(6) |
| C95C -H95H | 0.950 | Ru -N4 -C14 | 125.6(6) |
| C96C -H96G | 0.950 | Ru -N4 -C17 | 125.7(6) |
| C96C -H96H | 0.950 | C2 -C1 -Cl1 | 128.7(7) |
| C96C -H96I | 0.950 | C20 -C1 -Cl1 | 122.5(7) |
| | | C20 -C1 -C2 | 108.4(8) |
| | | N1 -C2 -C1 | 107.9(7) |
| | | C3 -C2 -C1 | 127.9(8) |
| | | C3 -C2 -N1 | 123.7(8) |
| | | C19 -N1 -C2 | 107.9(7) |
| | | C4 -C3 -C2 | 126.2(8) |
| | | C21 -C3 -C2 C21 -C3 -C4 | 116.6(8) |
| | | | 117.3(8) 125.5(8) |
| | | N2 -C4 -C3 C5 -C4 -C3 | 126.5(8) |
| | | C5 -C4 -N2 | 107.9(8) |
| | | OO -O4 -M2 | 101.9(0) |

Table 4. (Cont.)

| Angle | (°) | An | gle(°) |
|---------------|----------|---------------|-----------|
| C7 -N2 -C4 | 108.1(7) | C17 -C16 -C15 | 108.6(9) |
| Cl2 -C5 -C4 | 129.5(7) | | 130.4(8) |
| C6 -C5 -C4 | 108.2(8) | C16 -C17 -N4 | 108.1(8) |
| C6 -C5 -C12 | 122.0(8) | C18 -C17 -N4 | 124.8(8) |
| Cl3 -C6 -C5 | 122.6(8) | C18 -C17 -C16 | 127.0(8) |
| C7 -C6 -C5 | 107.7(9) | C19 -C18 -C17 | 126.8(8) |
| C7 -C6 -C13 | 129.6(8) | C51 -C18 -C17 | 115.7(8) |
| C6 -C7 -N2 | 108.0(8) | C51 -C18 -C19 | 117.4(8) |
| C8 -C7 -N2 | 125.3(8) | C18 -C19 -N1 | 124.6(8) |
| C8 -C7 -C6 | 126.4(9) | C20 -C19 -N1 | 107.8(7) |
| C9 -C8 -C7 | 125.7(9) | C20 -C19 -C18 | 127.7(8) |
| C31 -C8 -C7 | 117.5(8) | C19 -C20 -C1 | 107.9(8) |
| C31 -C8 -C9 | 116.8(8) | C18 -C20 -C1 | 122.7(7) |
| N3 -C9 -C8 | 125.7(8) | Cl8 -C20 -C19 | 129.2(7) |
| C10 -C9 -C8 | 127.4(9) | C22 -C21 -C3 | 122.9(9) |
| C10 -C9 -N3 | 106.9(8) | C26 -C21 -C3 | 121.1(8) |
| C12 -N3 -C9 | 108.9(7) | C26 -C21 -C22 | 116.0(9) |
| Cl4 -C10 -C9 | 129.5(8) | C23 -C22 -C21 | 122.1(10) |
| C11 -C10 -C9 | 108.7(9) | F22 -C22 -C21 | 118.2(9) |
| C11 -C10 -Cl4 | 121.7(8) | F22 -C22 -C23 | 119.7(9) |
| Cl5 -C11 -C10 | 122.2(8) | C24 -C23 -C22 | 119.4(10) |
| C12 -C11 -C10 | 107.5(9) | F23 -C23 -C22 | 119.0(10) |
| C12 -C11 -C15 | 130.3(7) | F23 -C23 -C24 | 121.6(10) |
| C11 -C12 -N3 | 108.0(8) | C25 -C24 -C23 | 120.1(11) |
| C13 -C12 -N3 | 125.2(8) | F24 -C24 -C23 | 117.9(10) |
| C13 -C12 -C11 | 126.6(9) | F24 -C24 -C25 | 122.0(10) |
| C14 -C13 -C12 | 125.2(8) | C26 -C25 -C24 | 121.0(10) |
| C41 -C13 -C12 | 117.2(8) | F25 -C25 -C24 | 120.1(10) |
| C41 -C13 -C14 | 117.5(8) | F25 -C25 -C26 | 119.0(9) |
| N4 -C14-C13 | 125.7(8) | C25 -C26 -C21 | 121.4(9) |
| C15 -C14 -C13 | 126.1(8) | F26 -C26 -C21 | 119.6(8) |
| C15 -C14 -N4 | 108.2(8) | F26 -C26 -C25 | 119.0(9) |
| C17 -N4 -C14 | 108.2(7) | C32 -C31 -C8 | 120.9(9) |
| Cl6 -C15 -C14 | 129.2(7) | C36 -C31 -C8 | 122.8(9) |
| C16 -C15 -C14 | 106.8(9) | C36 -C31 -C32 | 116.3(10) |
| C16 -C15 -Cl6 | 123.6(8) | C33 -C32 -C31 | 121.3(10) |
| Cl7 -C16 -C15 | 120.9(8) | F32 -C32 -C31 | 120.4(9) |

Table 4. (Cont.)

| An | ngle(°) | | Angle | (°) |
|---------------|-----------|------------|-------|-----------|
| F32 -C32 -C33 | 118.2(9) | C54 -C53 · | -C52 | 120.2(11) |
| C34 -C33 -C32 | 119.1(11) | F53 -C53 - | -C52 | 120.0(11) |
| F33 -C33 -C32 | 119.5(10) | F53 -C53 - | -C54 | 119.8(11) |
| F33 -C33 -C34 | 121.3(10) | C55 -C54 - | -C53 | 120.3(12) |
| C35 -C34 -C33 | 119.9(11) | F54 -C54 | -C53 | 121.3(11) |
| F34 -C34 -C33 | 118.2(10) | F54 -C54 · | -C55 | 118.3(11) |
| F34 -C34 -C35 | 121.9(10) | C56 -C55 | -C54 | 121.5(11) |
| C36 -C35 -C34 | 119.4(11) | F55 -C55 | -C54 | 121.2(11) |
| F35 -C35 -C34 | 117.6(10) | F55 -C55 | -C56 | 117.3(11) |
| F35 -C35 -C36 | 123.0(10) | C55 -C56 | -C51 | 118.9(10) |
| C35 -C36 -C31 | 123.9(10) | F56 -C56 | -C51 | 119.6(10) |
| F36 -C36 -C31 | 118.5(9) | F56 -C56 | -C55 | 121.5(10) |
| F36 -C36 -C35 | 117.6(10) | O2 -C72 | -C71 | 124.5(15) |
| C42 -C41 -C13 | 123.3(9) | O3 -C72 | -C71 | 113.1(14) |
| C46 -C41 -C13 | 119.4(9) | O3 -C72 | -O2 | 122.2(14) |
| C46 -C41 -C42 | 117.3(10) | C73 -O3 | -C72 | 119.2(16) |
| C43 -C42 -C41 | 120.1(11) | C74 -C73 | -O3 | 113.0(26) |
| F42 -C42 -C41 | 120.4(10) | O4 -C82 | -C81 | 115.5 |
| F42 -C42 -C43 | 119.5(11) | O5 -C82 | -C81 | 134.5 |
| C44 -C43 -C42 | 120.8(13) | O5 -C82 | -04 | 108.6 |
| F43 -C43 -C42 | 118.8(12) | C83 -O5 | -C82 | 122.2 |
| F43 -C43 -C44 | 120.3(12) | C84 -C83 | -O5 | 111.7 |
| C45 -C44 -C43 | 120.0(14) | C93A -C92A | -C91A | 110.7 |
| F44 -C44 -C43 | 121.0(13) | C94A -C93A | -C92A | 109.7 |
| F44 -C44 -C45 | 119.0(13) | C95A -C94A | -C93A | 111.0 |
| C46 -C45 -C44 | 119.9(13) | C96A -C95A | | 112.0 |
| F45 -C45 -C44 | 119.8(13) | C93B -C92B | -C91B | 110.5 |
| F45 -C45 -C46 | 120.3(12) | C94B -C93B | -C92B | 111.8 |
| C45 -C46 -C41 | 121.8(11) | C95B -C94B | | 111.5 |
| F46 -C46 -C41 | 119.4(10) | C96B -C95B | -C94B | 111.1 |
| F46 -C46 -C45 | 118.8(11) | C93C -C92C | | 113.1 |
| C52 -C51 -C18 | 121.2(9) | C94C -C93C | | 114.3 |
| C56 -C51 -C18 | 121.1(9) | C95C -C94C | | 111.8 |
| C56 -C51 -C52 | 117.7(9) | C96C -C95C | | 111.9 |
| C53 -C52 -C51 | 121.4(10) | | -C72 | 109.9 |
| F52 -C52 -C51 | 119.2(9) | | -C72 | 110.1 |
| F52 -C52 -C53 | 119.4(10) | H71C -C71 | -C72 | 109.6 |

Table 4. (Cont.)

| | Angle(°) | | Angle(°) | |
|------------|-------------|-------|------------------|-------|
| H71B -C71 | -H71A | 109.4 | H92A -C92A -C91A | 109.2 |
| H71C -C71 | -H71A | 108.7 | H92B -C92A -C91A | 109.2 |
| H71C -C71 | -H71B | 109.1 | H92A -C92A -C93A | 109.2 |
| H73A -C73 | -03 | 109.9 | H92B -C92A -C93A | 109.2 |
| H73B -C73 | -O3 | 109.3 | H92B -C92A -H92A | 109.5 |
| H73A -C73 | -C74 | 109.4 | H93A -C93A -C92A | 109.4 |
| H73B -C73 | -C74 | 104.4 | H93B -C93A -C92A | 109.4 |
| H73B -C73 | -H73A | 110.7 | H93A -C93A -C94A | 109.4 |
| H74A -C74 | -C73 | 107.9 | H93B -C93A -C94A | 109.4 |
| H74B -C74 | -C73 | 105.6 | H93B -C93A -H93A | 109.5 |
| H74C -C74 | -C73 | 112.7 | H94A -C94A -C93A | 109.1 |
| H74B -C74 | -H74A | 105.3 | H94B -C94A -C93A | 109.1 |
| H74C -C74 | -H74A | 114.0 | H94A -C94A -C95A | 109.1 |
| H74C -C74 | -H74B | 110.8 | H94B -C94A -C95A | 109.1 |
| H81A -C81 | -C82 | 109.5 | H94B -C94A -H94A | 109.5 |
| H81B -C81 | -C82 | 109.5 | H95A -C95A -C94A | 108.8 |
| H81C -C81 | -C82 | 109.5 | H95B -C95A -C94A | 108.8 |
| H81B -C81 | -H81A | 109.5 | H95A -C95A -C96A | 108.8 |
| H81C -C81 | -H81A | 109.5 | H95B -C95A -C96A | 108.8 |
| H81C -C81 | -H81B | 109.5 | H95B -C95A -H95A | 109.5 |
| H83A -C83 | -O 5 | 108.9 | H96A -C96A -C95A | 109.5 |
| H83B -C83 | -O 5 | 108.9 | H96B -C96A -C95A | 109.5 |
| H83A -C83 | -C84 | 108.9 | H96C -C96A -C95A | 109.5 |
| H83B -C83 | -C84 | 108.9 | H96B -C96A -H96A | 109.5 |
| H83B -C83 | -H83A | 109.5 | H96C -C96A -H96A | 109.5 |
| H84A -C84 | -C83 | 109.5 | H96C -C96A -H96B | 109.5 |
| H84B -C84 | -C83 | 109.5 | H91D -C91B -C92B | 109.5 |
| H84C -C84 | -C83 | 109.5 | H91E -C91B -C92B | 109.5 |
| H84B -C84 | -H84A | 109.5 | H91F -C91B -C92B | 109.5 |
| H84C -C84 | -H84A | 109.5 | H91E -C91B -H91D | 109.5 |
| H84C -C84 | -H84B | 109.5 | H91F -C91B -H91D | 109.5 |
| H91A -C91A | | 109.5 | H91F -C91B -H91E | 109.5 |
| H91B -C91 | | 109.5 | H92D -C92B -C91B | 109.2 |
| H91C -C91 | | 109.5 | H92E -C92B -C91B | 109.2 |
| H91B -C91 | | 109.5 | H92D -C92B -C93B | 109.2 |
| H91C -C91 | | 109.5 | H92E -C92B -C93B | 109.2 |
| H91C -C91 | A -H91B | 109.5 | H92E -C92B -H92D | 109.5 |

Table 4. (Cont.)

| Angle(°) | | Angle(°) |) |
|------------------|----------------|------------------|-------|
| H93D -C93B -C92B | 108.9 | H94H -C94C -C93C | 108.9 |
| H93E -C93B -C92B | 108.9 | H94G -C94C -C95C | 108.9 |
| H93D -C93B -C94B | 108.9 | H94H -C94C -C95C | 108.9 |
| H93E -C93B -C94B | 108.9 | H94H -C94C -H94G | 109.5 |
| H93E -C93B -H93D | 109.5 | H95G -C95C -C94C | 108.9 |
| H94D -C94B -C93B | 108.9 | H95H -C95C -C94C | 108.9 |
| H94E -C94B -C93B | 108.9 | H95G -C95C -C96C | 108.9 |
| H94D -C94B -C95B | 108.9 | H95H -C95C -C96C | 108.9 |
| H94E -C94B -C95B | 108.9 | H95H -C95C -H95G | 109.5 |
| H94E -C94B -H94D | 109.5 | H96G -C96C -C95C | 109.5 |
| H95D -C95B -C94B | 109.1 | H96H -C96C -C95C | 109.5 |
| H95E -C95B -C94B | 109.1 | H96I -C96C -C95C | 109.5 |
| H95D -C95B -C96B | 109.1 | H96H -C96C -H96G | 109.5 |
| H95E -C95B -C96B | 109.1 | H96I -C96C -H96G | 109.5 |
| H95E -C95B -H95D | 109.5 | H96I -C96C -H96H | 109.5 |
| H96D -C96B -C95B | 109.5 | | |
| H96E -C96B -C95B | 109.5 | | |
| H96F -C96B -C95B | 109.5 | | |
| H96E -C96B -H96D | 109.5 | | |
| H96F -C96B -H96D | 109.5 | | |
| H96F -C96B -H96E | 109.5 | | |
| H91G -C91C -C92C | 109.5 | | |
| H91H -C91C -C92C | 109.5 | | |
| H91I -C91C -C92C | 109.5 | | |
| H91H -C91C -H91G | 109.5 | | |
| H91I -C91C -H91G | 109.5 | | |
| H91I -C91C -H91H | 109.5 | | |
| H92G -C92C -C91C | 108.6 | | |
| H92H -C92C -C91C | 108.6 | | |
| H92G -C92C -C93C | 108.6 | | |
| H92H -C92C -C93C | 108.6 | | |
| H93G -C93C -C92C | 108.3 | | |
| H93H -C93C -C92C | 108.3 | | |
| H93G -C93C -C94C | 108.3 | | |
| H93H -C93C -C94C | 108.3 | | |
| H93H -C93C -H93G | 109.5 108.9 | | |
| H94G -C94C -C93C | 100.9 | | |

Table 5. Intermolecular Distances Less Than 3.5 Å for Aquo, Carbonyl Tetrakis(Pentafluorophenyl)octachloroporphyrin Ruthenium(II).

| | Dis | tance(A) | Dista | $nce(ilde{A})$ |
|-----|-------|-----------|-----------|-----------------|
| CII | -F25 | 3.140(7) | F23 -F36 | 3.411(10) |
| | -F43 | 3.423(12) | F24 -F53 | 3.439(10) |
| - | -F43 | 3.353(11) | F24 -F54 | 2.981(10) |
| | -04 | 3.436 | F24 -F44 | 3.359(11) |
| | -F33 | 3.415(10) | F24 -F35 | 3.036(10) |
| | | 3.250(13) | F24 -F25 | 3.314(9) |
| | -C91B | 3.460 | F24 -F26 | 3.378(9) |
| | -F25 | 3.152(7) | F25 -F53 | 2.862(10) |
| - | -F43 | 3.471(12) | F25 -F25 | 3.264(9) |
| | -F43 | 2.998(12) | F26 -F33 | 2.982(9) |
| C20 | -F43 | 3.057(12) | F26 -F34 | 3.080(9) |
| C23 | -F54 | 3.191(13) | F32 -C71 | 3.249(19) |
| C24 | -F53 | 3.400(14) | F32 -C72 | 3.057(17) |
| C24 | -F54 | 3.039(13) | F32 -O2 | 3.422(12) |
| C24 | -F25 | 3.087(13) | F32 -O3 | 3.208(13) |
| C25 | -F53 | 3.140(13) | F32 -C74 | 3.47(4) |
| C25 | -C25 | 3.417(15) | F32 -C91A | 3.283 |
| C25 | -F25 | 3.060(12) | F33 -C91A | 3.203 |
| C33 | -F26 | 3.032(13) | F33 -C92A | 3.353 |
| C34 | -F26 | 3.100(13) | F33 -C61 | 3.369(12) |
| C35 | -F24 | 3.394(13) | F33 -O61 | 3.176(11) |
| C43 | -F34 | 3.246(15) | F34 -F43 | 3.170(11) |
| C44 | -F34 | 3.189(17) | F34 -F44 | 3.088(11) |
| C44 | -F35 | 3.409(17) | F34 -O61 | 3.035(11) |
| | -F35 | 3.300(16) | F35 -F44 | 3.400(11) |
| | -F45 | 3.104(16) | F35 -F45 | 3.169(11) |
| | -C96A | 3.456 | F35 -C71 | 3.442(19) |
| | -F45 | 3.157(15) | F35 -O3 | 3.367(13) |
| | -C96A | 3.444 | F36 -O3 | 3.323(13) |
| | -C81 | 3.490 | F36 -C91A | 2.576 |
| | -C82 | 3.154 | F36 -C91B | 2.652 |
| | -05 | 3.004 | F36 -C91C | 3.022 |
| | -F54 | 3.296(10) | F42 -F52 | 3.318(10) |
| | -C91A | 3.083 | F43 -F52 | 3.033(11) |
| | -C91B | 2.409 | F43 -C61 | 3.362(13) |
| | -C91C | 2.711 | F43 -061 | 3.170(12) |
| F23 | F35 | 3.491(10) | F45 -F54 | 3.013(12) |

Table 5. (Cont.)

Distance(Å)

| F45 -F55 | 3.174(12) |
|-----------|-----------|
| F45 -C96A | 3.393 |
| F46 -C95A | 3.328 |
| F46 -C96A | 3.253 |
| F46 -C95B | 3.230 |
| F46 -C96B | 3.465 |
| F46 -C95C | 3.214 |
| F52 -C74 | 3.47(4) |
| F55 -C96A | 2.975 |
| F55 -C96B | 3.448 |
| F55 -C96C | 3.228 |
| F55 -C71 | 3.47(2) |
| F55 -C81 | 3.245 |
| | 3.305 |
| F55 -O4 | 3.449 |
| F56 -C81 | 3.428 |
| F56 -C96A | 3.017 |
| O61 -C92A | 3.305 |
| O61 -C92C | 3.389 |
| O1 -C81 | 3.210 |
| O1 -C82 | 3.371 |
| 01 -04 | 2.668 |
| O1 -C96C | 3.362 |
| O1 -O2 | 2.683(12) |
| O2 -C96C | 3.306 |
| O4 -C83 | 3.060 |
| O5 -O5 | 3.309 |
| O5 -C84 | 2.343 |
| C84 -C84 | 2.453 |

Table 6. Observed and Calculated Structure Factors for Aquo, Carbonyl Tetrakis(pentafluorophenyl)porphyrin Ruthenium(II)

The columns contain, in order, ℓ , $10F_{obs}$, $10F_{calc}$ and $10\sigma F_{obs}$. A minus sign preceding F_{obs} indicates that F_{obs}^2 is negative.

| Aquo. Carbonyl Tetrakis(pentafluoro | phenyl)octachloroporphyr | in Ru(II) | | Page 1 |
|---|--|--|--|---|
| | 8 -13 2 1 8 1 785 759 17 1 2 389 339 20 0 3 1205 1179 18 1 4 406 444 19 9 5 215 114 27 7 6 292 264 23 8 7 330 316 21 8 78 163 52 | 9 72 66 59 10 794 773 18 11 405 409 21 -13 7 1 1 205 155 29 2 248 257 26 3 -29 75 81 4 181 237 32 | 9 -147 92 29 10 -126 112 34 11 278 300 23 12 257 233 24 13 313 316 22 14 225 230 27 15 111 137 44 16 531 522 19 17 614 587 19 | 9 253 252 25 10 396 387 20 11 150 195 36 12 503 488 19 13 217 267 29 14 52 84 68 15 148 222 39 -12 7 1 |
| 1 433 380 21 2 879 871 19 3 427 440 21 4 383 385 22 1 335 336 2 5 547 531 20 2 327 229 5 547 531 20 5 282 255 6 176 7 7 31 2 -15 2 1 5 282 255 2 -74 23 56 8 300 281 2 3 557 479 20 9 345 326 2 4 404 373 21 10 150 201 5 418 405 21 6 227 259 29 -14 5 1 1 608 584 19 3 694 705 1 2 9111 870 1 1 608 584 19 3 694 705 1 2 127 58 43 4 650 608 1 3 417 424 21 5 325 341 4 4 179 108 34 6 451 495 2 4 170 231 45 4 165 201 2 663 641 25 3 69 24 405 2 1 170 231 45 4 165 201 6 897 867 25 5 -43 42 8 179 205 44 6 459 466 10 631 579 26 7 366 335 12 600 555 27 -14 1 1 1 222 157 12 600 555 27 -14 1 1 1 222 157 12 600 555 27 -14 1 1 1 222 157 12 600 555 27 -14 1 1 1 222 157 12 600 555 27 -14 1 1 1 222 157 12 600 555 27 -14 7 1 1 1 246 217 26 5 5 44 6 459 466 10 631 579 26 7 366 335 12 600 555 27 -14 7 1 1 1 246 217 26 25 550 537 2 513 31 529 31 234 169 28 12 531 529 11 234 169 28 12 531 529 11 234 169 28 12 531 529 11 234 169 28 12 531 529 11 21 -155 38 31 14 963 972 | 8 78 163 52 9 391 413 20 10 493 517 19 11 228 197 27 13 12 79 136 54 15 790 766 19 3 14 464 443 20 16 464 443 20 3 268 179 24 18 29 36 390 20 3 268 179 24 18 8 -76 42 51 18 8 -76 42 51 18 8 -76 42 51 18 8 -76 42 51 18 8 -76 42 51 18 9 156 66 344 33 10 459 385 19 156 63 380 400 20 18 8 -76 42 51 18 9 156 66 34 33 10 459 385 19 15 16 6 380 400 20 18 13 41 15 15 277 260 28 16 238 243 26 17 4458 438 20 18 5 19 445 19 19 9 906 911 359 10 151 70 36 11 359 243 265 11 359 243 265 11 359 393 223 12 16 2 38 519 445 19 19 9 906 911 359 393 12 1 1 55 277 260 23 13 4 140 131 36 15 277 260 23 16 238 243 265 17 468 271 260 23 18 519 445 19 19 9 906 911 18 19 10 151 70 36 19 11 359 393 22 11 1 2-124 2 38 13 355 337 23 14 433 420 15 7 456 418 19 16 2 150 265 27 17 456 426 27 18 2 150 265 27 18 2 17 2 250 257 19 2 266 27 10 247 256 27 11 -92 66 48 11 7 12 490 529 20 18 13 716 750 19 12 -13 6 1 | 1 205 155 29 2 24 27 75 81 4 181 237 32 6 571 556 28 77 7 554 441 20 9 992 27 10 267 237 27 -13 8 1 1 223 183 28 2 470 491 20 3 229 207 28 4 399 466 21 5 143 196 39 6 76 108 58 6 76 108 58 7 146 131 39 8 62 37 65 -13 9 1 1 472 444 20 2 195 188 32 3 -156 77 315 2 222 218 40 4 -229 18 22 6 1027 177 755 -12 0 1 2 222 218 40 4 -229 18 22 6 1027 177 6 2 2 2 2 2 8 6 1027 177 753 3 -156 21 115 10 -207 6 27 14 663 568 25 16 462 422 285 -12 1 1 1 8 287 370 20 1 1 472 444 20 2 195 188 32 3 -156 77 315 2 320 402 24 3 -166 21 28 5 287 340 35 -12 1 1 1 8 287 370 24 1 9 -115 21 34 6 10 257 315 24 1 1 27 167 38 8 -122 125 346 1 1 27 167 38 8 -122 127 243 23 1 1 27 167 38 8 -122 127 243 23 1 1 27 167 38 8 -122 17 243 23 1 1 27 167 38 8 -122 127 243 23 1 1 27 167 38 8 -122 27 243 23 1 2 2 2 2 2 2 2 2 2 2 2 2 2 2 2 2 2 2 2 | 16 531 522 19 17 614 587 19 -12 3 1 1 -135 50 30 2 321 309 20 3 14 602 620 17 5 -591 64 43 602 620 17 7 184 202 29 8 4 203 18 9 513 551 18 10 -176 34 24 11 20 18 11 140 121 37 115 752 18 13 193 176 30 14 140 121 37 15 752 18 16 148 112 37 17 279 156 26 -12 4 1 1 526 550 17 2 466 433 18 13 193 176 30 14 140 121 37 15 752 18 16 148 112 37 17 279 156 26 -12 4 1 1 526 550 17 2 4 3 19 4 399 408 19 5 437 492 18 3 372 373 19 4 399 408 19 5 437 492 18 3 373 19 10 196 117 29 11 372 378 29 11 373 373 19 | |
| 8 351 88 22 8 -127 85 9 250 252 26 9 -119 100 10 164 44 35 10 205 173 11 722 695 19 11 696 677 -14 3 1 12 917 852 -14 3 1 13 85 35 14 186 27 1 600 610 18 15 256 170 | 18 9 235 205 27 17 10 247 265 27 18 12 490 529 20 18 13 716 750 19 17 10 250 20 18 13 716 750 19 17 10 10 10 10 10 18 13 1 -127 24 35 18 3 -129 70 34 18 3 1-127 24 35 18 3 -129 70 34 18 3 15 296 22 18 5 10 516 19 | 1 117 222 41 2 -131 87 31 3 187 196 28 4 -95 51 41 5 650 686 17 6 227 234 25 7 519 528 17 8 -117 1 36 | 1 354 324 20 2 -189 53 22 3 -10 144 93 4 -126 47 34 5 481 503 18 6 415 396 19 7 233 208 26 8 -67 47 56 | 14 788 760 24 16 390 466 28 18 201 258 42 20 638 603 27 -11 1 1 1 -113 24 38 |

| Aquo. Carbonyl Tetrakis(pentafluorophe | enyl)octachloroporphyrin Ru(II) | Page 3 |
|---|---|---|
| 1 53 119 70 7 41 89 66 2 172 189 35 8 455 448 18 3 197 279 32 9 459 453 19 10 163 187 32 | 10 157 70 36 -9 10 1 11 773 775 19 12 339 321 20 1 148 146 3 13 286 308 22 2 289 329 | 24 237 249 29 1 1135 1158 16 4 2 1035 1115 16 -8 4 1 2 3 571 562 15 |
| -9 0 1 11 1098 1085 19 12 -164 73 26 | 13 286 308 22 2 289 329 2 14 606 615 17 3 309 287 15 308 296 22 4 146 155 16 145 172 36 5 369 389 | 1 1135 1158 16 4 2 1035 1115 16 2 3 571 562 15 2 4 467 485 16 5 5 425 447 16 0 6 362 361 17 3 729 755 16 4 7 571 581 16 4 426 453 17 8 8 1250 1175 17 5 483 522 17 9 9 364 339 18 6 469 438 17 |
| 1 53 119 70 6 682 627 17 189 63 197 279 32 9 459 453 19 10 163 187 32 11 1098 1085 19 12 -164 73 26 48 24 11 1098 1085 19 12 -164 73 26 48 24 11 1098 1085 19 12 -164 73 26 48 24 11 1098 1085 19 12 -164 73 26 48 24 11 1098 1085 19 12 -164 73 26 16 153 185 33 10 649 625 24 17 836 845 17 12 594 649 25 18 267 300 24 14 470 511 28 19 184 214 31 16 347 401 28 20 99 183 47 18 -58 94 77 21 237 270 27 27 147 226 49 22 128 158 42 22 399 350 30 | 4 838 800 18 | 55 10 711 768 16 7 1020 1004 17 18 11 1347 1289 19 8 597 587 17 13 12 585 602 17 9 1305 1351 19 14 13 333 378 21 10 186 114 28 14 14 699 747 18 11 1071 1082 18 18 15 -41 165 71 12 392 355 20 16 -103 109 43 13 156 245 34 11 17 38 119 69 14 188 160 31 |
| 1 1110 1053 17 1 585 621 16 2 335 333 19 2 439 396 17 3 963 950 17 3 462 451 17 4 460 382 18 4 431 390 17 5 -72 11 48 5 287 306 20 6 772 774 17 | 1 158 186 33 14 -36 55 12 477 461 19 15 117 181 48 38 800 18 5 473 470 20 -9 11 1 6 295 270 24 7 254 236 26 1 212 208 8 513 512 20 2 393 389 9 314 357 24 3 255 241 10 249 276 23 18 5 12 460 522 18 6 259 249 11 476 435 18 5 665 592 12 460 522 18 6 259 249 13 80 171 51 7 158 158 161 15 114 122 42 9 320 374 16 337 360 22 10 29 69 17 243 260 26 11 144 178 18 625 672 19 12 -99 123 19 66 243 61 13 -149 0 | 18 561 557 17 15 597 597 19 19 407 367 19 16 264 233 22 20 581 579 18 17 -31 54 75 21 -66 29 56 18 146 225 35 25 23 -86 119 51 20 32 116 77 26 24 146 183 39 21 454 464 20 28 -8 21 22 242 208 29 25 -8 2 1 23 -35 122 80 |
| 8 220 222 24 9 514 544 19 10 -66 81 52 11 152 170 35 11 139 195 35 12 210 157 12 57 99 61 13 -156 57 29 13 131 191 38 14 277 265 14 -119 26 38 15 494 541 18 15 746 747 19 16 708 725 17 16 148 221 33 17 62 79 59 17 475 538 18 18 448 503 19 18 444 490 19 19 739 749 18 19 -164 79 27 20 149 93 37 20 99 137 46 21 475 494 20 21 211 252 29 22 32 34 83 23 32 109 83 -9 5 1 | 20 122 160 44 14 50 207 -9 8 1 -9 12 1 | 21 -66 |
| 2 -110 27 35 1 262 219 21 3 1127 1121 18 2 -139 133 25 4 450 481 18 3 23 10 74 5 538 501 18 4 -74 9 44 6 742 737 17 | 12 456 457 19 12 233 279 13 -126 0 35 14 14 142 91 -9 13 1 15 469 509 19 16 302 308 23 1 98 51 | 57 18 256 231 24 16 -95 138 42 41 19 336 323 21 17 51 182 63 45 20 438 445 19 18 -122 94 36 48 21 581 556 18 19 192 216 30 22 156 67 35 20 357 360 21 23 688 678 19 21 129 212 41 24 -166 34 30 22 15 58 94 48 -8 3 1 36 -8 6 1 |
| -9 2 1 1 354 391 19 2 -110 27 35 1 262 219 21 3 1127 1121 18 3 23 10 74 5 538 501 18 4 -74 9 44 6 742 737 17 5 559 540 17 7 277 310 23 6 287 283 21 8 146 148 35 7 1408 1397 19 9 994 944 18 8 626 666 17 10 626 663 19 9 421 363 19 11 60 55 62 10 -107 77 38 12 411 408 21 11 194 153 29 13 -70 78 51 12 -126 44 34 14 523 514 17 13 562 542 19 15 398 379 19 14 -85 82 49 16 825 786 17 12 -126 44 34 14 523 514 17 13 555 594 30 26 17 212 232 28 16 551 600 17 18 152 232 28 16 551 600 17 18 152 232 28 16 551 600 17 18 152 134 35 17 -78 122 49 19 374 452 21 18 460 488 19 20 44 114 72 19 72 112 55 21 184 260 33 20 423 433 20 21 29 185 82 -9 6 1 22 43 157 74 23 91 77 53 1 64 127 55 2 500 533 18 2 2 183 157 74 23 91 77 53 1 64 127 55 2 500 533 18 3 185 184 29 2 183 157 26 6 327 337 73 1 292 288 20 5 470 463 19 2 183 157 26 6 327 37 73 1 1 292 288 20 5 470 463 19 2 183 157 26 6 327 37 73 1 1 292 288 20 5 470 463 19 2 183 157 26 6 327 37 73 1 1 292 288 20 5 470 463 19 2 183 157 26 6 327 37 73 1 1 292 288 20 5 470 463 19 2 183 157 74 37 74 18 434 20 4 1165 1147 18 8 497 551 19 | 16 302 308 23 1 98 51 17 102 157 48 2 159 226 18 205 251 31 3 -95 7 19 -169 12 29 4 388 347 -9 9 1 5 104 58 1 444 456 21 8 353 326 2 454 380 21 8 353 326 2 454 380 21 8 353 326 2 454 37 115 44 5 21 8 353 326 2 454 380 21 8 353 326 2 454 380 21 8 353 326 2 454 380 21 8 353 326 2 454 380 21 8 353 326 2 523 328 23 2 1524 1513 6 190 218 28 4 559 608 7 283 256 22 6 126 71 8 602 649 17 8 605 588 9 580 550 18 10 61 105 10 93 153 47 12 300 245 11 290 280 23 14 507 557 12 -73 111 53 16 537 526 13 214 328 28 18 984 1008 14 -115 45 39 20 406 358 14 -15 -99 81 45 22 853 911 16 -18 147 92 24 300 391 17 349 358 23 | 47 1 766 835 15 8 1 417 412 18 48 33 425 441 16 2 375 353 19 35 4 11 11 69 31 3 800 791 17 47 5 1564 1565 19 4 546 526 17 23 6 89 82 40 5 683 669 17 7 372 422 18 6 1123 1174 18 8 61 128 52 7 518 485 18 8 9 936 996 17 8 749 710 18 425 11 1 578 595 17 10 776 770 18 427 11 1 578 595 17 10 776 770 18 42 12 13 15 78 12 12 13 15 78 12 12 13 15 12 12 13 13 13 13 15 15 15 15 15 15 15 16 16 16 16 16 16 16 16 16 16 16 16 16 |
| 1 292 288 20 5 470 463 19 2 183 157 26 6 327 335 22 3 85 77 43 7 418 434 20 4 1165 1147 18 8 497 531 19 5 1395 1411 19 9 -74 0 54 | 16 -18 147 92 24 300 391 17 349 358 23 -8 1 1 | 35 21 460 510 19 20 103 150 46 22 -101 98 44 21 336 265 23 23 448 430 20 22 326 338 24 |

| 7 -31 25 75 8 989 935 21 11 716 692 16 7 8 122 89 39 10 389 402 24 12 226 174 24 8 9 563 548 18 12 871 903 23 13 98 188 43 9 | 112 132 37 249 233 23 | 10 146 155 38 |
|--|---|--|
| 15 255 265 24 | 557 562 18 -80 66 50 -80 66 50 -80 66 50 -80 66 50 -80 66 50 -80 67 44 19 -91 242 50 -80 132 157 42 -7 7 1 308 366 20 -78 710 16 -78 770 17 -80 772 17 -80 773 132 29 -954 937 132 29 -954 937 132 29 -954 937 132 29 -954 937 132 29 -954 937 132 29 -954 937 132 29 -954 937 132 29 -80 177 17 -80 122 29 -80 177 17 -80 180 190 19 -80 177 17 -80 190 177 -90 190 190 190 190 -90 170 190 190 190 -90 170 190 190 190 -90 170 190 190 190 -90 170 190 190 190 -90 170 190 190 190 -90 170 190 -90 170 190 | 10 146 155 38 112 146 150 112 150 112 150 112 1436 1455 18 115 150 31 115 18 149 155 136 16 167 136 137 191 18 18 190 154 31 19 158 197 72 17 10 1 1 1 1 1 1 1 1 1 1 1 1 1 1 1 1 1 |

| Aquo. Carbonyl Tetrakis(pent | tafluorophenyl)octachloropo | rphyrin Ru(II) | | Page 6 |
|---|---|--|---|--|
| 19 1395 1373 20 10 314 20 -83 6 52 11 893 21 72 117 53 12 576 22 421 391 19 13 654 23 332 321 22 14 -76 24 190 220 31 15 100 25 284 334 25 16 333 26 37 113 79 17 688 -5 3 1 19 271 | 393 19 5 536 498 882 16 6 711 706 536 16 7 -75 61 711 17 8 145 144 138 47 9 415 430 | 17 8 491 478 20 16 9 586 576 20 332 11 -56 59 59 19 12 357 275 20 17 13 434 484 19 18 14 239 231 25 19 15 420 472 20 135 16 -103 89 42 25 17 -79 100 52 11 18 106 131 47 17 19 163 154 36 20 20 214 287 31 26 27 28 284 343 21 27 28 284 343 21 28 384 343 21 29 21 384 343 21 20 21 384 343 21 21 382 361 23 | 7 357 394 21 8 294 258 24 9 167 117 35 10 -60 73 64 -5 16 1 1 243 238 27 2 52 130 67 3 212 251 29 4 166 93 35 5 421 383 21 | 18 82 142 50 19 354 403 22 20 827 805 19 21 186 218 33 22 378 441 20 23 249 289 25 24 89 24 50 25 635 608 18 26 410 326 21 27 236 256 29 |
| 6 854 855 14 7 229 310 19 -5 6 8 -114 139 27 1 406 20 12 19 2 -70 11 1007 958 16 3 582 12 260 622 16 4 450 12 6 561 12 62 6 561 12 6 561 12 6 561 12 6 561 15 659 650 670 17 7 679 16 63 221 56 8 103 11 120 52 6 561 15 659 670 17 7 679 16 63 221 56 8 103 11 120 52 6 561 11 122 12 784 11 12 12 12 12 12 12 12 12 12 12 12 <td>352 15</td> <td>266 10 19 19 20 20 21 21 24 27 28 28 28 29 27 27 27 26 22 243 26 22 244 27 26 26 26 26 27 27 27 26 27 27 26 27 27 26 27 27 26 27 27 27 27 27 27 27 27 27 27 27 27 27</td> <td>-4 0 1 2 1019 617 17 4 3098 2866 33 6 634 814 17 8 141 94 33 10 1407 1533 22 12 -145 61 30 14 526 491 22 16 105 87 52 18 910 892 24 20 184 266 44 22 239 345 34 24 353 342 26 589 624 26 -4 1 1 1 -97 46 28 2 815 875 12 3 1587 1474 16 4 1194 1246 14 5 194 336 18 6 512 550 12 7 186 61 20 9 1326 1302 16 10 -58 40 11 356 361 16 12 366 321 16 13 569 680 15 14 888 860 16 15 847 896 16 10 58 40 11 356 361 16 12 366 321 16 13 699 680 15 14 888 860 16 15 847 896 16 15 847 896 16 15 847 896 16 15 847 896 16 15 847 896 16 15 847 896 16 15 847 896 16 15 847 896 16 17 -90 37 335 22 17 186 1302 16 18 453 490 19 19 -92 137 42 20 436 458 20 21 -38 92 76 22 156 137 20 22 292 24 27 158 186 37 24 2 1 25 216 270 28 26 292 292 24 27 158 186 37 28 1210 1123 15 9 238 195 18 10 869 898 195</td> <td>1 668 613 12 828 833 13 3 1023 99 13 4 218 156 18 5 571 595 13 6 552 595 13 6 552 595 13 7 1324 1272 16 8 -122 175 24 10 755 752 14 11 1078 1084 16 12 099 900 16 13 541 540 16 14 217 225 23 15 651 611 16 16 253 268 23 17 190 1108 18 18 557 538 18 19 245 232 26 20 204 237 20 21 285 237 22 22 127 213 38 18 19 245 232 26 22 127 213 38 23 302 309 22 24 -147 2 31 25 254 212 26 26 -129 213 37 27 34 28 17 17 13 4 657 655 13 5 199 208 19 6 1057 73 15 5 199 208 19 6 1057 937 143 58 171 147 23 18 324 657 655 13 5 199 208 19 6 1057 937 15 19 1044 1075 15 19 1044 1075 15 19 1044 1075 15 19 1044 1075 15 19 1044 1075 15 19 1044 1075 15 19 1044 1075 15 19 1044 1075 15 19 1044 1075 15 19 1044 1075 15 19 1044 1075 15 19 1044 1075 15 19 1044 1075 15 19 1044 1075 15 19 1044 1075 15 19 1044 1075 15 19 105 106 106 106 106 106 106 106 106 106 106</td> | 352 15 | 266 10 19 19 20 20 21 21 24 27 28 28 28 29 27 27 27 26 22 243 26 22 244 27 26 26 26 26 27 27 27 26 27 27 26 27 27 26 27 27 26 27 27 27 27 27 27 27 27 27 27 27 27 27 | -4 0 1 2 1019 617 17 4 3098 2866 33 6 634 814 17 8 141 94 33 10 1407 1533 22 12 -145 61 30 14 526 491 22 16 105 87 52 18 910 892 24 20 184 266 44 22 239 345 34 24 353 342 26 589 624 26 -4 1 1 1 -97 46 28 2 815 875 12 3 1587 1474 16 4 1194 1246 14 5 194 336 18 6 512 550 12 7 186 61 20 9 1326 1302 16 10 -58 40 11 356 361 16 12 366 321 16 13 569 680 15 14 888 860 16 15 847 896 16 10 58 40 11 356 361 16 12 366 321 16 13 699 680 15 14 888 860 16 15 847 896 16 15 847 896 16 15 847 896 16 15 847 896 16 15 847 896 16 15 847 896 16 15 847 896 16 15 847 896 16 17 -90 37 335 22 17 186 1302 16 18 453 490 19 19 -92 137 42 20 436 458 20 21 -38 92 76 22 156 137 20 22 292 24 27 158 186 37 24 2 1 25 216 270 28 26 292 292 24 27 158 186 37 28 1210 1123 15 9 238 195 18 10 869 898 195 | 1 668 613 12 828 833 13 3 1023 99 13 4 218 156 18 5 571 595 13 6 552 595 13 6 552 595 13 7 1324 1272 16 8 -122 175 24 10 755 752 14 11 1078 1084 16 12 099 900 16 13 541 540 16 14 217 225 23 15 651 611 16 16 253 268 23 17 190 1108 18 18 557 538 18 19 245 232 26 20 204 237 20 21 285 237 22 22 127 213 38 18 19 245 232 26 22 127 213 38 23 302 309 22 24 -147 2 31 25 254 212 26 26 -129 213 37 27 34 28 17 17 13 4 657 655 13 5 199 208 19 6 1057 73 15 5 199 208 19 6 1057 937 143 58 171 147 23 18 324 657 655 13 5 199 208 19 6 1057 937 15 19 1044 1075 15 19 1044 1075 15 19 1044 1075 15 19 1044 1075 15 19 1044 1075 15 19 1044 1075 15 19 1044 1075 15 19 1044 1075 15 19 1044 1075 15 19 1044 1075 15 19 1044 1075 15 19 1044 1075 15 19 1044 1075 15 19 1044 1075 15 19 1044 1075 15 19 1044 1075 15 19 105 106 106 106 106 106 106 106 106 106 106 |
| 1 -74 7 37 23 8 2 495 546 14 24 23 3 427 423 15 4 954 940 15 -5 5 1142 930 16 6 664 711 15 1 279 7 373 343 16 2 193 8 439 380 16 3 15 9 1131 1201 16 4 67 | 8 1 2 159 13 9 258 19 4 713 630 3 176 24 5 496 527 6 78 28 6 345 319 7 670 16 7 706 642 | 21 1 63 31 59 18 2 397 398 20 18 3 249 142 25 19 4 308 354 22 22 5 135 121 38 19 6 -78 82 52 | 11 828 768 15 12 430 451 16 13 1625 1673 19 14 301 333 19 15 472 550 17 16 825 840 17 17 -65 154 53 | 1 307 322 15 2 911 985 14 3 383 425 14 4 382 331 15 5 856 902 14 6 991 970 15 |

| Aquo, Carbonyl Tetr | akis(pentafluoropher | nyl)octachloroporphym | rin Ru(II) | | Page 7 |
|--|---|---|--|--|---|
| 7 156 39 25 8 750 700 15 9 472 530 15 10 1374 1345 17 11 919 836 16 12 745 788 16 13 777 789 16 14 323 343 20 15 148 6 32 16 1399 1424 19 17 962 915 18 18 271 214 25 19 56 68 65 20 104 176 42 21 137 10 36 22 443 459 19 22 3316 254 22 24 -118 69 39 25 331 331 23 26 216 228 31 | 1 490 438 15 2 1538 1520 18 3 212 165 22 4 326 317 18 5 351 237 18 6 199 191 24 7 435 450 17 8 1296 1268 18 9 442 453 18 10 362 19 11 339 347 20 12 145 201 34 13 435 434 19 | 1 232 228 25 2 303 295 21 3 138 22 34 4 380 399 20 5 554 427 18 6 48 27 65 7 510 482 19 8 3316 351 23 9 318 351 23 10 -124 52 37 11 -72 29 50 12 64 63 56 14 237 231 25 15 232 206 26 16 -45 151 68 17 489 503 19 18 70 77 58 19 328 357 23 20 42 0 75 | 13 -92 58 48 14 604 584 19 15 185 31 33 -4 15 1 1 124 128 39 2 78 81 52 3 205 236 28 4 341 361 21 5 142 14 36 6 224 226 27 7 224 226 27 14 36 8 -106 6 42 8 -106 6 42 8 -106 6 42 10 43 11 122 10 43 11 122 10 43 12 277 295 26 | 1 78 125 34 2 529 602 11 3 555 685 11 4 165 83 20 5 1683 1453 17 6 1974 1787 19 7 1933 1953 19 8 1124 1076 14 9 930 874 14 10 400 409 14 11 189 193 21 11 2 365 375 16 13 699 721 15 14 234 282 21 15 -88 65 38 | 18 134 165 37 19 422 43 48 20 20 431 402 21 21 493 477 17 22 302 281 22 23 379 432 20 24 301 277 23 25 108 6 45 26 -152 20 32 27 276 259 26 -3 5 1 1 71 122 37 |
| -4 6 1 1 183 110 21 2 1271 1366 16 3 392 416 15 4 413 403 15 5 646 603 14 6 178 229 23 7 1039 991 16 8 643 651 15 9 797 809 15 10 909 957 16 11 140 163 30 12 344 363 19 13 -41 160 63 14 1021 976 18 15 1011 1030 18 16 613 595 18 17 -42 9 70 18 270 194 25 19 166 146 30 20 1143 1138 18 21 729 713 17 22 600 569 18 23 132 149 39 24 129 198 41 25 164 146 36 | 1 490 438 15 2 1538 1520 18 2 1538 1520 18 3 1521 165 222 3 1321 165 223 4 326 317 18 5 3551 237 18 6 199 191 24 7 8 1296 1268 18 9 442 442 433 18 10 362 302 19 11 339 347 20 12 145 201 34 12 145 201 34 12 145 201 34 15 637 619 16 -51 106 67 17 8 238 27 33 19 500 445 18 201 434 474 19 21 -130 44 35 122 3-87 56 51 17 22 3-87 56 51 14 152 81 36 16 16 16 16 17 7 568 956 17 24 10 14 152 81 18 500 502 18 19 265 567 19 14 152 81 36 15 275 313 26 16 -180 20 23 17 270 350 20 23 17 270 350 20 23 17 270 350 20 23 17 270 350 20 23 17 270 350 20 20 20 20 20 20 20 20 20 20 20 20 20 | 8 316 351 23 338 351 23 10 -124 52 37 11 -72 29 50 12 64 63 56 13 224 235 26 14 237 231 25 15 232 206 26 16 -45 151 68 17 489 503 19 18 70 77 58 20 42 357 23 21 1 20 279 274 24 21 279 274 24 22 279 274 24 23 28 30 75 24 12 1 1 391 408 20 22 279 274 24 23 52 85 19 19 27 4 24 27 5 19 8 40 29 108 107 22 29 108 107 23 20 42 413 20 20 42 413 20 20 42 413 20 20 22 29 274 24 3 528 546 19 6 434 460 20 7 28 239 177 23 10 13 36 379 10 10 38 39 10 110 38 39 10 110 38 39 10 110 38 39 11 204 100 28 11 204 100 28 | -4 16 1 1 393 343 21 2 294 289 24 3 260 194 25 4 213 239 29 5 178 198 33 6 -132 35 36 7 135 103 40 -3 0 1 2 1253 306 20 6 2861 2643 31 8 2720 2786 30 1 2963 918 20 14 706 748 21 16 215 268 33 18 1127 1189 25 11 670 26 22 421 447 26 24 549 528 25 26 301 356 33 28 915 827 26 | 78 125 34 125 34 125 34 125 32 33 3 1 125 36 37 12 125 34 327 252 34 125 138 26 131 30 22 25 264 222 25 25 264 222 25 25 264 222 25 25 264 222 25 25 264 222 25 25 264 222 25 25 264 222 25 25 264 222 25 25 264 222 25 25 264 222 25 25 264 222 25 25 264 25 264 25 25 264 25 25 264 25 25 264 25 25 264 25 25 264 25 25 264 25 26 264 264 265 264 265 264 264 265 | |
| 2 376 946 18 2 378 404 16 3 173 197 24 4 1325 1230 17 5 617 604 15 6 367 356 17 7 1029 991 16 8 595 570 16 9 500 502 16 10 662 652 16 11 1301 1310 18 12 690 682 17 13 250 271 24 14 227 253 17 -51 90 66 15 548 543 19 16 164 277 33 17 -51 90 66 18 801 765 16 19 250 271 24 20 402 371 19 21 138 5 37 22 406 47 59 24 734 705 19 25 358 374 23 | 1 213 198 24 2 112 21 36 3 363 385 19 4 1600 202 30 5 2772 315 22 6 35 112 70 7 381 424 20 8 129 166 37 9 513 507 19 10 199 225 29 11 26 42 82 12 76 14 88 16 13 63 17 62 14 188 16 18 15 500 515 18 15 500 515 18 17 -166 42 82 17 -167 48 26 19 458 425 19 20 170 97 34 21 480 474 20 22 203 208 31 | 16 599 587 19 17 248 170 28 -4 14 1 1 240 210 24 2 258 175 23 3 91 182 46 4 177 173 30 5 394 409 19 6 506 437 18 7 95 93 45 8 176 45 30 9 190 162 29 10 183 181 31 11 195 207 30 12 -98 3 45 | 1 2191 2054 20 2 1811 1798 17 3 1128 1085 13 4 155 149 21 5 781 876 12 6 154 11 22 7 2156 2246 21 8 2619 2485 24 9 1619 1636 17 10 131 130 26 11 626 560 14 12 976 994 15 13 533 582 15 14 653 614 15 15 253 272 12 16 798 781 16 17 332 340 20 18 245 227 24 19 664 693 18 20 704 691 18 21 301 355 24 22 269 253 23 23 -25 72 81 24 304 222 269 253 23 23 -25 72 81 24 304 222 223 25 337 319 222 26 404 425 21 27 108 44 47 28 339 288 24 | 1 503 501 12 2 251 414 16 3 927 1030 13 4 1654 1642 17 5 1943 1997 19 6 1095 996 14 7 853 828 14 9 824 833 14 10 1178 1218 16 11 1411 1414 17 12 627 593 16 14 423 378 17 15 83 159 44 16 315 411 20 17 679 633 17 | 20 526 456 17 21 59 42 60 22 366 306 20 23 275 349 24 24 302 269 24 25 292 340 25 26 -139 1 36 -3 7 1 1 649 538 14 2 308 328 16 3 329 240 16 4 -53 99 47 5 532 455 15 6 550 575 15 7 512 449 15 |

| Aquo, Carbonyl Tetrakis(pentafluoroph | enyl)octachloroporphyrin Ru(II) | | Page 8 |
|---|--|--|--|
| 8 726 774 15 5 284 251 21 9 380 397 17 6 567 549 17 10 270 381 20 7 -73 49 18 11 -70 51 46 8 267 278 23 12 628 626 17 9 335 301 21 13 454 435 18 10 493 480 19 14 1057 1028 18 11 732 651 18 15 105 87 42 12 122 57 41 16 -59 73 59 13 136 152 39 17 529 446 19 14 -45 63 71 18 114 137 44 15 89 17 47 19 109 2 41 16 183 212 29 20 67 77 717 17 17 525 544 18 21 132 154 38 18 223 245 27 22 247 295 25 19 522 505 18 21 131 149 44 20 105 11 45 24 245 180 27 21 669 589 18 23 113 149 44 20 105 11 45 24 245 180 27 21 669 589 18 23 113 149 44 20 105 11 45 24 245 180 27 21 669 589 18 23 113 149 44 20 105 11 45 24 245 180 27 21 669 589 18 24 151 153 1024 16 5 310 325 21 6 638 634 15 6 23 310 325 21 6 638 634 15 6 23 310 325 21 6 638 634 15 6 23 310 325 21 6 638 634 15 6 23 310 325 21 6 638 634 15 6 23 310 325 21 6 638 634 15 6 6 231 325 21 1 401 388 18 11 -76 26 53 1 104 470 456 17 10 318 267 23 1 1401 388 18 11 -76 26 53 1 470 456 17 10 318 267 23 1 140 138 18 11 77 17 10 318 267 23 1 140 138 18 12 61 408 207 1 401 388 18 11 77 17 203 31 1 512 436 445 18 12 61 408 207 1 401 388 18 11 77 17 203 31 1 512 436 375 20 2 32 177 191 77 18 411 408 20 2 453 375 20 2 32 156 51 36 52 17 703 358 21 1 512 430 31 5 333 335 22 2 457 549 20 2 1 18 177 59 17 18 411 408 20 2 169 167 32 20 96 98 50 2 1 2 24 30 31 5 333 335 22 2 457 549 20 2 1 18 177 203 31 1 512 436 375 20 2 3 156 51 36 5 27 17 19 19 555 447 19 19 419 394 19 19 555 447 19 19 419 394 19 19 555 447 19 19 419 394 19 19 19 555 447 19 19 419 394 19 19 19 555 447 19 19 419 394 19 19 19 555 447 19 19 419 394 19 19 19 555 447 19 10 426 473 19 11 414 456 18 10 500 1035 17 11 414 456 18 10 500 1035 17 11 414 456 18 10 500 29 10 127 140 36 11 414 415 19 14 129 132 38 11 512 436 439 19 16 428 414 120 67 32 77 703 358 21 1 516 517 441 18 127 28 655 18 15 14 129 132 38 15 15 466 430 20 18 259 207 26 16 371 416 19 19 361 392 22 11 203 33 31 72 216 256 207 26 11 416 605 582 18 | 12 | 23 381 382 20 24 -77 38 52 25 -136 3 34 26 69 94 60 27 234 229 28 28 -133 135 38 -2 4 1 1 1437 1247 151 2 591 602 114 4 223 114 17 5 2625 476 12 7 36 63 54 8 894 856 14 9 631 548 13 10 194 92 21 11 1270 1248 16 12 505 476 12 7 36 69 63 12 20 1248 16 12 505 488 17 11 1270 1248 16 12 505 488 17 13 724 697 15 14 244 225 21 15 883 944 16 16 505 488 17 17 100 121 428 16 69 69 22 549 544 17 23 32 61 77 24 45 69 69 25 651 572 28 27 396 382 22 27 396 382 22 28 28 28 132 29 104 99 28 19 5 1668 1655 18 6 1136 1117 15 7 1145 137 15 9 1040 992 16 11 1133 1144 16 11 1131 1198 17 1198 177 15 7 1145 133 134 15 9 1040 992 16 10 350 268 15 11 1133 1144 16 11 1131 1198 17 11 198 17 11 198 17 11 198 17 11 198 17 11 198 17 11 199 198 19 10 108 51 11 113 1144 16 12 1191 1198 17 13 45 135 57 14 823 942 16 15 919 91 198 13 4 199 298 19 5 1668 1334 1374 15 9 1040 992 15 10 350 268 15 11 1133 1144 16 11 1131 1198 17 11 198 17 17 57 55 59 18 209 221 26 19 10 18 57 19 10 18 13 19 19 992 21 10 350 268 15 11 1133 1144 16 12 1191 1198 17 17 17 57 55 59 18 209 221 257 26 18 229 221 26 27 28 28 29 28 297 257 257 257 28 297 257 257 29 129 297 257 257 29 129 297 257 257 29 129 297 257 257 20 129 297 257 257 20 129 297 257 257 21 129 257 257 257 22 129 257 257 257 23 39 24 | Page 8 10 416 435 16 11 149 182 28 12 786 832 16 13 537 552 16 14 683 755 16 15 -1007 17 27 18 -73 105 53 19 -107 103 42 20 304 351 45 22 -148 53 30 22 -148 53 30 22 -148 53 369 24 406 386 20 25 278 253 25 26 580 5537 19 -2 7 1 1 203 2000 19 2 828 779 14 3 1029 1070 15 4 828 779 14 5 666 671 14 7 834 772 15 8 1168 1185 16 6 666 671 14 7 834 772 15 8 1168 1185 16 10 414 399 17 11 192 268 24 16 666 671 14 7 834 772 15 18 237 216 10 414 399 17 11 192 268 24 16 613 657 19 18 237 216 10 414 399 17 11 192 268 24 444 15 13 616 17 15 188 212 28 16 419 426 20 17 613 657 19 18 237 216 28 23 183 304 23 24 157 33 25 25 1586 1642 18 20 366 418 20 21 194 262 29 23 1586 1642 18 23 1836 823 18 24 157 33 25 25 1586 1642 18 21 296 305 23 22 1586 1642 18 23 340 251 24 24 17 459 19 15 97 77 749 90 16 186 244 31 17 459 19 15 97 77 749 16 10 439 445 17 11 575 567 17 12 338 251 24 14 417 459 19 15 97 77 749 11 16 186 244 31 17 459 19 15 97 77 746 16 186 244 31 17 459 19 15 97 77 749 11 16 186 244 31 17 459 19 18 242 244 17 19 125 328 34 221 296 305 23 223 314 313 22 23 3500 514 19 224 278 234 252 23 500 514 19 224 278 234 252 225 255 257 |
| | 28 218 261 42 13 139 124 28 14 546 504 16 -2 1 1 15 1153 1138 17 16 110 150 37 | 1 809 732 13 2 1333 1342 15 3 1108 1163 14 | 20 426 305 23 21 296 305 23 22 314 313 22 23 500 514 19 24 278 234 25 |
| -3 10 1 5 98 48 42 6 579 567 17 7 218 258 25 1 145 128 30 8 286 249 21 2 74 53 46 9 -154 22 27 3 367 350 18 10 234 259 25 4 110 189 36 11 120 59 39 | 1 822 430 10 17 840 828 17 2 613 432 9 18 598 584 18 3 807 992 10 19 108 181 43 4 1603 1446 15 20 567 557 19 5 762 731 11 21 231 261 28 6 1189 1083 13 22 -128 8 33 | 1 809 732 13 2 1333 1342 15 3 1108 1163 14 4 558 488 13 5 838 934 14 6 438 416 14 7 871 933 14 8 737 727 14 | 25 254 217 28 -2 9 1 |
| 1 145 128 30 8 286 249 21 2 74 53 46 9 -154 22 27 3 367 350 18 10 234 259 25 4 110 189 36 11 120 59 39 | 2 613 432 9 18 598 584 18 3 807 992 10 19 108 181 43 4 1603 1446 15 20 567 557 19 5 762 731 11 21 231 261 28 6 1189 1083 13 22 -128 8 33 | 6 438 416 14 7 871 933 14 8 737 727 14 9 210 231 21 | 1 466 424 15 2 339 345 17 |

| Aquo, Carbonyl Tetrakis(pentafluoroph | enyl)octachloroporphyrin Ru(II) | | Page 9 |
|---|---|--|--|
| 3 360 416 17 4 455 431 19 4 977 911 16 5 282 299 23 5 1533 1568 19 6 296 308 23 5 507 505 16 7 486 496 19 7 260 126 20 8 511 539 19 8 25 4 71 9 460 488 20 9 418 451 18 10 164 195 29 10 284 296 21 11 184 246 28 11 299 336 21 12 403 409 19 12 -58 121 57 13 535 527 17 13 379 390 20 14 22 4 82 14 12 5 252 30 15 -144 46 30 15 294 256 27 16 -136 47 32 16 75 184 56 17 140 141 37 17 207 188 26 18 268 284 25 18 141 104 30 19 326 334 23 19 -145 27 30 20 114 164 46 20 266 226 24 1444 485 19 -2 13 1 22 140 31 33 31 23 587 524 19 1 222 149 27 24 177 150 35 2 250 238 26 24 177 150 35 2 250 238 26 25 267 149 20 7 195 182 27 24 336 335 18 9 272 310 22 2 267 149 20 7 195 182 27 3 404 477 17 8 152 34 32 2 267 149 20 7 195 182 27 3 404 477 17 8 152 34 32 2 267 149 20 7 195 182 27 3 404 477 17 8 152 34 32 2 267 149 20 7 195 182 27 3 404 477 17 8 152 34 32 2 267 149 20 7 195 182 27 3 404 477 17 8 152 34 32 2 267 149 20 7 195 182 27 3 404 477 17 8 152 34 32 2 19 105 1167 18 14 115 112 41 10 56 48 59 11 211 26 26 7 964 976 17 12 134 6 36 8 148 5 32 13 121 98 39 9 1065 1167 18 14 115 112 41 10 56 48 59 11 211 26 26 7 964 976 17 12 134 6 36 8 148 5 32 13 121 98 39 9 1065 1167 18 14 115 112 41 10 56 48 59 18 16 277 258 25 12 184 146 31 17 -144 13 33 15 289 310 21 -2 14 1 | 3 176 187 32 16 816 825 16 4 210 185 28 17 115 129 36 5 247 296 26 18 271 267 22 6 258 241 25 19 -90 41 44 7 370 356 21 20 383 405 21 8 -84 21 51 21 904 910 19 9 197 178 31 22 346 309 23 1 109 15 45 26 284 252 24 2 153 23 36 27 642 549 19 -1 0 1 2 1820 1874 19 4 3047 2601 31 1 1863 182 17 6 2037 1786 23 2 696 731 11 8 1940 1988 23 3 1502 1195 15 10 748 629 18 4 1478 1488 15 112 411 494 21 5 116 174 26 11 104 114 51 8 2123 2108 21 22 696 670 27 10 526 492 13 126 149 68 87 12 379 392 15 28 773 662 26 13 1267 1142 17 26 49 68 87 12 379 392 15 27 1 1 1 15 91 87 40 1 1227 1059 11 17 1079 1094 17 | 2 1067 1059 13 3 380 383 13 4 2124 2167 20 5 1266 1253 15 6 971 921 14 7 305 325 15 8 1056 1109 15 9 738 707 14 10 113 20 30 111 778 802 15 112 367 418 17 13 610 591 15 14 543 568 16 15 738 698 16 15 738 698 16 15 246 299 23 17 623 597 17 18 987 969 18 19 624 592 19 20 503 539 20 21 337 341 20 25 504 965 18 23 -63 132 58 24 341 350 22 25 504 965 18 23 -63 132 58 24 341 350 22 25 615 585 18 22 3 -63 132 58 24 341 350 22 25 615 581 18 27 246 293 28 -1 6 1 1103 1017 14 2 1303 1217 2 144 82 26 17 7 340 382 15 7 340 382 15 7 340 382 15 7 340 382 15 7 340 382 15 7 340 382 15 18 42 1490 17 9 144 82 26 10 814 766 15 11 852 845 15 12 828 800 16 13 949 1000 16 14 589 576 16 13 3949 1000 16 14 589 576 16 13 3949 1000 16 14 589 576 16 15 326 373 20 16 1277 2 1236 19 17 629 593 18 18 422 499 20 19 -124 139 37 20 212 232 30 17 232 30 21 -66 51 55 22 -154 29 23 -163 4 27 24 190 30 26 63 127 664 | Page 9 21 478 522 18 22 322 338 22 23 225 263 27 24 415 396 20 25 110 106 46 26 217 258 30 -1 8 1 1 244 331 18 2 403 340 15 3 527 550 14 4 501 445 15 5 6 50 616 15 6 52 59 51 7 235 258 20 4 45 613 16 10 144 16 29 11 1032 980 17 12 290 357 21 11 032 980 17 12 290 357 21 13 211 224 26 14 -130 22 31 15 316 334 22 11 5 316 334 22 11 5 316 334 22 11 5 316 334 22 11 5 316 334 22 12 290 357 21 12 290 357 21 12 290 357 21 13 211 224 26 14 -130 22 31 15 316 334 22 16 4 28 60 19 323 389 21 20 426 435 19 21 20 426 435 19 22 515 475 19 23 287 317 24 24 -90 75 49 25 -164 37 30 -1 9 1 1 377 316 313 31 24 275 272 19 25 -164 37 30 -1 9 1 1 377 316 16 2 118 113 31 3 16 3 17 365 17 6 253 149 20 7 12 25 179 22 6 179 22 7 18 226 179 22 |
| 17 164 162 32 1 86 36 46 18 156 186 33 2 374 356 19 19 263 281 24 3 109 87 40 20 189 196 30 15 -85 39 45 22 181 155 33 6 351 367 20 23 190 224 33 7 195 157 28 -2 11 1 9 169 58 31 1 351 18 31 134 211 35 2 338 338 19 12 5 -43 558 18 3 687 661 17 13 131 124 39 4 -68 38 50 14 194 210 30 5 344 398 20 15 -5 161 102 6 256 334 23 16 49 21 71 337 348 20 8 224 188 26 -2 15 1 9 750 763 18 10 136 21 37 1 160 121 32 11 379 457 21 2 258 289 23 12 176 64 33 3 241 239 25 13 -28 69 75 4 366 313 20 14 152 242 33 5 194 158 29 15 462 408 18 6 -57 23 60 16 -17 143 87 7 314 320 22 17 370 330 22 12 125 11 41 1 158 66 32 2 1370 330 22 12 125 11 41 1 158 66 32 2 5569 586 18 1 490 434 19 3 176 72 30 2 143 44 36 | 1 1227 1059 11 17 1079 1094 17 2 1020 1264 10 18 296 257 22 3 345 152 10 19 1057 1045 18 4 1123 753 12 20 309 310 23 5 799 658 11 21 236 201 28 6 586 640 11 22 -52 104 61 7 148 172 22 23 166 261 32 8 196 225 19 24 79 58 53 9 829 876 13 25 397 361 20 10 787 729 13 26 131 60 40 11 999 965 14 27 293 252 25 12 1783 1810 19 28 -144 122 35 13 448 373 15 -1 4 1 2 1 1 1 1 1 1 1 1 1 1 1 1 1 1 1 1 | 17 629 593 18 18 422 409 20 19 -124 139 37 20 212 232 30 21 -66 51 55 22 -154 29 29 23 -163 4 27 24 190 172 31 25 -117 30 40 -1 7 1 1 609 579 13 2 348 339 15 3 384 401 14 4 360 397 15 5 1072 1110 15 6 1952 1986 20 7 281 268 17 8 945 897 15 9 423 377 16 10 830 780 15 11 663 594 16 12 32 32 33 66 12 32 33 66 12 32 33 66 12 32 33 66 12 32 33 66 12 32 33 66 12 32 33 66 12 32 33 66 13 -83 957 17 14 969 957 17 204 177 29 18 650 645 19 19 -122 62 38 20 -162 27 26 | 1 377 316 16 2 118 113 31 3 76 6 41 4 275 272 19 5 1307 1365 17 6 253 149 20 7 1243 1315 17 8 226 179 22 9 615 17 10 442 493 18 11 509 615 17 12 -55 20 57 13 267 240 23 14 325 405 22 13 319 339 23 16 -95 103 46 13 319 339 23 16 -95 103 46 17 319 339 23 18 148 195 33 18 148 195 33 18 148 195 33 18 148 195 33 18 12 339 339 23 21 -113 62 37 22 -124 37 35 21 -115 62 37 22 -124 37 35 21 -115 62 37 22 397 393 21 24 27 10 1 1 501 458 16 2 390 397 17 3 600 636 16 4 214 81 23 5 561 516 16 6 76 135 399 19 8 -98 65 37 9 905 966 17 10 209 143 26 11 626 586 19 10 209 143 26 11 626 597 61 11 -152 98 29 |

| Aquo. Carbonyl Tetrakis(pentafluorophenyl)octachloroporphyrin Ru(II) | · | Page 10 |
|--|---|--|
| 15 407 390 21 | 3 1974 1997 20 4 740 794 13 5 902 803 14 6 2164 2172 21 7 780 802 14 8 807 783 14 10 1174 1169 16 111 1408 431 16 112 765 750 15 13 344 225 15 13 344 225 15 13 344 225 15 14 294 346 22 15 135 154 33 115 135 154 33 12 295 20 15 135 154 229 15 13 739 388 20 15 135 154 229 15 13 739 388 20 15 137 139 388 20 15 137 139 388 20 15 137 139 388 20 16 111 1122 12 17 379 388 20 18 224 255 276 24 23 136 443 20 25 274 261 25 26 71 26 20 27 1 101 239 16 27 179 420 477 16 27 179 420 477 16 28 1371 1483 17 16 706 680 15 11 261 255 204 17 179 420 477 16 10 706 680 15 11 261 255 204 17 179 420 477 16 10 706 680 15 11 261 255 20 307 306 21 21 191 239 16 14 584 638 17 15 605 531 17 16 908 80 14 2 937 977 15 3 466 433 37 2 298 37 17 156 680 761 165 3 17 256 27 23 156 84 337 22 671 689 17 23 156 84 337 24 127 45 37 25 247 256 27 26 374 298 37 3 466 766 386 21 22 177 132 129 383 16 16 7 660 761 155 8 123 797 15 3 466 7660 761 165 17 782 797 16 18 183 313 360 22 17 132 129 383 360 12 17 132 129 383 360 12 17 132 129 383 360 12 17 132 129 39 18 18 363 2498 18 20 724 752 17 175 26 31 | 22 113 158 43 222 233 338 324 222 223 243 349 376 222 233 263 299 0 9 1 1 682 684 15 270 234 430 17 128 25 5944 886 16 6 428 441 16 7 372 443 17 18 19 120 39 982 16 15 535 464 20 13 746 755 17 18 119 120 39 16 526 259 26 17 18 19 120 39 16 16 260 259 26 17 18 19 120 39 16 16 260 259 26 17 18 19 120 39 16 16 260 259 26 17 18 19 120 39 16 16 260 259 26 17 18 19 120 39 16 16 260 259 26 17 18 19 120 39 16 16 260 259 26 17 18 19 120 39 16 16 260 259 26 17 18 19 120 39 16 16 16 16 16 16 16 16 16 16 16 16 16 |

| Aquo. Carbonyl Tetrakis(pentafluoroph | nenyl)octachloroporphyrin Ru(II) | | Page 11 |
|---------------------------------------|--|---|--|
| 18 | 11 1298 1356 16 26 90 93 52 12 742 721 14 27 168 60 36 13 1947 1911 21 | 7 730 689 15 1 844 8 8 935 970 16 2 243 2 9 237 301 21 3 399 4 10 419 405 17 4 636 6 11 383 405 18 5 826 7 112 429 513 17 6 134 2 14 653 681 17 8 464 5 15 235 195 25 9 161 1 16 556 490 19 10 180 1 17 582 629 19 11 952 10 18 -25 115 85 12 444 3 19 348 309 20 13 586 5 20 799 829 17 14 -93 21 501 452 18 15 109 1 22 286 260 23 16 446 4 23 228 244 28 17 565 5 24 235 198 28 18 256 2 25 642 602 19 19 456 4 23 228 244 28 18 15 109 1 24 255 198 28 18 256 2 25 642 602 19 19 456 4 1 9 1 21 164 1 0 536 515 11 1 12 1 1500 1485 18 2 2 221 122 20 0 403 4 4 676 595 15 2 512 4 4 138 384 403 18 6 287 2 9 370 355 18 7 141 1 9 370 355 18 7 141 1 9 370 355 18 7 141 1 10 94 88 41 8 545 5 1 11 12 188 237 27 10 329 4 | 6 33 7 4 2 20 11 12 20 11 13 20 11 14 45 17 19 18 18 19 19 19 19 19 19 19 19 19 19 19 19 19 |

| Aguo, Carbonyl Tetr | akis(pentafluoropher | nyl)octachloroporphyr | rin Ru(II) | | Page 12 |
|---|---|--|---|---|---|
| 12 122 21 37 13 365 377 19 14 424 436 19 15 209 1111 27 16 140 79 35 17 -88 64 46 18 114 99 42 19 120 89 42 20 305 377 24 1 13 1 0 745 789 13 1 179 126 31 2 440 399 20 3 159 38 34 4 231 237 27 5 223 234 28 6 242 255 23 7 132 24 34 8 49 26 62 9 164 7 31 10 57 577 17 11 302 328 22 12 718 713 17 13 281 261 23 14 405 374 19 15 -136 51 32 14 405 374 19 15 -136 51 32 14 405 374 19 15 -136 51 32 16 295 22 17 -47 97 68 18 499 482 19 1 14 1 0 151 107 23 1 299 262 21 2 567 595 17 3 108 420 19 5 78 55 50 16 163 176 31 | 7 139 224 38 8 85 115 52 9 454 478 20 10 210 140 30 1 17 1 1 179 190 32 2 52 52 57 4 163 82 35 2 0 1 1 1 1 1 1 1 1 1 1 1 1 1 1 1 1 1 1 | 13 479 408 15 14 247 245 20 15 360 325 18 16 950 951 17 17 127 67 35 18 816 764 17 19 649 596 18 20 109 31 44 21 -152 49 30 22 494 464 17 23 578 546 17 24 194 75 29 25 635 609 18 26 32 24 80 27 105 71 48 28 184 41 34 2 3 1 0 178 219 13 1 135 1224 12 2 2251 2131 15 3 605 369 11 2 2 2 2 251 2131 15 3 605 369 11 2 2 2 2 2 2 2 2 2 2 2 2 2 2 2 2 2 2 | 2 5 1 0 465 518 9 1 398 373 12 2 505 569 12 3 559 484 12 4 751 684 12 4 751 684 12 5 1786 1556 18 6 540 426 13 8 782 642 14 10 240 255 19 11 410 430 15 12 335 330 17 13 1059 1092 16 14 626 611 16 14 626 611 16 15 -89 60 39 16 337 277 20 17 1043 1018 18 18 262 286 25 19 479 478 20 20 305 300 24 21 -98 111 41 22 198 111 47 23 469 479 19 24 -99 96 47 21 -98 111 47 23 469 479 99 24 -99 96 25 117 213 43 26 3 130 106 27 14 71 98 2 6 1 0 590 552 13 | 14 1190 1262 18 15 169 96 30 16 743 684 18 17 189 230 30 18 184 204 35 20 718 745 17 21 264 216 24 22 142 224 36 23 209 205 29 24 -150 129 31 25 -83 9 53 2 8 1 0 797 81 91 1 5511 462 14 2 280 284 17 3 742 752 14 4 653 698 14 5 126 171 29 6 891 772 283 17 8 142 110 5 898 144 195 33 114 41 38 14 21 0 39 17 -161 189 27 18 473 506 17 13 114 41 38 14 -67 85 51 15 218 213 26 16 -107 0 39 17 -161 189 27 18 473 506 17 | Page 12 6 488 444 78 9 30 41 73 10 116 94 39 11 571 632 18 12 699 647 18 13 329 647 18 13 329 402 22 14 169 227 33 16 501 456 17 17 505 579 17 18 354 372 20 19 204 181 28 20 86 59 50 21 -53 62 65 22 -154 30 31 23 543 513 20 2 11 1 0 366 318 13 1 304 342 20 2 87 42 44 3 4172 195 28 2 11 1 0 366 318 13 1 304 342 20 2 2 7 42 44 3 4 172 195 28 5 254 216 23 6 259 185 23 7 449 507 19 8 197 53 28 9 996 1008 18 10 145 120 36 11 -93 77 45 12 160 94 35 11 -93 77 45 12 160 94 35 11 -93 77 45 12 160 94 35 11 -93 77 45 12 160 94 35 11 -93 77 45 12 160 94 35 11 -93 77 45 12 160 94 35 11 -93 77 45 12 150 94 35 11 -93 77 45 12 150 94 35 11 -93 77 45 12 150 94 35 11 -93 77 45 12 150 551 19 |
| 0 151 107 23 1 299 262 21 2 567 595 17 3 108 119 40 4 388 420 19 5 78 55 50 6 16 16 34 256 23 8 516 48 18 9 214 100 27 10 346 334 21 11 102 0 0 44 12 -56 97 61 13 253 185 25 14 472 492 19 15 66 134 60 16 290 311 25 1 15 1 0 433 423 13 1 197 91 27 2 -74 70 50 3 69 67 54 4 370 325 20 5 148 131 34 6 488 449 18 7 -91 48 44 8 134 22 21 1 16 1 0 150 71 25 1 240 310 25 2 169 78 32 3 428 449 19 4 225 141 27 5 102 21 45 6 145 100 36 | 0 240 407 9 9 1 683 400 9 1 683 400 9 1 12 3 1509 1489 14 14 5 186 134 18 6 365 249 12 18 17 18 16 18 18 1307 1278 15 10 418 368 14 11 2 694 676 14 13 209 198 21 16 716 716 715 716 716 716 717 15 718 17 4 9 19 15 716 717 15 719 17 73 14 21 15 719 | 19 887 83 68 20 65 31 68 20 65 31 66 20 22 -148 84 66 18 24 455 419 19 25 484 461 19 26 109 213 46 27 615 571 19 2 24 1 2156 61 266 1726 17 234 324 256 18 285 252 23 19 549 546 29 20 156 222 73 174 53 1657 1659 10286 1288 16 11 1405 1375 17 12 170 73 24 13 1027 1056 16 14 669 702 16 15 189 212 25 16 148 148 31 17 1657 1659 20 18 285 252 23 19 549 546 29 20 156 222 73 174 53 23 691 657 1659 20 122 73 174 53 23 691 657 172 24 482 452 19 92 27 -116 2 42 | 1 590 552 13 2 1050 11103 14 2 1033 226 17 4 283 225 124 6 1047 1025 15 7 851 950 14 9 699 720 14 10 647 638 15 11 236 321 20 12 178 596 15 13 628 596 15 14 261 234 21 15 370 385 19 16 1409 1377 19 17 257 252 24 18 5 960 861 18 19 54 74 66 20 -67 93 53 20 738 728 17 20 27 273 23 22 738 728 17 20 111 120 43 24 -17 190 90 25 -161 193 125 21 114 165 47 2 7 1 0 91 40 24 1 364 359 14 2 800 735 14 3 251 252 17 4 807 901 14 5 406 275 15 6 353 404 16 7 11 4 67 91 1 5 406 275 15 6 353 404 16 7 11 69 212 25 10 419 409 15 10 419 409 15 11 169 212 25 12 177 204 26 13 194 158 25 | 2 9 1 0 568 599 11 1 457 476 15 2 566 503 15 3 38 109 58 4 113 102 28 6 558 582 16 7 767 769 16 8 1023 1096 17 9 443 409 17 12 217 247 25 13 651 618 18 14 340 37 21 15 425 477 20 16 500 482 19 21 109 121 18 241 271 24 19 757 769 18 2 10 1 0 288 208 14 1 547 23 23 79 24 165 154 36 2 10 1 0 288 208 14 1 547 36 31 3 355 274 18 4 409 958 17 | 2 12 1 0 423 489 18 2 144 102 34 3 214 128 26 4 576 628 18 5 414 319 20 6 370 389 21 7 534 502 19 8 440 427 20 9 192 55 31 10 249 106 23 11 573 608 17 12 290 242 22 13 494 516 18 14 154 171 33 15 27 86 78 16 524 516 18 14 154 171 33 15 27 86 78 16 524 399 19 18 374 361 21 19 181 22 32 2 19 217 29 2 13 1 0 516 548 14 1 185 23 30 2 652 586 18 3 521 510 19 4 443 398 20 5 133 106 39 6 128 0 35 7 183 169 28 |

| Aquo. Carbonyl Tetrakis(pentafluorophe | nyl)octachloroporphyrin Ru(II) | | Page 13 |
|---|---|---|--|
| 8 668 649 16 16 352 288 26 9 223 274 25 18 910 846 24 10 345 424 20 20 1352 1303 27 11 287 229 22 22 -176 30 33 12 171 121 31 24 670 608 24 13 335 261 21 26 49 132 88 14 381 447 20 28 217 69 43 15 109 133 43 16 252 307 25 3 1 1 17 219 209 28 18 381 383 21 0 1243 1019 11 | 5 888 806 13 21 8 161 94 6 -51 165 44 22 745 780 17 7 628 565 13 23 601 551 18 8 -53 10 44 24 -24 17 84 9 1010 1002 14 25 483 515 20 10 150 64 24 26 351 360 23 11 1584 1540 18 12 125 49 29 3 6 1 13 200 264 23 14 117 86 34 0 329 299 10 15 461 493 17 1369 1243 16 16 208 125 25 2 799 674 13 | 10 347 361 18 11 -49 94 57 12 441 424 18 13 787 783 17 14 851 815 18 15 58 194 60 16 -106 156 40 17 190 213 31 18 -108 152 37 19 302 304 21 20 761 749 17 21 199 204 29 22 462 471 19 22 462 471 19 23 269 247 25 24 167 65 35 | 7 635 654 18 8 106 82 43 9 57 63 61 10 485 448 19 11 859 823 19 12 131 151 35 13 523 535 17 14 328 250 20 15 107 239 41 16 174 157 30 17 295 278 22 18 -157 1 27 19 294 32 45 21 144 6 38 |
| 0 660 638 12 4 2557 5245 23 1 185 42 28 5 1955 1985 19 2 69 9 7 57 7 707 693 12 4 124 82 37 8 -91 135 29 5 146 1 33 9 -99 28 28 6 510 474 17 10 272 270 16 7 212 182 26 11 235 257 19 8 110 111 41 12 1621 1595 18 9 144 277 67 13 74 136 42 10 354 393 20 14 329 321 11 55 189 159 159 12 598 669 18 16 914 921 17 13 155 119 35 17 284 256 21 13 145 258 203 26 19 351 350 21 14 221 203 28 18 635 610 18 15 258 203 26 19 351 350 21 16 27 15 1 26 24 34 411 18 15 258 203 26 19 351 350 21 16 2 306 322 21 26 354 377 22 3 282 227 22 27 -119 7 41 2 3 282 227 22 27 -119 7 41 1 114 118 44 37 370 2551 11 1 2 -58 0 63 21 2 35 24 126 191 40 2 3 186 187 33 5 150 594 31 10 186 191 31 2 2 288 417 14 11 114 118 44 37 370 2551 11 12 -58 0 63 4 927 89 91 3 186 187 33 5 150 594 31 10 186 191 31 2 2 288 417 14 11 114 118 44 37 702 555 11 12 -58 0 63 4 927 89 91 13 186 187 33 5 150 5943 13 10 186 187 33 5 150 5943 13 10 186 187 33 5 150 5943 13 10 186 187 33 150 180 180 180 180 180 180 180 180 180 18 | 3 4 1 15 50 932 17 17 52 118 62 13 208 26 17 736 840 12 18 -161 15 27 22 412 396 12 19 121 54 42 39 11031 13 20 682 683 17 4 -99 143 26 21 235 155 25 153 107 22 22 179 92 18 -161 15 27 13 20 996 14 23 361 331 21 7 1032 996 14 23 361 331 21 7 1032 996 14 23 361 331 21 7 1032 996 14 23 361 331 21 27 15 719 15 15 27 15 719 15 15 27 15 719 15 15 27 15 719 15 15 27 15 719 15 15 27 15 719 15 15 27 15 719 15 15 27 15 719 15 15 27 15 719 15 15 27 15 719 15 15 27 15 719 15 15 27 15 719 15 15 27 15 719 15 15 27 15 719 15 15 27 15 719 15 15 27 15 719 15 15 27 15 719 15 15 27 15 15 15 27 15 15 27 15 15 15 16 27 15 15 16 15 16 16 16 16 16 16 16 16 16 16 16 16 16 | 23 269 247 25 24 167 65 35 3 9 1 0 788 778 11 1 417 437 16 2 151 116 27 3 214 163 22 4 479 509 16 7 169 213 27 4 18 466 18 9 -92 105 39 10 100 160 41 11 752 714 17 12 737 730 17 13 199 205 28 14 171 148 32 15 70 50 56 16 432 430 17 17 17 423 443 18 18 262 265 23 19 221 261 261 26 653 19 27 169 889 885 16 2 4 65 41 2 2 15 30 2 2 1 2 15 30 2 2 1 2 15 30 2 2 1 2 2 15 30 2 2 1 8 8 9 8 8 5 16 2 4 4 5 5 2 4 9 2 2 1 6 6 6 5 3 19 3 10 1 0 9 6 102 28 1 889 885 16 2 4 65 41 42 4 6 183 177 27 7 7 7 6 6 6 6 6 6 6 6 6 6 6 6 6 6 6 6 6 | 3 12 1 0 78 74 38 1 140 37 29 2 322 274 21 3 790 787 18 4 250 125 25 5 471 418 19 6 40 22 711 7 72 15 55 8 355 255 22 9 749 752 16 10 154 137 31 11 -15 220 86 12 162 124 31 13 248 304 20 15 285 315 23 11 157 173 34 16 129 35 34 17 157 173 34 18 277 283 24 19 -124 57 37 3 13 1 0 653 633 13 17 157 173 34 18 277 283 24 19 -124 57 37 3 13 1 0 653 633 13 1 31 1 1 153 312 23 3 195 94 26 4 148 91 31 5 499 467 17 6 847 884 16 7 304 137 21 8 306 397 21 9 88 40 47 10 191 133 28 11 153 112 33 12 35 367 20 13 124 56 39 14 -105 79 41 15 218 270 28 16 309 286 23 17 40 65 74 3 14 1 0 243 217 28 3 16 309 286 23 17 40 65 74 3 14 133 135 35 5 71 9 51 10 191 133 188 19 3 226 282 25 4 133 135 35 5 71 9 9 1 10 191 133 188 19 3 226 282 25 4 133 135 35 5 71 9 9 1 10 191 133 188 19 |
| 0 2946 2686 26 2 432 551 15 3 3 1 4 197 65 23 6 3377 3168 35 0 1075 1102 10 8 279 233 21 1 1255 2024 18 10 693 720 18 2 1450 1347 10 12 597 609 20 3 323 343 13 14 2750 2698 33 4 2022 1938 19 | 7 986 939 14 25 363 372 23 8 531 527 14 3 8 1 10 972 964 15 11 1691 1674 19 0 1111 1138 12 12 557 567 15 1 601 621 14 13 449 459 16 2 1412 1352 17 14 541 565 16 3 120 75 30 15 505 513 17 4 847 820 15 16 1002 972 18 5 343 306 17 17 759 764 18 6 278 156 19 18 280 327 24 7 930 939 16 19 105 126 46 8 701 686 16 20 357 432 23 9 -15 91 78 | 0 19 33 64 1 656 682 17 2 180 168 28 3 390 350 19 4 469 530 18 5 660 599 17 6 182 139 29 | 6 102 141 43 7 180 198 29 8 599 584 17 9 181 184 30 10 142 272 36 11 169 110 32 12 -15 1 91 13 12 318 23 14 322 318 23 15 -88 81 50 |

```
Page 16
Aquo. Carbonyl Tetrakis(pentafluorophenyl)octachloroporphyrin Ru(II)
                                                                                                                                                                                                                                                                                                                                                                                                                                                                                                                                                                                                                                                                                                                                                                                                                                                                                                                                                                                                               2153
476
1866
1330
154
70
432
7
84
864
                                                                                                                                                                                                                                                                                                                                                                                                                                                                                                                                                                                                                                                                                                                                                                                                                                                                                                                                                           2122
396
1950
1411
233
263
400
165
175
843
                                                                                                                                                                                                                                                                                                                                                                                                                                                                                                                                                                                                                                                                                                                                                                                                                                                                                                                                                                                                                                                                                                                                                                                            1059
632
793
107
83
170
463
129
684
49
678
176
-75
153
659
25
215
109
20
                                                                                                                                                                                                                                                                                                                                                                                                                                                                                                                                                                                                                                                                                                                                       -91
303
49
225
                                                                                                                                                                                                                                                                                                                                                                                                                                                                                                                                                                                                                                                                                                                                                                                                 91
303
31
266
                                                                                                                                                                                                                                                                                                                                                                                                                                                                                                                                                                                                                                                                                                                                                                                                                                                                                                                                                                                                                                                                                      27
22
27
24
33
32
29
43
43
25
                                                                                                                                                                                                                                                                                                                                                                                                                                                                                                                                                                                                                                                                                                                                                                                                                                                                                                                                                                                                                                                                                                                                                          7 8 9 10 11 2 13 14 15 16 17 18 19 20 1 22 23 24 25
                                                                                                                                                                                                                                                                                                                                                                                                                                                                                                                                                                                                                                                                                                                                                                                                                                                                                                                                                                                                                                                                                                                                                                                                                                                                                                                       16
15
16
35
43
28
18
61
92
49
33
17
28
46
92
                                                                                                                                                                                                                                                                                                                                                                                                                                                                                                                                                                                                                                                                                                                                                                                                                                                                                                                         6
10
12
14
16
18
20
22
24
                                                                                                                                                                                                                                                                                                                                                                                                                                                                                                                                                                                                                                                                                                16
17
18
19
                                                                                                                                                                                                                                                                                                                                                                                                                                                                                                                                                                                                                                                                                                                                                                                                                                                        46
23
69
29
                                                                                                                                                                                                                                                                                                                                                                                                                                                                                                                                                                     40
133
267
687
51
382
83
170
577
624
                                                                                                                                                                                                                                                                                                                                                                                                                                                                                                                                                                                                                            45
54
22
17
59
20
50
26
18
                                                                                                                                                                                                                                                                                                                                                                                                                                                                                                              -95
-76
276
649
61
367
86
241
634
625
                                                                                                                                                                                                                                                                                                                                    556
28
274
524
158
563
367
                                                                                                                                                                                                                                                                                                                                                                                                                                                                 13
14
15
16
17
18
19
21
22
                                                                                                                                                                                                                                                                          562
-126
238
526
280
574
378
                                                                                                                                                                                                                                                                                                                                                                                             17
34
25
18
24
19
22
                                                                                                                                                                                                                                                                                                                                                                                                                                                                                                                                                                                                                                                                                                                                                                                                                                                                                                                                                                                                                                                                                                                                                                                                                                                                653
756
56
54
95
443
61
663
20
709
44
10
186
655
32
261
187
35
01234567890112314567890122345
                                                                                           1011
676
249
1317
308
4
335
366
739
131
1241
1241
138
637
148
818
8138
362
339
282
314
555
150
                                                                                                                                                          975
645
269
1288
273
59
234
459
784
600
94
1199
400
303
3212
326
557
494
                                                                                                                                                                                                                                                                                                                                                                                                                                                                                                                                                                                                                                                                                                                               6
                                                                                                                                                                                                                                                                                                                                                                                                                                                                                                                                                                                                                                                                                                                                                            12
                                                                                                                                                                                                                                                                                                                                                                                                                                                                                                                                                                                                                                                                                                                                                                                                        1
                                                                                                                                                                                                                                                                                                                                                                                                                                                                                                                                                                                                                                                                                                                                          105
110
664
182
639
276
573
405
231
452
249
216
125
274
310
124
                                                                                                                                                                                                                                                                                                                                                                                                                                                                                                                                                                                                                                                                                                                                                                                                 107
104
656
117
613
21
329
567
410
171
425
268
256
79
150
266
301
94
                                                                                                                                                                                                                                                                                                                                                                                                                                                                                                                                                                                                                                                                                                                                                                                                                                                        29
39
16
28
16
44
22
17
19
25
18
24
27
39
40
24
23
43
                                                                                                                                                                                                                                                                                                                                                                                                                                                                                                                                                                                                                                                                                                     012345678910112131451617
                                                                                                                                                                                                                                                                                                            6
                                                                                                                                                                                                                                                                  6
                                                                                                                                                                                                                                                                                                                               433
1173
1015
320
1068
1195
357
641
738
333
113
732
481
1052
372
295
481
1052
372
126
357
570
550
                                                                                                                                                                                                                                012345678910112314567181902122324
                                                                                                                                                                                                                                                                413
1206
1056
316
1023
1230
405
594
758
382
758
366
125
105
105
1034
1263
1218
117
413
818
818
12111
                                                                                                                                                                                                                                                                                                                                                                                                                                                                                                                                                                                                                                                                                                                                                                                                                                                                                                                                                              7
                                                                                                                                                                                                                                                                                                                                                                                                9
                                                                                                                                                                                                                                                                                                                                                                                                                                                                                                                                                                             1
                                                                                                                                                                                                                                                                                                                                                                                                                                                                                                   6
                                                                                                                                                                                                                                                                                                                                                                                                                                                                                                                                                                                                                                                                                                                                                                                                                                                                                                                                                                                                                            369
635
1437
964
793
7552
402
769
566
639
481
729
408
896
274
35
566
61
61
61
61
61
61
62
484
                                                                                                                                                                                                                                                                                                                                                                                                                                                                                                                                                                                                                                                                                                                                                                                                                                                                                                                              0123456789101123145167819021223455
                                                                                                                                                                                                                                                                                                                                                                                                                                                                                                                                                                                                                                                                                                                                                                                                                                                                                                                                                                297
689
1518
1050
733
548
432
584
432
667
207
423
431
862
240
862
240
865
110
130
130
130
130
130
130
130
                                                                                                                                                                                                                                                                                                                                                                                                                                                                                                                                                                                                                                                                                                                                                                                                                                                                                                                                                                                                                                                                                      241
1140
387
323
375
796
464
1498
103
313
184
228
-154
211
-165
140
160
681
404
213
                                                                                                                                                                                                                                                                                                                                                                                                                                                                                                                                                          217
1197
323
316
364
841
409
1498
53
131
357
176
187
298
10
210
210
210
54
626
395
167
                                                                                                                                                                                                                                                                                                                                                                                                                                                                                                                                                                                                                              0123456789101123145167819021
                                                                                                                                                                                                                                                                                                                                                                                                                                                                                                                                                                                                                                                                                                                                                                                                                                                                                                                                                                                                                                                                                                                                                                                                 7
                                                                                                                                                                                                                                                                                                                                                                                                                                                                                                                                                                                                                                                                                                                                                                                                                                                                                                                                                                                                                                                                                                                                                                                                                                                                                1
                                                                                                                                                                                                                                                                                                                                                                                                                                                                                                                                                                                                                                                                                                                                                                                                                                                                                                                                                                                                                                                                                                                                                                                                                                           4
                                                                                                                                                                                                                                                                                                                                                                                                                                                                                                                                                                                                                                                                                                                                                                                                                                                                                                                                                                                                                                                                                                                                                                                                    517
920
157
356
158
638
786
1792
192
193
194
112
871
428
238
864
152
1208
42
-194
254
394
                                                                                                                                                                                                                                                                                                                                                                                                                                                                                                                                                                                                                                                                                                                                                                                                                                                                                                                                                                                                                                                                                                                                                                                                                                                           563
958
1995
347
133
628
1716
1756
1716
125
167
898
453
274
3565
45
1240
270
2427
                                                                                                                                                                                                                                                                                                                                                                                                                                                                                                                                                                                                                                                                                                                                                                                                                                                                                                                                                                                                                                                                                                                                                                  01234567891011231456781902122324
                                                                                                                                                                                                                                                                                                                                                                                                                                                                                                                                                                                                                                                                                                                                                                                                                                                                                                                                                                                                                                                                                                                                                                                                                                                                                                                            115267
12615
150228
14438
17926
19229
1882
19229
19229
19229
19229
19229
19229
19229
19229
19229
19229
19229
19229
19229
19229
19229
19229
19229
19229
19229
19229
19229
19229
19229
19229
19229
19229
19229
19229
19229
19229
19229
19229
19229
19229
19229
19229
19229
19229
19229
19229
19229
19229
19229
19229
19229
19229
19229
19229
19229
19229
19229
19229
19229
19229
19229
19229
19229
19229
19229
19229
19229
19229
19229
19229
19229
19229
19229
19229
19229
19229
19229
19229
19229
19229
19229
19229
19229
19229
19229
19229
19229
19229
19229
19229
19229
19229
19229
19229
19229
19229
19229
19229
19229
19229
19229
19229
19229
19229
19229
19229
19229
19229
19229
19229
19229
19229
19229
19229
19229
19229
19229
19229
19229
19229
19229
19229
19229
19229
19229
19229
19229
19229
19229
19229
19229
19229
19229
19229
19229
19229
19229
19229
19229
19229
19229
19229
19229
19229
19229
19229
19229
19229
19229
19229
19229
19229
19229
19229
19229
19229
19229
19229
19229
19229
19229
19229
19229
19229
19229
19229
19229
19229
19229
19229
19229
19229
19229
19229
19229
19229
19229
19229
19229
19229
19229
19229
19229
19229
19229
19229
19229
19229
19229
19229
19229
19229
19229
19229
19229
19229
19229
19229
19229
19229
19229
19229
19229
19229
19229
19229
19229
19229
19229
19229
19229
19229
19229
19229
19229
19229
19229
19229
19229
19229
19229
19229
19229
19229
19229
19229
19229
19229
19229
19229
19229
19229
19229
19229
19229
19229
19229
19229
19229
19229
19229
19229
19229
19229
19229
19229
19229
19229
19229
19229
19229
19229
19229
19229
19229
19229
19229
19229
19229
19229
19229
19229
19229
19229
19229
19229
19229
19229
19229
19229
19229
19229
19229
19229
19229
19229
19229
19229
19229
19229
19229
19229
19229
19229
19229
19229
19229
19229
19229
19229
19229
19229
19229
19229
19229
19229
19229
19229
19229
19229
19229
19229
19229
19229
19229
19229
19229
19229
19229
19229
19229
19229
19229
19229
19229
19229
19229
19229
19229
19229
19229
19229
19229
19229
19229
19229
19229
19229
19229
19229
19229
19229
19229
19229
19229
19229
19229
19229
19229
19229
                                                                                                                                                                                                                                                                                                                                                                                                                                                                                                                                                                                                                                                                                                                                                                      13
                                                                                                                                                                                                                                                                                                                                                                                                                                                                                                                                                                                                                                                                                                                                                                                                              1
                                                                                                                                                                                                                                                                                                                                                                                                                                                                                                                                                                                                                                                                                                                                       6
                                                                                                                                                                                                                                                                                                                                                                                                                                                                                                                                                                                                                                                                                                                                                                                                      198
360
111
125
18
231
194
121
395
18
292
197
243
177
441
153
                                                                                                                                                                                                                                                                                                                                                                                                                                                                                                                                                                                                                                                                                                                                               206
353
154
33
113
250
166
124
440
112
358
211
282
119
436
207
                                                                                                                                                                                                                                                                                                                                                                                                                                                                                                                                                                                                                                                                                                                                                                                                                                                               1
                                                                                                                                                                                                                                                                                                                                                                                                                                                                                                                                                                                                                                                                                                          0 1 2 3 4 5 6 7 8 9 10 11 2 13 14 15
                                                                                   4
                                         6
                                         533
159
580
971
655
90
595
1348
241
1798
603
788
-116
168
920
132
291
346
484
484
484
2-51
                                                                                                0 1 2 3 4 5 6 7 8 9 10 112 13 14 15 16 7 18 19 22 12 22 22 25
                                                                                                                                                                                                                                                                                                                                                                                                                                                                                                                                                                                     1
                                                                                                                                                                                                                                                                                                                                                    1
                                                                                                                                                                                                                                                                                                                                                                                                                                                                                                           6
                                                                                                                                                                                                                                                                                                                                                                                                                                                                                                                                   10
                                                                                                                                                                                                                                                                                                                    7
                                                                                                                                                                                                                                                                          6
                                                                                                                                                                                                                                                                                                                                                                                                                                                                                                                   56
319
114
963
155
169
257
220
408
257
220
408
257
130
456
234
59
456
234
119
                                                                                                                                                                                                                                                                                                                                                                                                                                                                                                                                                                             128
322
26
983
8
443
157
250
104
34
174
471
205
554
11
58
                                                                                                                                                                                                                                      0 1857
1 926
2 377
3 203
4 1096
6 1277
7 5681
10 187
11 370
12 453
13 428
14 190
15 110
17 122
18 707
19 365
21 486
21 486
22 248
                                                                                                                                                                                                                                                                                                                               1818
871
382
84
1099
581
1218
1218
492
215
129
4415
495
266
163
698
300
443
201
291
                                                                                                                                                                                                                                                                                                                                                                                                   012345678901123145167181920
                                                                                                                                                                                                                                                                                                                                                                                                                                                                                                                                                                                                                                 1
                                                                                                                                                                                                                                                                                                                                                                                                                                                                                                                                                                                                                                                                                                                                                                                                                                                                                                                                                                                                                     2
                                                                                                                                                                                                                                                                                                                                                                                                                                                                                                                                                                                                                                                                                                                                                                                                                                                                                                                                                                        7
                                                                                                                                                                                                                                                                                                                                                                                                                                                                                                                                                                                                                                                                                                                                                                                                                                                                                                                                                                                                                                  1150
1794
195
356
362
1974
776
1155
1040
1214
890
423
423
423
423
217
365
389
219
217
563
489
217
563
489
217
                                                                                                                                                                                                                                                                                                                                                                                                                                                                                                                                                                                                                                                                                                                                                                                                                                                                                                                                                                        1166
1860
218
326
374
1918
795
1110
1079
1248
363
1624
884
395
393
333
412
381
140
256
471
456
760
                                                                                                                                                                                                                                                                                                                                                                                                                                                                                                                                                                                                                                                                                                                                                                                                                                                                                                                                           01234567890111231451678902223425
                                                                                                                                                                                                                                                                                                                                                                                                                                                                                                                                                                                                                                                                                                                                                                                                                                                                                                                                                                                                                                                                                                14
                                                                                                                                                                                                                                                                                                                                                                                                                                                                                                                                                                                                                                                                                                                                                                                                                      1
                                                                                                                                                                                                                                                                                                                                                                                                                                                                                                                                                                                                                                                                                                                                            6
                                                                                                                                                                                                                                                                                                                                                                                                                                                                                                                                                                                                                                                                                                                                                       98
111
282
156
236
48
129
43
287
189
269
71
175
                                                                                                                                                                                                                                                                                                                                                                                                                                                                                                                                                                                                                                                                                                                                                                                                              37
78
238
61
143
111
57
64
324
172
261
139
35
                                                                                                                                                                                                                                                                                                                                                                                                                                                                                                                                                                                                                                                                                                                  012345678910112
                                                                                                                                                                                                                                                                                                                                                                                                                                                                                                                                                                                                                                                                                                                                                                                                                                                                     33
41
23
33
25
65
38
69
23
25
58
34
                                                                                                                                                                                                                                                                                                                                                                                                                                                                                                                                                                                                                                                                                                                                                                                                                                                                                                                                                                                                                                                                                                                                                                                                         7
                                                                                                                                                                                                                                                                                                                                                                                                                                                                                                                                                                                                                                                                                                                                                                                                                                                                                                                                                                                                                                                                                                                                                                                                                                                      5
                                                                                                                                                                                                                                                                                                                                                                                                                                                                                                                                                                                                                                                                                                                                                                                                                                                                                                                                                                                                                                                                                                                                                                                                                                                                                     1
                                                                                                                                                                                                                                                                                                                                                                                                                                                                                                                                                                                                                                                                                                                                                                                                                                                                                                                                                                                                                                                                                                                                                                          01234567890111213145167181922122324
                                                                                                                                                                                                                                                                                                                                                                                                                                                                                                                                                                                                                                                                                                                                                                                                                                                                                                                                                                                                                                                                                                                                                                                                                 254
-20
768
393
445
433
405
563
405
318
477
392
414
414
591
172
266
294
186
237
195
                                                                                                                                                                                                                                                                                                                                                                                                                                                                                                                                                                                                                                                                                                                                                                                                                                                                                                                                                                                                                                                                                                                                                                                                                                                                          309
3 794
1440
362
1440
363
387
387
387
551
693
367
352
550
429
421
635
614
8
8
228
225
164
363
218
                                                                                                                                                                                                                                                                                                                                                                                                                                                                                                                                                                                                                                                                                                                                                                                                                                                                                                                                                                                                                                                                                                                                                                                                                                                                                                                                       6
                                                                                                                        1
                                               1297
1452
252
676
713
865
369
681
752
207
415
1217
1053
595
85
269
1156
                                                                                                        1243
1501
237
622
701
770
354
699
687
153
142
1178
1049
626
9
294
1169
                                                                                                                                                                          13
17
19
14
15
16
15
15
16
18
18
18
18
18
25
27
27
                                                                                                                                                                                                                                                                                                                                                                                                                                                                                                                                             11
                       012345678910112131415167
                                                                                                                                                                                                                                                                                                                                                                                                                                                                                                                   6
                                                                                                                                                                                                                                                                                                                                                                                                                                                                                                                                                                                                                                                                                                                                                  6 15
                                                                                                                                                                                                                                                                                                                                                                                                                                                                                                                                                                                                                                                                                                                                                                                                                           1
                                                                                                                                                                                                                                                                                                                                                                                                                                                                                                                                                                                     301
408
161
31
145
311
685
52
73
207
373
30
374
217
376
                                                                                                                                                                                                                                                                                                                                                                                                                                                                                                                              326
385
155
111
149
325
682
137
47
86
248
374
-99
365
278
                                                                                                                                                                                                                                                                                                                                                                                                                                                                                                                                                                                                                                              16
20
34
38
35
22
18
33
62
46
23
41
20
25
23
                                                                                                                                                                                                                                                                                                                                                                                                                                                                                      0 1 2 3 4 5 6 7 8 9 10 11 12 13 14 15
                                                                                                                                                                                                                                                                                                                                                                                                                                                                                                                                                                                                                                                                                                                                                            307
-50
240
-145
219
276
273
-106
247
                                                                                                                                                                                                                                                                                                                                                                                                                                                                                                                                                                                                                                                                                                                                                                                                                      358
189
33
178
236
208
23
157
                                                                                                                                                                                                                                                                                                                                                                                                                                                                                                                                                                                                                                                                                                                                                                                                                                                                       16
66
26
31
28
24
25
42
27
                                                                                                                                                                                                                                                                                                                                                                                                                                                                                                                                                                                                                                                                                                                          012345678
                                                                                                                                                                                                                                                                                     6
                                                                                                                                                                                                                                                                                                                                                           1
                                                                                                                                                                                                                                                                                                                                 8
                                                                                                                                                                                                                                                                                                                                                      138
191
783
757
670
549
197
224
1005
860
171
288
                                                                                                                                                                                                                                                                                                                                                                                                             21
16
16
17
24
28
26
18
29
25
                                                                                                                                                                                                                                                        012345678910112
                                                                                                                                                                                                                                                                                             159
214
845
780
645
534
206
176
207
1029
877
193
259
                                                                                                                                                                                                                                                                                                                                                                                                                                                                                                                                                                                                                                                                                                                                                                                                                                                                                                                                                                                     7
                                                                                                                                                                                                                                                                                                                                                                                                                                                                                                                                                                                                                                                                                                                                                                                                                                                                                                                                                                                                                                            142
301
106
1299
1022
885
672
                                                                                                                                                                                                                                                                                                                                                                                                                                                                                                                                                                                                                                                                                                                                                                                                                                                                                                                                                                                          149
293
136
1311
955
920
635
                                                                                                                                                                                                                                                                                                                                                                                                                                                                                                                                                                                                                                                                                                                                                                                                                                                                                                                                                              0123456
                                                                                                                                                                                                                                                                                                                                                                                                                                                                                                                                                                                                                                                                                                                                                                                                                                                                                                                                                                                                                                                                                                             18
17
27
17
15
15
                                                                                                                                                                                                                                                                                                                                                                                                                                                                                                                                                                                                                                                                                                                                                       7
                                                                                                                                                                                                                                                                                                                                                                                                                                                                                                                                                                                                                                                                                                                                                                                                   0
                                                                                                                                                                                                                                                                                                                                                                                                                                                                                                                                                                                                                                                                                                                                                                                                                                1
                                                                                                                                                                                                                                                                                                                                                                                                                                                                                                                                                                                                                                                                                                                                                                                                                854
141
1307
                                                                                                                                                                                                                                                                                                                                                                                                                                                                                                                                                                                                                                                                                                                                                       978
72
1407
                                                                                                                                                                                                                                                                                                                                                                                                                                                                                                                                                                                                                                                                                                                                                                                                                                                                                                                                                                                                                                                                                                                                                                                                                         7
                                                                                                                                                                                                                                                                                                                                                                                                                                                                                                                                                                                                                                                                                                                                                                                                                                                                                                                                                                                                                                                                                                                                                                                                                                                                   6
```

| Aquo. Carbonyl Tetrakis(pentaflu | oronhenylloctachlocoporphy | rin Ru(II) | | Page 17 |
|---|--|---|---|---|
| 0 1379 1356 14 0 -64 78 1 340 277 18 1 243 279 2 100 87 37 2 578 575 3 415 374 17 3 867 888 4 176 238 26 4 201 156 5 353 392 18 5 171 33 6 1441 1458 18 6 189 111 7 980 959 17 7 320 332 8 137 134 32 8 862 842 9 158 215 29 9 491 492 10 137 71 34 10 -59 65 11 164 119 31 11 753 716 12 394 414 20 12 38 51 13 106 84 43 13 -114 3 14 527 534 19 14 220 15 15 74 55 56 15 607 570 | 3 41 10 98 14 45 3 25 11 132 79 38 5 18 12 469 435 19 3 18 13 339 358 22 14 372 352 21 3 31 15 400 398 21 1 2 2 7 13 1 2 18 5 19 0 171 159 22 5 61 1 107 58 41 | 13 1086 1084 18 14 1000 972 18 15 210 93 27 16 217 256 27 17 432 441 17 18 265 308 22 19 490 494 17 20 404 476 19 21 323 332 21 22 251 209 25 23 -99 38 45 24 372 415 22 8 2 1 | 8 459 474 17 9 892 870 17 10 56 54 56 11 305 318 21 12 125 15 37 13 844 852 18 14 282 319 23 15 255 236 25 16 409 425 18 17 146 255 33 18 243 181 24 19 659 698 17 20 509 531 18 21 254 271 25 22 112 92 44 23 356 367 22 8 5 1 | 6 1310 1286 19 7 574 542 18 8 243 131 24 9 131 89 37 10 610 632 18 11 238 195 26 12 543 449 19 13 322 361 20 14 409 427 19 15 65 165 56 16 485 528 18 17 312 291 22 18 641 577 18 19 186 85 31 20 481 459 20 21 325 313 23 |
| 20 272 312 24 20 544 588 21 178 207 32 26 27 10 1 2 2 2 545 502 2 2 545 502 2 2 545 502 2 2 2 2 2 2 2 2 2 2 2 2 2 2 2 2 2 | 11 8 29 98 119 12 219 199 28 13 150 66 37 199 28 13 150 66 37 191 199 28 13 150 66 37 191 199 28 199 28 199 28 199 28 199 28 199 28 199 28 199 28 199 28 199 28 199 28 199 28 199 28 199 28 199 37 15 1 10 150 93 37 15 1 10 150 93 37 15 1 10 150 93 37 15 1 10 150 93 37 15 1 10 150 93 37 15 1 10 150 93 37 15 1 10 150 93 37 15 1 10 150 93 37 15 1 10 150 193 193 193 193 193 193 193 193 193 193 | | | 8 8 1 0 82 138 37 1 173 118 30 2 1012 990 18 3 781 761 188 4 1385 1385 20 5 374 292 20 6 347 335 21 7 551 520 19 8 857 886 18 9 10 1 274 277 22 11 274 277 22 11 274 277 22 12 492 498 17 13 470 443 18 14 382 425 19 15 428 432 19 16 351 382 21 17 223 248 27 18 77 18 55 19 443 400 20 479 477 20 8 9 1 0 597 585 13 1 882 850 18 2 320 287 23 3 105 19 45 4 164 22 34 8 71 18 6 759 756 19 8 10 1 0 597 585 13 1 882 850 18 2 320 287 23 3 105 19 45 6 759 756 19 14 164 22 34 8 -71 27 50 9 -61 16 55 10 -44 59 65 11 407 416 19 12 499 548 18 13 117 95 40 14 -87 106 42 17 519 521 19 18 227 229 28 19 534 503 20 8 10 1 |
| 10 438 493 20 16 341 26 11 201 236 29 17 465 41 12 -149 53 30 7 12 1 14 293 292 21 15 398 392 19 0 684 70 16 24 126 81 1 153 13 17 358 310 21 2 318 26 18 551 530 18 3 285 28 19 454 409 19 4 337 32 20 293 311 24 5 535 47 21 201 212 31 6 219 7 343 37 7 9 1 8 445 42 9 112 14 | 2 -22 5 69 3 87 92 39 35 32 4 930 888 16 681 20 5 144 250 28 681 22 6 216 222 22 26 20 7 483 537 16 78 17 8 1189 1245 17 18 25 9 220 192 22 10 10 822 818 16 27 18 11 837 777 17 18 18 37 777 17 | 8 4 1 0 672 673 11 1 1030 1081 16 2 869 825 16 3 504 473 16 4 -114 74 30 5 86 10 41 6 74 59 45 7 238 213 22 | 21 298 259 24 22 449 477 21 8 7 1 0 1027 1027 13 1 22 9 78 2 64 106 54 3 -66 95 51 4 194 87 27 5 586 533 17 | 0 290 290 18 1 277 201 25 2 230 174 28 3 946 928 19 4 249 115 23 5 185 122 28 6 433 379 18 7 687 664 16 8 120 45 38 9 820 850 17 10 205 76 27 11 223 215 26 |

| Aquo. Carbonyl Tetrakis(pentafluoropher | nyl)octachloroporphyr | in Ru(II) | | Page 18 |
|--|---|--|---|--|
| 12 363 343 20 10 273 273 31 13 394 458 20 12 124 37 51 14 -166 24 26 14 316 21 32 15 299 324 23 16 858 828 22 15 174 191 33 18 -104 82 52 17 312 270 24 20 56 118 72 22 491 493 27 | 14 434 431 20 15 595 645 16 16 582 560 17 17 202 20 27 18 420 418 19 19 338 320 21 20 194 255 29 21 244 268 26 22 186 219 32 | 15 239 236 24 16 580 560 18 17 94 47 18 321 337 22 19 581 587 19 20 191 209 31 21 154 201 49 | 0 116 177 29 1 -125 47 34 22 288 199 22 3 540 509 17 4 339 297 20 5 711 741 17 6 141 54 35 7 252 259 24 8 113 80 41 | 18 182 215 41 20 363 406 29 10 1 1 0 748 720 12 1 150 110 32 2 581 532 17 3 96 148 43 |
| 8 11 1 9 1 1 9 1 1 1 1 1 1 1 1 1 1 1 1 1 | 9 4 1 0 24 145 16 1 1693 1674 20 2 316 298 20 3 -63 43 50 4 391 387 18 5 1232 1228 18 6 261 296 22 7 82 65 47 8 -79 100 45 9 61 296 22 7 82 65 47 8 11 1399 1373 20 12 157 51 33 13 664 677 19 14 103 71 15 516 496 17 17 488 534 18 18 -74 39 330 23 20 161 190 45 17 488 534 18 18 -74 39 330 23 20 161 190 45 21 110 124 23 22 444 464 21 29 5 1 0 -135 50 21 1 450 33 38 21 1 10 124 45 22 444 467 18 21 110 124 45 22 444 467 18 21 110 124 45 22 444 467 18 21 12 139 388 21 12 39 388 21 12 39 388 21 12 39 388 21 12 139 385 21 147 190 365 31 348 21 6 284 258 22 7 470 436 18 9 779 784 18 10 213 92 27 11 580 535 18 12 147 190 365 18 242 270 25 14 931 901 16 15 514 509 17 17 179 232 27 11 580 535 578 10 213 82 27 14 509 17 17 179 232 27 15 508 20 9 6 1 | | 0 116 177 29 1 -125 47 34 2 288 199 27 3 540 599 17 4 339 297 20 5 7111 741 17 6 141 54 35 7 252 259 24 8 113 80 41 10 216 212 27 11 215 263 28 12 -156 23 29 13 163 163 163 20 14 -92 93 48 15 218 207 29 16 -77 120 55 9 11 1 0 93 13 8 35 1 512 485 18 2 427 374 19 4 209 116 27 5 141 137 36 1 205 147 27 3 73 361 363 20 9 12 1 0 9 12 1 1 0 197 200 19 4 78 421 19 1 108 81 44 1 109 99 11 18 1 108 81 44 1 109 99 11 18 1 108 81 44 1 109 99 11 18 1 108 81 44 1 108 81 44 1 109 115 40 1 108 81 44 1 109 115 40 1 108 81 44 1 109 115 40 1 109 115 40 | 748 720 12 1 150 132 2 1581 532 17 3 96 148 43 4 5 64 156 54 6 2622 245 23 10 237 271 25 11 513 570 18 12 163 90 33 13 308 274 20 11 515 457 465 18 19 101 106 42 201 232 226 27 21 370 21 10 2 1 10 2 1 10 4 19 488 18 19 101 106 42 201 232 26 21 370 367 21 20 413 348 19 20 413 4.97 12 21 1398 1342 19 20 413 4.97 12 21 1398 455 18 12 116 155 488 460 18 8 421 499 498 19 10 415 429 20 11 655 642 19 25 18 11 655 642 18 12 409 392 21 13 663 646 16 18 12 11 18 19 12 11 16 13 1 18 247 252 25 10 1 254 237 25 10 2 2 2 2 2 2 2 2 2 2 2 2 2 2 2 2 2 2 2 |
| 2 569 599 18 0 162 194 20 3 120 12 41 1 89 181 41 4 70 161 57 2 102 163 38 5 -137 81 33 3 299 286 20 6 135 20 39 4 151 97 30 7 92 53 50 5 -72 42 46 9 0 1 7 671 658 17 9 0 1 7 671 658 17 2 646 683 22 10 379 376 20 4 1423 1478 24 11 348 320 21 6 265 322 29 12 508 468 123 8 246 123 31 13 984 947 18 | 1 87 15 46 2 423 429 19 3 197 22 27 4 1264 1244 19 5 508 487 18 6 464 405 19 7 139 2 35 8 383 398 20 9 324 282 22 10 1251 1225 19 11 647 646 19 12 409 437 18 13 725 719 18 14 270 217 22 | 13 -145 15 30 14 242 254 26 15 107 163 45 16 236 263 27 17 247 153 27 9 10 1 | 0 1345 1307 19 2 1776 1653 27 4 -111 75 47 6 884 944 24 8 1652 1656 27 10 678 714 25 12 271 260 34 14 1248 1258 23 16 200 120 38 | 15 331 331 231 16 157 197 32 17 686 686 17 18 -134 80 32 19 269 271 24 20 128 101 40 21 406 383 21 |

| Aquo. Carbonyl Tetrakis(pentafluorophe | nyl)octachloroporphyrin R | u(II) | | Page 19 |
|---|--|--|--|---|
| 10 4 1 | 3 158 164 34 10 4 112 43 43 11 5 714 703 18 12 6 234 522 27 13 7 304 302 23 14 8 240 229 27 14 10 12 1 16 10 233 116 41 16 10 233 232 27 17 11 248 248 27 18 10 12 1 19 10 12 1 19 10 12 1 19 10 265 303 18 1 85 115 53 0 2 302 281 24 1 3 148 166 37 2 4 39 77 75 3 5 140 94 39 44 1 3 148 166 37 2 2 19 34 4 5 20 5 140 97 33 4 5 6 6 17 7 228 265 28 6 7 8 402 374 21 7 10 13 1 90 0 126 131 32 11 1 -71 89 59 12 2 63 23 64 13 3 52 3 86 14 11 0 1 16 16 0 453 434 19 18 2 773 82 25 38 6 6 311 353 31 1 -71 89 59 12 2 63 23 64 13 3 52 3 86 14 11 0 1 16 16 0 453 434 19 18 2 773 82 25 38 6 6 311 353 31 1 1 -56 825 38 6 6 311 353 31 1 1 -71 81 50 6 6 311 32 32 64 13 3 52 3 86 14 14 -146 47 39 12 2 777 815 23 19 14 -146 47 39 26 15 4 -50 43 64 13 18 634 704 25 44 20 154 171 50 6 154 171 50 6 157 -39 18 31 16 17 -739 18 31 16 18 79 166 61 18 12 2 777 89 566 19 16 17 573 13 19 10 18 6534 506 19 16 17 573 13 19 10 18 6534 506 61 18 12 17 257 288 21 11 1 1 1 7 67 11 1 1 7 77 13 158 17 266 60 12 512 502 17 13 158 17 266 60 12 512 502 17 13 158 17 266 60 12 512 502 17 247 288 21 1 1 156 193 134 229 33 10 150 213 248 25 18 213 213 248 25 | 355 378 19 666 725 18 18 219 269 259 251 231 231 25 -88 13 45 240 211 25 -181 19 11 19 11 11 11 11 11 11 11 11 11 11 | 11 6 1 0 713 678 12 1 359 381 197 3 428 428 18 4 558 556 566 176 6 556 566 176 6 563 68 177 18 110 1 99 475 18 111 99 475 18 111 99 475 18 111 99 475 18 111 99 475 18 111 99 475 18 111 99 475 18 111 99 475 18 111 99 475 18 111 99 475 18 111 99 475 18 111 142 167 38 14 335 361 17 17 3 18 53 153 153 153 153 153 153 153 153 153 | Page 19 0 21 8 69 1 -65 86 57 2 87 135 50 3 326 337 222 4 405 416 20 5 347 142 15 37 8 441 476 20 10 1-136 138 25 11 11 1 |
| 10 7 1 13 423 416 21 14 -67 111 60 | 16 193 134 299 25 4 18 213 240 28 5 19 165 246 34 6 11 2 1 8 0 529 494 13 10 1 -60 134 59 11 2 606 617 18 12 3 221 240 27 18 5 146 269 35 15 6 557 579 19 16 7 189 132 30 17 8 96 102 47 18 9 489 475 17 | 526 488 17 203 252 26 -119 63 34 114 199 39 393 404 19 | 0 283 259 16 1 562 545 18 2 433 427 19 3 717 711 17 4 138 13 36 5 428 365 19 6 386 386 20 7 518 505 18 8 200 140 29 9 324 272 22 10 403 482 20 11 278 279 24 12 265 280 23 11 174 43 | 16 359 377 21 17 -166 71 28 12 2 1 0 628 626 14 1 226 312 24 2 190 262 27 3 -168 42 24 4 819 792 16 5 561 578 17 6 248 191 23 7 1087 1094 17 8 254 125 23 9 243 180 24 10 208 137 26 |
| 0 260 278 18 10 11 1 1 -115 100 39 2 809 789 19 0 -101 0 32 3 -62 11 59 1 310 284 23 4 -67 57 57 2 308 291 23 | 7 189 132 30 17 8 96 102 47 18 9 489 475 17 | -132 24 34 316 331 23 | 13 121 174 43 | 8 254 125 23 9 243 180 24 10 208 137 26 |

| 11 1 255 160 25 2 1 124 2 28 8 | Aquo. Carbonyl Tetrakis(pentafluorophenyl)octachloroporphyrin Ru(II) | | | | Page 20 | |
|---|---|--|---|---|--|--|
| 5 401 398 199 12 | 11 135 160 35 12 -68 74 53 13 232 243 25 14 243 321 25 15 -168 36 26 16 182 277 31 17 -149 101 31 12 3 1 0 368 392 14 1 1 341 344 20 1 2 228 234 25 1 3 503 558 17 1 4 235 152 24 | 1 124 2 38 2 878 903 17 3 119 128 39 4 -119 36 36 5 383 407 20 6 313 308 22 7 -76 50 50 8 -135 93 52 10 -75 76 51 11 129 112 38 125 520 552 19 13 -78 84 51 4 332 383 22 | 13 0 1 0 200 97 28 2 68 108 72 4 612 690 24 6 563 543 24 8 741 732 24 10 765 720 24 12 239 194 36 14 542 574 26 13 1 1 0 994 1003 13 | 1 621 603 17 2 195 19 29 3 743 667 17 4 -86 81 47 5 252 239 24 6 552 487 18 7 91 89 48 8 293 306 23 9 784 778 18 10 262 233 24 11 267 243 24 12 116 171 42 13 286 304 24 | 14 0 1 | 14 5 1 0 308 273 17 1 183 158 32 2 246 166 27 3 666 679 18 4 367 316 22 5 139 3 39 6 377 355 21 7 86 125 53 8 521 455 19 |
| 1 347 407 20 | 5 401 398 19 6 827 796 17 7 385 397 19 8 398 402 19 9 964 989 17 10 -134 93 31 11 421 433 19 12 32 134 74 13 81 110 50 14 114 19 42 15 580 608 18 16 268 309 25 17 -92 179 48 1 | 0 318 329 15 1 256 173 24 2 686 621 17 3 136 46 36 4 705 675 17 5 395 402 20 7 181 215 30 8 113 170 42 9 -56 95 61 10 305 278 23 | | 1 395 392 20 2 190 43 29 3 127 103 39 4 196 98 29 5 199 123 43 6 441 396 19 7 411 417 20 8 190 142 30 9 170 162 22 34 10 162 22 34 11 623 644 18 12 302 344 24 | 0 259 254 18 1 254 237 25 2 474 487 19 3 423 366 20 4 1173 1142 19 5 311 284 23 6 227 129 27 7 450 420 19 8 511 492 19 9 347 306 22 10 797 811 18 11 -64 125 60 | 0 829 817 13 1 219 61 29 2 541 497 19 3 214 73 29 4 500 485 20 5 386 410 22 6 579 19 14 7 1 0 290 251 18 1 384 290 22 2 1036 1036 19 3 261 102 27 |
| 13 78 140 53 0 -133 55 26 12 180 161 31 3 529 17 12 17 267 34 13 667 652 18 4 567 550 19 3 36 47 76 15 15 358 375 22 2 251 227 26 14 398 366 21 5 203 56 30 4 319 242 23 15 4 1 12 6 1 4 207 128 30 13 4 1 7 117 59 44 6 241 151 27 0 280 270 10 258 259 17 6 213 163 30 0 331 312 15 13 9 1 8 316 232 23 | 12 5 1 0 638 636 12 1 -74 53 50 2 431 409 18 3 316 317 21 4 448 462 18 5 501 501 7 18 6 -148 43 29 7 289 306 22 8 193 260 28 9 -139 2 30 10 143 35 11 241 300 25 12 -132 74 33 13 78 140 53 | 1 199 144 29 2 398 442 20 3 371 355 20 4 273 240 24 5 66 39 39 35 6 411 397 20 7 206 149 29 8 215 258 28 9 112 196 43 10 -56 34 63 11 -56 34 63 11 108 40 12 9 1 0 -148 18 22 1 7 1 63 55 2 89 86 50 3 662 634 18 4 232 135 27 5 313 327 23 6 191 3 3 7 234 145 27 8 403 407 21 9 104 87 47 10 139 111 52 | 0 874 854 13 1 465 396 18 2 337 313 21 3 16 72 87 4 90 123 47 5 -137 44 31 5 -137 44 32 7 281 80 23 8 534 513 18 10 264 256 24 13 34 256 24 13 34 256 24 13 380 371 21 13 31 0 0 335 295 15 1 843 804 17 2 3 226 155 26 4 459 418 19 1 304 256 214 25 3 226 155 26 4 459 418 19 1 304 351 22 6 129 35 38 7 1034 1036 18 8 226 212 26 9 247 272 25 10 117 105 41 11 399 429 20 12 189 161 31 | 1 261 142 24 2 805 751 18 3 278 197 24 4 437 438 199 6 10 37 95 7 491 458 19 9 459 458 19 9 451 503 19 10 519 503 19 11 176 95 33 13 7 1 0 796 798 13 1 180 75 32 2 2 55 24 4 -133 28 38 6 680 676 18 7 89 105 51 8 305 265 24 9 229 184 28 10 316 286 23 13 8 1 0 280 247 18 1 102 57 47 2 386 367 250 19 4 567 550 19 5 203 56 30 19 5 203 56 30 19 5 203 56 30 19 5 203 56 30 19 | 0 444 446 14 1 614 565 18 2 171 104 32 3 605 560 18 4 400 309 20 5 184 123 31 6 623 594 18 7 478 415 19 8 149 155 36 9 220 196 28 10 384 241 18 1 456 389 19 1 3 860 825 18 4 407 418 20 5 222 250 28 6 147 107 36 7 588 530 19 1 34 47 1 107 36 7 588 530 19 1 69 141 34 14 4 1 0 374 47 15 1 906 855 18 2 175 129 32 | 0 242 231 27 2 489 539 28 4 606 592 27 6 470 515 28 15 1 1 0 621 613 14 1 262 277 26 2 323 228 23 3 629 559 19 5 355 368 22 6 464 422 20 15 2 1 0 372 422 15 1 323 287 23 2 579 572 19 3 590 351 15 1 635 648 19 2 173 649 35 3 122 102 44 4 183 147 33 15 4 1 |

Appendix 5

Transient Spectra of RuTFPPCl₈(CO) at 415 nm

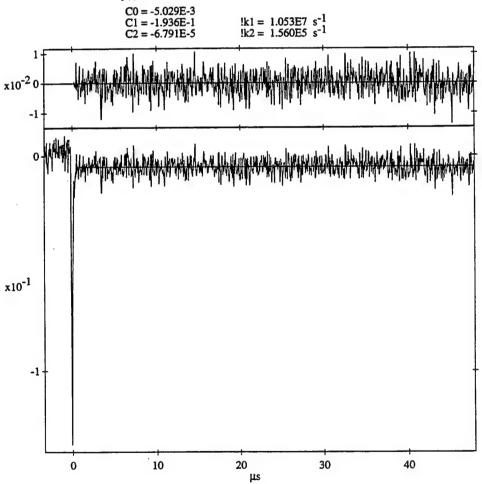
1995-2-23 9:19:52 INPUT OFFSET: 0 % DATA FILE: RUO2.001 DATA FILE: RUO2.001
TIME RANGE: 50 µs INPUT V RANGE: 0.320V
EXPERIMENT: TRANSIENT ABSORBTION
FAST (200 MHz) QUASI-DIFFERENTIAL AMP
MODE: SINGLE-ENDED

SHOTS PRE CYCLE: 10 CYCLES: 5 PMT VOLTIGE: EXCITATION WAVELENGTH: 355 nm OBSERVATION WAVELENGTH: 415 nm SAMPLE: Rucl8(CO) SOLVENT: CH2Cl2
TEMPERATURE: rt
COMMENT: under dioxygen
COMMENT: PMT VOLTIGE: 702 V

---> FIXED PARAMETER; ! ---> FIXED SIGN

$$y(t) = C0 + C1*e^{-k1*t} + C2*e^{-k2*t}$$

 $!k1 = 1.053E7 \text{ s}^{-1}$ $!k2 = 1.560E5 \text{ s}^{-1}$



DATA FILE: RUET.002

1995-2-23 9:24:35 INPUT OFFSET: 0 %

TIME RANGE: 50 µs INPUT V RANGE: 0.320V EXPERIMENT: TRANSIENT ABSORBTION FAST (200 MHz) QUASI-DIFFERENTIAL AMP

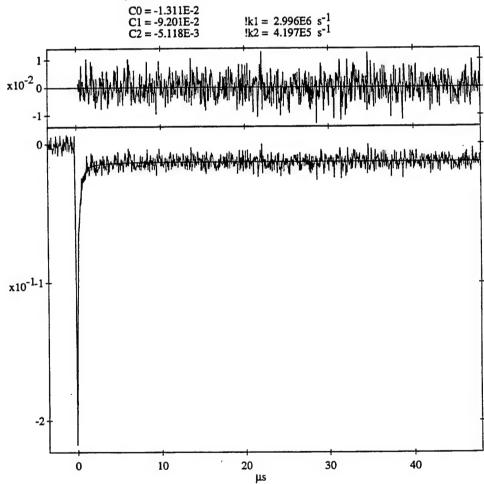
MODE: SINGLE-ENDED

SHOTS PRE CYCLE: 10 CYCLES: 5 PMT VOLTIGE: EXCITATION WAVELENGTH: 355 nm OBSERVATION WAVELENGTH: 415 nm PMT VOLTIGE: 702 V

SAMPLE: RuCl8(CO) SOLVENT: CH2Cl2 TEMPERATURE: n COMMENT: under ethylene COMMENT:

---> FIXED PARAMETER; ! ---> FIXED SIGN

$$y(t) = C0 + C1*e^{-k1*t} + C2*e^{-k2*t}$$



1995-2-23 9:14:31 INPUT OFFSET: 0 %

DATA FILE: RUAR.005

TIME RANGE: 50 µs INPUT V RANGE: 0.320V EXPERIMENT: TRANSIENT ABSORBTION FAST (200 MHz) QUASI-DIFFERENTIAL AMP MODE: SINGLE-ENDED

PMT VOLTIGE: 702 V

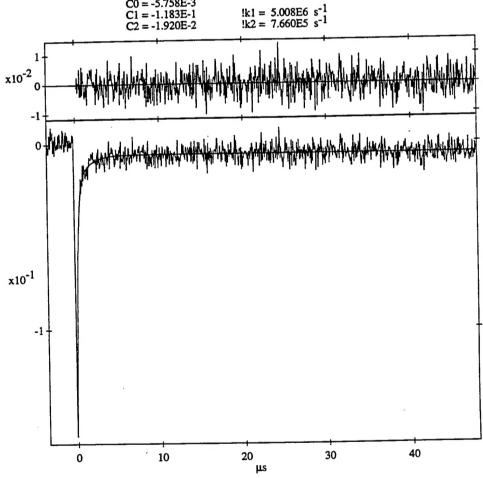
SHOTS PRE CYCLE: 10 CYCLES: 5 PMT VOLTIGE: EXCITATION WAVELENGTH: 355 nm OBSERVATION WAVELENGTH: 415 nm SAMPLE: Rucl8(CO) SOLVENT: CH2Cl2 TEMPERATURE: rt COMMENT: under argon COMMENT:

COMMENT:

---> FIXED PARAMETER; ! ---> FIXED SIGN

$$y(t) = C0 + C1*e^{-k1*t} + C2*e^{-k2*t}$$

C0 = -5.758E-3 C1 = -1.183E-1



DATA FILE: RUO2.000

1995-2-23 9:18:40 INPUT OFFSET: 0 %

TIME RANGE: 5.0 µs INPUT V RANGE: 0.320V EXPERIMENT: TRANSIENT ABSORBTION FAST (200 MHz) QUASI-DIFFERENTIAL AMP

MODE: SINGLE-ENDED

SHOTS PRE CYCLE: 10 CYCLES: 5 PMT VOLTIGE: EXCITATION WAVELENGTH: 355 nm OBSERVATION WAVELENGTH: 415 nm SAMPLE: Rucl8(CO) PMT VOLTIGE: 702 V

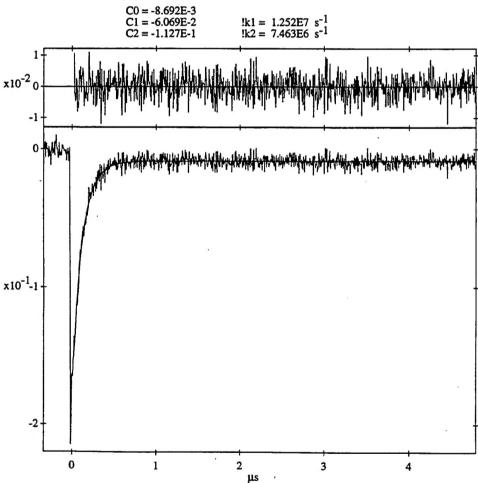
SOLVENT: CH2Cl2 TEMPERATURE: n

COMMENT: under dioxygen

COMMENT:

---> FIXED PARAMETER; ! ---> FIXED SIGN

$$y(t) = C0 + C1*e^{-k1*t} + C2*e^{-k2*t}$$



1995-2-23 9:23:24 INPUT OFFSET: 0 %

DATA FILE: RUET.001 TIME RANGE: 5.0 µs INPUT V RANGE: 0.320V EXPERIMENT: TRANSIENT ABSORBTION FAST (200 MHz) QUASI-DIFFERENTIAL AMP

MODE: SINGLE-ENDED

SHOTS PRE CYCLE: 10 CYCLES: 5 PMT VOLTIGE: 702 V EXCITATION WAVELENGTH: 355 nm OBSERVATION WAVELENGTH: 415 nm SAMPLE: Rucl8(CO) SOLVENT: CH2Cl2

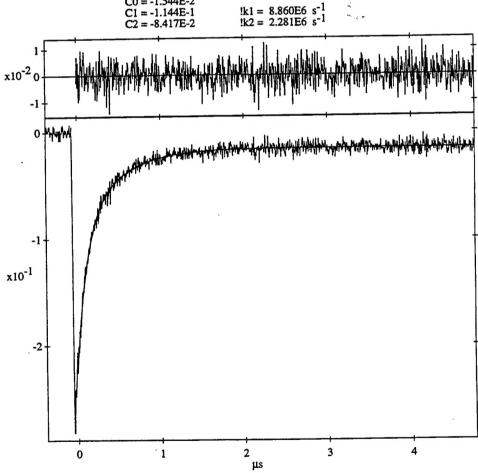
TEMPERATURE: rt
COMMENT: under ethylene
COMMENT:

---> FIXED PARAMETER; ! ---> FIXED SIGN

$$y(t) = C0 + C1*e^{-k1*t} + C2*e^{-k2*t}$$

C0 = -1.544E-2

C1 = -1.144E-1



DATA FILE: RUAR.004 TIME RANGE: 5.0 µs INPUT V RANGE: 0.320V EXPERIMENT: TRANSIENT ABSORBTION_ 1995-2-23 9:13:21 INPUT OFFSET: 0 %

FAST (200 MHz) QUASI-DIFFERENTIAL AMP MODE: SINGLE-ENDED

SHOTS PRE CYCLE: 10 CYCLES: 5 PMT VOLTIGE: EXCITATION WAVELENGTH: 355 nm OBSERVATION WAVELENGTH: 415 nm SAMPLE: Ruc18(CO) PMT VOLTIGE: 702 V

SOLVENT: CH2C12 TEMPERATURE: n COMMENT: under argon

COMMENT:

---> FIXED PARAMETER; ! ---> FIXED SIGN

$$y(t) = C0 + C1*e^{-k1*t} + C2*e^{-k2*t}$$

C0 = -9.262E-3C1 = -6.495E-2

